Multiwavelength fluorescence studies of *Bacillus* bacterial spores

A thesis submitted in partial fulfilment
of the requirements for the degree
of
Doctor of Philosophy in Medical Physics

by

Sivananthan Sarasanandarajah
B.Sc (Hons), P.G.Dip.Sc, M.Sc

at the
University of Canterbury
Christchurch, New Zealand

2007

Supervisor: Associate Professor Lou Reinisch Ph.D.

ABSTRACT

Fluorescence techniques are being considered for the detection and identification of bacterial spores. This thesis sets out to empirically characterize the detailed autofluorescence spectroscopic properties of spores and their target molecules. The multiwavelength fluorescence studies from a unique endogenous biomarker, dipicolinic acid (DPA) and its calcium salt (CaDPA) in bacterial spores are found to be useful for fluorescence characterization of spores. A systematic determination of the fluorescence profile of the major chemical components of *Bacillus* spores and the effect of UV irradiation on them has been performed in dry samples, wet paste and in aqueous solution. The thesis applies reliable tools for accurately describing complex nature of spectral profile from bacterial spores, and for interpreting and identifying their spectral properties. We show that multiwavelength fluorescence technique combined with Principal Component Analysis (PCA) clearly indicates identifiable grouping among dry and wet *Bacillus* spore species. Differences are also observed between dried, wet and redried spores, indicating the stark effect of hydration on fluorescence fingerprints. The study revealed that changes in fluorescence of spores due to hydration/drying were reversible and supports a recent model of a dynamic and dormant spore structure. The spectra were analysed with PCA, revealing several spectroscopically characteristic features enabling spore species separation. The identified spectral features could be attributed to specific spore chemical components by comparing the spore sample signals with spectra obtained from the target molecules. PCA indicated underlying spectral patterns strongly related to species and the derived components were correlated with the chemical composition of the spore samples. More importantly, we examined and compared the fluorescence of normal spores with a mutant of the same strain whose spores lack DPA. We discovered that the dramatic fluorescence enhancement of *Bacillus* spores can be caused by UV irradiation in the spectral region of this unique biomarker without any pre treatment. Differences between spectra of spores, spore strains and other biological samples are very marked and are due to the dominance of the dipicolinate features in the spore spectra. This could lead to a cheap, more sensitive, faster and reagentless bacterial spore detector.

Index Heading: Fluorescence; Excitation-Emission matrix; Hydration; Bacterial spores; Principal Components Analysis; Dipicolinic acid; UV irradiation

List of publications and scholarly work originating from work described in this thesis.

Peer reviewed publications in Journals:

1. **Sivananthan Sarasanandarajah**, Joseph Kunnil, Burt.V.Bronk and Lou Reinisch. Two dimensional Multi Wavelength Fluorescence Spectra of Dipicolinic Acid and Calcium Dipicolinate. Applied Optics, volume 44, Issue 7, 1182-1187 (2005).
2. **Sivananthan Sarasanandarajah,** Joseph Kunnil, Easaw Chacko, Burt.V.Bronk and Lou Reinisch. Reversible changes in fluorescence of bacterial endospores found in aerosols due to hydration/drying. Journal of Aerosol Science (Elsevier). Volume 36, Issue 5-6, 689-699 (2005).
3. Lou Reinisch, Joseph Kunnil and **Sivananthan Sarasanandarajah**. Anthrax detector development. New Zealand Science Review, Volume 62, Issue 1-2, 23-25 (2005).

Patent:

Lou Reinisch and **Sivananthan Sarasanandarajah** (2005), System for spore detection, Patent no: 60/719 930.

Peer reviewed Conference proceedings:

1. **Sivananthan Sarasanandarajah,** Joseph Kunnil, Easaw Chacko and Lou Reinisch. Effects of hydration on the detection and identification of *Bacillus* bacterial spores using two-dimensional fluorescence spectroscopy. The conference on Engineering & the Physical Sciences in Medicine (EPSM), Adelaide, Australia, 23rd – 27th October, 2005 .
2. **Sivananthan Sarasanandarajah,** Joseph Kunnil, Easaw Chacko, Burt.V.Bronk and Lou Reinisch. Reversible effect of Hydration on *Bacillus* globigii probed with Fluorescence Spectroscopy. The Pittsburgh Conference (pittcon) on Analytical Chemistry and Applied Spectroscopy, Orlando, FL, USA, Feb 27 –March 4, 2005.
3. **Sivananthan Sarasanandarajah**, Joseph Kunnil, Easaw Chacko, Burt V Bronk and Lou Reinisch. Reversible effect of hydration on bacterial spores probed with fluorescence spectroscopy. The conference on NZPEM, Christchurch, New Zealand, 22nd &23rd November, 2004

Manuscripts in preparation from work described in this thesis:

- Distinguishing *Bacillus* spores from other biological and non biological samples using fluorescence technique.
- Identifying components of the multiwavelength fluorescence of *Bacillus* spores.
- Principal Component Analysis of Fluorescence data to probe the effect of hydration on identification of *Bacillus* spores.
- Effect of Autoclaving on *Bacillus* bacterial spores studied by Principal Components Analysis combined with fluorescence spectroscopy.
- Fluorescence Quantum Efficiency of major *Bacillus* spore components and spores in suspension.

List of additional publications partially arising or supporting from work described in this thesis:

1. Joseph Kunnil, **Sivananthan Sarasanandarajah**, Easaw Chacko, Barry Swartz and Lou Reinisch, Identification of *Bacillus* spores Using Clustering of Principal Components of Fluorescence Data. Aerosol Science and Technology, volume 39, 842-848 (2005).

2. Joseph Kunnil, **Sivananthan Sarasanandarajah**, Easaw Chacko, and Lou Reinisch, Fluorescence Quantum Efficiency of dry *Bacillus globigii* spores Optics Express, volume 13, Issue 22, 8969-8979 (2005)

3 Joseph Kunnil, **Sivananthan Sarasanandarajah**, Easaw Chacko, Barry Swartz and Lou Reinisch, Effect of Washing on the Identification of *Bacillus* spores by Principal Components Analysis of Fluorescence Data. Applied Optics, volume 45, Issue 15, 3659-3664 (2006).

ACKNOWLEDGEMENTS

First and foremost, my sincere and heartfelt gratitude goes to my supervisor, Associate Professor Lou Reinisch, Director of Medical Physics, for his constant motivation, academic guidance, and support throughout the course of this investigation. I take this opportunity to express sincere and heartfelt thanks to my co-supervisor Professor Phil Butler for his constant inspiration, encouragement and moral support. His interest has been ongoing since I was doing my IAEA fellowship training in Medical Physics in Japan in 2001. He was instrumental in this great opportunity to conduct my Ph.D research work at the University of Canterbury. I would like to thank my associate supervisor Dr. Easaw Chacko for his valuable suggestions and timely discussions especially in the statistical analysis part of my thesis. I also would like to acknowledge the support and advice from our collaborator, Dr Burt V Bronk, U.S.Air Force Research Lab. My research could not have been completed without the support and help of Craig Galilee, Senior Technician, School of Biological Sciences of this University. I extend a very special thanks to my friends, N. Mittinity, P. Smale, T. Francis, J. Kunnil, E. Jhala, and A. Bell for their help in many ways. I would like to thank Head and staff of the Department of Physics and Astronomy for their moral support, administrative assistance, technical assistance and for providing a good environment for carrying out my studies. I also acknowledge the support and help from Dr Brian McArdle in the analysis part of my thesis. I thank to Dr Petra Sauer for her interest in my research work and providing some useful comments and fruitful discussion. I acknowledge the support and help from the Learning skill center and UCSA. Finally, I would like to thank Angela Davies, Assistant Librarian for helping me to edit the references by using EndNote.

I would like to acknowledge financial support in the forms of a scholarship (University of Canterbury doctoral scholarship, US Department of Defence and NovaSol, USA), a Teaching and research Assistant position and conference attendance for presentations (Novasol and Department of Defence, USA, University of Canterbury, and ACPSEM). My motivation for the earnest pursuance of the PhD degree comes from the devotion, expectation, love and support of my family. My parents, Sarasanandarajah Nageswary and the late Paramalingam Sarasanandarajah and my wife Malini Sivananthan, and my daughter's Sharnika Sivananthan and Ashveka Sivananthan, are always in the warmest part of my heart and the driving force of my life.

CONTENTS

List of Figures

List of Tables

Abbreviations

BA	*Bacillus anthracis*
BG	*Bacillus globigii*
BG1	*Bacillus globigii* 1
BG2	*Bacillus globigii* 2
BG3	*Bacillus globigii* 3
BC	*Bacillus cereus*
BS	*Bacillus subtilis*
BT	*Bacillus thuringiensis*
E.coli	*Escherichia.Coli*
DNA	Deoxyribonucleic acid
SP	Spore photoproduct
DPA	Dipicolinic acid
CaDPA	Calcium dipicolinate
(+DPA)	Normal strain of *Bacillus subtilis* (with DPA)
(–DPA)	Mutant strain of *Bacillus subtilis* (lack of DPA)
Tb-DPA	Terbium dipicolinate
NADH	Nicotinamide adenine dinucleotide
EEM	Excitation-Emission Matrix
nm	Nanometers
2D	Two dimensional
PCA	Principal Component Analysis
PCs	Principal components
UV	Ultraviolet
UV-Vis	Ultraviolet-Visible
O.D.	Optical density
a.u	Arbitrary unit
QE	Quantum Efficiency
Wet	Hydrated spores on filter paper
Aqueous	Hydrated spores in water suspension

CHAPTER 1

1 GENERAL INTRODUCTION

1.1 Motivation

> "*Bacteria represent the great success story of life's pathway. They occupy a wider domain of environments than any other group. They are adaptable, indestructible and astoundingly diverse. We cannot even imagine how anthropogenic intervention might threaten their extinction, although we worry about our impact on nearly every other form of life…. This is the 'age of bacteria'---as it was in the beginning, is now and ever shall be*."

-Stephen Jay Gould.[1]

There is currently increasing anxiety all over the world about the possibility of chemical and biological terrorism. Biological warfare agents of critical concern include bacterial spores such as *Bacillus anthracis* (anthrax), *Clostridium tetani* (tetanus*)* and *Clostridium Botulinum* (botulism). Certain spore-forming bacterial species are pathogenic and the toxins produced by the bacteria**,** the causative agents of food poisoning or serious acute diseases, are extremely resistant to antibiotics and disinfectants. Bacterial endospores are an important source of bacterial contamination and are currently hard to detect. It is therefore vital to understand and develop rapid, specific methods for their detection.

The biological agent detection systems currently available are large, expensive devices that, despite their complexity, are still prone to giving false alarms. Costly reagents that possess high sensitivity are required in many detectors.[2] There is also a large gap between the minimum number of spores required to induce illness and the minimum number of spores required for detection using current equipment. More research and investment in fast, sensitive and reliable biological detection techniques is needed.

Since fluorescence techniques are to be considered for the detection and identification of bacterial spores, it is important to understand and characterize the relevant optical properties of bacterial spores and their target molecules. This thesis mainly investigates the auto fluorescence of *Bacillus* spores using multi wavelength fluorescence spectroscopy. These studies may be useful in the future to develop bacterial spore detectors that are useful for monitoring the environment without any disturbance. Monitoring of aerosolised bacterial spores is desirable in locations such as mail sorting, food preparation, and healthcare facilities. A key advantage of optical methods is that many wavelengths can be dealt with simultaneously without the signals interfering with one another. The single wavelength excited luminescence characteristics of many biological and environmental substances overlap. However, a variety of optical methods have been developed by various research groups to separate the individual contribution from the target and its background.

Although vegetative cells of endospore-forming bacteria are most commonly found in the soil, endospores exist almost everywhere on the planet.[3] The huge number of similar micro-organisms present in the environment act as a challenge to the detection and measurement of the biological agents of interest.[4] Existing methods for detection and identification of bacterial spores include chemical or biological processes such as polymerase chain reaction (PCR),[5, 6] immunofiltration assay,[7, 8] polymorphism analysis,[9] direct detection of DNA sequences[10] and liquid chromatography.[11] Some optical processes have also been studied such as Fourier Transform Infrared Spectroscopy (FT-IR)[12] and those which indicate bacterial spore presence by detection of dipicolinic acid (DPA).[13-23] Detection of anthrax biomarkers by surface-enhanced Raman spectroscopy is also an active area of current research in this field.[24] Most of these techniques are time consuming and require trained personnel for sampling and analysis. Few biological detection systems provide a sensitive, real-time capability to detect, identify and quantify the bacterial endospores. There is a need for better systems that give an early warning so that infection can be avoided.

Dipicolinic acid (2,6-pyridinedicarboxylic acid or, briefly, DPA) and its salts (mainly calcium) are major constituents of bacterial endospores and are rather uncommon elsewhere in nature. As has been emphasized elsewhere, the presence of DPA and its

calcium salt gives a ready-made fluorescence biomarker for endospores. The present study is motivated by the fact that more detailed excitation-emission studies of these compounds and bacterial spores are needed to understand the fluorescence of endospores. The DPA and CaDPA in the spore correspond more closely to a solid sample or a wet paste than to DPA in solution.[25] Previous studies did not include fluorescence from DPA/CaDPA in this form. Thus further experimental measurements of multiwavelength fluorescence spectra with wet paste, dry crystalline and solution preparations of DPA and CaDPA, including the effect of broad band UV irradiation, were necessary to further characterize the fluorescence from bacterial spores. The fluorescence signals from spores of normal strain (+DPA) were compared with signals from a strain of a same spore species that lacked DPA (−DPA) in this thesis. The effects of UV irradiation on fluorescence profiles of *Bacillus* spores are studied to understand the unique fluorescence signal from *Bacillus* spores.

Distinguishing bacterial spores at the species level is also extremely important in order to understand and differentiate between pathogenic and non- pathogenic bacterial spore species in both dry and water environments. Some aerosol detectors use fluorescence in an attempt to detect bacterial spores. However, these detectors have not been able to indicate reliably the presence of spores. In order to tackle the problems with current aerosol detectors using fluorescence, it was necessary to understand the fluorescence spectra from different species of *Bacillus* spores due to hydration/drying using multiwavelength fluorescence spectroscopy and attempt to distinguish dry spores from wet spores. Fluorescence quantum efficiency (QE) measurements of bacterial spores and their major probable fluorophores were also investigated in this thesis to further understand the optical properties of these samples.

1.2 Fluorescence studies of Bacterial spores

The autofluorescence technique has been tried on a number of occasions for bacterial identification.[26-33] The fluorescence from bacteria and bacterial spores is due to emissions of intrinsic fluorophores.[34, 35] Single-wavelength excitation and single-wavelength or wide-band emission fluorescence is, for example, used in several particle analyzers.[36] Acquiring fluorescence spectra at several excitation wavelengths

may further increase the possibility of classifying the biological particles,[37-40] but it also increases the complexity of the instrument and the data analysis. Multiwavelength fluorescence spectroscopy measurements have been shown to be useful for detecting shape, chemical composition and changes in internal structure.[41]

Fluorescence has a number of parameters (for example, excitation wavelength, emission wavelength or fluorescence lifetime). This affords a number of possibilities when tailoring the technique to fit the problem. The emission peak from a single excitation wavelength is often seen as a broad peak without significant features. Therefore, sample identification with fluorescence techniques generally involves a double discrimination technique. Double discrimination means that the identification is made by varying two different parameters. The double discrimination can involve generation of a fingerprint in the form of an excitation-emission matrix (EEM).[28] In this research, the fingerprinting data are acquired in the form of a matrix of fluorescence intensity as a function of multiple exciting and emitting wavelengths,[42] and the two varied parameters are the excitation and emission wavelengths. Measurement of two-dimensional fluorescence spectroscopy for bacterial spores is a crucial step in understanding the endogenous fluorophores and determining which excitation-emission wavelength region contains the most information for further analysis.

Fluorescence spectroscopy has been selected for several reasons in this research. It is a resonance process and fluorophores often have a large cross section. The fluorescence technique is also fast. While the traditional methods of identification generally take several hours, it is possible to measure a fluorescence spectrum in less than one second. Fluorescence spectroscopy can also be used in remote detection which is especially useful in the event of bacterial warfare. Compared with non-resonance phenomena like Raman spectroscopy, this method is very sensitive, requiring very few bacterial samples or a low concentration of fluorophore to give a representative spectrum. Since the fluorescence signal is shifted in wavelength away from the exciting signal, detection of very low concentrations is possible with a good signal to noise ratio. The small sample size also decreases risk to laboratory personnel during the development and testing of the technique.

Fluorescence is a valuable tool in probing different chemicals, bacterial spores and other materials. Because the surrounding medium influences the emissions from intrinsic fluorophores, subtle differences in the emission spectra can be used to identify their environment. Such environmental differences can be linked to the species of the microbes or to the growth stages of the bacteria. Analysis of whole samples of bacterial cells and spores with this technique has given rise to unique protein and other chemical fingerprints that can be used for classification at the species and strain levels.[43]

1.3 Mathematical treatment of data

The complex nature of the spectral profile from bacterial spores and other biological samples makes their interpretation a difficult task. The main problem for interpretation of high dimensional spectroscopy is the partial or complete overlap of signals from the different constituents in the multi-component samples, such as bacterial spores. For this reason, current methods using spectroscopy for understanding and classification of biological samples have their shortcomings. To assist with the development of robust spectroscopic methods, one needs reliable tools for accurately describing bacterial spores, and for interpreting and identifying their spectral properties. This thesis applies multivariate data analysis to the spectral data to reduce the dimensionality of the data set. In order to understand the samples' composition, shape and grouping by their fluorescence characteristics, it is necessary to analyze signals at several sets of excitation and emission wavelengths. Ideally, complete emission spectra obtained at several excitation wavelengths would cover the combination that is required to pick up the signature from each of the fluorophores in the samples.

Statistical multivariate analysis detects differences in spectral characteristics (shape and pattern) of spectroscopic data from biological samples and enables one to disentangle the detail information.[44] This statistical techniques are used to analyze more than two variables simultaneously. Principal Component Analysis (PCA) is the most commonly used multivariate analytical technique for representing the original

data with a reduced number of variables and makes it possible to draw similarity maps of the samples in order to understand the physical or chemical system.

PCA has found many applications in optical spectroscopy. PCA has been used for the analysis of UV/visible fluorescence data,[32, 40, 45, 46] and for laser- induced breakdown spectroscopy in the UV-Vis region.[47, 48] Its usefulness has also been demonstrated for high-performance liquid chromatography[49, 50] and time resolved Fourier transform infrared spectroscopy.[51,52] Leblanc and Dufour[40] were able to successfully discriminate suspensions of vegetative bacterial samples using four excitation wavelengths and PCA. Very recently, Bhatta, Goldys and Learmonth used fluorescence combined with PCA to differentiate between yeast and bacteria and between different yeast species.[46] PCA was applied to obtain a map describing physical and chemical variations between the samples studied. PCA finds combinations of variables that describe major trends in the data set. In PCA, each sample is represented as a point in a multidimensional coordinate system in which the number of axes is equal to the number of variables. Points with similar properties will end up closer to each other than points with less similarity.[32, 40, 46] PCA produces a set of expression patterns known as Principal Components (PCs), and linear combinations of these patterns can be assembled to represent the behavior of all of the objects in the data set. PCs can also be used to obtain the major contribution to the fluorescence spectra.

1.4 Overview of the thesis

The work presented in this thesis is part of the whole project carried out in our laboratory entitled "Pathogen detection and identification using two-dimensional fluorescence spectroscopy". The purpose of this thesis is aimed to empirically characterize the autofluorescence of *Bacillus* spores under certain physical conditions on the basis of multiwavelength fluorescence spectroscopy. We apply exploratory methods to the fluorescence profiles of different species of *Bacillus* spores to discover sample groups and to understand the relative contribution of major chemical components (fluorophores). This study has gone to considerable depth in the exploration of fluorescence of spores.

This study focused on the following to address the main objective of this thesis:

* Multi wavelength fluorescence studies of major probable chemical components of the *Bacillus* spores.
* Multi wavelength fluorescence studies of different species of *Bacillus* spores.
* Reversible changes in fluorescence of *Bacillus* spores due to hydration and drying
* Effect of Autoclaving and washing on spore fluorescence
* Understanding the relationship between the fluorescence of major chemical components and the fluorescence of *Bacillus* spores.
* Multi wavelength fluorescence studies on *Bacillus* spores under enhanced UV irradiation
* The determination of fluorescence QE of major *Bacillus* spore components and spores in water suspension.

Fluorescence excitation-emission spectra provide a probe for the internal structure (composition) of biological samples and the environment of the fluorophores. We investigated the detailed excitation-emission spectra of major *Bacillus* spore chemical components, DPA, CaDPA and tryptophan and related these to the fluorescence studies of *Bacillus* spores. The contribution of these chemicals to the autofluorescence of the *Bacillus* spores was examined by comparing excitation-emission spectra taken from a normal strain (+DPA) of *Bacillus subtilis* (BS) spores and from spores of a mutant strain (⁻DPA) derived from the same (+DPA) strain. We examined the PCA loadings vector components to discover whether they corresponded to the underlying spectra of the fluorescent chemical compounds and tried to assign the principal components to these chemical components (fluorophores). We also performed a simulation study of these mixture components and compared it to the fluorescence profile of *Bacillus* spores to identify the major fluorophores in spores.

We used different species of *Bacillus* spores to determine whether the fluorescence profiles were unique and could be distinguished. We investigated the reversible effect of hydration on *Bacillus* spores and attempted to distinguish dry spores from wet spores from different species systematically under similar conditions and to see any differences between dry and re-dried spores.

We tried to understand the effect of UV irradiation on fluorescence spectroscopic properties of the *Bacillus* spores. The fluorescence spectra were measured in water suspensions to determine specific and quantifiable UV-induced changes. The results seem to indicate the occurrence of a peculiar response in some specific spectral regions of the UV-induced fluorescence emission spectra. The attribution of the observed changes in the potential bio-indicator role of *Bacillus* spores is discussed in the light of our studies of DPA, CaDPA and tryptophan. We used this study to understand the unique fluorescence property of *Bacillus* spores. This research shows that UV irradiation on *Bacillus* spores could lead to a rapid, reagentless and cheap bacterial spore detector.

An Excitation-Emission Matrix (EEM) is a two-dimensional contour plot that displays the fluorescence intensities as a function of a range of excitation and emission wavelengths. We used the EEM technique to visualize the fluorescence fingerprints of the samples investigated. Each contour represents points of equal fluorescence intensities. Assignment of the inherent fluorophores and the understanding of the physical/chemical system were performed using EEM and PCA. This required the development of algorithms for plotting the EEM and for PCA. The fluorescence of a sample or biological molecule is characterized by its spectrum, quantum efficiency (QE) and its life time.[53] In this thesis, we calculated the QE of the major *Bacillus* spore chemical components, before and after UV irradiation using the QE value of a standard sample of anthracene in ethanol. We also calculated the QE of some *Bacillus* spores in suspension, before and after washing the samples.

This thesis has the following structure. In this Chapter 1 the topic has been introduced, its importance, and the reasons for selecting the fluorescence technique for this research are discussed. Chapter 2 is devoted to a more comprehensive review of the literature relating to each area of the sub objectives. Chapter 3 outlines the materials and methods of the research. We also discuss the methodology of formation of EEM and the PCA procedure. In Chapter 4 the results and data analysis are presented and in Chapter 5 we discuss the important findings of this research in the light of current literature. In Chapter 6, the achievements of the whole study are summarized and conclusions drawn.

CHAPTER 2

2 LITERATURE REVIEW AND BACKGROUND

2.1 Overview

The thrust of this Chapter is to review the topics and the background information pertinent to this thesis research. Section 2.2 provides a brief background information on *Bacillus* spores and spore structure. Section 2.2 also reviews the physical and microbiological aspects of spores, including their response to hydration. Section 2.3 describes the basic principles of fluorescence spectroscopy: absorbance and transmittance, fluorescence instrumentation and the basic theory behind the formation and interpretation of EEM. In Section 2.4 we describe the major probable fluorophores in *Bacillus* spores including DPA and CaDPA. We describe the QE measurements in Section 2.5. Section 2.6 gives a brief outline of the basic theory of PCA.

2.2 *Bacillus* bacterial spores

At the end of the 19th century Tyndall, Kohn and Koch independently discovered that certain species of bacteria, particularly *Bacillus* and *Clostridium* bacteria, form dormant cellular structures known as endospores (or simply spores).[54] Spores are known to be the hardiest form of life. Spore dormancy is a response to the stress of starvation. Spores can remain in a viable dormant state for long periods of time (in some cases millions of years) and when conditions permit (e.g: nutrients) they may develop into a vegetative bacterium.

2.2.1 The structure of a *Bacillus* spore

The spores of *Bacillus* consist of several layers of protective coatings surrounding a core of DNA and enzymes. Figure 2.1 illustrates the compartmentalized and layered structure of the spore.

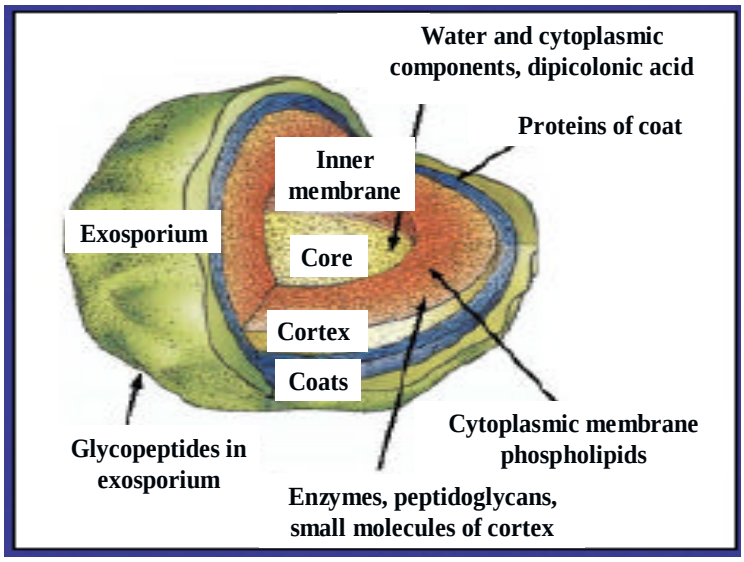

Figure 2.1: Structure of a *Bacillus* spore (Extracted from http://www.chemimage.com)

The spores of *Bacillus* vary according to species and can even exhibit different properties among strains of the same species. Further, environmental factors such as temperature and available metabolites (amino acids, growth factors, etc.) have been shown to affect sporulation (spore formation) and the resulting spore structure.[55]

The external surfaces of spores of *Bacillus anthracis* (BA), *Bacillus cereus* (BC) and *Bacillus thuringiensis* (BT) are enclosed in a structure known as exosporium which is not well studied.[56] In the well-studied *Bacillus subtilis* (BS) species the exosporium is absent. It is not known whether the spores of *Bacillus globigii* (BG) have an exosporium. Studies by Matz *et.al*[57] have found the exosporium to be composed of protein (~50%), polysaccharide (~20%) and lipid (~7%) with smaller amounts of calcium (~0.7%) and DPA (~0.2%).[58] Beneath the exosporium is a multilayered proteinaceous spore coat.[59] The construction of the spore coat – such as the number of layers and whether the spore coats surface is grooved, ridged or dimpled – varies with spore species .[56, 60]

The cortex, composed of peptidoglycan, can shrink or swell in response to environmental conditions, and is thought to be essential for establishing relative dehydration in the central part of the spore.[59, 61, 62] "Compared with the cortex, the spore core is significantly dehydrated. It contains the nucleoid, enzymes, ribosomes and much of the DPA, and it varies with different spore species".[59]

Overall, spore structure is dynamic and complex. "Spores form slowly (6-10 hours) and can accumulate metabolic byproducts from the culture media".[63] This complicates any analysis. Because environmental conditions affect the chemical composition of the spore, the structure of the spore cannot be considered as fixed. The spore forms as a result of environmental conditions and reflects these conditions in its structure.

The process of condensation of bacterial DNA into a core within a series of membranes that accumulate calcium, DPA and protein layers is known as sporulation. There are different stages in sporulation. Initially, the spores' central region accumulates DPA synthesized by the mother cell.[64] "Large amounts of divalent cations (mainly Ca^{2+}) are absorbed in parallel with the DPA.[64] Finally, the spore core dehydrates".[64]

"Spores are metabolically temporarily inactive and therefore carry out no detectable catabolism of exogenous or endogenous metabolites.[65] Consequently, spores of both *Bacillus* and *Clostridium* species in particular do not have significant levels of the common high-energy compounds found in growing cells, such as nucleoside triphosphates, reduced pyridine nucleotides and acyl-coenzyme A molecules".[65] The exact reasons for the lack of activity of spore-core enzymes are not clear, but a major contributing factor appears to be the extremely low water content in the spores' core.[66] Further, a recent theoretical analysis led to the suggestion that the spore core is in a glassy state.[67]

2.2.2 Effect of hydration on *Bacillus* spores

The sorption of water vapour by bacterial spores has been investigated by researchers for many years. Bacterial spores have a significant affinity for water. The amount of water adsorbed varies with spore species. The permeability of spores to water has been reviewed on several occasions.[68-71] The demonstration of the permeability of spores to water is based on the experimental observations. There appears to be no restriction to the movement of water vapour in or out of the spore.[68, 72-75] Neihof et al.[68] used a quartz spring balance to measure the uptake of water by *Bacillus* spores and from this study they conclude that the spore coat is permeable to water vapour. They also showed that the interior of the spore is not maintained as anhydrous because they observed similar curves for water adsorption and desorption as a function of the relative humidity with intact and crushed BS endospores. It is claimed that the relationship between water content in the spores and the environmental relative humidity at a constant temperature varies with the preparation of the spores, the hydration history and the condition of adsorption.[68]

The hydration of bacterial spores is particularly complex because of the wide range of hydrophilic sites, physical structures and solubilities of the spore components.[76] A recent study revealed that the molecular mobility of spore core component phosphorous due to addition or removal of water indicates that water can readily diffuse between the inner core and the surroundings.[77] This was not observed in the case of another core-specific component, DPA, when spores were hydrated. It is known that spores can absorb their own weight in water and still remain viable.[78] There is a growing consensus that the central protoplast remains in a relatively dehydrated state even when spores are exposed to an excess of water.[79]

Leuschner and Lillford[77] proposed that DPA could exist in the core immobilized in a water-insoluble network. Black and Gerhardt have developed a model which shows that, “the cross linking of macromolecules to form a high-polymer matrix containing entrapped free water, has an insolubly gelled core”.[70] Hydration studies analysed by Leuschner and Lillford using ^{13}C NMR (Nuclear Magnetic Resonance spectroscopy) revealed a dependence on the water concentration and a considerable mobility in the cortex and proteins of dormant, fully hydrated spores.[77] Their data also revealed a

strong effect of hydration on spore dimensions because the breadth and length of spores changed significantly as water was absorbed.

The recent results of Westphal[80] and his co-workers are particularly illuminating. They showed that the spore is capable of relatively rapid expansion and contraction while maintaining spore dormancy. They discovered that the spores consistently swell in response to increased relative humidity, and shrink to near their original size on re-exposure to dry air (reversible changes). Their results suggests that individual spores respond consistently to changes in humidity.[80] The observed swelling of spores of *Bacillus thuringiensis* may be diagnostic of all *Bacillus* spores and may provide a means of distinguishing between different types of *Bacillus*. The study by Westphal *et.al* found that distinguishing of spores on the basis of size or swelling could be achieved by tests that took between several seconds and a few minutes.[80]

According to Driks[81] the flexibility of the exosporium, coat, and/or cortex have been demonstrated to be flexible enough to allow the volume changes while retaining the integrity of the spore. The Morphological consequences of changes in bacterial spores due to changes in relative humidity are illustrated in a cartoon shown in Figure 2.2.

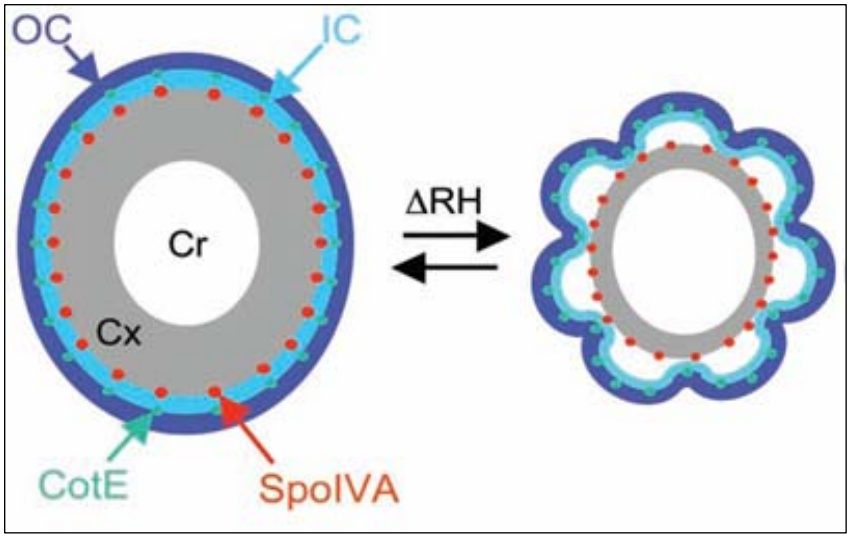

Figure 2.2: Morphological consequences of changes in relative humidity. The layers comprising the spore are colour-coded: white, core (Cr); grey, cortex (Cx); light blue, inner coat (IC); dark blue, outer coat (OC). RH, relative humidity. The exosporium is not illustrated, for simplicity. Thin-section electron microscope analysis shows significant variation in the degree of folds in the coat, reflected in the two cartoons (the folds in the right spore coat are somewhat exaggerated for clarity). Possibly, the ability of the coat to fold and unfold permits changes in spore size as relative humidity varies (extracted from Driks, 2003,[81]).

2.3 Principles of fluorescence spectroscopy

"Spectroscopy is the study of the interaction of electromagnetic radiation with matter that occurs at UV, VIS, near-infrared (NIR) and infrared (IR) wavelengths".[82] Almost all chemical and biological samples absorb energy from at least one region of the spectrum of electromagnetic radiation.

"The energy at which the absorption occurs depends on the available electronic, vibrational and rotational energy levels of the molecule".[82] When absorption is from the UV-Vis region of the spectrum, transitions occur between electronic energy levels, and it is these transitions that form the basis of UV-Vis spectrometry. The analysis of autofluorescence has the advantage of providing information about the molecular species responsible for the emission as well as about the physiological changes taking place in cells under perturbation (e.g, hydration, UV radiation) without interfering with the native cellular environment. "Techniques based on fluorescence spectroscopy have the potential to link the biochemical and morphological properties of biological samples and to characterize physical-chemical changes occurring in cells".[83]

There are three aspects to a spectroscopic measurement: irradiation of a sample with electromagnetic radiation; measurement of the absorption, spontaneous emission (fluorescence, phosphorescence) and/or scattering (Rayleigh scattering, Raman scattering) from the sample; and analysis and interpretation of these measured parameters to give useful biological information.[82] In the UV-Vis spectral regions, absorption spectroscopy and fluorescence spectroscopy have been explored extensively as diagnostic tools for medical and biological applications. The goal of the present study is to apply UV-Vis fluorescence spectroscopy to understand the fluorescence characteristics of *Bacillus* spores and their target molecules.

2.3.1 Rayleigh scattering and Raman scattering

In general, the scattered light that interferes with fluorescence measurements can be divided into Raman scatter and Rayleigh scatter, according to its origin.[53] Scattering provides no information about the fluorescence properties of the sample and must be removed from the measurements. The elastic Rayleigh scatter refers to the scattering of light by particles and molecules smaller than the wavelength of incident light. In this case, the wavelength of scattered light coincides with the incident light.

An inelastic Raman scattering and fluorescence emission are two competing phenomena mainly in liquid sample measurements. Raman scatter originates due to absorption (or perturbation) and re-emission of light couples with vibrational states of the molecules. The scattered light will have a higher or lower wavelength than the exciting light, with a constant difference in wavenumbers.

In the data analysis of this thesis, both Rayleigh and Raman scatter are non-desirable phenomena. Therefore, eliminating of various signals of scattering light is necessary to obtain the correct spectrum in fluorescence analysis. Theoretically, the elastic scatter can be removed by measuring the fluorescence signal between 1st and 2nd order scatter. However, the instrumental setups with large bandwidths normally cause the Rayleigh scatter a significant interference to fluorescence emission with small Stokes shifts. For highly fluorescent samples, the fluorescence emission spectrum generally overwhelms the Raman peak.[53] Raman scatter can be neglected in most cases due to its sparse contribution and will be separated from the data analysis in liquid sample measurements in this thesis research.

2.3.2 Absorbance and transmittance

A fundamental aspect of spectroscopy is the measurement of light absorption. Many molecules absorb ultraviolet or visible light. Different molecules absorb radiation at different wavelengths. Absorbance is directly proportional to the path length, d, and the concentration, c, of the absorbing molecules. The *Beer-Lambert* law assumes that

the fraction of light absorbed or scattered from the measurement path by each layer of solution is the same.[53] This is expressed in the following equation.

$$\text{Absorbance, } A = \log (I_0 / I) = \varepsilon\, d\, c \qquad (2.1)$$

Where I_0 is the incident intensity, I is the transmitted intensity, d is the pathlength of the sample, that is, the pathlength of the cuvette in which the sample is contained. The proportionality constant ε is called the absorbtivity. The Beer-Lambert law, even with its deviations and limitations (eg, it is not valid at high concentrations), forms a major basis for all the quantitative measurements in UV-Vis spectroscopy as it relates absorbance directly to concentration.

2.3.3. Luminescence

Luminescence spectroscopy measurements play an important role in current clinical and biochemical analyses due to their high sensitivity and selectivity. Luminescence is the emission of light from any substance resulting from the decay of electronically excited states. Optically stimulated luminescence is formally divided into two major classes, fluorescence and phosphorescence, depending on the characteristics of the excited state. "The study of fluorescence can provide some information about the chemical composition of the emitting system and the processes that take place after the absorption of the excitation energy". [53]

2.3.4 The phenomenon of fluorescence

"Optical spectroscopy probes the energy levels of a molecule defining its characteristic state, and is influenced by molecular structure and to the energetics and dynamics of any chemical processes the molecule may be undergoing".[82] At room temperature most molecules are in the lowest level of the ground electronic state (S_0) as shown in Figure 2.3. From this state upward transitions occur upon the absorption of light. For molecules in solution the rotational energy levels are so closely spaced that they cannot be distinguished by optical spectroscopy.

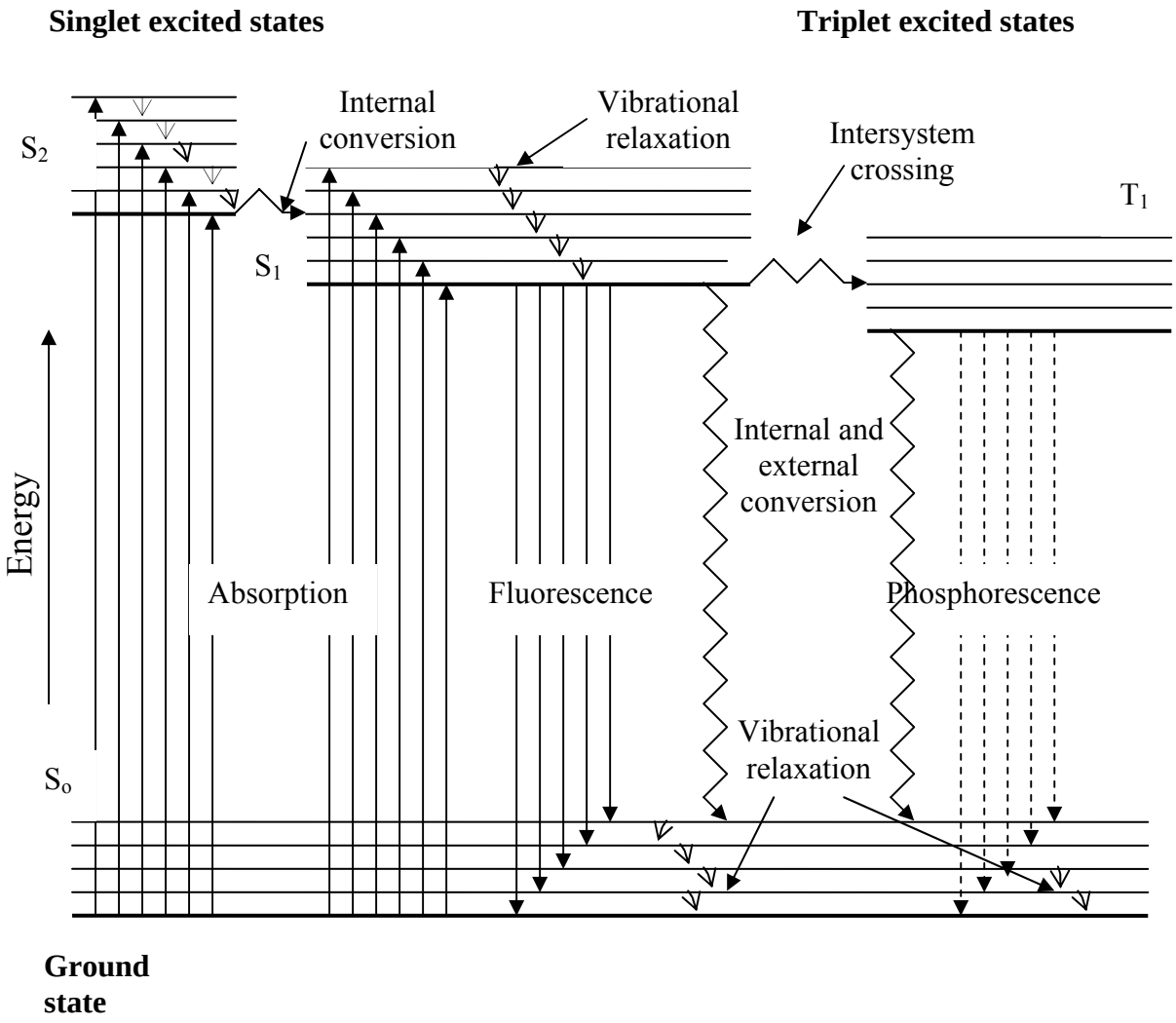

Figure 2.3: Simplified energy level diagram

Figure 2.3 shows a simplified energy level diagram of a molecule with ground state (S_0) and higher energy excited electronic states (S_1). In turn, these energy states contain several vibrational energy levels.[53] If a molecule is illuminated with radiation of a wavelength that lies within the absorption spectrum of the molecule, it will absorb the energy and be activated from its ground state (S_0) to an excited singlet state (S_1 or S_2), with the electron having the same spin as it had in the ground state. The molecule then relaxes back from the excited state to the ground state by the generation of energy either radiatively or nonradiatively, depending on the local environment.[83] In a nonradiative transition, relaxation occurs by thermal energy transfer (dashed arrows). In a radiative transition, relaxation occurs via fluorescence at specific emission wavelengths (solid arrow). The generation of fluorescence occurs in the following three steps: firstly, a nonradiative transition to a vibrational level of the first

excited state occurs to maintain thermal equilibrium; secondly, there is a radiative transition from the first excited state to one of the vibrational levels of the ground state; and thirdly, there is another nonradiative transition to the lowest vibrational ground state. It can also happen that an electron in the lowest vibrational state of an excited energy level can make a nonradiative transition to a vibrational state of another energy level of slightly lower energy, provided the two energy levels have the same spin multiplicity. Such a transition is called an internal conversion.[83]

Phosphorescence is a different process: it results from an inter-system crossing in which the spin of the electron is flipped in the excited state (see fig 2.6). This spin change increases the time taken for radiative transition from the excited state to the ground state. This excited state is termed a triplet state (T_1).[83] The radiative transition from the excited triplet state to the ground state is generally called phosphorescence.

Fluorescence has three general characteristics common to all molecules, whether biological or non-biological. First, due to energy losses between absorption and emission fluorescence occurs at emission wavelengths that are almost always red-shifted relative to the excitation wavelength. Second, generally the emission wavelength is independent of the excitation wavelength. Third, the fluorescence spectrum of a molecule is generally a mirror image of its absorption spectrum.[83]

2.3.5 Steady-state fluorescence

Fluorescence measurement techniques can be broadly classified into two types: steady-state and time-resolved.[53] Most commonly used because of its convenience, a steady-state measurement is performed with constant illumination and observation. The sample is illuminated with a continuous beam of exciting light, and the intensity or emission spectrum is recorded. Since the timescale for fluorescence is of the order of nanoseconds, most measurements are steady-state type. When the sample is initially illuminated, the steady state is reached almost immediately. A time-resolved measurement is generally more complex, requiring a high-speed detection system.[53] The research work presented in this thesis used only steady-state measurements in order to facilitate construction of simple and cost effective detectors in the near future.

2.3.6 Fluorescence instrumentation

Success in fluorescence spectroscopy depends on attention to experimental details and a good enough understanding of the apparatus. The techniques are highly sensitive, thus there are many potential artefacts that can misrepresent the data. For instance, amplifying instrument output can help to produce an observable signal[53], but signals seen at high amplification, may not originate entirely from the fluorophore of interest. Background fluorescence from the solvents, stray light in the optics, light leaks in the instrumentation, light scattered by turbid solutions, Rayleigh scattering and Raman scattering are all possible source of interferences in the measurements.[53] There is no ideal spectrofluorometer and the available instruments do not necessarily yield true excitation or emission spectra. This is because the light sources produce a non uniform spectral output while the monochromators and the detectors are wavelength dependent. Detectors are usually based on photomultiplier tubes because of their sensitivity to UV and visible light[53]. The polarization or anisotropy of the emitted light can also affect the fluorescence intensities[53].

2.3.7 Excitation and emission spectra

An emission spectrum is the wavelength distribution of the emitted light measured at a single excitation wavelength. An excitation spectrum is defined by the wavelength distribution of exciting light, measured at a single emission wavelength. Either a wavelength scale or a wavenumber scale is used to present such spectra.[53] For most fluorophores, the emission spectra are independent of excitation wavelength. Hence, the excitation spectrum of a fluorophore is typically a mirror image of its absorption spectrum. “However, this is almost never observed because the wavelength responses of almost all spectrofluorometers are dependent on wavelength. Such correspondence also requires the presence of only a single type of fluorophore and no other complicating factors. These can include a nonlinear response resulting from the high optical density of the sample or the presence of other chromophores”.[53]

2.3.8 Fluorescence excitation –emission matrix (EEM)

An EEM is a 2D matrix whose elements, I (λ_{ex}, λ_{em}), are the fluorescence intensity as a function of the excitation (λ_{ex}) and emission (λ_{em}) wavelengths. For single molecular species, the EEM provides a unique fluorescence signature of the molecule. For a complex medium such as bacterial cells or tissues, the EEM indicate the relative contributions of the component molecules. However, *Bacillus* spores and other biological samples are microscopically heterogeneous in the distribution of fluorophores, chromophores and scattering. Hence, the measured EEM may depend strongly also on the measurement geometry, which varies according to the application.[84]

When a mixture of two or more components is examined spectrally, the emission spectrum is no longer independent of the excitation wavelength, and the excitation spectrum is no longer independent of the monitoring wavelength.[85] In this case, a conventional one dimensional spectrum is not adequate to describe the fluorescence intensity behaviour, and an EEM representation is necessary.

2.4 Fluorophores in biological samples (Biofluorophores)

Figure 2.4 shows the biological molecules that exhibit endogenous fluorescence, along with their excitation and emission maxima in biological samples. These fluorophores are commonly found in most microorganisms. As mentioned in the above sections, there are no significant amounts of NADH (Nicotinamide adenine dinucleotide) and other high energy components in bacterial spores.

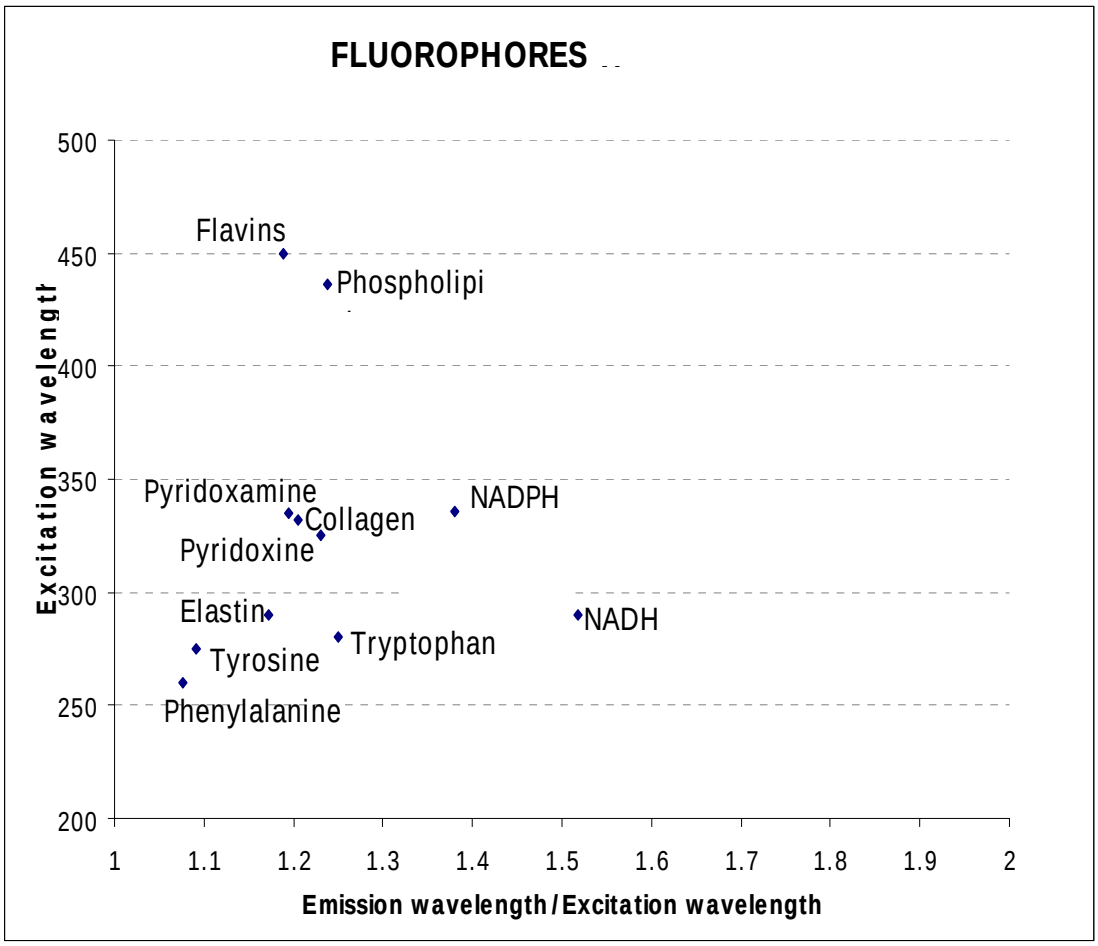

Figure 2.4: Fluorophores in biological samples[83]

The aromatic amino acids, tryptophan, tyrosine, and phenylalanine are mainly responsible for intrinsic protein fluorescence.[86] "In native proteins the emission of tyrosine is often quenched, which may be due to its interaction with the peptide chain or energy transfer to tryptophan. The major cause of UV absorbance and emission in proteins are the presence of indole groups of tryptophan residues. It was found that at excitation wavelengths longer than 295 nm only tryptophan is fluorescent".[53] From 280 nm to 295 nm, both tyrosine and tryptophan are fluorescent. However, energy transfer from tryptophan to tyrosine is common.[53] Below 280 nm, all three amino acids can be excited, although the QE of phenylalanine is relatively low compared with that of tryptophan and tyrosine.[53]

"The emission of tryptophan is highly sensitive to its local environment, and it is thus often used as a reporter group for protein conformational changes. Spectral shifts have been observed as a result of several phenomena, such as binding of ligands and protein-protein association".[53] Tryptophan fluorescence is subject to being quenched by nearby electron-deficient groups and protonated histidine residues. "Multi wavelength excitation can be useful to probe different chromophores in target biological materials".[38] For example, 260-280 nm excites the aromatic amino acids tyrosine, tryptophan and phenylalanine so that each have characteristic emission bands between 300nm and 400 nm.[83] These natural chromophores are universal markers for biological aerosols since these aminoacids are present to some extent in nearly all proteins.

"Fluorescence at visible wavelengths has frequently been attributed to reduced nicotinamide adenine dinucleotide (NADH) associated with cell metabolism and flavins, such as riboflavin, although there are other biogenic compounds such as carotenoids and chlorophylls that also fluoresce".[87] The 349 nm excitation wavelength was originally chosen to excite biogenic chemicals associated with cell metabolism, such as NADH[88] and riboflavin which have characteristic broad emission bands peaking at 450 nm and 560 nm, respectively.[87, 88] However, the chemical origin of visible band emission from bacterial spores has remained somewhat mysterious. Since, by their nature, bacterial spores exist in a nearly dormant state with almost no detectable metabolic activity, they therefore do not contain much NADH or riboflavin.[89]It is now reasonably well known that fluorescence spectra of different types of bacteria are very similar, and that actual species-level identification based on these single excitation wavelength spectra is nearly unlikely.[39] The ideal biomarker molecule should have an intrinsic fluorescence spectrum that distinguishes it from other materials, and have sufficient fluorescence intensity to produce a strong signal. In general, shorter excitation wavelengths have higher energy and thus are likely to produce fluorescence in more types of material. DPA and CaDPA are unique biomarkers of bacterial spores and this thesis analyses the detail fluorescence properties of these components.

2.4.1 Dipicolinic acid and Calcium dipicolinate

The presence of DPA in bacterial spores was first reported by Powell in 1953.[90] Mostly in the form of CaDPA, it has been found to be the second largest component by weight in dried spores of *Bacillus megaterium*, coming after the totality of proteins, with RNA a close third.[91]

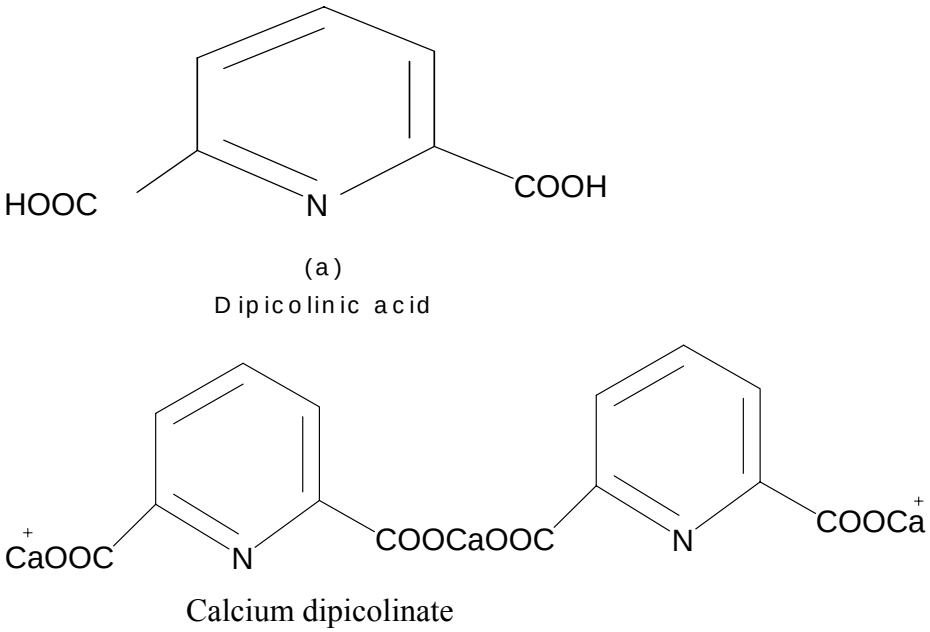

Figure 2.5: A chemical structure of DPA and CaDPA.

Figure 2.5 shows the chemical structure of DPA and CaDPA. It has been suggested that it is involved in spore dormancy,[92, 93] stability,[94] germination,[95] heat resistance[92, 93, 96, 97] and ultraviolet (UV) and gamma irradiation resistance.[98, 99] There is no direct evidence indicating the location of DPA, but some researchers hold that it is located primarily in the spore core,[100, 101] linked with proteins or amino acids, or intercalated with DNA. However, small amounts of DPA have been detected in exosporium.[57] Since it is unusual for a single organic compound to be present in such high quantities in a microorganism, it may be that DPA is linked to the evolutionary success of these endospore - forming organisms.

The absorption spectrum of CaDPA has its characteristic peaks at 269 and 277 nm with a shoulder at 263 nm.[102] Previous single fluorescence excitation–emission studies by Nudelman *et al.* and Bronk *et al.* for DPA, CaDPA, and DPA^- ion in aqueous solution indicated minimal or no fluorescence for solutions of DPA, but substantial fluorescence was found after irradiation at 255 nm.[103-105] CaDPA in aqueous solution has very weak fluorescence when excited at wavelengths near 300 nm.[103] Bronk *et al*. also observed an increase in fluorescence following the steps of suspending the bacterial spores in a water suspension, heating of the suspension to cause the release of DPA by the spores into the water and then exposing the supernatant to UV light.[105a]

DPA, is not absolutely necessary to the survival and formation of *Bacilus* spores, or for the survival of the bacteria in their spore form.[97, 106, 107] " However, dried (+DPA) spores are significantly more resistant to being killed by sunlight than dried isogenic (–DPA) spores".[108] In contrast, the (–DPA) spores are less sensitive in aqueous suspension, where they can be killed by 255 nm UV (in the UV-C range).[109] However, irradiation by 255 nm UV is unlikely in the natural environment, since extremely little UV-C penetrates to the earth's surface. The (– DPA) spores used in the present study were found to have significantly less core water than the comparable (+DPA) spores.[109] This led to reduced wet-heat resistance. This corresponds to the results of Gerhardt *et al*.[110] who found a positive correlation between core water content and heat sensitivity over several species of spores. For technical reasons, these experiments were done with lysozyme- sensitive spores, but it is suggested that this correlation is typical, if not universal.

There is convincing evidence that the calcium component in endospores along with the DPA, is almost totally concentrated in the core (also called protoplast).[111] The calcium is thought to be mostly complexed with the DPA. For example, when the spores are heated in suspension, the two components are released in equimolar amounts.[112] This suggestion is further supported by the measurement of the Raman band for CaDPA in lyophilized spores.[113] A recent investigation utilizing mid-IR absorption of the same (+DPA) and (–DPA) spores used in the present study also confirmed that most of the DPA is complexed with calcium.[114]

2.5 Quantum efficiency (QE)

The fluorescence QE of a compound is the ratio of photons emitted through fluorescence to photons absorbed by the compound**.** This quantity is not the same as the total number of emitted photons which escape a bulk sample divided by the total number of absorbed photons, although in many instances the two quantities are nearly equal. Practically, QE is important to assess the sensitivity of a proposed fluorometric determination of materials and the extent of interferences.[115]

Several techniques for measuring the QE have been described in the literature.[116-118] The majority of measurements have been made by reference to one of a few fluorescence standards for which absolute yields had been measured previously. Most emission quantum yield determinations found in the literature are relative measurements versus a standard whose QE has been accurately determined by absolute methods or is otherwise generally agreed upon. A direct measurement of the absolute QE of photofluorescence is exceedingly difficult to produce even a moderate degree of accuracy.[119] "The fluorescence intensity is generally measured directly only within a particular solid angle. Therefore, some assumption must be made to estimate the total emission over the total sphere surrounding the emitting object and the assumptions are never found to give satisfactory results".[119] As a consequence of the difficult and time consuming nature of absolute methods, only a very small number of compounds have been investigated in this manner.[120] Both methods have been reviewed by Demas and Crosby.[121]

"In their method, Parker and Rees[116] reasoned that if the total fluorescence intensities of two compounds could be measured on the same instrument with the same intensity of exciting light, and if the optical densities of the two compounds could be measured individually, then the ratio of the QEs could be calculated". If the QE of one compound was known from previous studies, it would then be easier to calculate the QE of compounds in question. This comparison method depends on knowledge of the QE of the reference compound and the conditions under which it was measured (as obtained from the literature or measured independently).

Relative measurements fall conveniently into two classes: optically dense and optically dilute methods. In the first case the light is almost completely absorbed and the luminescent spot is a near-point source, whereas in the latter most of the exciting beam emerges unattenuated. There are many difficulties associated with the optically dense methods. “The high concentrations necessary to obtain total absorption magnify the possibilities for concentration-quenching and reabsorption-reemission phenomena, although excitation at an absorption maximum reduces the required concentration level”.[121]

The determination of QEs using optically dilute solutions is the most common method currently used. Because of the popularity of this procedure we use this technique in this research. The optically dilute measurement rests on Beer’s law. The fluorescence intensity of an optically dilute homogeneous medium can be expressed as a linear function of the concentration of the fluorophores in that medium (the sum of the optical densities at the excitation and emission wavelength, everywhere is less than unity).[53, 121] The number of quanta emitted per unit time is proportional to the number of quanta absorbed per unit time multiplied times the fluorescence QE. We can write this as:

$$F = k\, I_0\, (1-10^{-A})\, QE \qquad (2.2)$$

Where F is the total fluorescence intensity, I_0 is the intensity of incident light; A is the absorbance of the solution, which is the product of the extinction coefficient of the molecule ε, the concentration of the molecules c, and the optical path length l ($A = \varepsilon cd$). k is a fraction of photons measured over photons emitted. If concentration c is low and hence D is small, then the equation (2.2) can be approximated as

$$F \sim 2.303\, (\varepsilon cd)\, k\, I_0\, QE \qquad (2.3)$$

Although the QE measurements of the optically dilute, homogeneous media is well understood, the QE measurements of biological samples are complicated due to their absorbing and scattering properties.[122]

The most reliable method for recording QE is the comparative method of Williams *et al*.,[123] which involves the use of well characterized standard samples with known QE values. Hence, a simple ratio of the integrated fluorescence intensities/optical densities of the two samples (recorded under identical conditions) will yield the ratio of the QE values. Since QE for the standard sample is known, it is trivial to calculate the QE for the test sample. The standard samples must be well characterised and suitable for such use.[53] Anthracene in ethanol is accepted as a standard because of the consistency of the results obtained by different authors.[122-124] We use anthracene in ethanol as the standard in this research.

The QE of the unknown samples are calculated using the standard samples which have a fixed and known fluorescence QE value, according to the following equation [53, 122]

$$QE_X = QE_{ST}\,[Grad_X / Grad_{ST}] * (n_X/n_{ST})^2 \qquad (2.4)$$

where the subscripts *ST* and *X* denote the standard and unknown sample respectively. *Grad is* the gradient (slope) of the plot of the integrated fluorescence at a selected excitation wavelength versus the absorption of the unknown sample as well as the standard sample, n_X and n_{ST} are the refractive indexes of the unknown sample and the standard sample respectively.

2.6 Principal Component Analysis (PCA)

PCA has been used for many years to analyze the large data sets typically generated in monitoring and classification studies that employ computerized instrumentation. Many techniques have been developed for dimensionality reduction."The experimental noise and other unknown dependencies of the experimental conditions may add to the confusion when attempting to understand and distinguish highly dimensional data".[125] PCA has found many applications in optical spectroscopy,[126, 127] and is a powerful tool for the determination of correlations and classification from high dimensional data.

The multivariate statistical method of PCA is very useful tool for examining relationships among several quantitative descriptors or variables.[128-130] "PCA is considered as a set of ordination techniques to reduce and summarize the data set. Ordination is a process by which the relative distances among objects are displayed graphically in the form of a scatter plot of objects on linear combinations of the original variables".[131] PCA therefore provides a means of quantifying the similarity or dissimilarity between objects.

The aim of PCA is to summarize as much of the information (variation) in the data set as possible in the fewest number of dimensions. "By establishing a new set of orthogonal axes, we could clearly explain the variations still present from the original data set ".[131] Hence, by plotting the points in the new set of axes, the significant effects within the data can be more easily visualized. One significant quality of PCA is that it reproduces all of the variance in the original data set in to new set of components.

The standard PCA scheme in spectroscopy begins with input data matrix, X, constructed from experimental spectra. The R (R≤ min (I, J)) component PCA model is defined in equation (2.5) where the data matrix X (I, J) representing a table of I samples and J variables is decomposed into a score matrix A (I, R) and a loading matrix B (J, R).

$$\boldsymbol{X = A.B^T} \qquad (2.5)$$

Where superscript T means transposed. In this way, the multidimensional data in *X* is resolved into a set of orthogonal components, R, whose linear combinations represent the original data. The score values contain information about the samples according to each of the extracted principal components. The loading vectors contain information about the variables. For spectral data, the loading vector represents the spectral profile of the spectral components. In the case of PCA of fluorescence data, the loading vectors are directly related to the fluorophores (chemical components) present and therefore form a basis for the interpretation of differences in the structures.[132,133] This might be useful for extraction of structural differences of the fluorescing chemical components in different samples. From this, the variables responsible for the dissimilarity of the samples can be predicted.[132]

As the first few PCs hold most of the variation in the original data set, they are retained to be used for further analysis. Any remaining noise in the original data set will be captured by the last few PCs which are excluded in the analysis.[134] Therefore PCA filters noise from a data set**.** The signal-to-noise ratio is highest in the first PC and decreases as subsequent PCs are calculated. The final result is that the non significant PCs typically encode more noise than spectral signal and their exclusion removes noise from the original data set**.** The PCs are extracted successfully in the following way. The first PC identifies the major axis in the data set which is the direction of greatest variance then removes it from the data. The major axis in the remaining data is then identifies the second PC, which is orthogonal and uncorrelated with the first PC. Therefore, variation is stacked onto the first few PCs and taken away from the non-significant components. Even though the total amount of variation in the new data set after PCA is identical to that of original data set, the variations is not uniformly distributed in the new data set: the first PC points in the direction of greatest variance, the second in the direction of next-greatest variance and so on.[131,135]

Each original variable (sample) in the data set contributes to each PC, though not to the same extent.[130] As a result, the PCs can identify sets of variables that show correlated patterns of variation (which may have a common underlying cause). PCs are statistically independent (may be not biologically) from each other and explains a different feature of the total variation.[131]

"The PCA routine finds the eigenvalues (variance accounted for) and eigenvectors (components) using the variance-covariance matrix or the correlation matrix".[135] PCA based on covariance matrices has the drawback that the PCs are highly sensitive to the unit of measurement. A general rule of thumb is to define PCs using the correlation matrix if the variables are of different types or use different unit of measurements.[135] To be safe from scaling errors, we use the correlation matrix in our analysis. The correlation matrix is a symmetric matrix. We then extract the eigenvalues and eigenvectors from the symmetric matrix, such that the eigenvalue for each axis of variation among individuals is maximized. Then the original data are projected onto the space defined by the extracted PCs to generate a set of PC scores for the original objects.[135]The scores for the various PC axes can then be plotted to get a new picture of the patterns of variation among objects in the original data set.[131,135]

When using PCA as a data reduction technique, one must ask how many PCs are necessary to extract. Since the variance of PCs is ordered, usually the first few PCs are used in data analysis. The question is how best to choose the PCs so that it adequately represent the data. The decision is ultimately arbitrary, but there are some common rules of thumb.[135, 136]

1. Retain PCs with eigenvalues (or variance) greater than one. The PCs with eigenvalue less than one explain less variance than any of the original variables. This criterion, proposed by Kaiser[137], is probably the one most widely used especially in the case of PCA on a correlation matrix.
2. In some cases[135], the first two components which represent over 90% of the total variation are chosen.
3. The Scree plot (simple plot of eigenvalues versus component number) can also be used to choose the number of significant components. After this curve starts to flatten out, the corresponding components may be regarded as insignificant.[135] If no clear break appears the decision remains largely subjective.

Often just two PCs are retained because they can be drawn easily as a two dimensional plot.[135, 136] If the first one to three PCs represent most of the variance in the new data set, then the PCA is considered to be a successful one whereas it is considered a failure if the variance is distributed at approximately evenly among several components.[138] A modern analysis of PCA has shown that no subset of the PCs can be predetermined to give the best description of the data.[134] One must judiciously select the right subset of PCs. The output of PCA is normally capable of grouping the samples. There are also many other ways (hierarchical and partitioning methods) to cluster the data using the obtain PCs.[139]

CHAPTER 3

3 MATERIALS AND METHODS

3.1 Materials

3.1.1 *Bacillus* spores

The following powdered spores used for this research were a generous gift from the US Army SBCCOM (Soldier and Biological Chemical Command). The five different preparations of the spores were: BC, BT, BG 1, BG2, and BG3. The three preparations of BG (1, 2 and 3) were produced in different laboratories and at different times. Samples were received in individual vials in a lyophilized form. None of the details of spore production methods were made available to us, except for the fact that none of the spores were treated with any special flow agent or anti-clumping compounds. All the spore samples were measured as they were provided. They were stored in the original culture tubes in a cabinet at room temperature. The spores were not washed unless stated and were used without any further preparation.

Both strains of BS spore used in this study are derivatives of strain 168. BS was a generous gift from Peter Setlow, Department of Molecular, Microbial and Structural Biology, University of Connecticut Health Center, Farmington, Connecticut, USA. The (+DPA) strain is PS832 and the (–DPA) strain in turn was derived in the laboratory of Peter Setlow as follows. First, a strain (FB85) was isolated that lacked the three major receptors needed for nutrient-initiated germination. The three mutations responsible were denoted as Δger3. These mutations ordinarily stop germination of the spores in response to nutrients but the spores germinate normally in response to Ca^{2+} and DPA.[109] The (–DPA) strain used in the present study was then derived from FB85. This strain was denoted FB108 and has an additional mutation (spoVF) in one of the two cistrons coding for an enzyme necessary for DPA synthesis in the mother cell during sporulation.[109] The spores of the resulting strain (FB108) are stable, and they can be isolated and purified.

3.1.2 Other biological samples

We also used different vegetative bacterial samples of *E.Coli*, BS, BC, and *Psedomonous aeroginosa*. These samples were isolated by Mr Craig Galilee at the School of Biological Sciences, University of Canterbury, NZ. These bacterial samples were stored on agar plates at -80^0C. The bacterial samples were thawed before cultures could be prepared. Cultures were prepared in nutrient broth (Oxoid Ltd, Basingstoke, Hampshire, England) as stated below:

Nutrient broth pH- 7.4 +/- 0.2
'Lab-lemco' powder 1.0 g
Yeast extracts 2.0 g
Peptone 5.0 g
Sodium chloride 5.0 g

The bacterial cultures thus prepared were kept in incubation at 30^0 C static for 24 hours. These cultures were then centrifuged at 10000 rpm for 10 minutes. The bacteria forms a pellet after being centrifuged allowing the broth to be separated from the bacterial fluorophores. The broth was then disposed of. The bacterial pellet thus formed was suspended in sterile saline water (0.9 % NaCl). This process was repeated for two washes.

Also used in this research were other biological samples such as *Aspergillus niger*, a fungal spore (Lenoir, NC, Lot 8553-10), pigweed (pollen), *Pinus radiata* (pollen) and ovalbumin (egg white and a growth medium ingredient) (Sigma, St. Louis, MO USA).

3.1.3 Chemicals

DPA in powder form was purchased from Sigma-Aldrich corp (St. Louis, Missouri, USA) and used as provided. $CaCO_3$, $Ca(NO_3)_2$ and $Ca(OH)_2$ were obtained from the Aldrich chemical company (Milwaukee, Wisconsin). Anthracene was obtained from BDH Chemicals Ltd (Poole England). Table 3.1 shows a list of samples used in this study.

Table 3.1: List of *Bacillus* spores, other biological samples and chemicals used in this research study.

Samples	**Source**	**Characteristics**
AFIP *Bacillus globigii* (BG1)	US Army	B.spore/Anthrax stimulant
Merck *Bacillus globigii* (BG2)	US Army	B.spore/Anthrax stimulant
Dugway *Bacillus globigii* (BG3)	US Army	B.spore/Anthrax stimulant
Bacillus subtilis (BS)	Peter Setlow	B.spore168(PS832) (+DPA)
Bacillus subtilis (BS)	Peter Setlow	B.spore168(FB108) (–DPA)
Bacillus cereus (BC)	US Army	B.spore
Bacillus thuringiensis (BT)	US Army	B.spore
Pig weed	Carolina Biological supply	Pollen
Pinus radiata	School of Biological Sciences, Canterbury University, NZ	Pollen
Aspergillus niger	School of Biological Sciences, Canterbury University, NZ	Fungal spore
Ova Albumin	Sigma, St. Louis, MO USA	Protein
Psedomonous aeroginosa	School of Biological Sciences, Canterbury University, NZ	Gram negative vegetative bacteria
E.coli	School of Biological Sciences, Canterbury University, NZ	Gram negative vegetative bacteria

Bacillus subtilis (BS)	School of Biological Sciences, Canterbury University, NZ	Gram positive vegetative bacteria
Bacillus cereus (BC)	School of Biological Sciences, Canterbury University, NZ	Gram positive vegetative bacteria
Dipicolinic acid (DPA)	Sigma-Aldrich corp	Chemical compound
Calcium dipicolinate (CaDPA)	Prepared in our Lab	Chemical compound
Tryptophan	Fisher Scientific, Fairlawn,NJ,USA	Amino acid
Anthracene	BDH Chemical, Ltd, Poole, England.	Chemical compound
Ethanol	Scharlau Chemie S.A., Barcelona, Spain	Solvent

3.2 Methods

3.2.1 Spore measurements on filter paper/quartz slide/water suspension

3.2.1.1 Introducing a new substrate technique (Filter paper)

A bacterial endospore is one of the most likely biological components in the environment (or of an aerosol). For the collection and measurement of fluorescence of bacterial spores and other microorganisms, one should determine the optimal substrate. The chosen substrates must have a very small fluorescent signal that does not overlap very strongly with the fluorescence of the sample to be investigated. We used different types of substrates depending on the aim of the experiment and measured the fluorescence of the samples. We did not find any difficulties in collecting the dry spores. Initially, it was anticipated that the measurement of wet samples would be the most problematic. The spore collection system must be able to

collect individual spores or large clumps of spores. It must also retain the spores for additional testing, to help identify the source of the spores.

Not all the samples were dry and the tape collection system was not suitable for collection and measurement of wet samples. We proposed a filter paper method to solve this problem. Initially, it was thought that the filter paper would also produce fluorescence in the same region as our samples. The most suitable filter paper (GF/A, Glass Microfibre Filters, Whatman, Kent, UK) was selected from many different types of filter papers in order to measure the fluorescence of wet samples as well as dry samples. The chosen filter paper had a minimal fluorescence signal that overlapped very little with the fluorescence of the biological samples and chemicals used in this research. The different types of sample collection methods are shown in the Table 3.2 below.

Table 3.2: Substrates used for collection and measurement of samples.

Substrates/method of collection	**Source/method**
Filter Paper	GF/A, Glass Microfibre Filters, Whatman, Kent, UK
Quartz Slides	Esco, New Jersy, USA
Quartz Cuvette	Suspension, Deionized Milli Q water and Ethanol

The filter paper with samples were positioned in the spectrofluorometer at a 45 degree angle to the incident light and fluorescence light in a 1 cm pathlength quartz cuvette. A diagram of the set-up is shown in Figure 3.1.

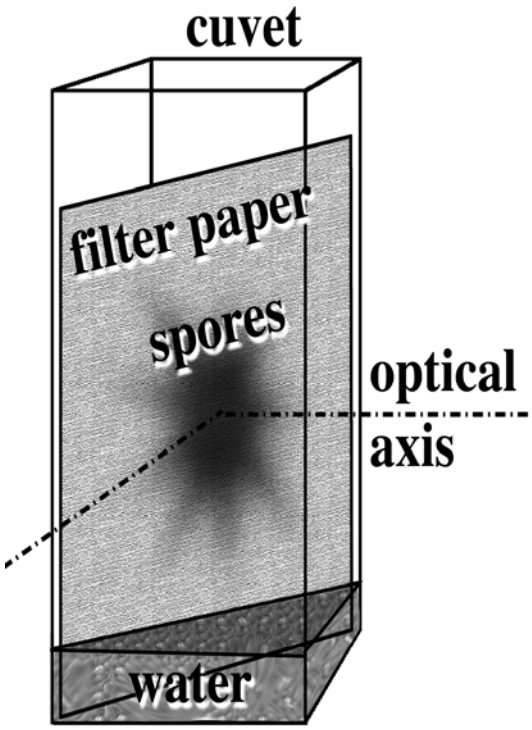

Figure 3.1: A drawing of the sample configuration for these experiments. The samples are placed on filter paper at 45 degrees in a 1 cm quartz cuvette.[140]

We also prepared quartz slides to measure the fluorescence in some experiments. The quartz slide has very low fluorescence compared to the filter paper. However it is not as convenient as the filter paper for some of the experiments. The quartz was cut into small slides of about 0.9 cm wide and 3 cm long. They were then coated with a very thin layer of low fluorescence adhesive (3M 4224 Adhesive, St. Paul, Minn, USA). The samples were fixed to a quartz plate and the coated slide was placed diagonally in a quartz cuvette. The cuvette was positioned in the spectrofluorometer so that the front face of the quartz slide (with the samples) was positioned at approximately a 30 degree angle to the excitation optical axis and at approximately a 60 degree angle to the emission optical axis. This procedure reduces reflected light entering the emission monochromator (see Figure 3.4).

3.2.2 Fluorescence measurements and spectral visualization

The fluorescence of each of the samples and chemicals was measured on a spectrofluorometer (SLM 8000C, Urbana, IL, USA) as shown in Figure 3.2. The spectrofluorometer consists of:

- a light source (450-W ozone-free xenon arc lamp)
- a monochromator for selecting the excitation wavelengths
- a sample compartment
- a monochromator for selecting the emission wavelengths
- a detector which converts the emitted light to electric signal
- a unit for data acquisition and analysis

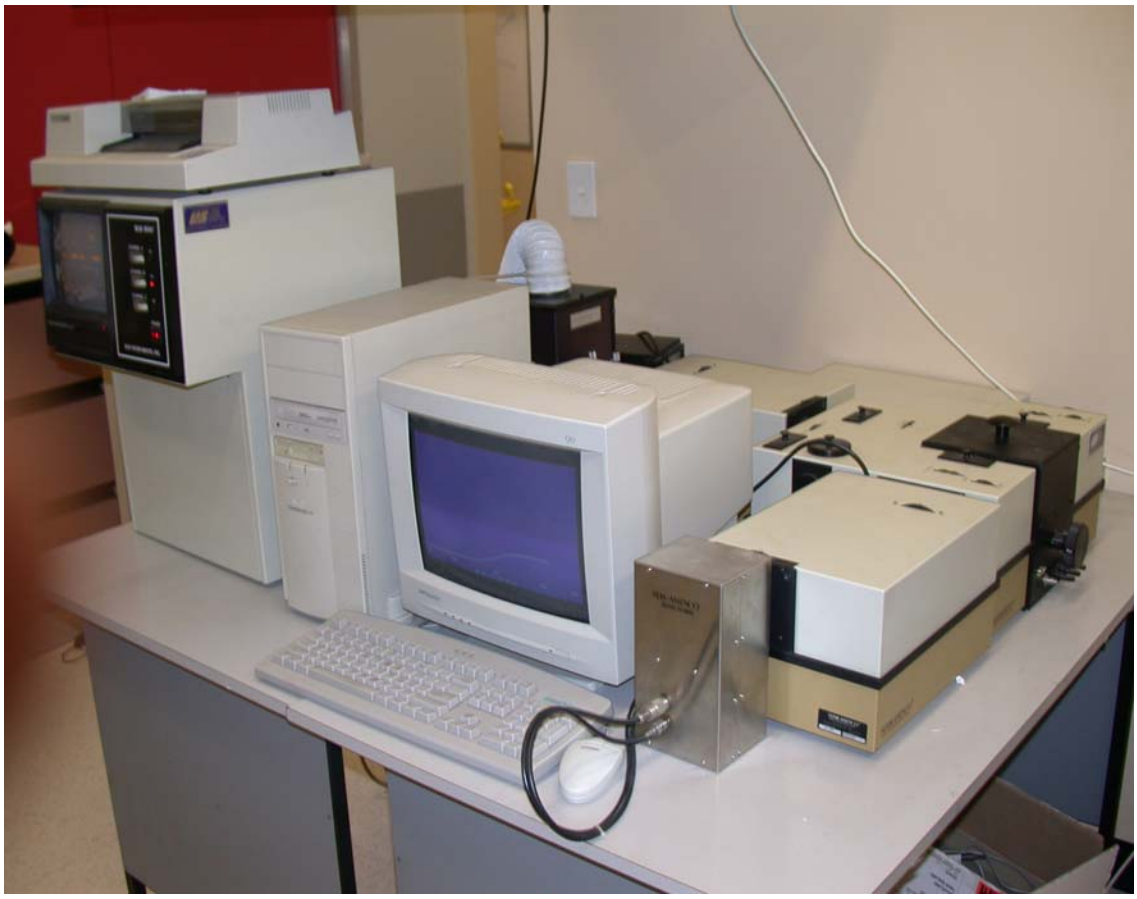

Figure 3.2: The SLM 8000C Spectrofluorometer

The xenon arc lamps are generally useful because of their high intensity at all wavelengths ranging from 250 nm. The instrument shown in this figure equipped with monochromators to select both the excitation and the emission wavelengths. The excitation monochromator contains concave gratings, which decreases stray light (i.e, light of wavelengths different from the chosen wavelength). The set up was with single monochromators with eagle design and a stigmatic concave diffraction grating of 900 lines/mm, blazed at 300 nm for excitation and at 400 nm for the emission. The emission monochromator is the same as excitation monochromator except that it includes one holographic grating which further decreases stray light. Both monochromators are motorised to allow automatic scanning of wavelength. The slits on both monochromators were set for a 4 nm bandwidth.

We used light from a mercury lamp to calibrate the monochromators. The light is allowed to directly enter the cuvette holder and locate dominant mercury lines using the emission monochromator and ensure that the line is assigned the correct wavelength. After calibration of the emission monochromator, the excitation monochromator was calibrated against this standard, with some of the excitation light scattered into the emission monochromator.

The excitation wavelength used to create each emission spectrum was varied in 10 nm increments from 200 to 600 nm. The emission spectrum was stepped every 1.0 nm from 10 nm longer than the excitation wavelength to 10 nm shorter than twice the excitation wavelength. All emission spectra presented in this thesis were acquired with identical instrument parameters. Table 3.3 outlines the multiple excitation wavelengths and the range of emission wavelengths used to acquire the fluorescence fingerprint of the samples being studied.

Table 3.3: Multiple excitation wavelengths and the range of emission wavelengths used to collect the EEM.

Excitation Wavelength (nm)	Emission Range of Wavelength Measured (nm)	Excitation Wavelength (nm)	Emission Range of Wavelength Measured (nm)	Excitation Wavelength (nm)	Emission Range of Wavelength Measured (nm)
200	210-390	340	350-670	480	490-700
210	220-410	350	360-690	490	500-700
220	230-430	360	370-700	500	510-700
230	240-450	370	380-700	510	520-700
240	250-470	380	390-700	520	530-700
250	260-490	390	400-700	530	540-700
260	270-510	400	410-700	540	550-700
270	280-530	410	420-700	550	560-700
280	290-550	420	430-700	560	570-700
290	300-570	430	440-700	570	580-700
300	310-590	440	450-700	580	590-700
310	320-610	450	460-700	590	600-700
320	330-630	460	470-700	600	610-700
330	340-650	470	480-700		

The measured fluorescence spectra were transferred to a Windows XP computer where they were analysed with *Mathematica* (Wolfram research, Urbana, IL). For visualization of the spectra by EEM, we divide the wavelengths of emission spectra by the wavelength of excitation spectra. The range of each spectra is then approximately 1.0 to 2.0. The analysis is not conventional[30] and allows us to use the full range of information from the measured data. It spreads out the important areas for better visualization. *Mathematica* then interpolates between the matrices of emission spectra to calculate the contour plot. Although this method is unconventional, the variable step size weights each spectrum equally. Figure 3.3 shows the conventional and modified presentation of fluorescence profile of tryptophan solution.

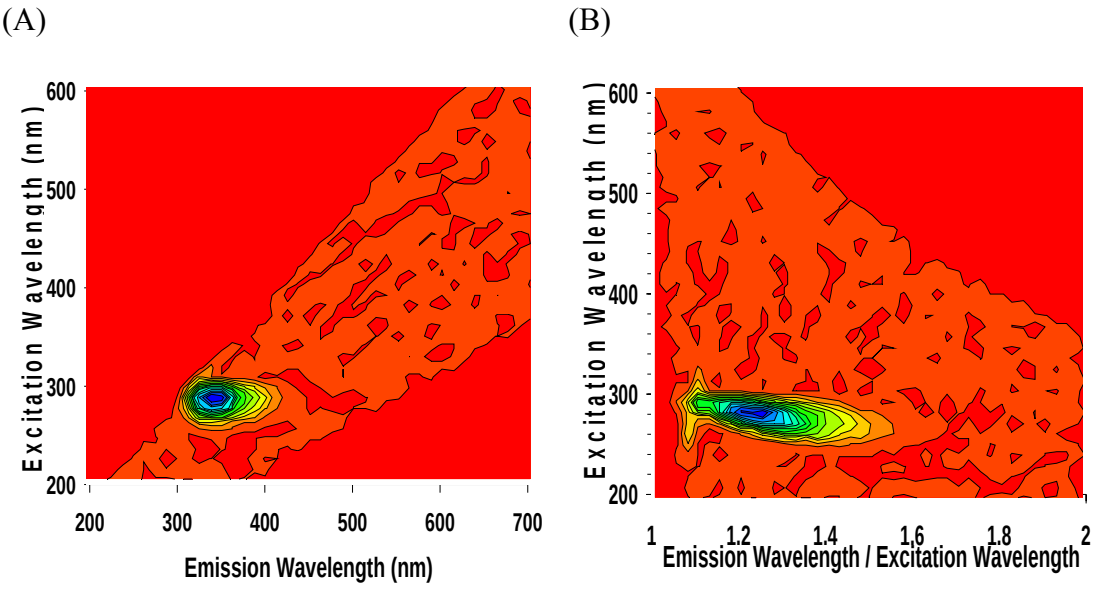

Figure 3.3: The fluorescence profile of tryptophan in water solution (A) conventional and (B) modified plots are displayed. In both cases, the contour represents equal changes in the fluorescence intensity and the peak intensity is normalized to one. The greatest intensity is blue and the least intensity is red.

Fluorescence emission is observed at wavelengths longer than the excitation wavelength. Typically the emission measurement is restricted to be at a wavelength shorter than twice the excitation wavelength. Generally, the second order transmission

through the monochromator dominates the fluorescence signal at wavelengths longer than twice the excitation wavelength.

3.2.3 Principal Component Analysis

The PCA is used to find the principal directions of variation in the fluorescence data. Relations between spore samples are thereby mapped out. It is then possible to draw similarity maps or score plots of the samples (variables) and to get spectral patterns.[141] Two neighbouring points on a PCA score plot describe two similar spectra. The spectral patterns exhibit the fluorescence bands that explain the similarities observed on the maps. They are similar to spectra and can be used to derive structural information at the molecular level. PCA is carried out on the measured fluorescence spectra using the R software package (GNU project, Version 2, Boston, MA, http://www.gnu.org).

The first step in PCA was to generate a matrix from the obtained fluorescence. We have written an algorithm to read and execute the data files obtained from fluorescence measurements. We decided to limit the data matrix to the fewer excitation wavelengths that showed reasonable fluorescence signals from the samples. Prior to analysis the column vectors containing the emission spectra at excitation wavelengths selected for evaluation were cropped to discard the tails and then concatenated into a vector. We have written a program code to select the data points in the emission range from 30nm longer than the excitation wavelength to 160 nm longer than the excitation wavelength (e.g. if 300 nm is the excitation wavelength, the emission was measured from 330 to 490 nm). Measurement over a 160 nm emission ranges permitted detection of the major fluorescence peaks of the sample fluorophores. Our spectrofluorometer measured the emission spectrum at 1nm intervals. Therefore we obtained a total of 160 data points for each excitation wavelength.

The next step in the PCA was to formulate a correlation matrix of the samples (variables) measured. The written algorithm will automatically make a correlation matrix from the measured fluorescence data according to the selection of excitation and emission wavelengths. The procedures to carry out a PCA on the measured set of fluorescence data involve finding the eigenvectors and eigenvalues of the correlation matrix. We also considered smoothing the data. After obtaining the eigenvectors and eigenvalues we transformed the original dataset by projecting the original points onto new axes. It is known that the eigenvalues give a measure of the variance for each corresponding eigenvector.[138] The percentage of variance accounted for by each of the components was also calculated.

The PCA was applied to see how many PCs were needed to express the information contained in the variables. As explained in Chapter 2, we selected the number of components based on either the Kaiser's selection criteria or scree plot.[137]

3.3 Multi wavelength fluorescence studies of major bacterial spore chemical components

DPA solutions (ca. 200 microMolar) were prepared freshly each day with deionized water. A ten-fold excess of DPA was added to the water and the concentration was determined by the limited solubility of the DPA. The concentration was measured from the absorption spectrum (ε_{270nm} = 9450 $M^{-1}cm^{-1}$). Calcium dipicolinate (CaDPA) was prepared by mixing the solution of DPA with excess of various calcium compounds. We measured the UV absorption spectrum of each sample and confirmed the formation of CaDPA by observing its characteristic absorption spectrum.[102] The CaDPA concentrations were ca. 9.6 microMolar, measured from the absorption spectrum ($\varepsilon_{269\ nm}$ = 138000 $M^{-1}cm^{-1}$). Figures shown here were measured from CaDPA made with $CaCO_3$, although, identical spectra were measured with the other salts. We also verified CaDPA production by repeating all the measurements with CaDPA prepared according to published methods.[15, 142] Again, the identical absorption and fluorescence spectra were measured. Absorption measurements were

made at room temperature with a Cintra 40 spectrophotometer (GBC, Dandenong, Vic, Australia) with 1 cm path length quartz cuvettes.

Initially, we measured the fluorescence emission spectrum of a saturated DPA solution at room temperature. We confirmed that this solution had no measurable fluorescence. Then the solution in the 1 cm quartz cuvette was exposed to broad-band UV light through a distance of 20 cm for 15 minutes. The full UV and visible spectrum of light from a 450 W ozone free xenon arc lamp (the fluorometer lamp) was used. We measured the Energy fluence to be approximately 80 J/cm^2 (240 J energy) with the 15 minute exposure. Immediately after exposure, the fluorescence spectra of the exposed solutions were measured. The exposed solution was then allowed to stand for two hours in the dark before another measurement was made. We also measured the fluorescence emission spectrum of the same concentration of DPA dissolved in ethanol.

Additional sets of DPA solutions with different calcium compounds were prepared and the absorption spectra and the fluorescence spectra of each sample of calcium dipicolinate were measured. Each of these solutions was then exposed to the UV lamp for 15 minutes and the absorption and fluorescence spectra were measured.

Pieces of filter paper were cut about 1 cm wide and 3 cm high. The solutions of DPA and CaDPA were pipetted onto the filter paper. The filter paper had a minimal fluorescence signal that did not overlap significantly with the DPA or CaDPA fluorescence. By multiple cycles of pipetting the solution onto the filter paper and allowing the filter paper to dry, we made wet and dry samples of solid or wet paste DPA and CaDPA sufficiently concentrated for fluorescence measurements. The filter paper with the wet or dried sample was placed at 45 degrees to the incident and fluorescence light in a 1 cm path length quartz cuvette and placed in the spectrofluorometer.

We measured the variation of fluorescence intensity of the UV exposed CaDPA solution as a function of time immediately after the exposure. The sample was exposed to the UV arc lamp for 15 minutes. A different UV arc lamp (150 W) was used to expose the sample in this experiment and the rest of the experiments in this

research study. We measured the energy fluence to be approximately 25 J/cm^2 (80 J). It was then placed in the fluorometer and the emission was measured by repeatedly scanning 409 to 411 nm in 0.1 nm steps using a 305 nm excitation light. Each scan took 10 s. We also performed experiments with these compounds at different doses of UV exposure. We measured the fluorescence at different time intervals (5 min, 15 min, 20 min, 30 min, 1h etc).

We also measured the enhanced fluorescence intensities after we exposed the CaDPA solution for 15 minutes at different wavelengths of UV light between 250 nm and 330 nm at 10 nm interval. We measured the enhanced fluorescence emission at 305 nm excitation wavelength (This particular measurement was done by Johannes Tran Gia with my assistance).

The diluted tryptophan solution were prepared in Milli Q deionized water with concentration of 5 mg in 1000 ml. The fluorescence measurements were made at room temperature in a conventional geometry at 90 degrees to the excitation light. By multiple cycles of pipetting the tryptophan solution onto the filter paper and allowing the filter paper to dry, we made the dry tryptophan samples. The fluorescence of the dried sample was measured at 45 degree geometry. Both of these samples were exposed to UV irradiation for 15 minutes. The exposed solution was then allowed to stand for two hours in the dark before the measurement was made.

3.4 Multi wavelength fluorescence studies of *Bacillus* spores

3.4.1 Reversible changes in fluorescence of bacterial endospores due to hydration/drying

3.4.1.1 Spore fluorescence

Two different stocks of BG spores were used in this experiment: BG1 and BG2. The spores were not washed and were used without any further preparation. The filter paper was cut about 1cm wide and 3 cm high. A wire loop was used to obtain a small number of lyophilized spores from their storage container and smear them on to the

filter paper. Initially, the fluorescence emission spectrum of a sample in dry form was measured. Then a small amount of sterile deionized water was pipetted to the bottom of the cuvette. The water level was only a millimeter or two in the cuvette, well below the position at which the cuvette that was probed in the fluorometer (see Figure 3.1). This was done to minimize the number of spores that might wash off the filter paper. The sample was allowed to sit undisturbed for 15-20 minutes at room temperature to allow the water to wick up the filter paper and hydrate the spores. We then measured the fluorescence emission spectrum of the wet sample. Then the filter paper with spores was dried in air for 24 hours. The emission spectrum of the re-dried spores was then measured.

3.4.1.2 Principal Component Analysis

In this experiment we were interested in looking at the fluorescence spectral signatures due to drying, hydration and subsequent dehydration (air dried) conditions. We tried different combination of excitation wavelengths to lead us to select five different excitation wavelengths: going from 300 nm to 500 nm in steps of 50 nm. These five excitation wavelengths contain the critical information to understand and distinguish BG spore samples in dry and wet environments. The selected wavelengths' regions elicited reasonable fluorescence signals from the BG spores. In this case with 200 data points (emission range) for each excitation wavelength, we had 1000 data points for each of the BG samples. With 27 samples, the data matrix consists of 27 X 1000 data points. The next step was to formulate a correlation matrix. The PCA was applied to see how many PCs were needed to express the information in the BG samples. We selected the number of components based on the table below. There were 27 PCs. Only seven components are mentioned in Table 3.4 below

Table 3.4: First seven eigenvalues for the correlation matrix, reversible fluorescence BG data.

Principal Components	PC1	PC2	PC3	PC4	PC5	PC6	PC7
Eigenvalue/ Variance	23.89 (20.93)	2.57 (4.39)	0.30 (0.86)	0.10 (0.42)	0.05 (0.20)	0.04 (0.07)	0.02 (0.05)
Variance %	88.48 (77.52)	9.52 (16.26)	1.11 (3.19)	0.36 (1.56)	0.19 (0.74)	0.13 (0.26)	0.06 (0.19)
Cum %	88.48 (77.52)	98.00 (93.78)	99.11 (96.97)	99.47 (98.53)	99.66 (99.27)	99.79 (99.53)	99.85 (99.72)

The combination of PC1 and PC2 explains 98.00% of the total variance of the original data set and the eigenvalues of these two components are greater than or equal to one. This means that the data are well described by these first two PCs. Many analysis schemes retain a small number of PCs, e.g, only those with eigenvalues greater than one. This selection rule, proposed by Kaiser [137] is often used. On the other hand, a more modern analysis of PCA has shown that no predetermined subset of the PCs can arbitrarily best describe the data.[134] One must judiciously select the right subset of PCs. In the analysis presented in this research we use only first two PCs because they account for approximately 90 % of the variance and provide good separation of the samples. This selection is also follows Kaiser's rule.

We also did the analysis using six excitation wavelengths from 280 nm to 430 nm in steps of 30 nm to see the effect of excitation wavelengths and the range of emission wavelengths in the analysis. In this case and hereafter with 160 data points for each excitation wavelength, we had 960 data points for each of the samples. With 27 BG samples, the data matrix consists of 27 X 960 data points The PCs and the corresponding eigenvalues are given in brackets in Table 3.4. We could not notice any major difference in the analysis (See Figure 4.28 in the results section)

We performed the similar experiments with BC spores under similar conditions except that the spores were redried in air for seven days instead of 24 hours. We selected six equally spaced excitation wavelengths for PCA: 280, 310, 340, 370, 400 and 430 nm.

3.4.2 Distinguishing wet Bacillus spore species from dry spores

3.4.2.1 Spore fluorescence

In this study we used BC and BT spores in addition to the two different stocks of BG spores used in the previous experiment in Section 3.4.1. All the spore samples were smeared on different pieces of filter paper and measured as they were provided and in a dry state. As in the previous experiment, the fluorescence emission spectrum of wet samples was also measured. The measurements were repeated four times with new spore samples on pieces of filter paper. There were 24 total measurements: 12 dry measurements and 12 wet measurements (four dry and four wet measurements with each of the spore species).

3.4.2.2 Principal Component Analysis

We applied PCA on the 24 sample measurements for the identification of the PCs, to see if they were able to discriminate the dry spores from the wet spores. In this study, we selected six different excitation wavelengths for spectral analysis: 280, 310, 340, 370, 400 and 430 nm. Since spectral differences among various spores are greater at these wavelengths, they facilitate analysis of differences among spore species in wet and dry environments. Fluorescence may be emitted by several chemical components of the spores in the excitation range from 280 to 430 nm. The PCA of these fluorescence spectra were done as indicated in the above section.

Table 3.5: First seven eigenvalues for the correlation matrix, fluorescence data of dry and wet *Bacillus* spores.

Principal Components	PC1	PC2	PC3	PC4	PC5	PC6	PC7
Eigenvalue (Variance)	22.19	6.48	2.31	0.53	0.19	0.11	0.09
Variance %	69.32	20.25	7.22	1.66	0.58	0.34	0.26
Cum %	69.32	89.57	96.79	98.45	99.03	99.37	99.63

The combination of PC1, PC2 and PC3 explains 96.79% of the total variance with eigenvalues greater than unity, satisfying Kaiser's criteria.[137]

3.4.3 *Bacillus globigii* spores in different hydration conditions

3.4.3.1 Spore fluorescence

The BG spores were suspended in sterilized Milli-Q deionized water in a quartz cuvette and measured in a more conventional manner at 90 degrees to the exciting light. Spores were suspended for at least 15 minutes before the measurements were made to allow the spores to hydrate fully. We required approximately two hours to make a full measurement. The same measurements were repeated with different *Bacillus* spores and in the time intervals of four hours and six hours to see if there were any major changes in the fluorescence spectrum. We also measured the fluorescence of sterilized Milli Q deionized water in a quartz cuvette. There was no measurable fluorescence other than the familiar Raman peak of water.

3.4.3.2 Principal Component Analysis

We applied PCA on the 27 samples of BG spores for the identification of the PCs, which were expected to be able to discriminate the dry spores from the wet spores and spores in suspension. Again, we selected six excitation wavelengths, 280, 310 340, 370, 400 and 430 nm for spectral analysis. Since spectral differences among spores

are greater in these wavelengths, the above wavelengths were selected to analyze different spore species in the different environments, dry spores, wet (hydrated) spores on filter paper and spores in suspension.

Table 3.6: First seven eigenvalues for the correlation matrix, fluorescence data of dry, wet and aqueous BG spores.

Principal Components	PC1	PC2	PC3	PC4	PC5	PC6	PC7
Eigenvalue (Variance)	18.163	7.987	0.406	0.187	0.072	0.044	0.029
Variance %	67.26	29.58	1.50	0.69	0.27	0.16	0.11
Cum %	67.26	96.84	98.342	99.035	99.303	99.465	99.572

The combination of PC1 and PC2 explains 96.84% of the total variance of the original data set, and the eigenvalues of these two components are greater than unity and are used in the analysis.[137]

3.4.4 Effect of Autoclaving and washing on spore fluorescence

3.4.4.1 Spore fluorescence

Endospores of BG2 were suspended in Milli Q deionized water and divided into two portions, one of which was prepared for washing and autoclaving and the other set for use as a reference for comparison. The samples prepared for washing and autoclaving were rinsed and centrifuged after which the supernatant was removed and discarded. The centrifugation using the centrifuge (Spectrafuge, TLS total Lab Systems Ltd, Edison,NJ,USA) was done at 10000 rpm for 10 minutes for three times to further clean the samples to remove the growth medium or fragments of the vegetative cells. The resulting pellet sample was resuspended in water and divided further into two portions, one of which was prepared for autoclaving and the other set for without autoclaving.

Samples prepared for autoclaving were transferred to a vented tube and autoclaved for 20 min at 121 ^{0} c (Astell Scientific, Kent, UK). One drop of each of these three set of samples was placed onto a filter paper and quartz slide. A total of 18 samples (six each, three samples on filter paper and three samples on quartz slide) were prepared for fluorescence measurements and subsequent analysis.

3.4.4.2 Principal Component Analysis

We again selected six equally spaced consistent excitation wavelengths for PCA: 280, 310, 340, 370, 400 and 430 nm.

Table 3.7: First seven eigenvalues for the correlation matrix, fluorescence data of autoclaved and washed BG2 spores

Principal Components	PC1	PC2	PC3	PC4	PC5	PC6	PC7
Eigenvalue (Variance)	10.37	6.52	0.80	0.13	0.08	0.03	0.02
Variance %	57.76	36.22	4.44	0.72	0.44	0.16	0.11
Cum %	57.76	93.98	98.42	99.14	99.58	99.74	99.85

The combination of PC1 and PC2 explains 93.98% of the total variance and the eigenvalues of these three components are greater than one and used in the analysis[137]

3.4.5 Principal Component analysis of fluorescence spectra to distinguish *Bacillus* spores in water suspension

3.4.5.1 Spore fluorescence

In this experiment we used BG, BC and BS (+DPA) spores in water suspension. There were 12 total measurements (four measurements each). The concentration of samples in each experiment was different. Each sample was suspended in water for 15 minutes before measurements were made.

3.4.5.2 Principal Component Analysis

The PCA of these fluorescence spectra were done as indicated in the above section. Therefore, in this study we again selected six different excitation wavelengths, 280, 310, 340, 370, 400 and 430 nm, for spectral analysis. The number of components to investigate the relationship between the original variables was chosen based on the table 3.8 below.

Table 3.8: First seven eigenvalues for the correlation matrix, fluorescence data of *Bacillus* spores in water suspension.

Principal Components	PC1	PC2	PC3	PC4	PC5	PC6	PC7
Eigenvalue (Variance)	9.14	1.41	1.22	0.07	0.06	0.03	0.02
Variance %	76.16	11.75	10.16	0.58	0.50	0.25	0.16
Cum %	76.16	87.91	98.07	98.65	99.15	99.40	99.56

The combination of PC1, PC2 and PC3 explains 98.07% of the total variance of the original data set and the eigenvalues of these three components are greater than one.[137]

3.5 Multi wavelength Fluorescence studies on *Bacillus* spores under enhanced UV irradiation

3.5.1 Fluorescence studies of *Bacillus subtilis* spores with and without (lack) of dipicolinic acid

3.5.1.1 Spore fluorescence

In this study, we compared the results of BS spores, one with DPA (+DPA) and one having a marked depletion of DPA (–DPA). Both strains of BS spores used in this study are derivatives of strain 168. The preparation method of these spores was explained clearly in the second paragraph of Section 3.1.1. Fluorescence emission of

the samples in aqueous suspension was measured. Then each of these solutions was exposed to the broad band UV at a distance of 20 cm for 15 minutes (80 J) and the absorption and fluorescence spectra were measured under similar conditions. Each of the measurements was made at least three times, each time with a newly prepared sample. One of each strain samples were also exposed to UV for further 15 minutes (additional 80 J).

3.5.1.2 Principal Component Analysis

We used PCA to investigate the association of the spectral properties of tryptophan, DPA and CaDPA in the two strains of BS spores very precisely before and after UV irradiation. In this study again we selected five different excitation wavelengths, 280, 310, 340, 370 and 400 nm and 430 nm for spectral analysis.

Table 3.9: First seven eigenvalues for the correlation matrix, fluorescence data of the (+DPA) and (- DPA) strain of BS spores in suspension.

Principal Components	PC1	PC2	PC3	PC4	PC5	PC6	PC7
Eigenvalue (Variance)	6.80842	4.0844	0.8492	0.0894	0.0523	0.0459	0.0309
Variance %	56.73	34.03	7.0766	0.7450	0.4358	0.3825	0.2575
Cum %	56.73	90.76	97.836	98.581	99.017	99.399	99.657

The combination of PC1 and PC2 explains 90.76% of the total variance of the original data set and the eigenvalues of these three components are greater than one.[137]

3.5.2 Identifying components of UV-Vis fluorescence of *Bacillus* spores

The BG1 spores were suspended in deionized water in a quartz cuvette. The absorbance and the fluorescence were measured from 200 to 600 nm. CaDPA crystals were prepared with deionised water as described by Ghiamati *et al.*[18] The resulting solution was cooled slowly to allow crystallization. The CaDPA crystals were

collected by vacuum filtration and recrystallized with hot distilled water. We did not know the exact amount of CaDPA and tryptophan inside the BG spores. Therefore, we tried different weighted amounts of tryptophan and CaDPA. The sample set covered a representative range of concentrations and mixtures with the sample mixtures (the amount of CaDPA is about 10 fold in excess in weight of the amount of tryptophan) being made up by mixing weights of CaDPA and tryptophan. From our earlier studies, we found that dry or wet paste CaDPA fluoresces strongly around 300 nm excitation and the emission is around 400 nm. Tryptophan fluoresces at around 290 nm excitation and emission is around 340 nm. We measured the absorbance and fluorescence spectra of this simulant mixture in aqueous solution and the fluorescence spectra in a wet paste on a filter paper. We compared the 2-D fluorescence matrix of this simulant with the 2-D fluorescence matrix of BG spores in suspension. All these measurements were done at room temperature. Then each of these samples was exposed to broad band UV for 15 minutes and the fluorescence spectra was made.

3.5.3 Distinguishing bacterial spores from other biological samples using fluorescence

3.5.3.1 Sample fluorescence

UV-irradiation experiments on bacterial spores and other biological samples (except vegetative bacteria) were carried out by exposing the spore suspensions in milli Q deionized water in a quartz cuvette. The vegetative bacteria were harvested and suspended in a physiological saline solution (NaCl 0.9%). We exposed the samples through a distance of 20 cm at room temperature for a period of 15 minutes (80 J). All the samples were irradiated under similar conditions. Fluorescence measurements have been performed on controls and on irradiated samples (at comparable doses). Each sample was irradiated only once for 15 minutes. The irradiated samples were kept for 15 minutes in the dark before the fluorescence measurements were made. The absorbance and fluorescence spectra were recorded at room temperature.

3.5.3.2 Principal Component Analysis

We applied PCA to classify the bacterial spores from other biological samples after broad band UV irradiation for 15 minutes in suspension. In this study, we selected six different excitation wavelengths, 300, 320, 340, 360, 380 and 400 nm, for spectral analysis. Fluorescence may be emitted by DPA and CaDPA of the spores in these ranges of excitation wavelengths (after UV irradiation, the tryptophan-like fluorescence was suppressed), we chose the above wavelengths to analyze the fluorescence spectra of UV irradiated *Bacillus* spores and other biological samples. The PCA was done as mentioned in the above sections. We chose the number of components to investigate the relationship between the original variables based on the table below. There are 28 components in the PCA output. Only seven components are mentioned in Table 3.9 below.

Table 3.9: First seven eigenvalues for the correlation matrix, fluorescence data of UV irradiated *Bacillus* spores and other biological samples.

Principal Components	PC1	PC2	PC3	PC4	PC5	PC6	PC7
Eigenvalue (Variance)	16.82 (18.13)	4.13 (3.21)	2.68 (2.37)	1.18 (1.28)	0.80 (0.86)	0.74 (0.49)	0.51 (0.33)
Variance %	60.05 (64.75)	14.73 (11.46)	9.58 (8.46)	4.23 (4.57)	2.87 (3.07)	2.64 (1.75)	1.81 (1.18)
Cum %	60.05 (64.75)	74.78 (76.21)	84.36 (84.67)	88.59 (89.24)	91.46 (92.31)	94.1 (94.06)	95.91 (95.24)

The combination of PC1, PC2 , PC3 and PC4 explains 88.59% of the total variance and the eigenvalues of these three components are greater than one and used in the analysis[137]. To be consistent with other experiments, we also did the analysis using six excitation wavelengths from 280 nm to 430 nm in steps of 30 nm to see the effect of excitation wavelengths in the analysis. The PCs and the corresponding eigenvalues are given in brackets in Table 3.9. We could not notice any major effect in the analysis (see results section).

3.6 Fluorescence quantum efficiency of *Bacillus* spores in suspension and its probable major chemical components

Solvents for the fluorescent measurements used in this study were deionized milli Q water and benzene-free spectroscopic grade absolute ethanol. The fluorescence standard used for this research work was anthracene. Anthracene has a molar extinction coefficient of 9,700 $M^{-1}cm^{-1.}$ at 356.25 nm [143] and a fluorescence QE of 0.27 in ethanol.[120] Solutions of anthracene were prepared by weighing dry anthracene powder in a measured volume of spectrograde ethanol. The UV-vis absorbance spectrum of anthracene in ethanol was recorded with varying concentrations in a scanning range 250-600 nm using the spectrometer in a conventional method and a quartz 10 mm pathlength cuvette. Care was taken to keep the concentration of anthracene below that giving an optical density (OD) in the wavelengths measured is less than 0.2 so that the fluorescence intensity is approximately uniform throughout the solution. We measured the fluorescence of ethanol and fluorescence intensities of the prepared anthracene solutions (concentration range 0.001mM - 0.1mM).

The QE of the solutions was determined by placing the detector at right-angles to the direction of excitation light. The fluorescence spectrum of the solution was measured in the same 10 mm fluorescence cuvette. We also measured the absorption of the ethanol and used this as a baseline that was subtracted from the absorption of the anthracene solutions. The index of refraction for ethanol was taken to be 1.36 (*CRC Handbook of Chemistry and Physics*, Cleveland, Ohio, USA).The integrated fluorescence intensity was recorded from the corrected fluorescence spectrum. This procedure was repeated for different concentrations of anthracene in ethanol. The concentration of the fluorescent solutions was approximately in the order of 10^{-5}-10^{-6} M. The fluorescence spectrum was measured with excitation wavelengths of 320, 340, 350, 356.2 and 360 nm. The emission spectrum was measured from 10 nm longer than the excitation wavelength to 10 nm shorter than twice the excitation wavelength. The integrated fluorescence was measured as a function of the concentration. The analogue to digital converter in the fluorometer changed the photomultiplier output voltage to “counts”, and thus we assumed all the counts over the emission wavelength range. The integrated fluorescence intensity versus

absorbance graph was drawn at different excitation wavelengths within the linear part of the spectrum. We found a straight line with slope m.

Initially, the fluorescence emission spectrum of a saturated DPA solution at room temperature was measured. We confirmed that this solution had no measurable fluorescence. Then the solution in the 1 cm quartz cuvette was exposed to broad-band UV light for 15 minutes. The full UV and visible spectrum of light from a 150 W ozone free xenon arc lamp was used. We measured the UV energy fluence to be approximately 25 J/cm^2 over the 15 minute exposure. We measured the absorbance and fluorescence with different concentrations of DPA solution.

CaDPA was prepared separately with deionized water as stated elsewhere in this section. We measured the UV absorption spectrum of each sample and confirmed the formation of CaDPA by its characteristic absorption spectrum.[102] As above, the absorbance and fluorescence with different concentrations of the CaDPA solution was measured. Then we exposed the CaDPA solution to broad band UV light, as mentioned before in the case of DPA solution.

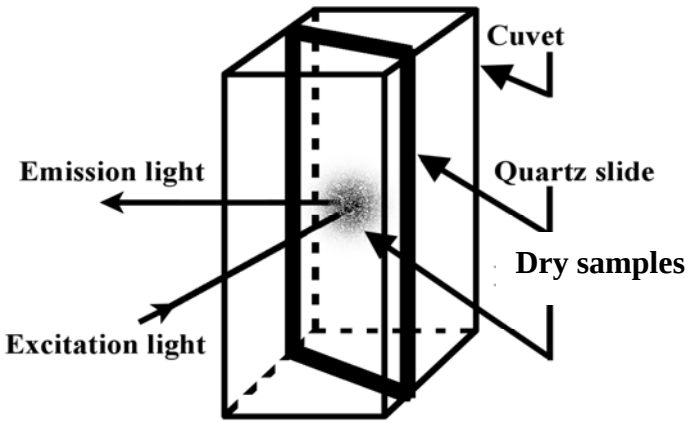

Figure 3.4: Schematic diagram of the dry samples mounted to the quartz slide and the optical geometry used in the fluorometer.[144]

In the measurement of dry DPA and CaDPA, the quartz slides with samples were placed diagonally in the quartz cuvette and placed in the spectrofluorometer, so that the front face of the quartz slide (with the samples) was positioned at a 30^0 angle to the excitation optical axis and at a 60^0 angle to the emission optical axis as shown in Figure 3.4. The quartz plate was not placed at 45^0 to decrease the amount of light directly reflected into the detection system. The illumination spot for this fluorometer is 1.7 ± 0.3 mm. The slits on the monochromators were set at a 4.0 nm bandwidth. The fluorescence spectrum was measured with a excitation wavelength of 360 nm for DPA crystals and 300 nm for CaDPA powder. The emission spectrum was measured from 10 nm longer than the excitation wavelength to 10 nm shorter than twice the excitation wavelength. When integrating the total fluorescence signal, the spectra were cut to exclude the light that was reflected off the quartz plate.

All fluorometer parameters, including the photomultiplier's high voltage (1000 V), step size (1.0 nm) and the data collection time (0.1 s per point), were kept the same for all the measurements. This quartz has a very negligible fluorescent signal that does not overlap very strongly with the dry sample fluorescence. The fluorescence of at least 10 slides, each containing a different amount of samples was measured both in the case of DPA and CaDPA. Absorption of the dried samples was measured using a GBC UV/VIS Cintra 40 spectrophotometer. The spectrophotometer was equipped with an integrating sphere to measure highly scattering or reflecting samples of dry DPA and CaDPA on quartz slide. The absorption was measured from 250 to 600 nm. The slits were set with a 2 nm bandwidth.

The spores were not washed and were used without any further preparation for our experiment with unwashed samples. The BG1 spores were suspended in deionized water in a quartz cuvette and the absorbance and the fluorescence was measured from 200 to 600 nm. We measured the absorbance and fluorescence of BG suspension in six different concentrations. For the washed spores, the same BG1 spores were prepared by washing the spores in cold deionized milli Q water and then centrifuging at 10000 rpm for five minutes using the centrifuge. The supernatant was removed in each washing. Samples were all washed three times and the pellet was resuspended in milli Q water and when measured, the absorbance and fluorescence in six different concentrations was similar to the unwashed samples. We also measured the

absorbance and the 2-D fluorescence spectra of the supernatant to see the spectral differences. The room temperature QEs were determined by comparing the integrated areas beneath the corrected emission spectra of the unknowns with that of a standard. The QE values were calculated by using the equation 2.4 in Section 2.5 Chapter 2. We found that we could exclude most of the scattered light by using the following ranges of emission wavelengths to determine the QE's of the unknown samples

1. Tryptophan : 300nm – 550 nm for 280 nm excitation
2. CaDPA : 330 nm – 570 nm for 290 nm and 300 nm excitation
3. DPA : 390 nm – 650 nm for 360 nm excitation
4. *Bacillus* spores : 330nm – 560 nm for 290 nm and 300 nm excitation

CHAPTER 4

4 RESULTS

4.1 Multi wavelength fluorescence studies of major *Bacillus* spore chemical components

4.1.1 Dipicolinic acid (DPA)

In Figure. 4.1(A) we show the 2-D multiwavelength fluorescence spectra of a DPA solution before exposure to the UV arc lamp. We did not observe any measurable fluorescence, but did observe the Raman scattering peak from water. We compared this spectrum with the measured spectrum of deionized Milli Q water (See Figure 4.2 (A)) and the wavenumber of the peak coincides with the literature value of the Raman spectrum of water (~3600 cm^{-1}).[53] The fluorescence of the same solution exposed to approximately 80 J/cm^2 of UV light is shown in Figure. 4.1 (B).

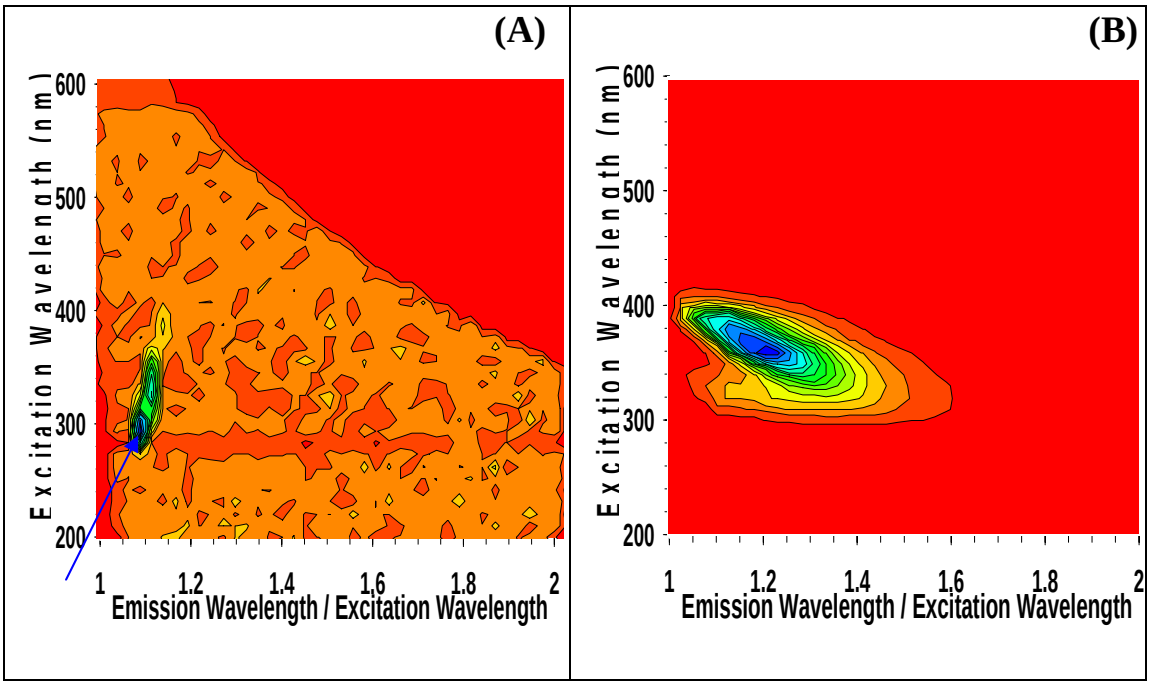

Figure 4.1: (A) Fluorescence spectrum of a freshly prepared DPA solution. The arrow points to the Raman scattering from the water. **(B)** Fluorescence spectrum of the same DPA solution after UV exposure. The greatest intensity is blue and the least intensity is red.

The DPA solution was exposed to UV light by an ozone free xenon arc lamp for 15 minutes and allowed to stand 2 hours in the dark before the fluorescence measurements were made. We also measured the fluorescence immediately after exposure and at different times in the following seven days to see the changes in fluorescence. The fluorescence spectrum looks very similar to Figure 4.1(B). We noticed that the fluorescence intensity continued to increase during the first few measurements and the peak intensity saturated after around 10 minutes (after the exposure lamp was turned off). The noise in Figure 4.1(A) is 0 to 3 "counts" (arbitrary units of intensity). The peak in Figure 4.1(B) has a maximum of 90 counts. The peak intensity has been enhanced by about a factor of 45 by the broad band of UV exposure for 15 minutes. The fluorescence observed in this figure has a peak emission wavelength at 440 nm and occurs with an excitation wavelength of 360 nm. Because of the poor solubility of DPA in water, we dissolved DPA in ethanol and found that DPA fluoresced in the blue as shown in Figure 4.2(B) and the shape of the spectrum looks similar to UV exposed DPA in solution (see Figure 4.1(B)).

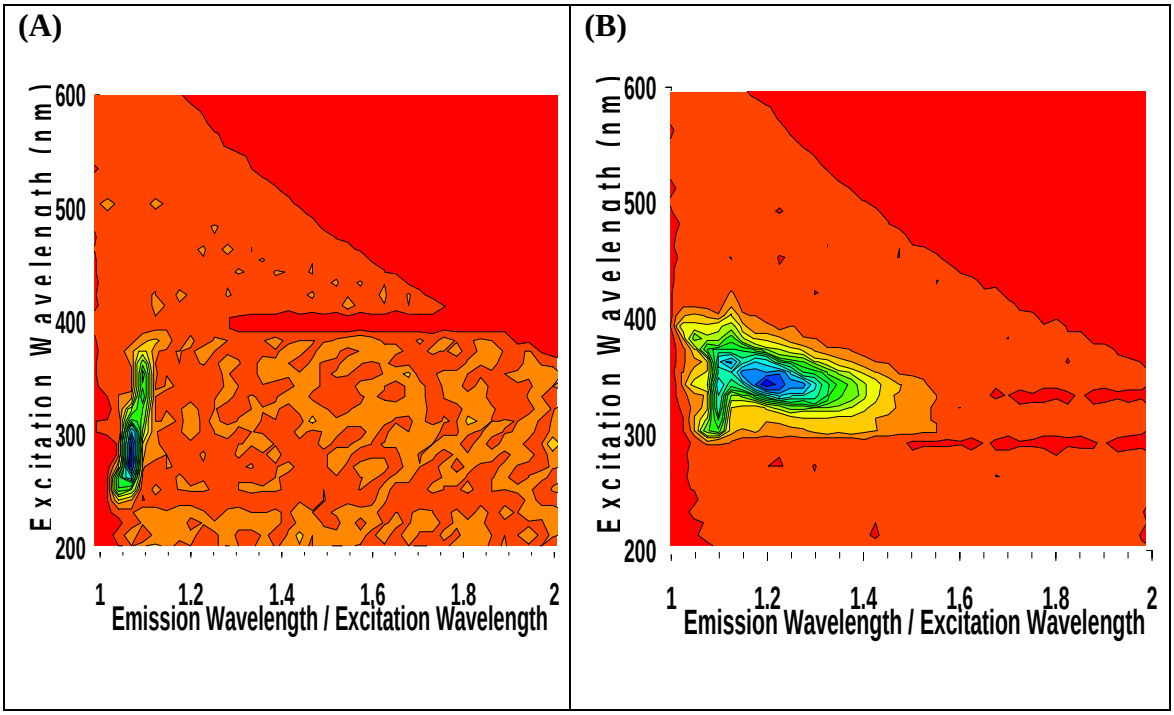

Figure 4.2: (A) Measured spectrum of pure water **(B)** Fluorescence spectra of DPA dissolved in ethanol. The greatest intensity is blue and the least intensity is red.

The DPA solution did show a well-defined absorption peak around 277 nm as can be seen in Figure. 4.3. We noted that the absorption spectrum of DPA shifted slightly (blue shifted) to shorter wavelengths upon exposure to UV light. There was also a very small increase in the absorption in the 300 to 400 nm wavelength region.

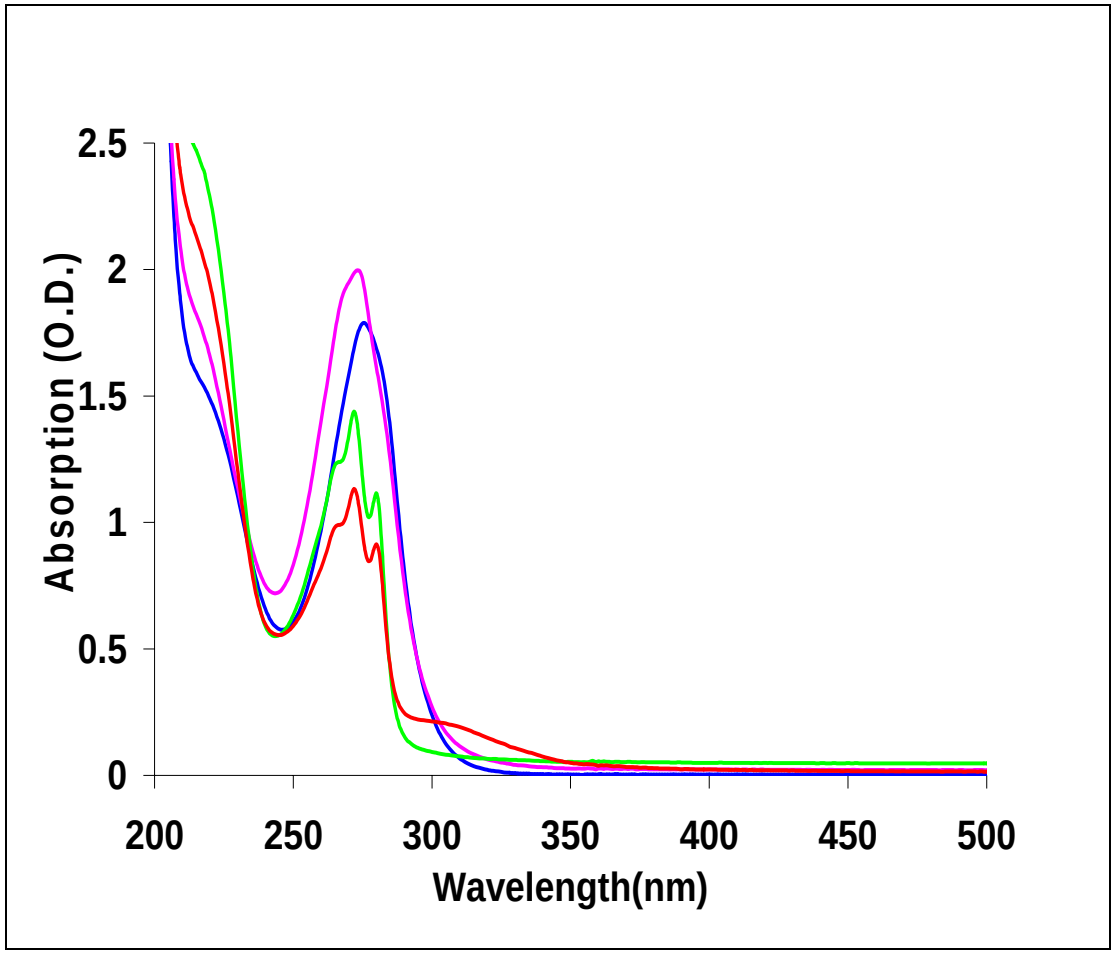

Figure 4.3: The absorption spectra of DPA before exposure to UV light (blue) and DPA after exposure to about 80 J/cm^2 of UV light (pink) are shown. Also shows the absorption of CaDPA before exposure to UV light (green) and after exposure to about 80 J/cm^2 of UV light (red). All samples were solutions measured in a 1 cm quartz cuvette. The same sample was measured before and after exposure.

Since the DPA inside the *Bacillus* spores is correspond to be similar to the dry crystalline state or wet paste of DPA not the DPA in solution, we also measured the fluorescence from the exposed DPA dried on filter paper to make a wet paste or a dry sample. Drying was done at room temperature and in the dark. The fluorescence for the wet paste is shown in Figure. 4.4(A). The dry crystal of exposed DPA is shown in

Figure 4.4(B). Both of these spectra are similar to Figure 4.1(B) (the UV exposed solution of DPA), with the fluorescence spread over a slightly wider spectral range.

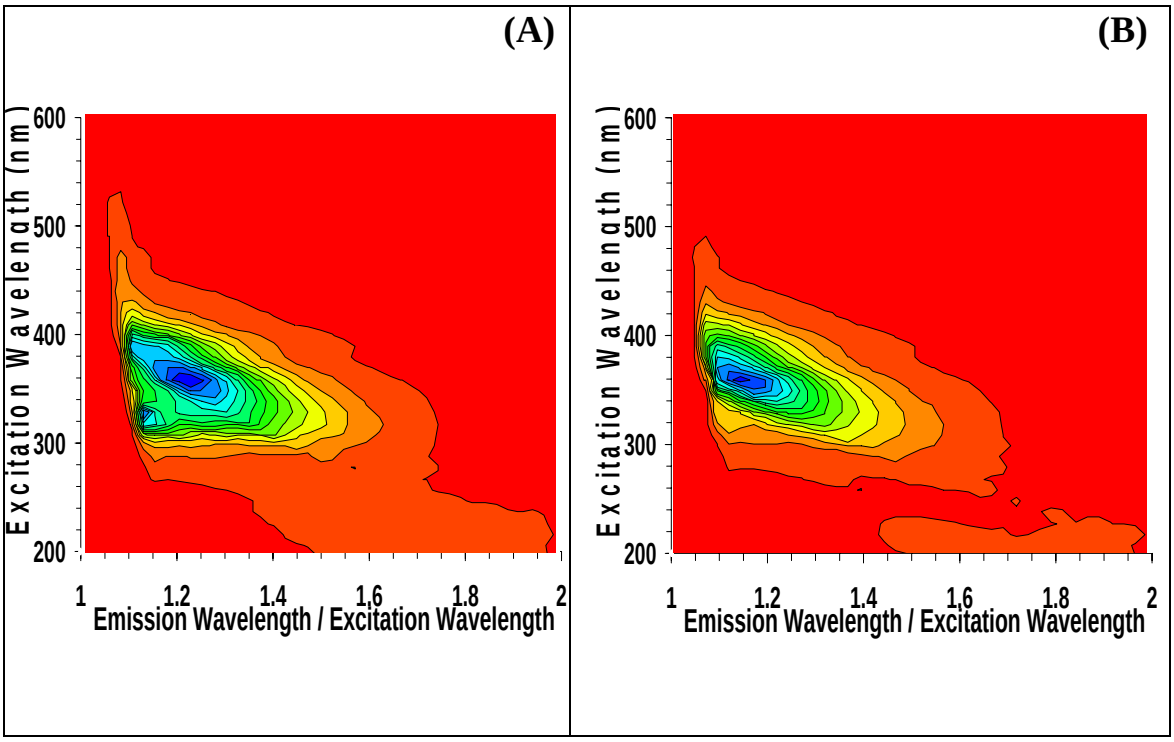

Figure 4.4: (A) Fluorescence spectrum of UV exposed DPA as a wet paste on filter paper. **(B)** Fluorescence spectrum of UV exposed DPA as dry crystals on filter paper. The sample preparations are described in the text. The greatest intensity is blue and the least intensity is red.

We then took crystals of DPA, not exposed to UV light and placed them on the filter paper and measured the fluorescence directly. This is shown in Figure. 4.5(A). Finally, we exposed the dry DPA crystals on the filter paper to the 80 J/cm^2 of broadband UV light. The UV enhanced fluorescence spectrum is shown in Figure. 4.5(B). The UV enhancement of the peak fluorescence intensity of the dry DPA sample was a factor of 1.8. The integrated fluorescence intensity over all wavelengths increased by a factor of 3.8. As mentioned elsewhere, the small trail of peaks that occur for short wavelength excitation is an anomalous signal at 420 nm that is observed whenever a large amount of light is reflected into the detection monochromator of the fluorometer.

We also checked whether the fluorescence of the dry crystals of DPA is enhanced compared to the small-to-zero fluorescence observed from DPA in solution. The fluorescence profile of dry, wet and re-dried DPA on filter paper is shown in Figure 4.6. We did not notice any major spectral shape changes other than the noticeable changes in intensity (Figures 4.6 (B) and 4.6 (C) were plotted on the same scale as 4.6 (A)). Initially we measured the fluorescence of dry DPA as shown in Figure 4.6(A). The fluorescence decreased by nearly a factor of three after the DPA was wet (see Figure 4.6(B)). We dried the same piece of filter paper with the DPA in the dark and the signal increased by a factor of two as shown in Figure 4.6(C).

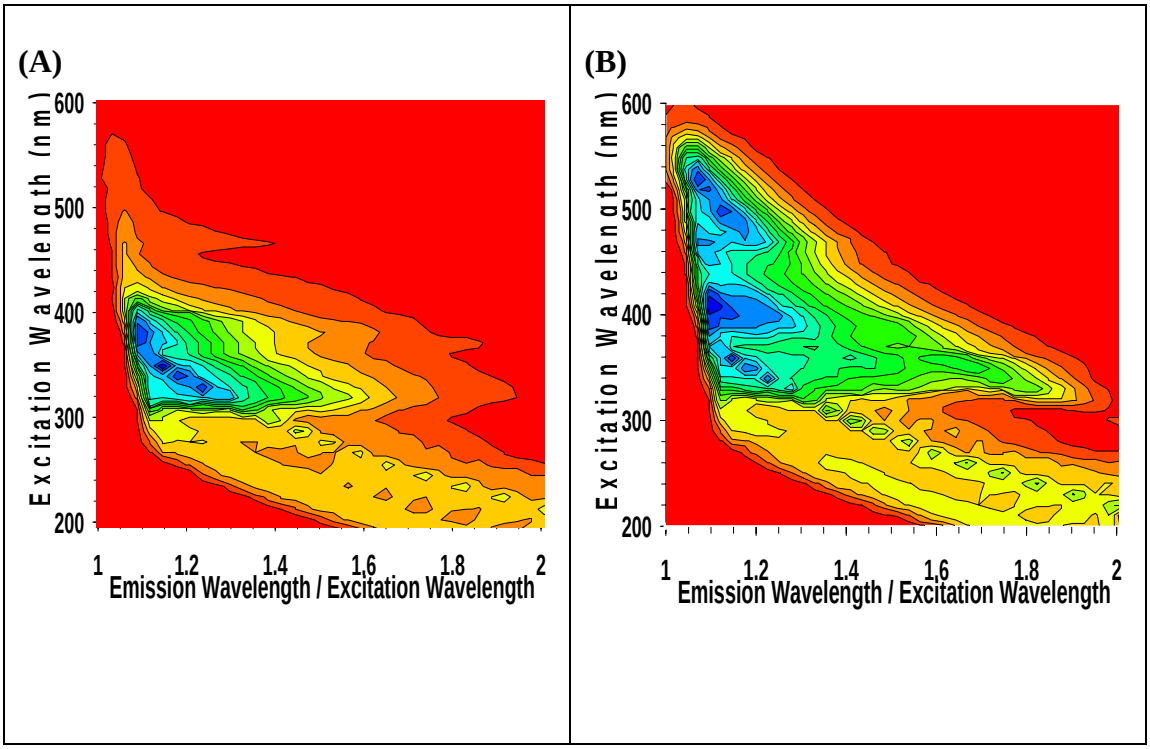

Figure 4.5: (A) Fluorescence spectrum of dry DPA without UV exposure on filter paper. **(B)** Fluorescence spectrum of UV exposed dry DPA crystals on filter paper. The maximum intensity on **(B)** is twice as large as the maximum intensity on **(A)**. The greatest intensity is blue and the least intensity is red.

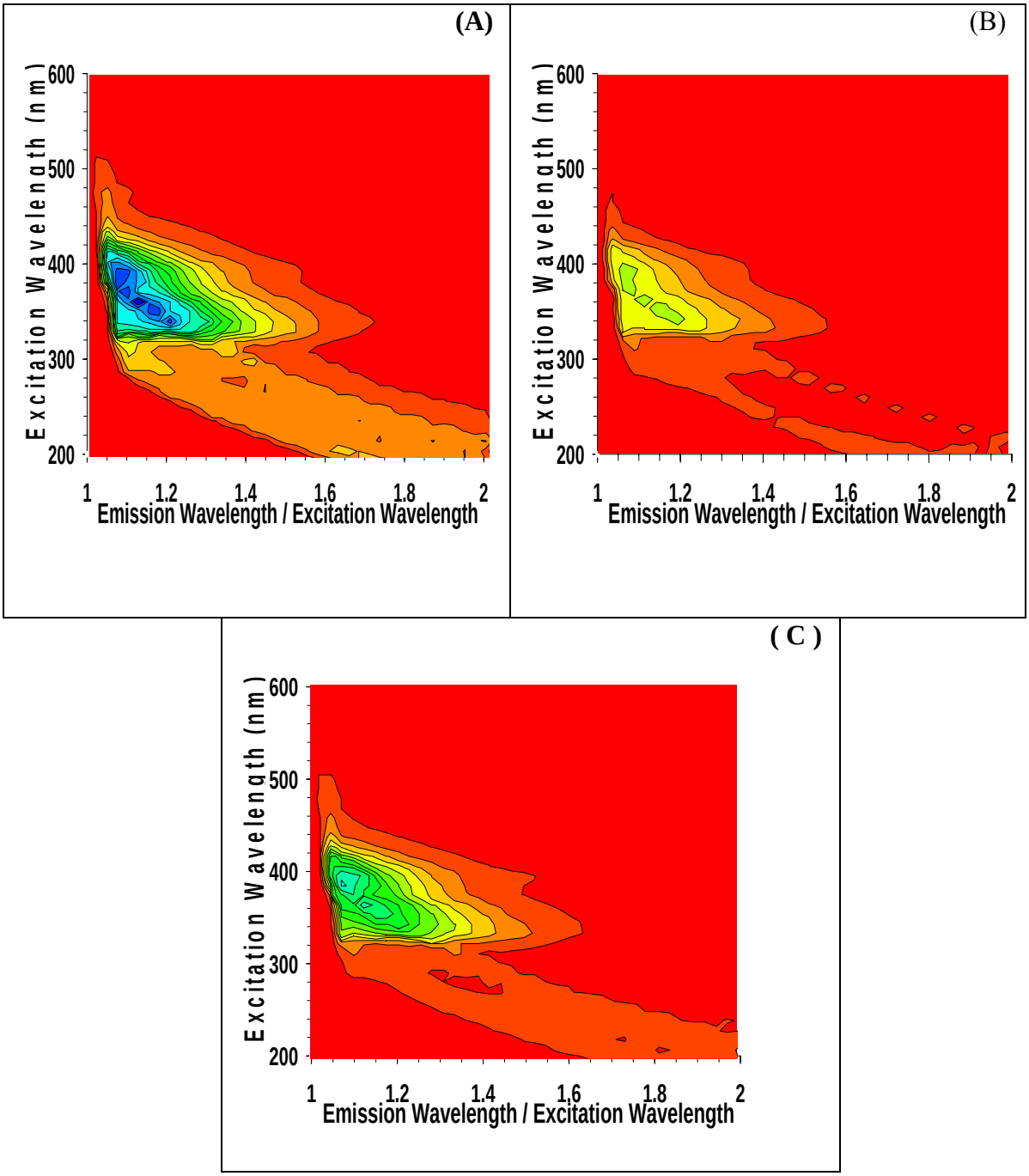

Figure 4.6: Fluorescence spectrum of (**A)** dry DPA (**B)** wet DPA crystals **(C)** re-dried DPA crystals on filter paper. Figures B and C were plotted on the same scale as **(A)** The maximum intensity on **(A)** is 3 times as large as the maximum intensity on **(B)** and about 2 times as large as on **(C).** The greatest intensity is blue and the least intensity is red.

4.1.2 Calcium dipicolinate (CaDPA)

In Figure 4.7 we show a modest fluorescence signal for DPA solution mixed with $CaCO_3$, with excitation in the range of 300 nm and emission peaking at about 400 nm. The arrow in the figure points to the Raman scattering of the water. During the sample preparations the solution was exposed to room light. Also, during the fluorescence measurements, which take about 90 minutes, the solution was exposed to UV light from the fluorometer. We always verified the presence of CaDPA by comparing absorbance with the compound's characteristic absorbance (see Figure 4.3).

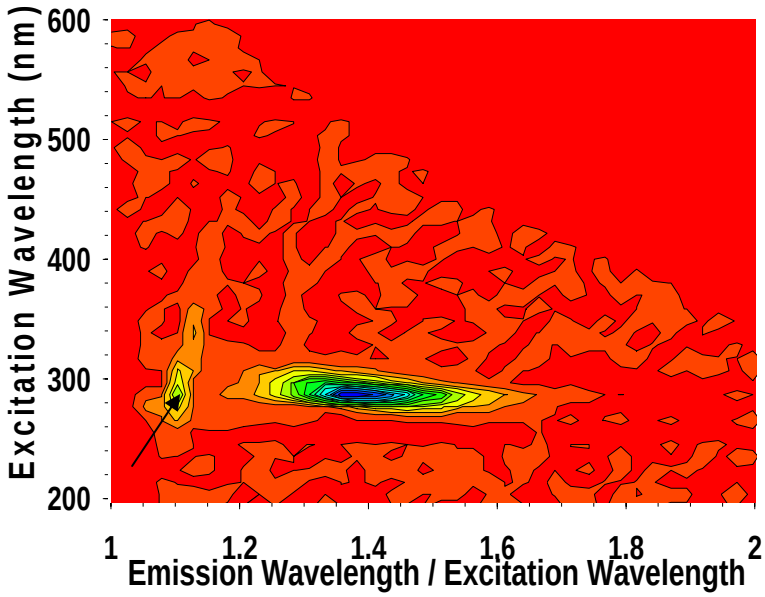

Figure 4.7: Fluorescence spectrum of a freshly prepared CaDPA solution. The arrow points to the Raman scattering from the water. The greatest intensity is blue and the least intensity is red.

The CaDPA solution was exposed to UV light (~ 80 J/cm^2 using the 15 min. exposure and 2 hour resting period) and the fluorescence was measured as shown in Figure 4.8. As we explained in the case of DPA and as shown in Figure 4.14 below, the peak intensity value saturated after around 10 minutes (after the exposure light was turned off). We notice that there were intensity changes up to around 10 minutes. So, we arbitrarily choose 2 hour resting period. We did not notice any major intensity changes after 10 minutes. We observed a large increase of fluorescence around the same range of emission and excitation as CaDPA solution without exposure (see

Figure. 4.8). The peak fluorescence increased by a factor of 85. In Figure 4.8, the excitation peak is slightly red shifted by 10 nm (from 290 nm to 300nm). The total volume under the curves increased by a factor of 50. As shown in Figure 4.3, the exposed absorption spectrum of CaDPA solution shows moderate changes compared with the absorption spectrum of an unexposed CaDPA solution. We noticed that the absorbance increased at around 300 nm excitation.

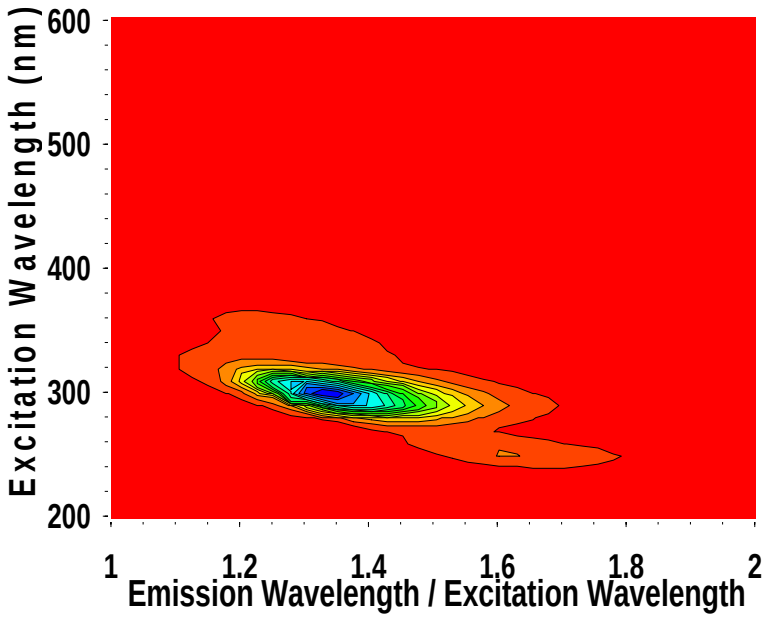

Figure 4.8: Fluorescence spectrum of the same CaDPA solution after UV exposure. The greatest intensity is blue and the least intensity is red.

Similar fluorescence and absorption spectra of CaDPA were obtained when solutions were made of DPA with different calcium compounds ($Ca((NO)_3)_2$, $Ca(OH)_2$). All samples were prepared on the day of the experiment.

Figure 4.9 shows the individual fluorescence spectra of CaDPA solution excited at 290 and 300 nm (before UV irradiation) and excited at 290, 300 and 310 nm (after UV irradiation). We noticed that the peak fluorescence of exposed CaDPA solution had shifted from 290 nm excitation (unexposed) to 300 nm excitation (exposed). We also measured the fluorescence of UV exposed CaDPA crystals in wet and dry form as shown in Figures 4.10 and 4.11. Similar to the DPA measurements, we measured

about a factor of 3.7 increases in the fluorescence of the dry crystals of CaDPA compared to wet crystals. We could not see any major difference in the fluorescence spectra of CaDPA in aqueous, dry and wet form other than a small increase in the spectral width of the fluorescence peaks and the peak excitation position was slightly red shifted about 10nm. The dry CaDPA before and after UV irradiation is shown in Figures. 4.12 and 4.13. The peak fluorescence increased by a factor of 1.5.

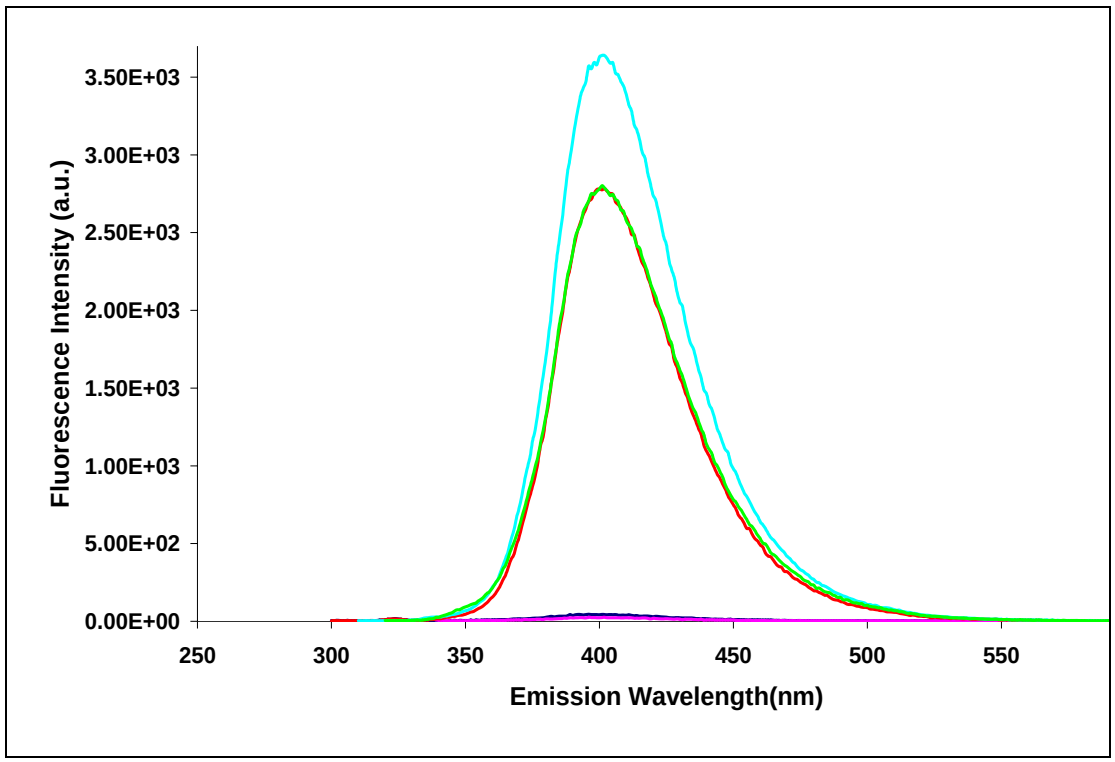

Figure 4.9: Fluorescence spectra of CaDPA solution, excited at 290nm (blue), 300nm (pink) (before UV irradiation) and excited at 290nm (green), 300nm (blue) and 310nm (red) (after UV irradiation). The same sample was used for all three measurements.

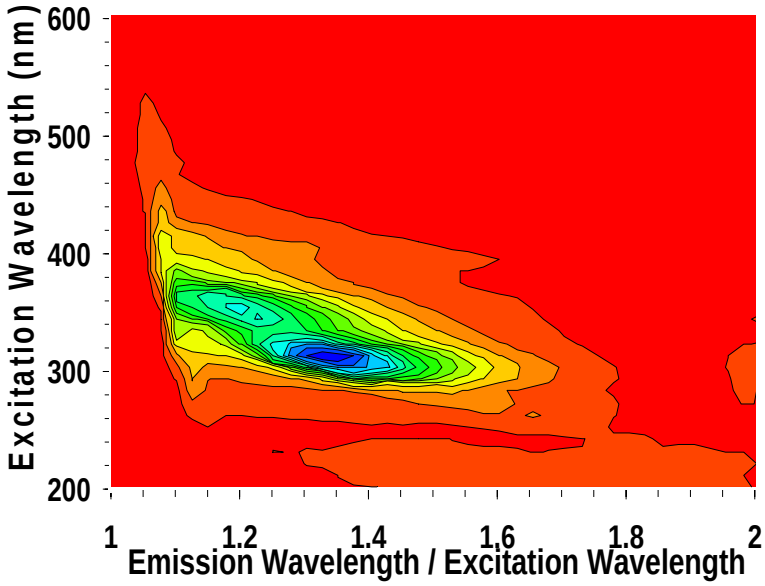

Figure 4.10: Fluorescence spectrum of UV exposed CaDPA as a wet paste on filter paper. The greatest intensity is blue and the least intensity is red.

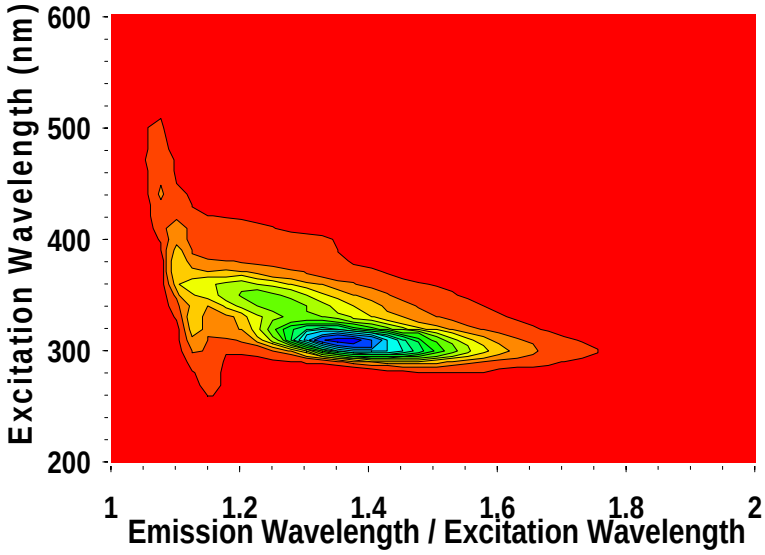

Figure 4.11: Fluorescence spectrum of UV exposed CaDPA as dry crystals on filter paper. The greatest intensity is blue and the least intensity is red.

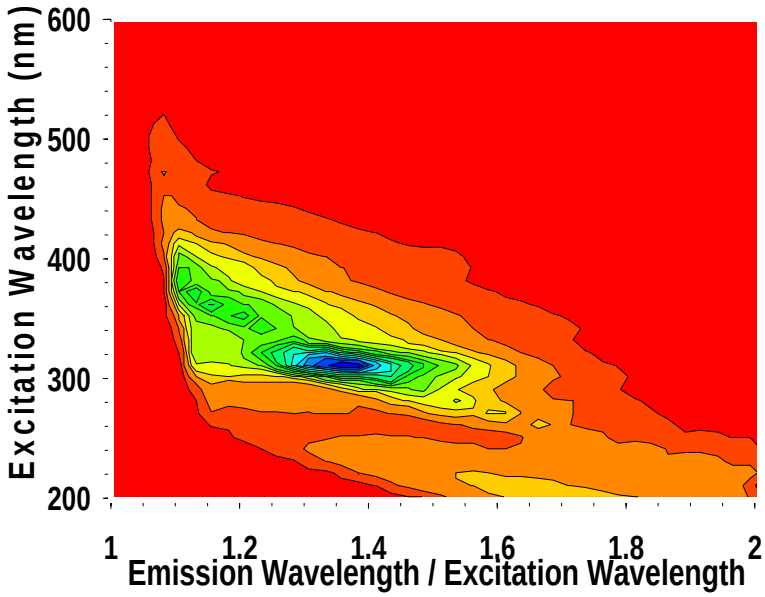

Figure 4.12: Fluorescence spectrum of dry CaDPA without UV exposure on filter paper. The greatest intensity is blue and the least intensity is red.

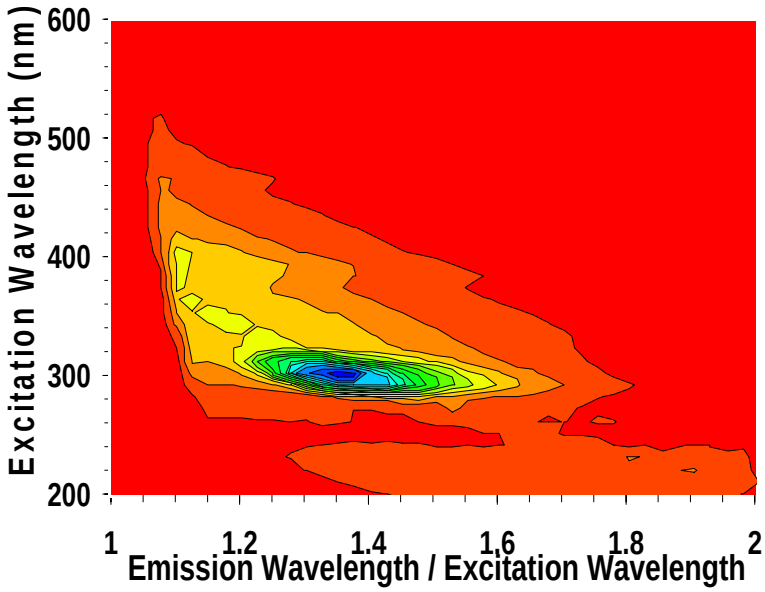

Figure 4.13: Fluorescence spectrum of UV exposed dry CaDPA crystals on filter paper. The greatest intensity is blue and the least intensity is red.

In order to further understand the nature of fluorescence enhancement in the UV exposed CaDPA solution, we measured the fluorescence intensity as a function of time immediately after the UV exposure. Figure 4.14 shows the variation of fluorescence intensity of the UV exposed CaDPA solution as a function of time. The

sample was exposed to the UV arc lamp for 15 minutes. It was then placed in the fluorometer and the fluorescence was measured with 305 nm excitation and the emission was measured by repeatedly scanning 409 to 411 nm in 0.1 nm steps. Each scan took 10 s. We then plotted the peak intensity as a function of time (the points plotted on Figure 4.14).

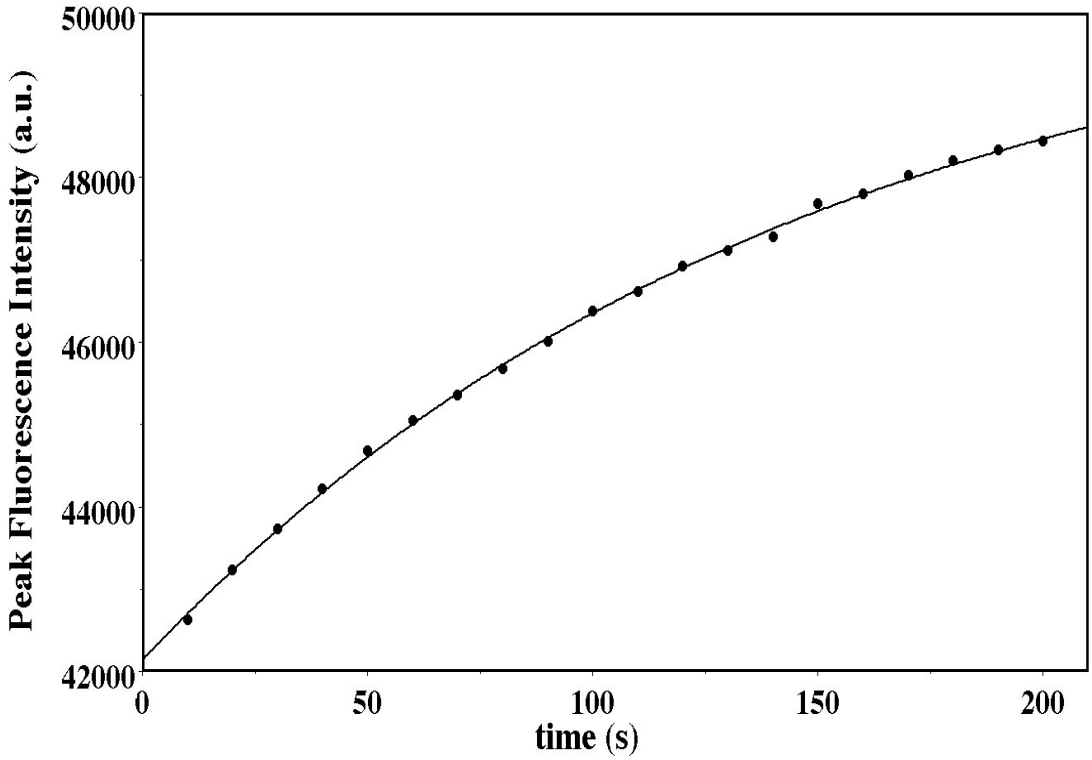

Figure 4.14: Fluorescence intensity of CaDPA solution measured at 410 nm and excited at 305 nm as a function of time after the UV exposure. The line is an exponential fit to the data points.

In order to further understand whether the UV-induced fluorescence increases were a continuous process or whether there was a threshold effect, we measured the fluorescence of CaDPA solution after we exposed the sample by UV at different exposure times under similar experimental conditions (2 hour resting period). The changes in the fluorescence intensity at 300 nm excitation and the absorbance of the CaDPA solution at different exposure times under similar conditions are shown in Figure 4.15. The UV irradiation of 5 minutes produced the peak fluorescence intensity. We note that the exposure time for optimal enhancement depends upon the intensity of the UV irradiation source and the concentration of the CaDPA solution.

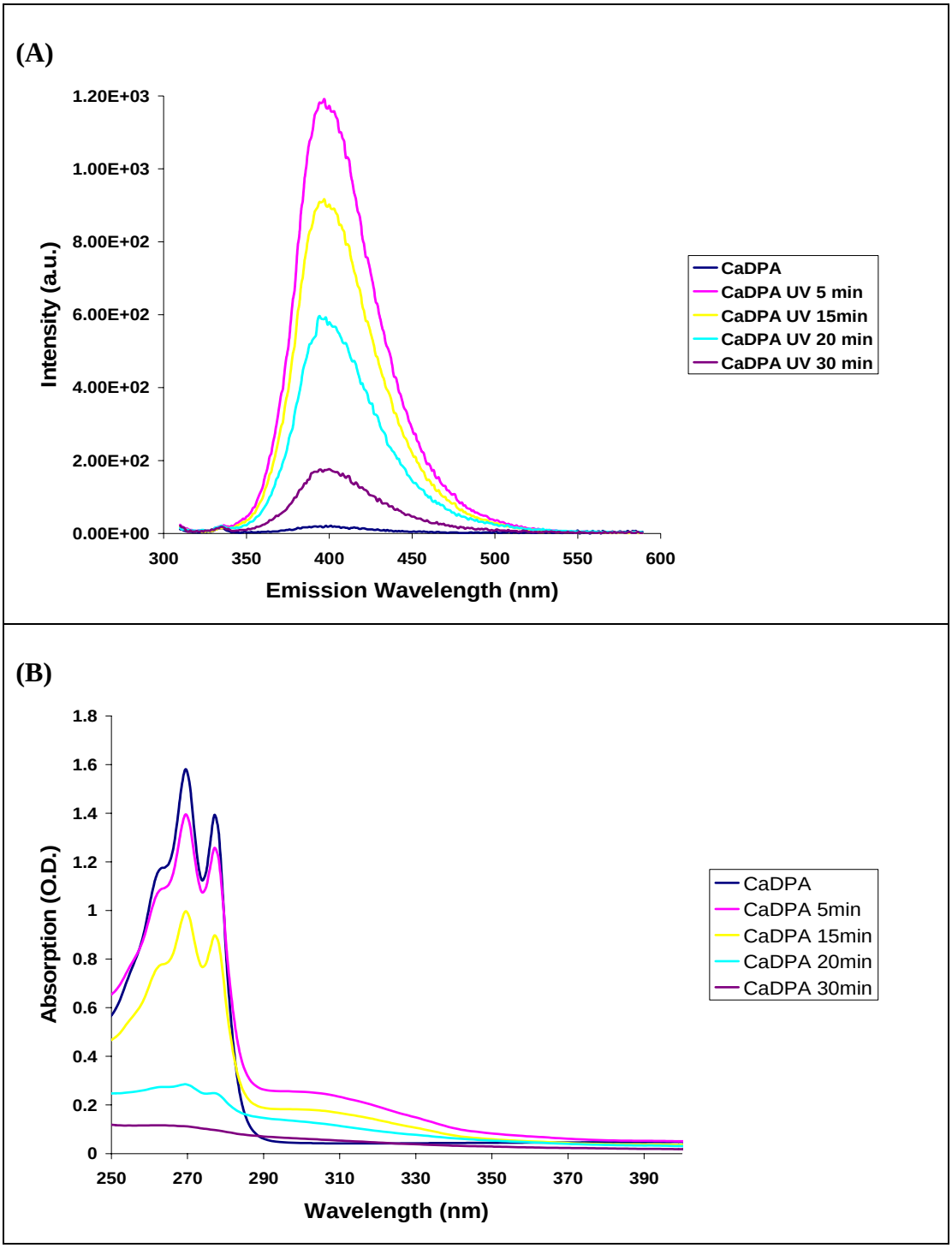

Figure 4.15: (A) Fluorescence intensity of CaDPA solution (excited at 300 nm) and **(B)** Absorption measured as a function of UV exposure time.

In order to understand whether any particular wavelengths or wavelength ranges are more effective at increasing the fluorescence than others, we measured the enhanced fluorescence intensities after we exposed the CaDPA sample for 15 minutes at different wavelengths of UV light between 250 nm and 330 nm at 10 nm intervals (15 min. exposure). Figure 4.16 shows the spectral response curve plotted on integrated fluorescence intensity versus wavelength of UV exposure.

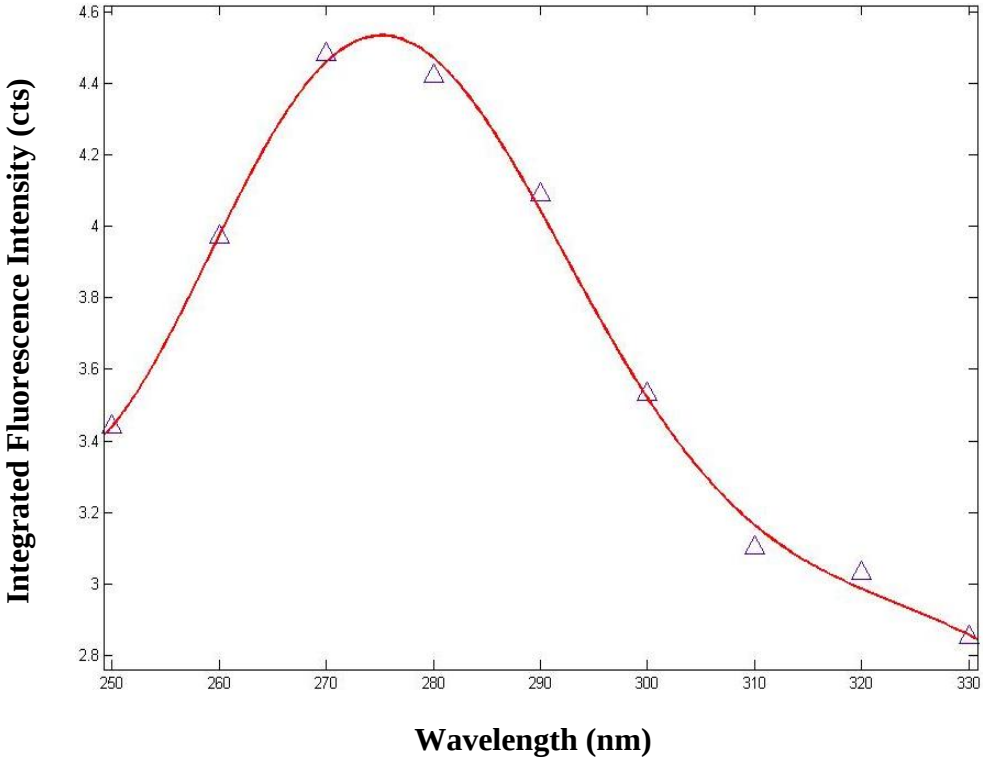

Figure 4.16: The graph of the integrated fluorescence intensity versus wavelength of exposure of the CaDPA in solution.

The triangles show the measured integrated fluorescence intensities. The line is a least squares fit of a Gaussian profile to the measured data. The maximum enhancement occurs with UV exposure at around 276 nm. This is an ideal region of the spectrum for assessing fluorescence enhancement.

4.1.3 Tryptophan

Tryptophan was identified as a major fluorophore in nearly all the biological samples including bacterial spores. Therefore, understanding the multiwavelength fluorescence profile of this component was necessary in order to understand and characterize the spore fluorescence and to assign inherent fluorophores. In this section we present the results of our 2-D fluorescence study of dry and wet tryptophan and the effect of UV irradiation in order to show its role in the fluorescence signature of *Bacillus* spores. We compare this result with our studies of dry and wet *Bacillus* spores in Section 4.2. Figure 4.17 shows the fluorescence contour plot of pure tryptophan in water solution. It produces a well defined emission peak at around 350 nm emission at 280 nm excitation.

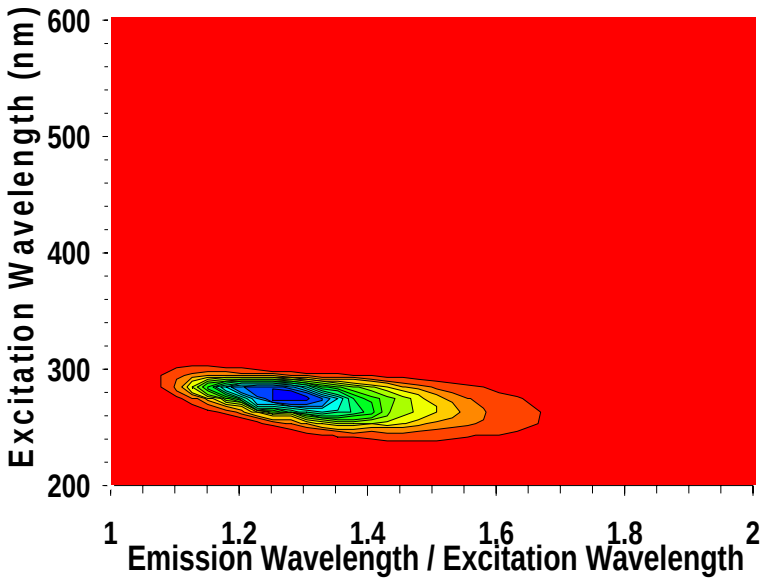

Figure 4.17: Fluorescence contour plot of pure tryptophan in water solution. The greatest intensity is blue and the least intensity is red.

Figure 4.18 shows the fluorescence profile of the same solution after irradiating the sample to our broad band UV for 15 minutes (~25 J/cm^2 using the 15 min. exposure and 2 hour resting period). The tryptophan peak almost disappears because of photoconversion of the tryptophan to a non-fluorescent form.

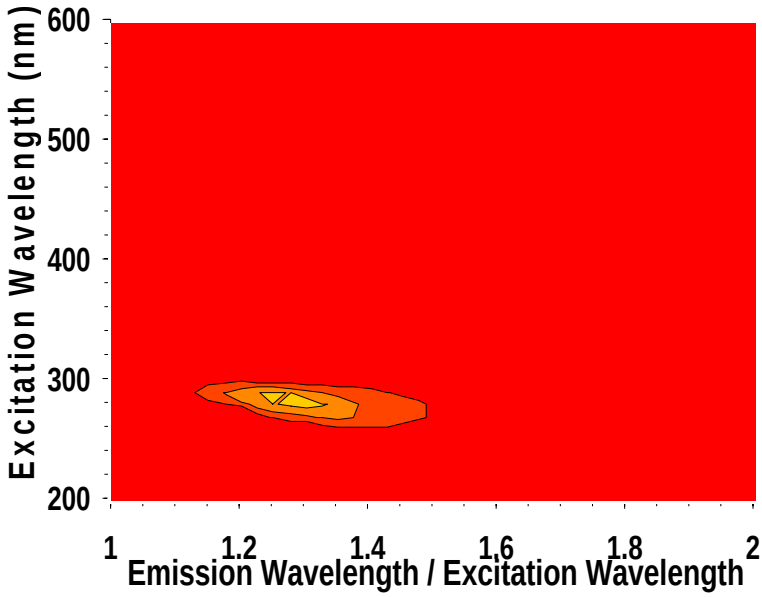

Figure 4.18: Fluorescence spectrum of the same tryptophan solution as shown in Figure 4.37 after being exposed to broad band UV irradiation for 15 minutes. The greatest intensity is yellow and the least intensity is red.

Figure 4.19 shows the absorption spectrum of the tryptophan in water before and after UV irradiation. The fluorescence spectra of the dry tryptophan smeared slightly on a piece of filter paper are shown in Figure 4.20. We note that the fluorescence peak is shifted to a shorter wavelength (blue shifted) compared with tryptophan in water suspension shown in Figure 4.17. We note that the fluorescence spectrum of dry tryptophan on filter paper and tryptophan in suspension at 290 nm excitation wavelengths with emission peaks at around 330 and 350 nm respectively. We also measured the fluorescence of the same dry sample after it was irradiated by broad band UV for 15 minutes and no measurable fluorescence was noted.

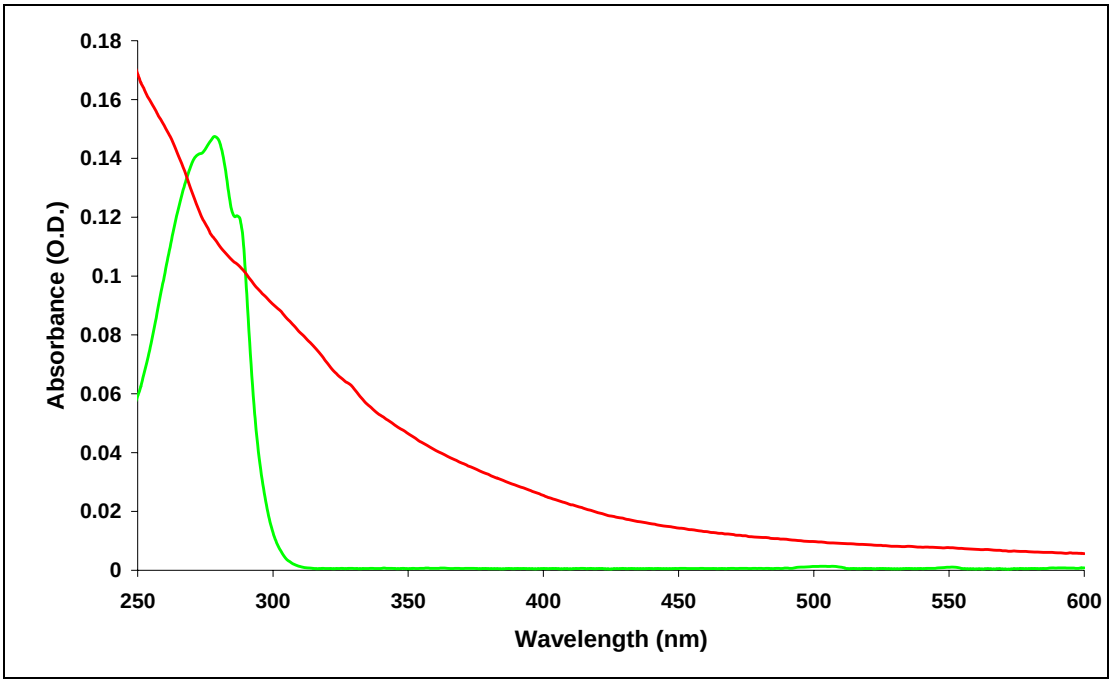

Figure 4.19: The absorption spectra of tryptophan in water before exposure to UV light (green) and tryptophan after being exposed to UV light (red).

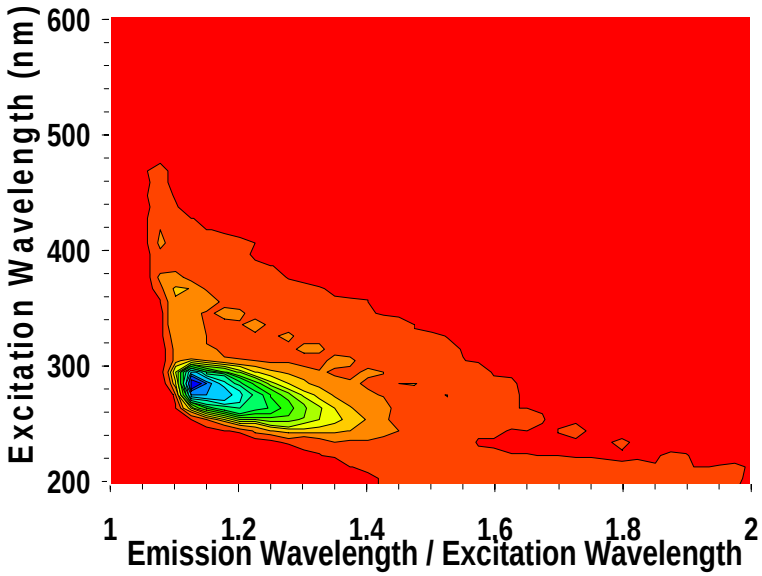

Figure 4.20: The Fluorescence spectrum of dry tryptophan without UV exposure on filter paper. The greatest intensity is blue and the least intensity is red.

4.2 Multi wavelength fluorescence studies of *Bacillus* bacterial spores

4.2.1 Reversible changes in fluorescence of *Bacillus globigii* spores due to hydration/drying

To better understand the nature of the fluorescence signal, we studied the intrinsic steady-state fluorescence spectra of BG spores in dry, wet and re-dried forms in this study. The two-dimensional autofluorescence excitation and emission profile for dried BG1 spores smeared on the filter paper is shown in Figure 4.21. The excitation was stepped every 10 nm. The intensity is equally divided by 15 contour lines. The greatest intensity is blue and the least intensity is red. This same style of representing the contour plot is used in all of the 2-D fluorescence fingerprints in this thesis. The spores essentially cover the filter paper where illuminated, so that very little signal comes from the filter paper. We estimate the order of 10^6 spores to be irradiated by the exciting beam.

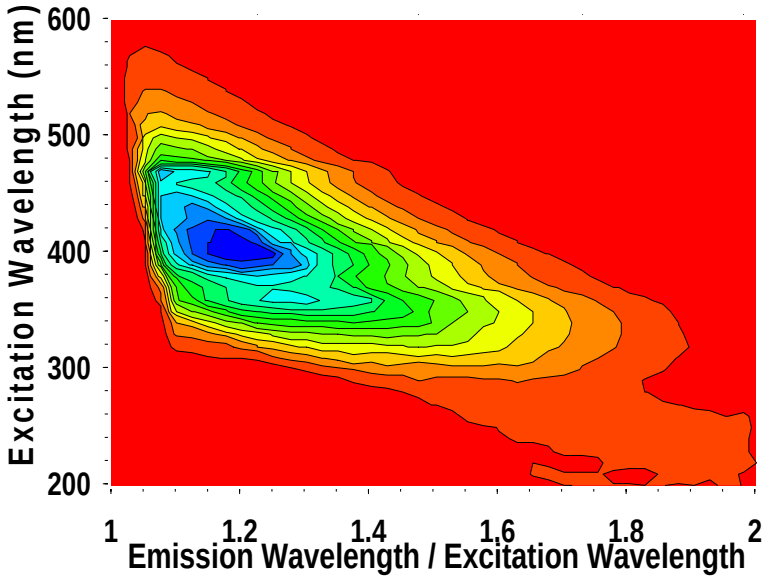

Figure 4.21: Fluorescence contour plot of dry BG1 endospores on filter paper. The greatest intensity is blue and the least intensity is red.

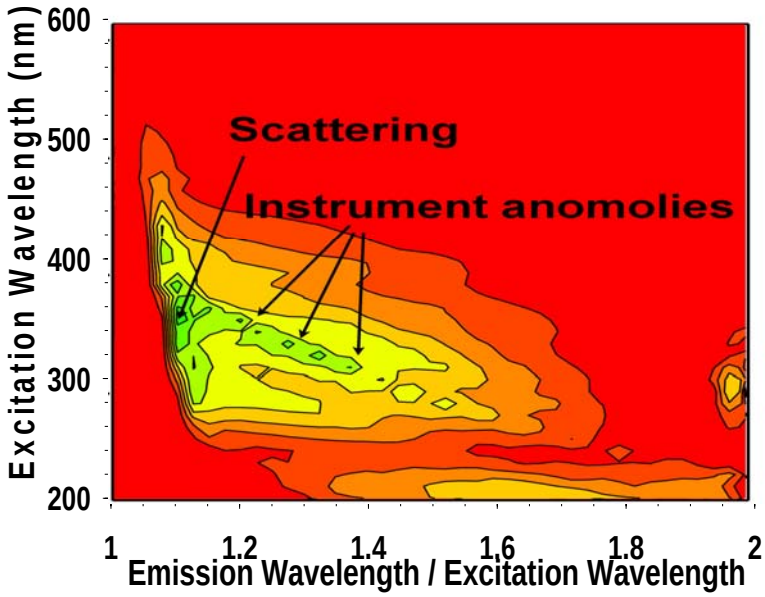

Figure 4.22: Fluorescence contour plot of the filter paper without any spores. The greatest intensity is blue and the least intensity is red.

For a reference, the weak fluorescence signal from the filter paper without any spores is shown in Figure 4.22. The intensity range and contours are the same as those used in Figure 4.21. The primary causes of this signal are from scattering and from instrument anomaly. Most of the signal is from the light scattered off the paper and leaking through the monochromators. In addition, the line of small spikes is caused by anomalies of the fluorometer. On each two-dimensional plot, fifteen equally spaced contours are drawn between zero and the maximum intensity. The dried spores show an emission peak near 410 nm excitation and 485 nm emission wavelength. The spores fixed to the filter paper were allowed to stand in water for 15-20 minutes to allow the spores to hydrate. Figure 4.23 shows the contour plot for wet BG1 spores on the filter paper. It should be noted that the peak fluorescence is shifted to a shorter excitation wavelength of about 350 nm for the excitation wavelength and 440 nm for the emission wavelength. After the data were collected, the filter paper with spores was dried in air for 24 hours. The fluorescence was measured again, and the contour plot for a re-dried BG1 sample is shown in Figure 4.24. It is very similar to the dried BG1 with an emission peak near 400 nm excitation. We did not notice any major photobleaching of the sample in this study.

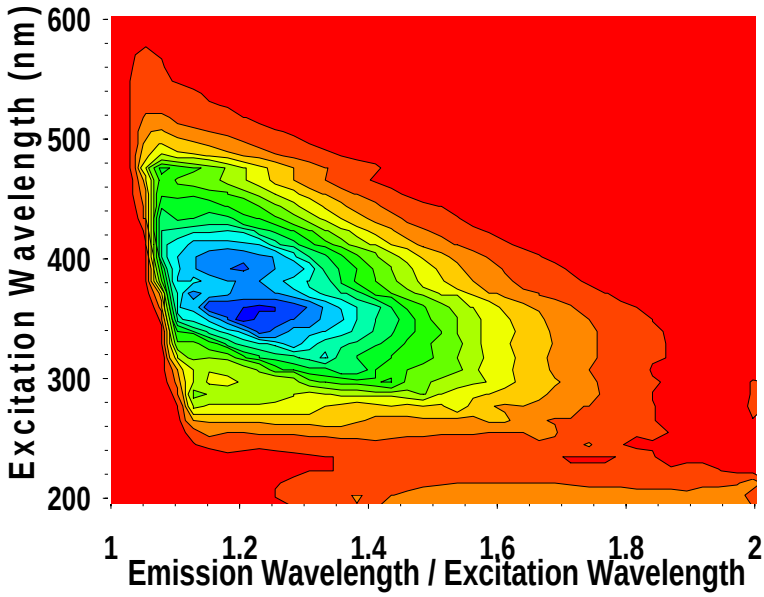

Figure 4.23: Fluorescence contour plot of wet BG1 endospores on filter paper. The greatest intensity is blue and the least intensity is red.

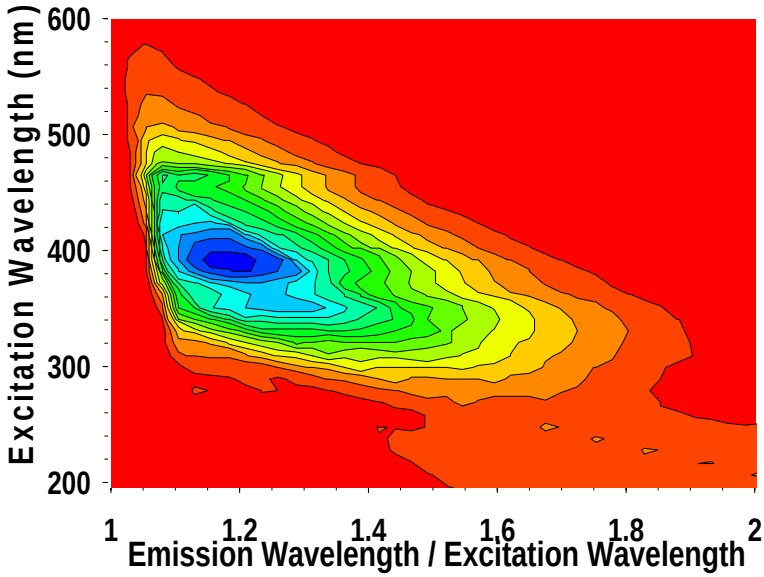

Figure 4.24: Fluorescence contour plot of re-dried BG1 endospores on filter paper. The greatest intensity is blue and the least intensity is red.

The spores essentially cover the filter paper, so we would expect very small signal from filter paper. We also show the conventional individual fluorescence spectra of a BG1 in a dry, wet and re-dried form at excitation 360 nm and 420 nm in Figures 4.25 and 4.26 respectively. Some of the decrease in the signal size between the dry and wet spores was due to a reduction in the fluorescence QE. Some of the decrease may have been due to a fraction of the spores being washed off the filter paper.

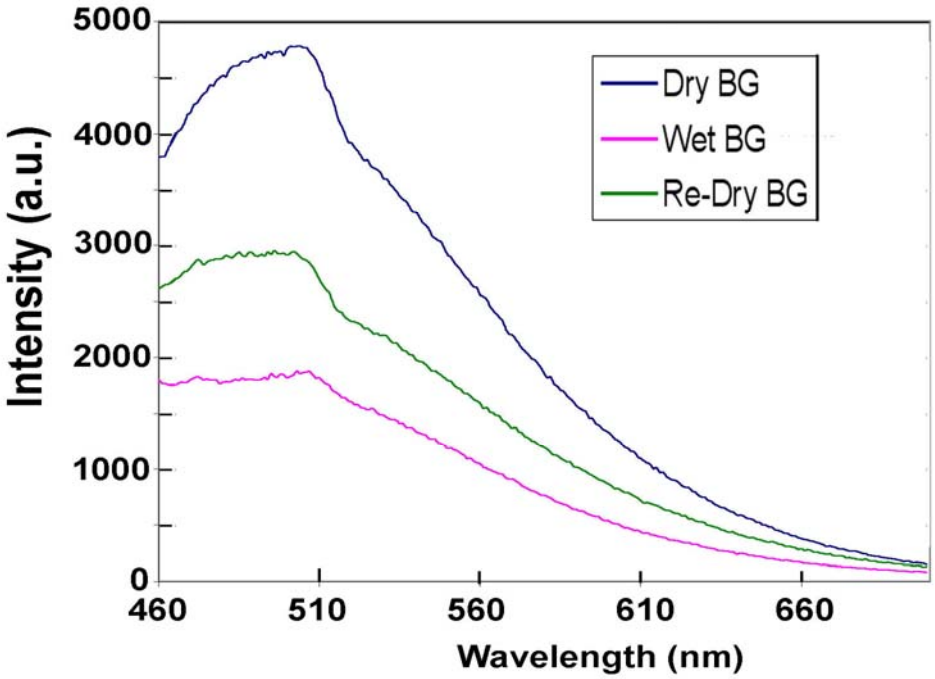

Figure 4.25: Fluorescence spectra, excited at 420 nm, of a BG1 in a dried, wet and re-dried form. The same sample was used for all three measurements.

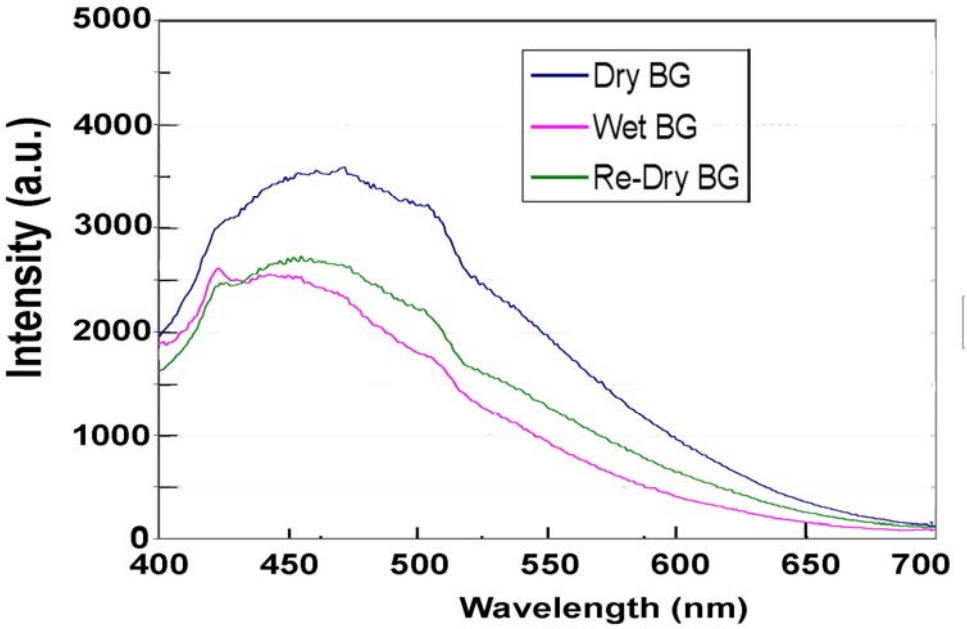

Figure 4.26: Fluorescence spectra, excited at 360 nm, of a BG1 in a dried, wet and re-dried form. The same sample was used for all three measurements.

We also did the same measurements with a BG2 sample as shown in Figure 4.27. The measurements were repeated multiple times with new BG spore samples on pieces of filter paper. Figure 4.28 shows the PC plot of the experiment performed 9 times (seven BG1 and two BG2 samples). We made 27 total measurements with nine of the dry spores, nine of the wet spores and nine of the redried spores. We show in Figure 4.28 these 27 measurements on a plot of the first PC versus the second PC. As the PCs are orthogonal to each other, and each spectral sample of spores can be represented by the linear combination of these PCs, it can be seen that the entire set of spectral spore samples is dominated by these two PCs. The data are clustered in three groups with some overlap between the dry samples and the redried samples. From the figure, it can be seen that the dry spores and the re-dried spores are well separated from the wet spores. The results in the PCA similarity plots are stable if small changes are made in the selection of excitation and emission wavelengths as shown in Figures 4.28 (A) and 4.28 (B).

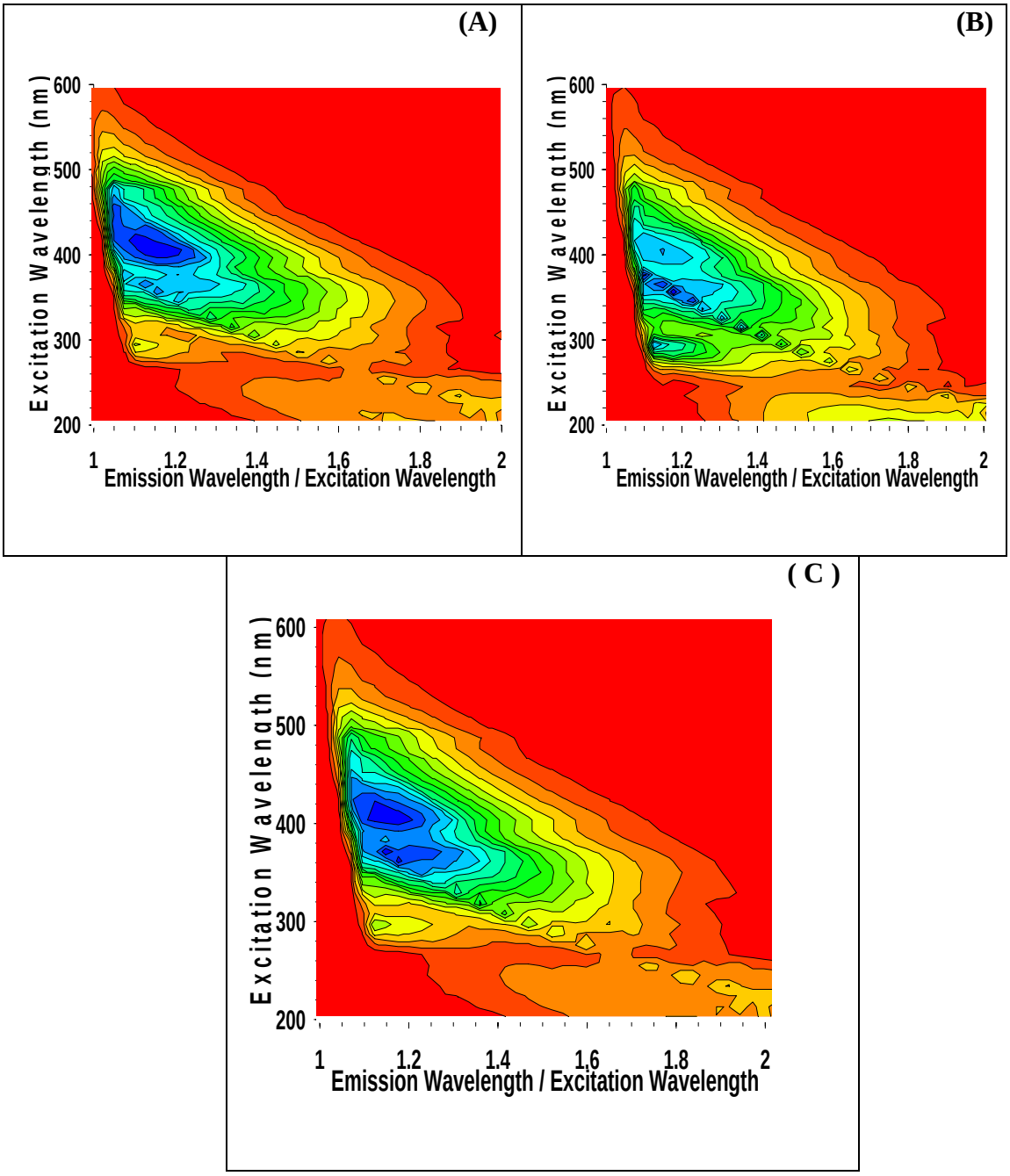

Figure 4.27: Fluorescence contour plot of (A) dry, (B) wet and (C) re-dried BG2 endospores on filter paper. The greatest intensity is blue and the least intensity is red.

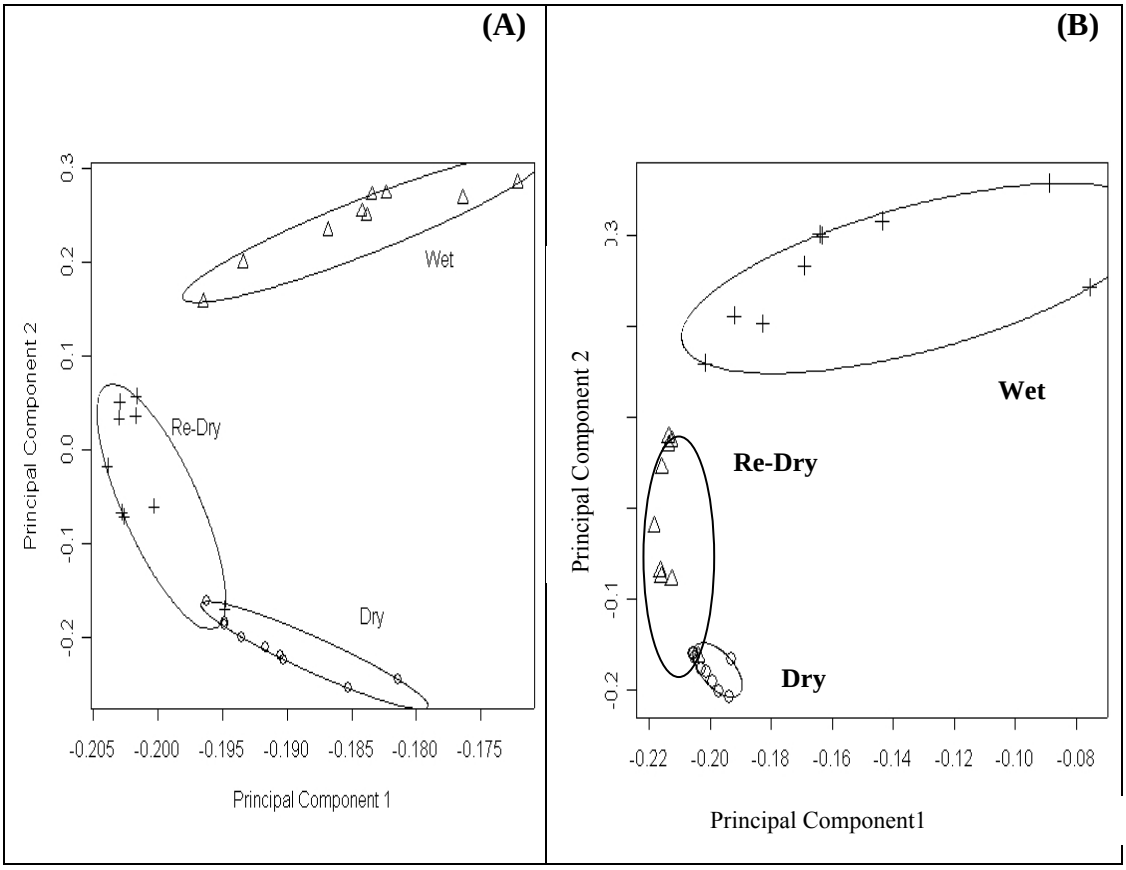

Figure 4.28: The first PC versus the second PC for the nine different concentrations of BG samples measured (A) using excitation wavelengths 300nm to 500 nm with steps 50 nm [140] (B) using excitation wavelengths from 280 nm to 430 nm with steps 30 nm. The ellipses are minimum area ellipses that contain all the 9 points for the particular sample state - dry, wet or re-dried.

4.2.2 Reversible changes in fluorescence of *Bacillus cereus* spores due to hydration/drying

The two-dimensional autofluorescence excitation and emission profile for dried, wet, re-dried BC spores on filter paper are shown in Figures 4.29, 4.30 and 4.31 respectively. To better understand the reversible changes in fluorescence, the filter paper with spores is re-dried in air for seven days instead of 24 hours in the previous experiment.

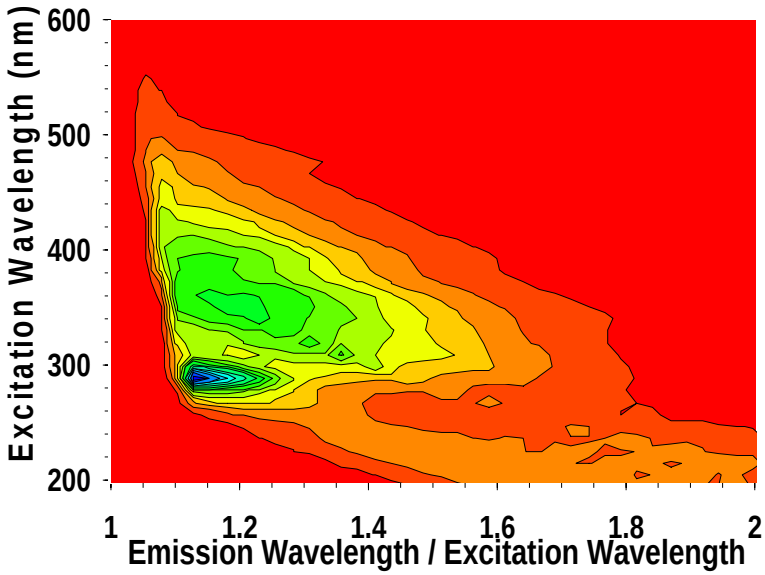

Figure 4. 29: Fluorescence contour plot of dry BC endospores on filter paper. The greatest intensity is blue and the least intensity is red.

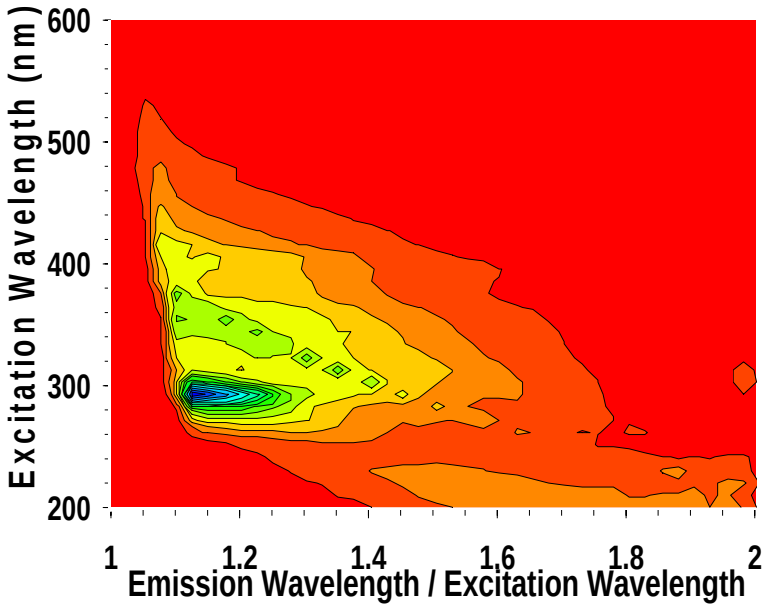

Figure 4.30: Fluorescence contour plot of wet BC endospores on filter paper**.** The greatest intensity is blue and the least intensity is red.

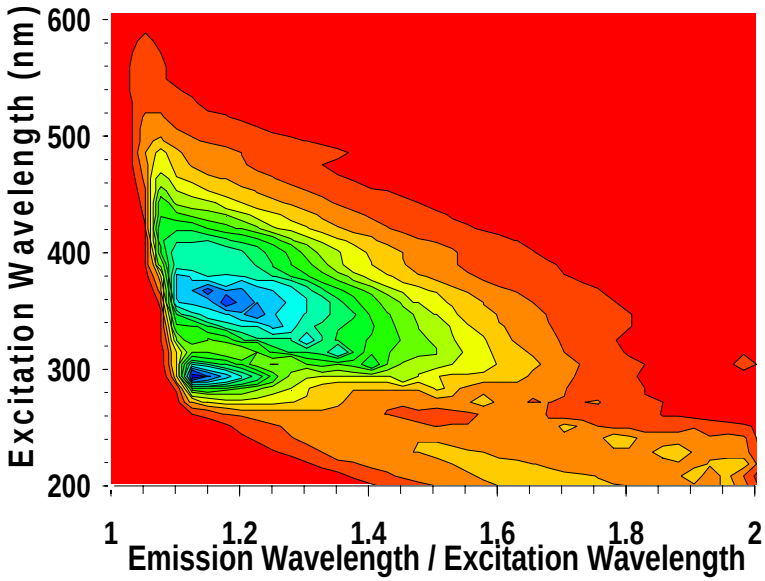

Figure 4.31: Fluorescence contour plot of re-dry BC endospores on filter paper. The greatest intensity is blue and the least intensity is red.

We could not see any major fluorescence shift between the dry, wet and redried spores as in the case of BG1 endospores. The tryptophan-like peak is more pronounced in the case of the wet BC sample. The measurements were repeated multiple times with new

spore samples on pieces of filter paper. Figure 4.32 shows the PCA plot of the experiment performed four times with a different concentration of BC spores. There are 12 measurements with four of the dry spores (circles), four of the wet spores (triangles) and four of the redried spores (crosses). We show these 12 measurements on a plot of the first PC versus the second PC. In this case the data are clustered in almost two groups. The dry spores and the re-dried spores are well within one group which is well separated from the wet spores.

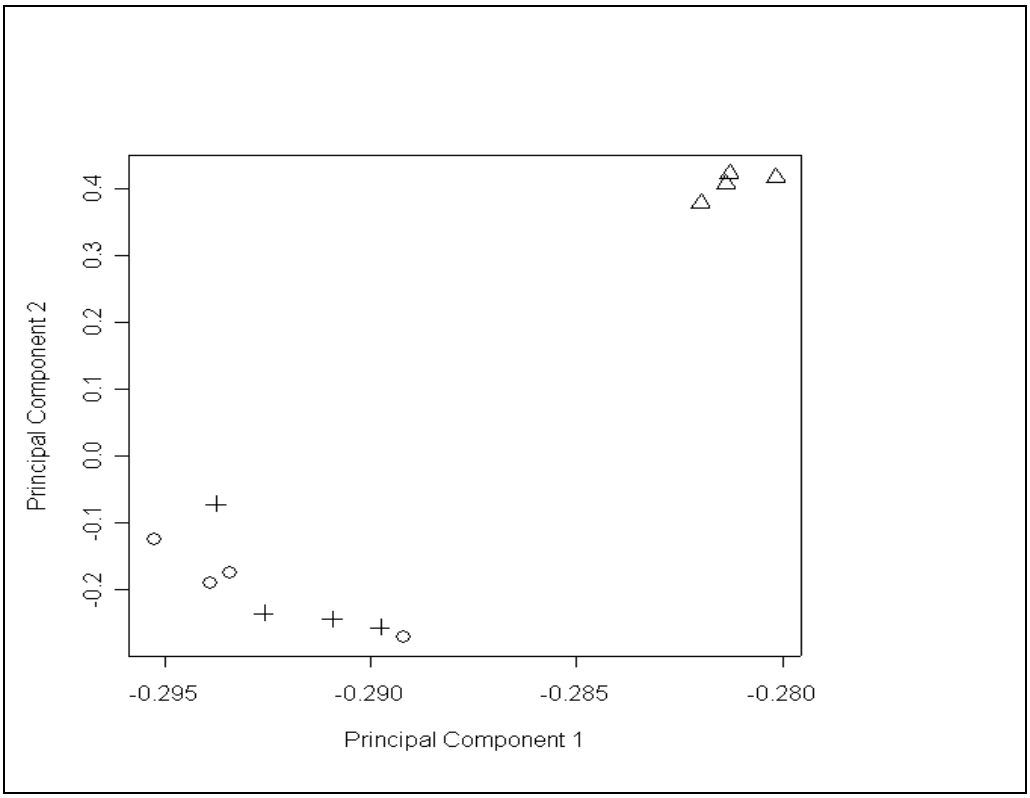

Figure 4.32: First PC versus the second PC for the 12 samples measured. The open circles are the original dry spores, the triangles are the hydrated spores and the crosses are the spores after being re-dried for seven days at room temperature. The excitation wavelengths are 280, 310, 340, 370, 400 and 430 nm.

4.2.3 Distinguishing wet *Bacillus* spore species from dry spores using PCA

In Figure 4.33 (A) we show the two-dimensional PCA plot (component one versus component two) of all the dry and wet samples of BG, BC and BT. Even though these samples contain a different concentration or hydration state of spores, one can see by the grouping of the data that the spore fluorescence signal is consistent and dependent on hydration state of a particular species of spores and therefore dominates in the analysis.

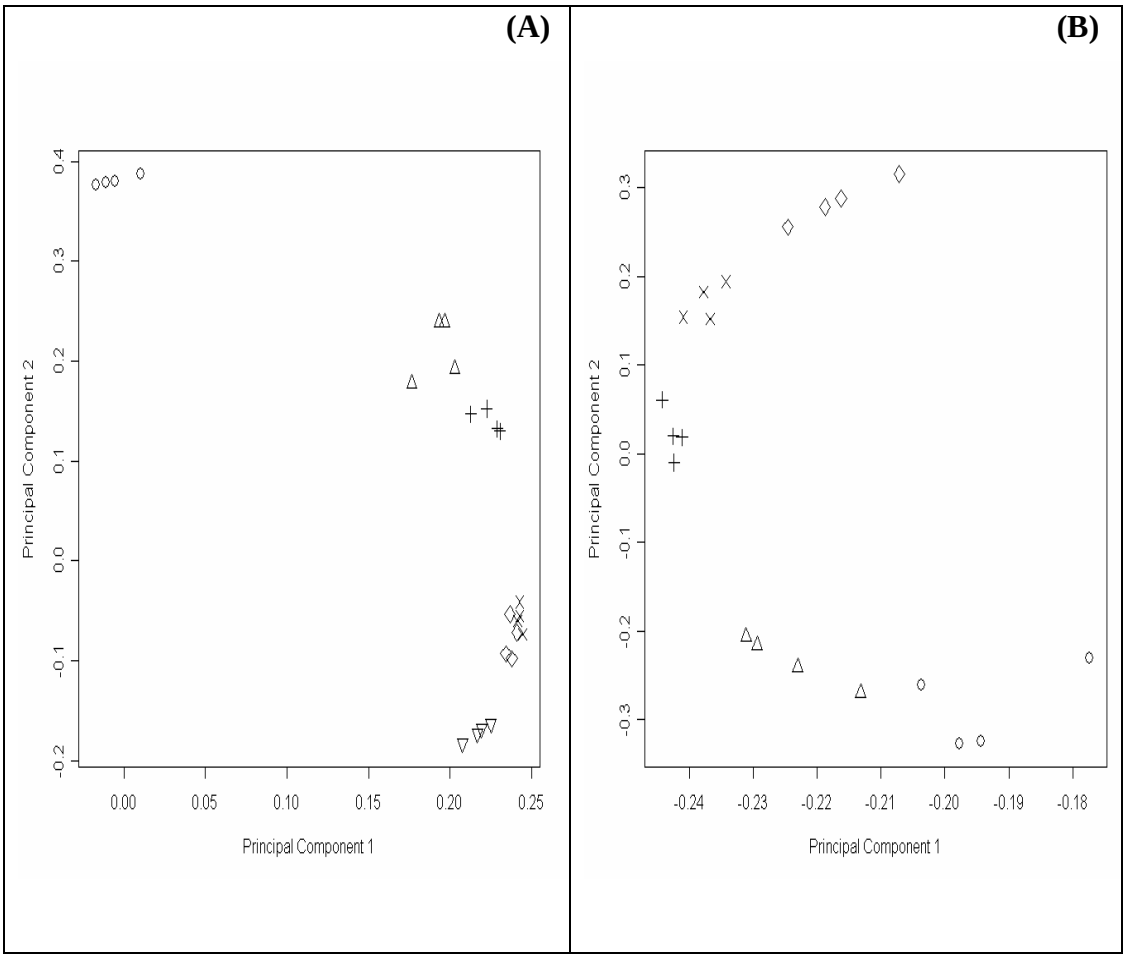

Figure 4.33: (A) The first PC versus the second PC for the 24 fluorescence measurements made on pieces of filter paper. The open circles are dry BG and triangles are wet BG. The plusses are dry BC and crosses are wet BC. The diamonds are dry BT and downward triangles are wet BT. **(B)** The first PC versus the second PC for the 20 measurements (excluding dry BG). The open circles are wet BG and triangles are dry BC. The plusses are wet BC and crosses are dry BT. The diamonds are wet BT.

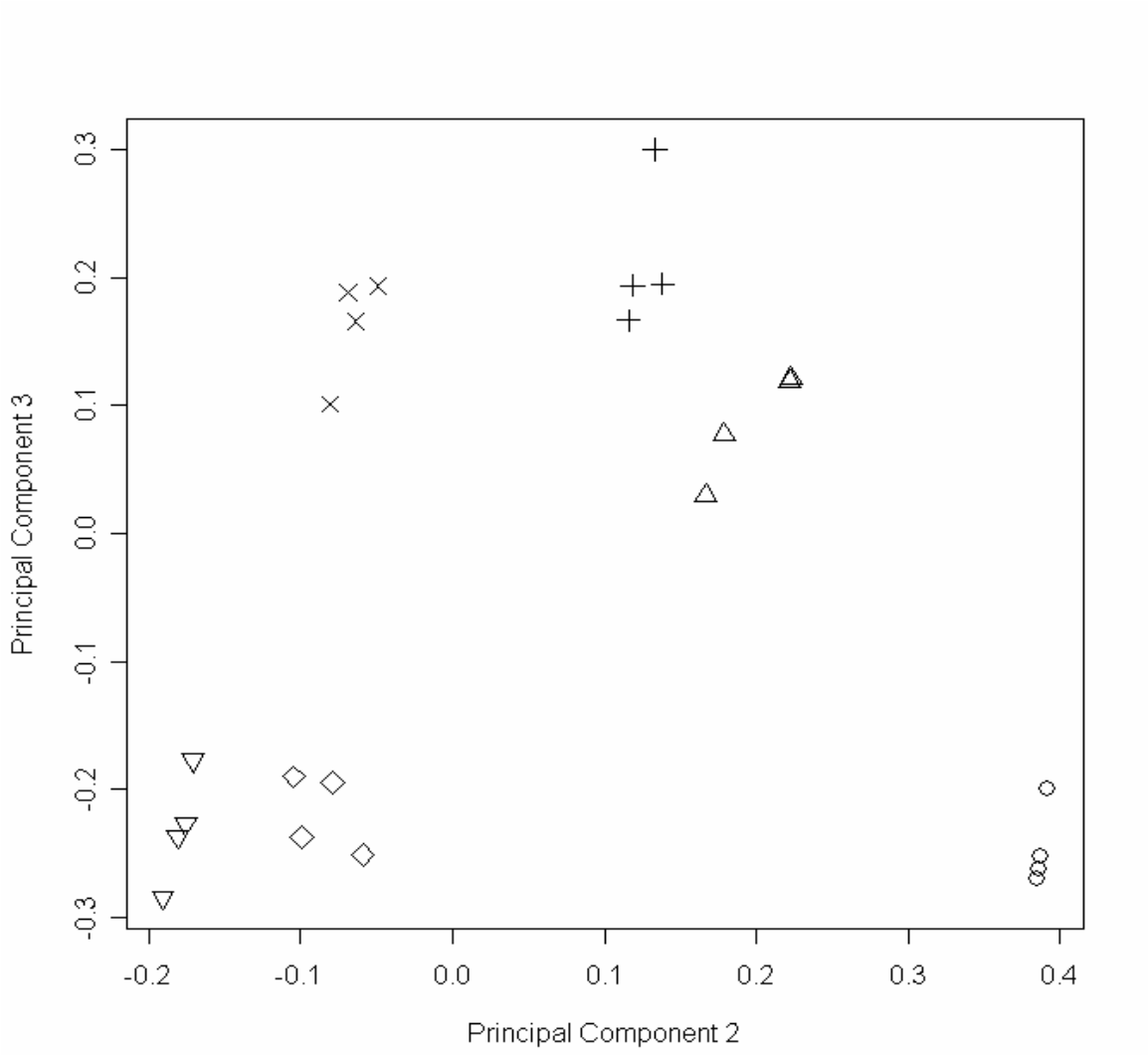

Figure 4.34: The second PC versus the third PC for the 24 fluorescence measurements made on pieces of filter paper corresponding to Figure 4.33(A). The open circles are dry BG and triangles are wet BG. The plusses are dry BC and crosses are wet BC. The diamonds are dry BT and downward triangles are wet BT

The first PC (horizontal axis in Figure 4.33(A)) explains the difference between the dry BG samples and the rest of the samples. This indicates that dry BG is very different from the other *Bacillus* spore samples and wet BG samples. Therefore, in Figure 4.33 (B) we show the PCA plot without including the dry BG spores. If we include the dry BG sample in the PCA, we notice that the third component (corresponding eigenvalue greater than one) also accounts for a significant contribution in this analysis as shown in Figures 4.34 and 4.35. One or two samples seem to show almost no change in PCs one and two when they are compared before and after hydration. If we look at the first three PCs, as shown in Figure 4.35, we can

see that significant changes along the third PC are seen before and after hydration for these samples. One can also see with the three PCs that the spore samples separate better than the first two PCs. As shown, the projection of the fluorescence spectra of the samples into the space of the first three instead of the first two PCs shows good separation between replicas. Since over 90% of the variance was captured within the first three PCs, we can be confident that differences in the samples scores are differences in the spore samples.

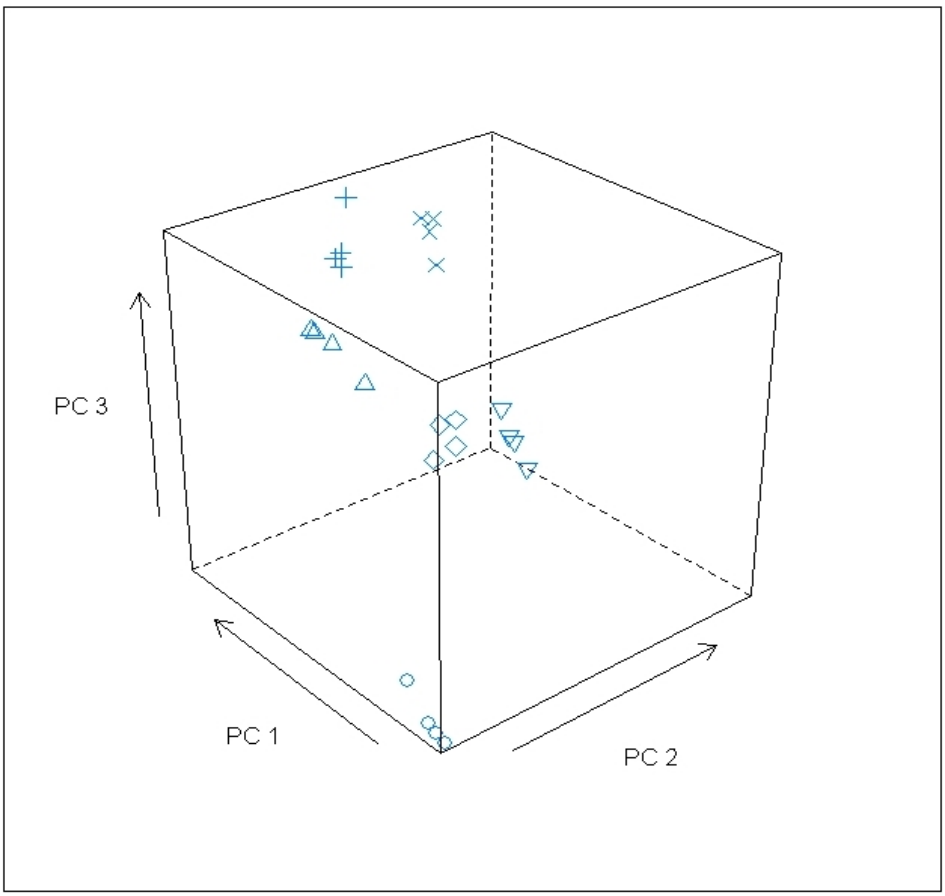

Figure 4.35: PCs one, two and three for the 24 fluorescence measurements (excitation from, 280 to 430 nm with 30 nm step) made on pieces of filter paper. The open circles are dry BG and triangles are wet BG. The plusses are dry BC and crosses are wet BC. The diamonds are dry BT and downward triangles are wet BT.

4.2.4 Fluorescence of *Bacillus globigii* spores in water suspension

Figure 4.36 shows the fluorescence two-dimensional excitation-emission profile of BG1 spores in suspension. Spores were suspended 15 minutes before the measurements were made to allow them to fully hydrate. The fluorescence profile is shifted to an excitation maximum at shorter wavelengths compared to dry and wet BG1 spores on filter paper as shown in Figures 4.21 and 4.23. It shows an additional bright emission peak near 300nm excitation and 400 nm emission wavelengths in addition to tryptophan-like fluorescence peak near 290 nm excitation and 340 nm emissions.

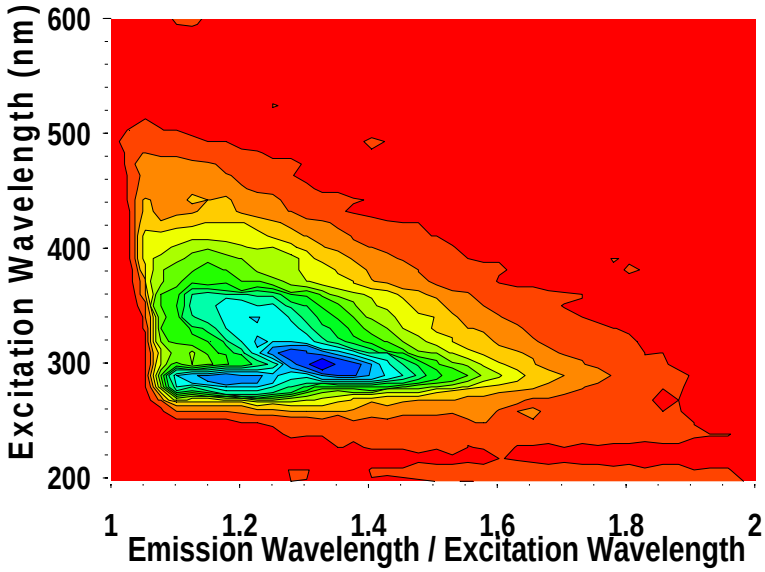

Figure 4.36: Fluorescence contour plot of BG1 endospores in suspension. The greatest intensity is blue and the least intensity is red.

.

We also repeated some of the multiwavelength fluorescence measurements in suspension (same sample) three times. With our scanning fluorometer, a full two dimensional fluorescence excitation/emission matrix requires more than 90 minutes to measure. We noticed photobleaching of the spore fluorescence around 340 nm at excitation 290 nm and slightly enhanced spore fluorescence around 400 nm at

excitation 300 nm. In Figure 4.37 we show the third measurement (after six hours in suspension) fluorescence profile of the same BG1 spores in suspension as shown in Figure 4.36.

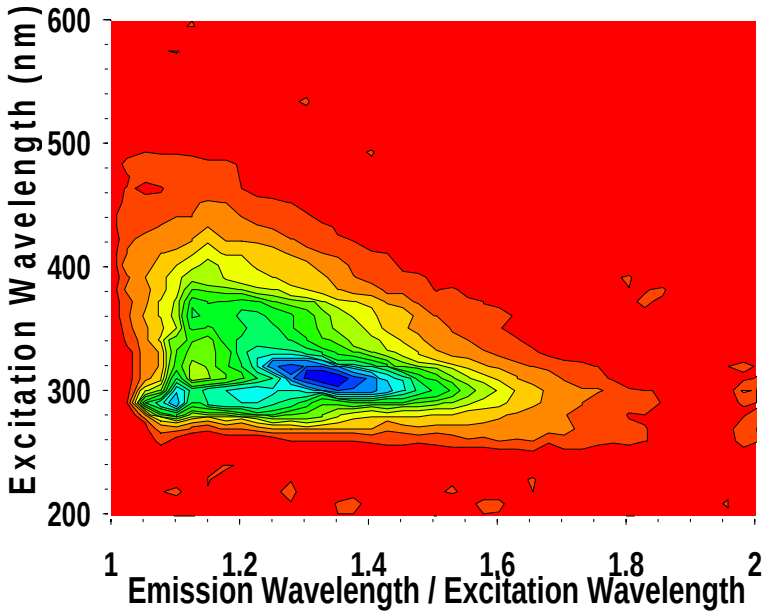

Figure 4.37: Third measurement (replicate) of multi wavelength fluorescence contour plot of BG 1 endospores in suspension. The greatest intensity is blue and the least intensity is red.

We also measured the fluorescence of milli Q deionized water that was used to suspend *Bacillus* spores. No fluorescence could be seen. However we could clearly see the familiar Raman peak of water (See Figure 4.2(A))

4.2.5 PCA analysis of *Bacillus globigii* spores in different hydration conditions

The measurements of BG1 spores in suspension were repeated nine times with new spore samples. The concentration of each sample was different. There are 27 total measurements with nine of the dry spores on filter paper (circles), nine of the wet spores on filter paper (plusses) and nine of the spores in suspension (triangles). We show these 27 measurements on a plot of the first PC versus the second PC in Figure 4.38. We also showed the output of the PCA results with major changes in selection parameters (selection of excitation wavelengths ranges for analysis). If we used six excitation wavelengths from 280 to 430 nm with step 30 nm as shown in the Figure 4.38(B), the data are separated in three groups. If we used three excitation wavelengths 280, 310 and 340 nm, the data are distinguished almost in two groups (see Figure 4.38(A)) with some overlap. From the figure, one can see that the fluorescence of spores changes very strongly with different environments or hydration states of the sample and the dry spore samples are well separated from wet spores on filter paper or spores in suspension, even if we choose different combinations of excitation wavelengths.

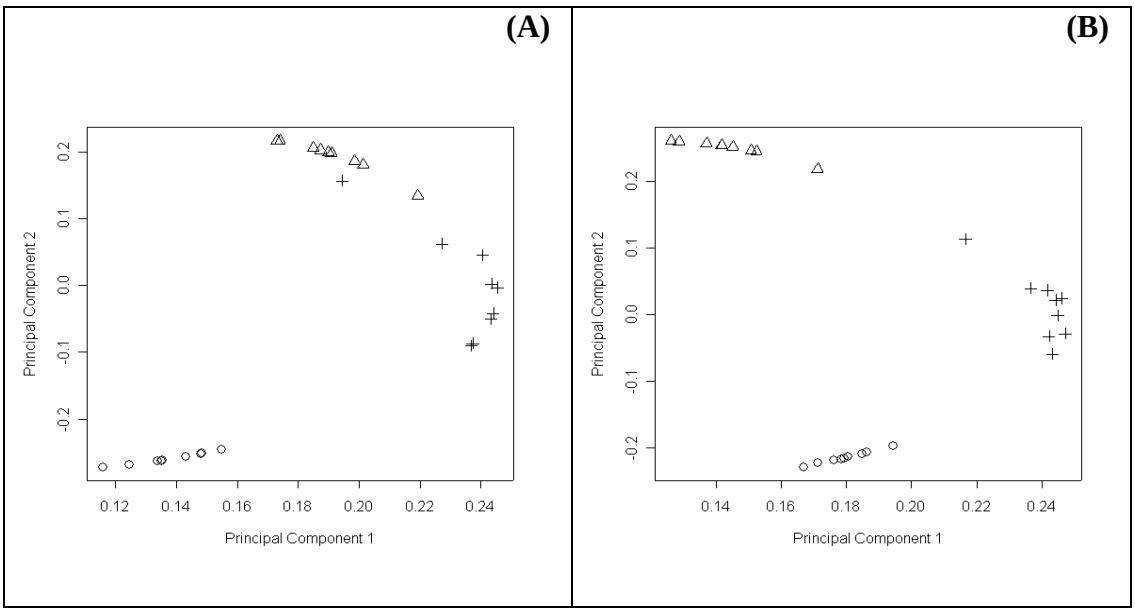

Figure 4.38: The first PC versus the second PC for 27 measurements. The open circles are the original dry spores, the triangles are the spores in suspension and the plusses are the wet spores on filter paper of the same dry samples. **(A)** three excitation wavelength, 280nm, 310nm and 340nm **(B)** six excitation wavelength, 280, 310, 340, 370, 400 and 430 nm.

4.2.6 Effect of Autoclaving and washing on spore fluorescence

In this study we tried to understand that fluorescence spectroscopy can be utilized to distinguish whether or not a sample of *Bacillus* spores has been washed and autoclaved. We measured the fluorescence fingerprint of the spores after the process of washing and autoclaving to see the changes in the fluorescence profile.

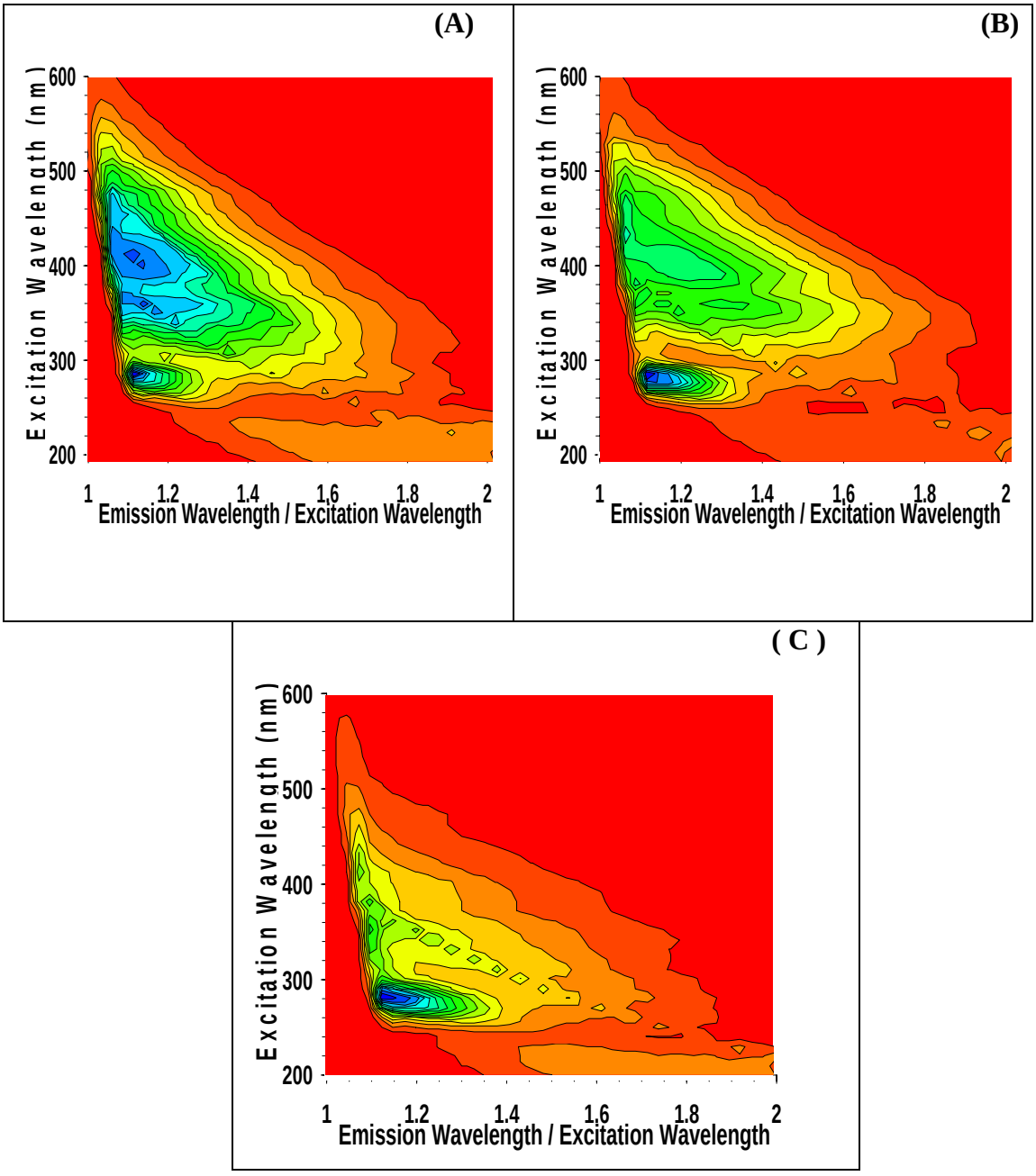

Figure 4.39: Fluorescence signatures from wet spores of BG2 on filter paper (A) before washing, (B) after washing, (C) after autoclaving (the washed spores)

Figure 4.39 shows the fluorescence fingerprint of the BG2 spores before and after washing three times by de ionized milli Q water. We also show the fluorescence profile of the same washed spores after autoclaved. For the discrimination of autoclaved from washed and untreated spores, fluorescence spectra were collected and grouped to give a set of six spectra each of untreated, washed and autoclaved samples. The resulting PCA score plot of BG2 spores, utilizing the first two components is shown in Figure 4.40. The spectra of autoclaved and washed samples are well separated from the untreated BG2 samples.

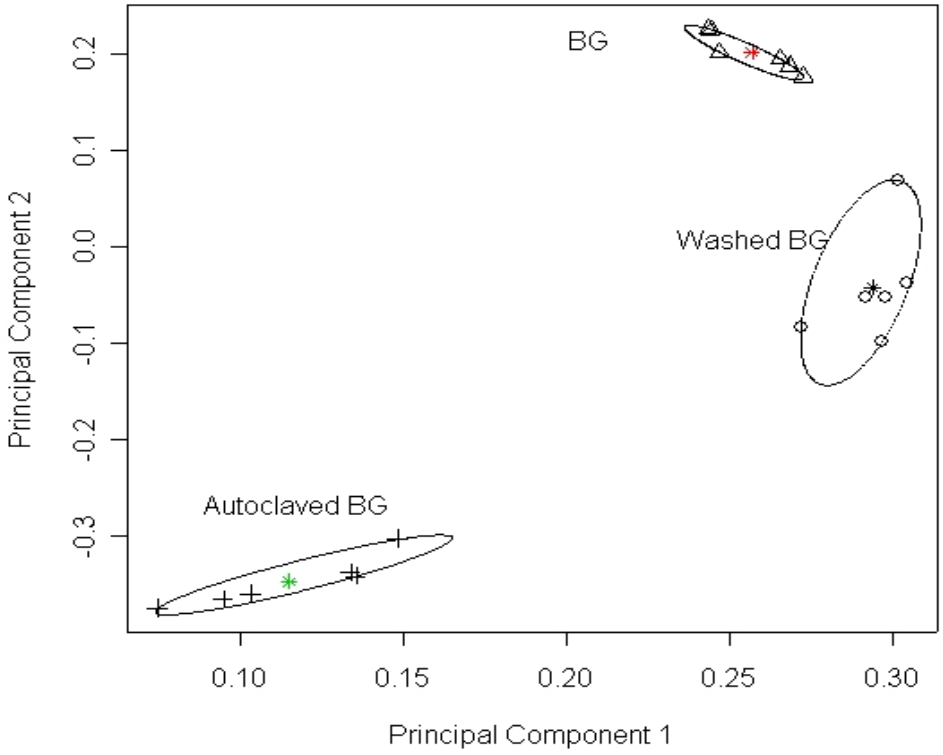

Figure 4.40: PCA scores plotted against the first two principal components for wet BG2 from data in Figure 4.39 illustrating the separation that exist between untreated samples, washed samples and autoclaved samples.

4.2.7 Principal Component analysis of fluorescence spectra from *Bacillus* spores species in water suspension

In this study, we tried to use PCA as a tool to understand and differentiate fluorescence results obtained from three closely related spore species of BG1, BS (+ DPA) and BC in water suspension. The 2-D fluorescence fingerprints of these samples are shown elsewhere in the thesis (see Figures 4.36, 4.43 and 4.56). PCA is used to extract spectral information that shows variance between the spore samples. In this study we selected six different excitation wavelengths, 280, 310, 340, 360, 400 and 430 nm, for spectral analysis. In Figure 4.41 we show the two dimensional PCA score plot of four samples of BG1, BS and BC. Using visual inspection, one can see that the three spore species are separated mainly along PC2.

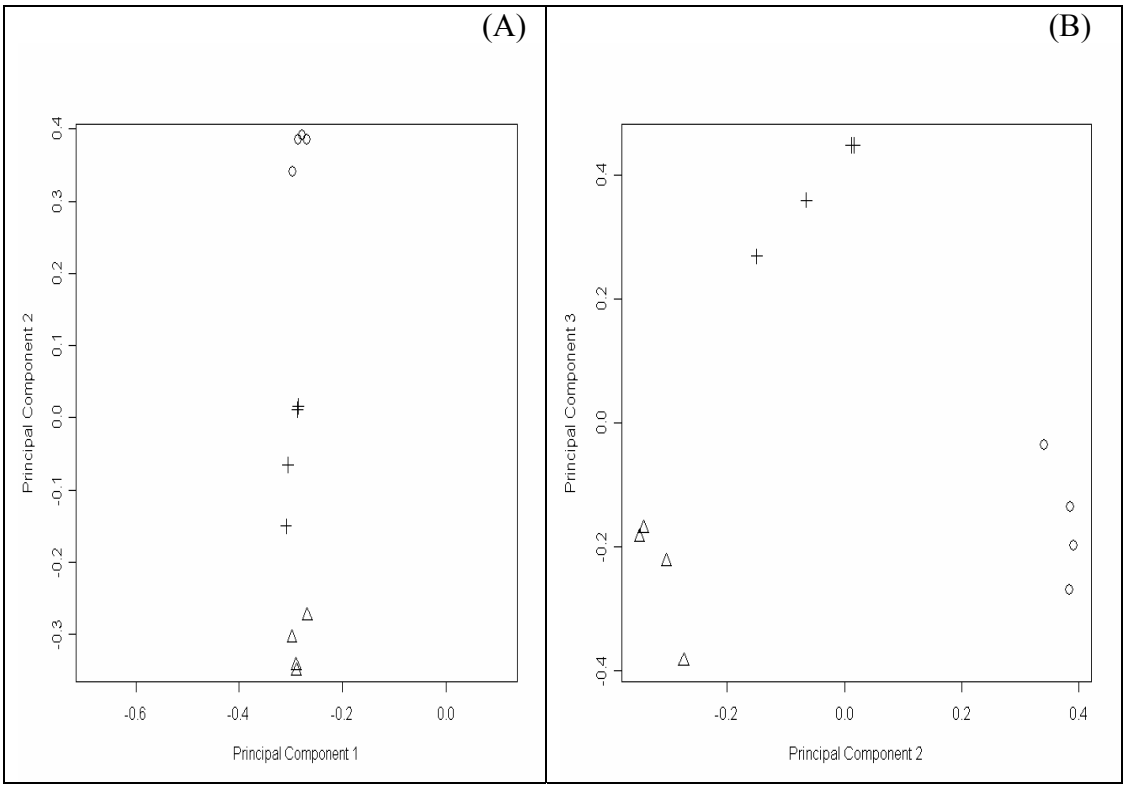

Figure 4.41: (A) PC1 versus PC2 **(B)** PC2 versus PC3 for the 12 fluorescence measurements of BG (circle), BS (plusses) and BC (triangles) spores in water suspension.

We also tried to physically interpret the obtained loading plots of PCs. Any PC accounting for a significant fraction of the total variance can be related to one or more underlying physical parameters, giving some physical insight. The corresponding loading plots of the PCs as shown in Figure 4.42 reveal the spectral profiles responsible for the distribution of the samples in the PCA score plot shown in Figure 4.41. BC spores have the well below the average score values and BG spores have the well above the average score values along PC2. PC2 has mainly contributed to differentiate between the three species of *Bacillus* spores. This separation is mainly due to CaDPA, as it can be seen from the large loadings around 300 nm excitation wavelengths and around 400 nm emission wavelength (see Figure 4.42(B)). CaDPA is likely to be the main contribution in PC2, because of the similarity between PC2 loading vector and the fluorescence profile of this chemical component. (The position and shape of loadings indicate that CaDPA was the most influential component in PC2). Tryptophan is likely to be the main contribution in PC1, because of the similarity between PC1 loadings and the fluorescence spectrum of this compound.

The general shape of fluorescence signal contribution from tryptophan is not much related to the type of spore species in suspension. This explains why the three types of *Bacillus* species cannot be distinguished along PC1 (see Figure 4.41(A)). This result also supports other studies that the fluorescence emission spectra for several species of bacterial spores in water suspension excited by 280 nm light (tryptophan region) appeared quite similar to each other.[27] Unlike PC2, PC1 does not distinguish well between the three species of *Bacillus* spores, meaning that the PCA model cannot distinguish the spore species in water on the basis of their tryptophan content.

As we indicated elsewhere, Raman spectra are a major interfering factor for the fluorescence measurements of samples and fluorophores in water. The arrow in Figure 4.42 (D) shows the Raman scattering-like component in the data set. We also noticed raman spectral features in the PCs analyzed at single excitation wavelength and looks similar to the Raman-like peak. It is evident from the shape of the loading vector of PC4 that the Raman scattering component in the measured fluorescence spectra of the samples can be separated from the strong fluorescence signal. PCA worked properly for the separation of various components, including the Raman spectra from the data set.

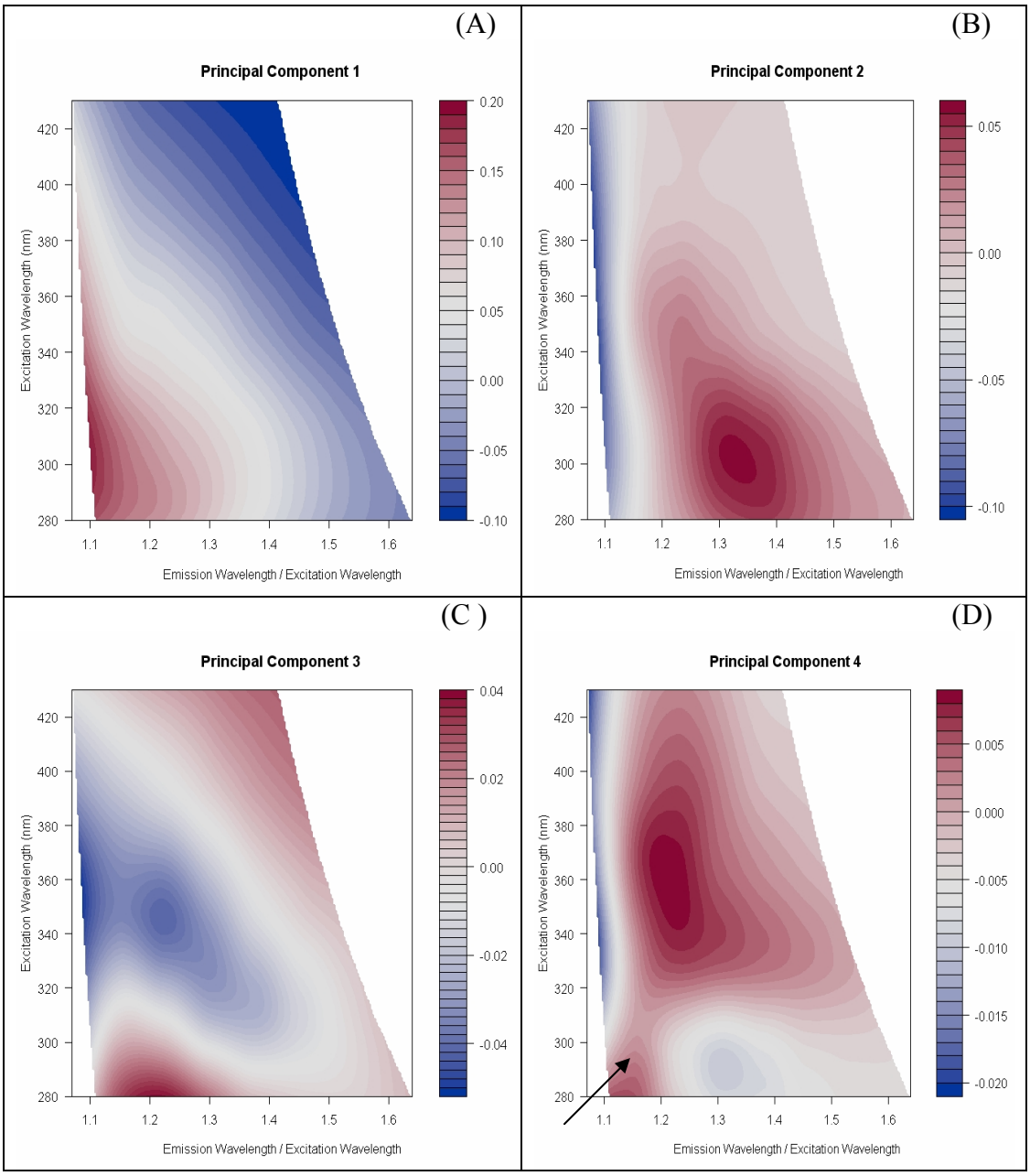

Figure 4.42: Contour plot of the Loading spectra of the (A) first and (B) second (C) third and (D) fourth principal components from fluorescence emission spectra of spore species in water suspension.

4.3 Multi wavelength fluorescence studies on *Bacillus* spores in water under enhanced UV irradiation

4.3.1 Fluorescence studies of *Bacillus* subtilis spores with and without (lack) of dipicolinic acid

A 2-D multiwavelength fluorescence spectra of the unirradiated (+DPA) BS spores in aqueous suspension is shown in Figure. 4.43. Comparing this to the 2-D graph of a dry tryptophan in Figure. 4.20 and tryptophan solution in Figure 4.17, we see that the major peak in this case, from excitation at around 280 nm and peak emission at around 330 nm arises from tryptophan. After exposing the suspension to our broad-band UV irradiation of 80 J (15 minutes exposure) , the fluorescence spectrum changes substantially as seen in Fig. 4.44. The tryptophan peak almost disappears due to photoconversion of the tryptophan to a non-fluorescent form. The same thing happens to the pure tryptophan solution after exposure to UV light as shown in Figure 4.18 and also in the case of dry tryptophan. But interestingly a new peak has appeared as shown in Figure 4.44.

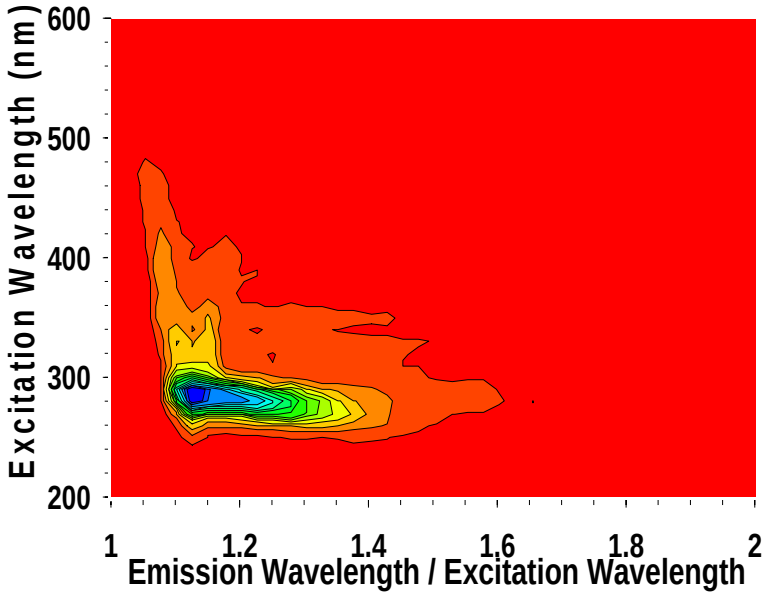

Figure 4.43: Fluorescence spectrum of BS spores (+DPA) in water without UV irradiation. The greatest intensity is blue and the least intensity is red.

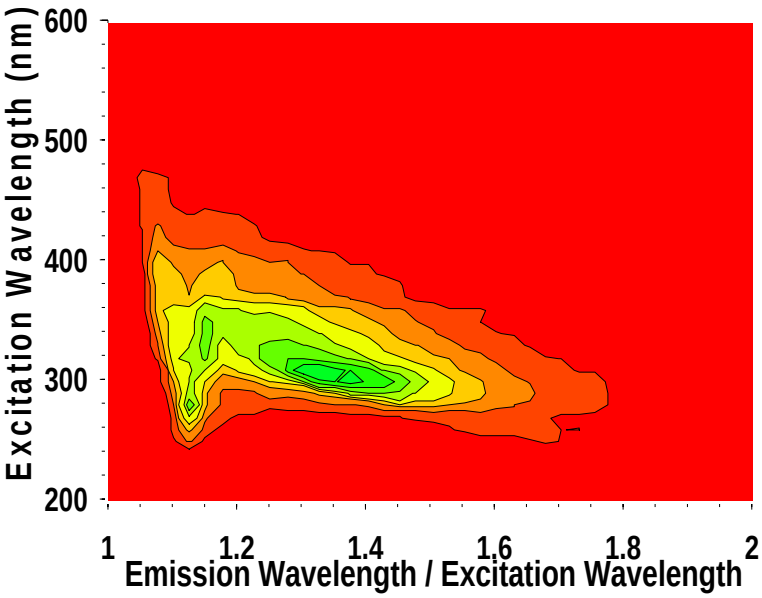

Figure 4.44: Fluorescence spectrum of standard UV irradiated (15minutes) BS spores (+DPA) in water. The greatest intensity is blue and the least intensity is red.

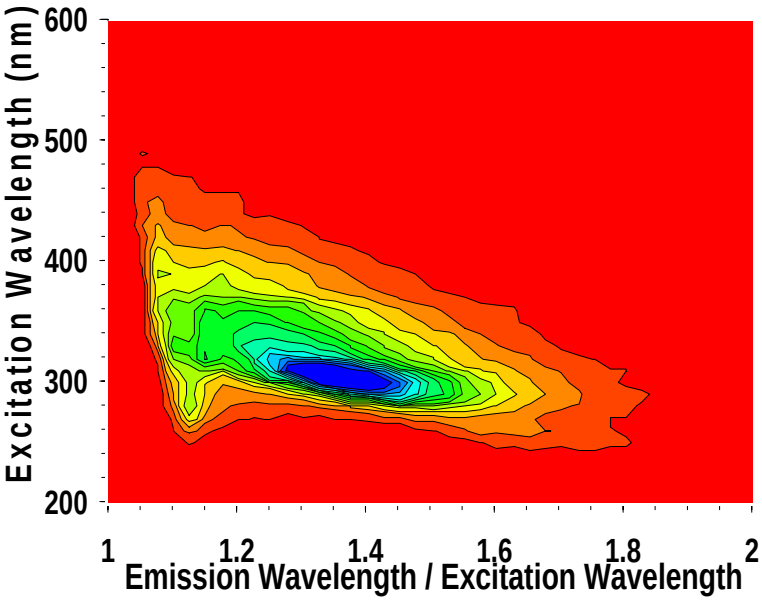

Figure 4.45: Fluorescence spectrum of additional UV irradiated (15 minutes) BS spores (+DPA) in water. The greatest intensity is blue and the least intensity is red.

By comparing the graph with that for CaDPA (see Figures 4.8, 4.11 & 4.13), we see that the major peak for CaDPA at around 300 nm excitation becomes pronounced for the irradiated (+DPA) spores. Further, by comparing the graph with that for dry pure DPA (see Figure. 4.5(A)), we see additional fluorescence in the region where dry DPA fluoresces. In Figure 4.45, the 2-D fluorescence spectrum for the (+DPA) spores after an additional 80 J UV irradiation is shown. The tryptophan peak has completely disappeared and most of the fluorescence from the region where dry pure DPA fluoresces (~400 nm excitation) and that the CaDPA peak was enhanced.

A 2-D fluorescence profile of a similarly prepared aqueous suspension of unirradiated (–DPA) BS spores is shown in Figure. 4.46 and the fluorescence profile for the same suspension after exposure to our broad band UV irradiation for 15 minutes (80 J) is shown in Figure 4.47. In Figure 4.48, the fluorescence spectrum of the (– DPA) spores after an additional 80 J UV irradiation is shown.

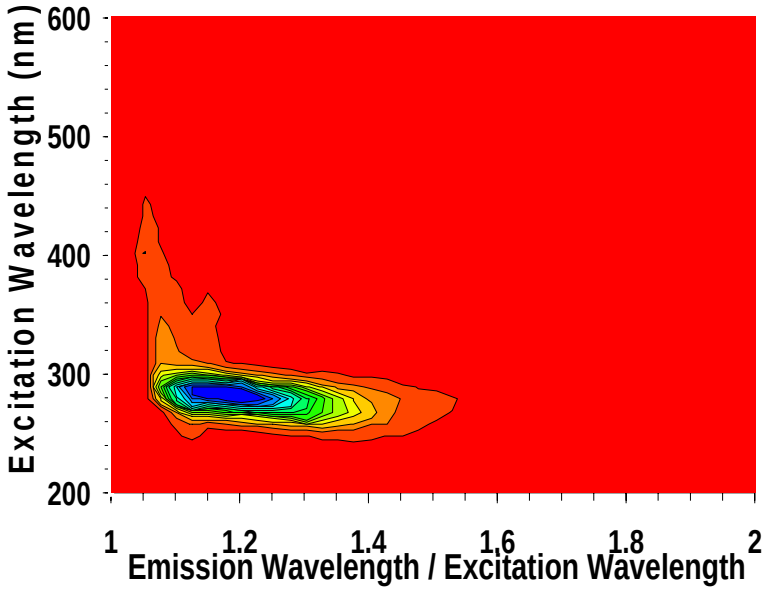

Figure 4.46: Fluorescence spectrum of BS spores (–DPA) in water without UV irradiation. The greatest intensity is blue and the least intensity is red.

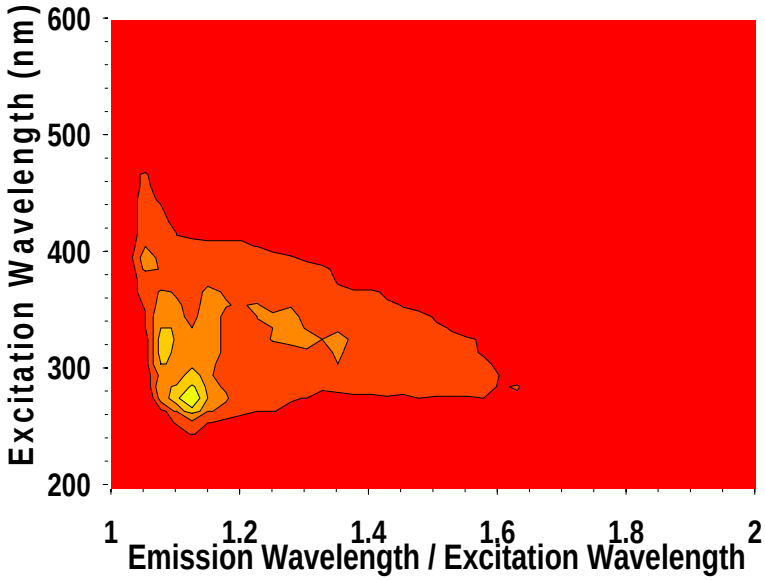

Figure 4.47: Fluorescence spectrum of standard UV irradiated (15minutes) BS spores (+DPA) in water. The greatest intensity is yellow and the least intensity is red.

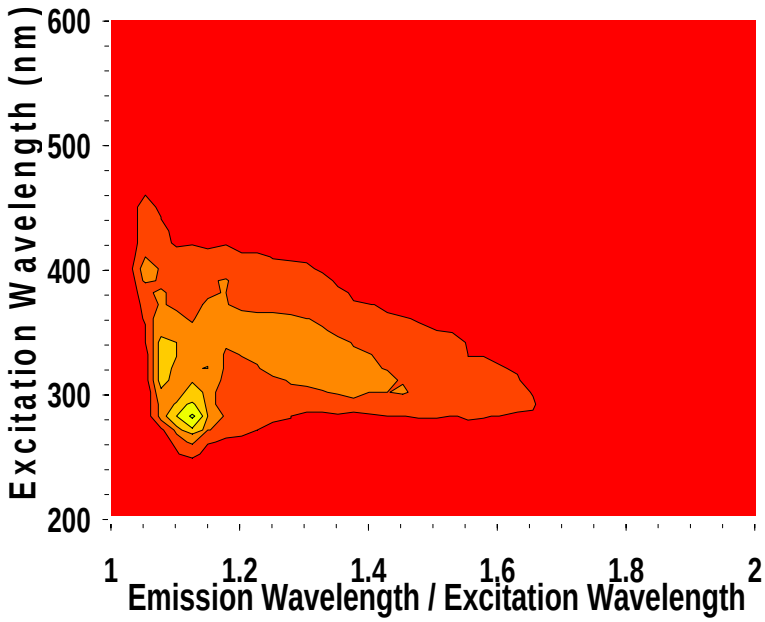

Figure 4.48: Fluorescence spectrum of additional UV irradiated (total 30 minutes) BS spores (–DPA) in water. The greatest intensity is yellow and the least intensity is red.

The unirradiated sample again shows the peak attributable to tryptophan. We also note that the tryptophan peaks in Figures 4.43 and 4.46 are different might be due to the contribution of fluorescence from CaDPA in the case of (+DPA) spores (since tryptophan and CaDPA fluoresce around the same excitation wavelength region). Figure 4.47 shows this peak disappears after our broad band UV irradiation, but the features attributable to CaDPA as seen in Figures 4.44 and 4.45 for the (+DPA) spores after irradiation did not appear. In this case, additional emission bands in the visible (DPA region) region also do not appear. We did not even observe any changes after an additional UV irradiation for 15 minutes as shown in Figure 4.48.

The measurements of (+DPA) and (–DPA) spores were repeated multiple times with new spore samples in water suspension. All these measurements were done before and after irradiation of broadband UV. Figure 4.49 shows the PCA plot of the experiment performed three times in water suspension. We selected six different excitation wavelengths, 280, 310, 340, 370, 400 and 430 nm, for spectral analysis. There are 12 total measurements with six of the (+DPA) spores in suspension (UV and without UV) and six of the (–DPA) spores in suspension (UV and without UV). We show these 12 measurements on a plot of the first PC versus the second PC. The data are separated based on each strain of BS spores and the discrimination of these strains was pronounced after UV irradiation. From the figure, one can clearly see that the (+DPA) spores are separated from the (–DPA) spores even before exposure to broad band UV irradiation.

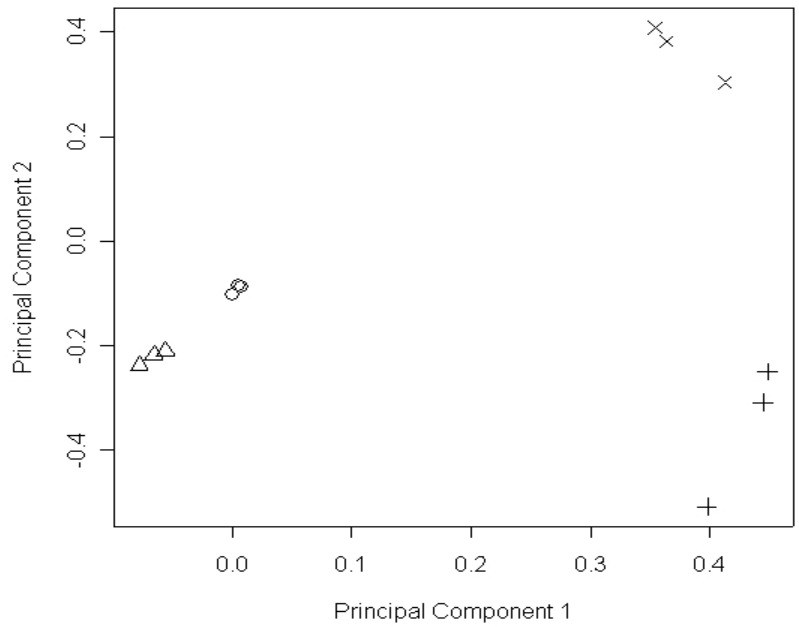

Figure 4.49: The first PC versus the second PC for the 12 fluorescence measurements made on both strains of B.sub spores (+DPA) and (–DPA) in suspension before and after broad band UV irradiation for 15 minutes. The circles are (+DPA) spores and the triangles are (–DPA) spores before UV irradiation. The plusses are (+DPA) spores and the crosses are (–DPA) spores after UV irradiation.

4.3.2 Identifying components of the UV-Vis fluorescence of *Bacillus globigii* spores

Figure 4.50 shows the 2-D fluorescence profile of the mixture of tryptophan and CaDPA in wet form. The sample preparation was explained in the material and method section. The two bright peaks appearing in this plot look similar to the 2-D fluorescence spectra of BG1 spores in suspension as shown in Figure 4.51. We identified CaDPA as a probable major component of BG1 spore fluorescence along with tryptophan. Since we could not find the exact amount of tryptophan and CaDPA inside the BG1 spores, we mixed the samples of tryptophan and CaDPA with different combinations of concentration. After we tried different weighed amounts of tryptophan and CaDPA, it was established that the best results were obtained at certain stage (the amount of CaDPA exceeds by a factor of 10 by weight from tryptophan). If one of the components predominates in producing fluorescence, the other component would be masked by this component. If two components are approximately producing the same fluorescence, we could see the two different peaks corresponding to each of these components as shown in Figure 4.50.

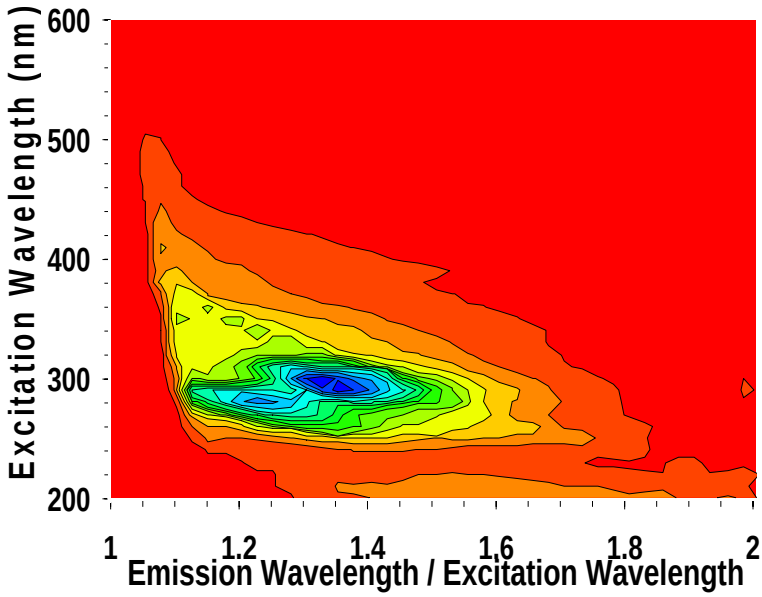

Figure 4.50: Fluorescence spectrum of the mixture of tryptophan and CaDPA wet paste on filter paper. The greatest intensity is blue and the least intensity is red.

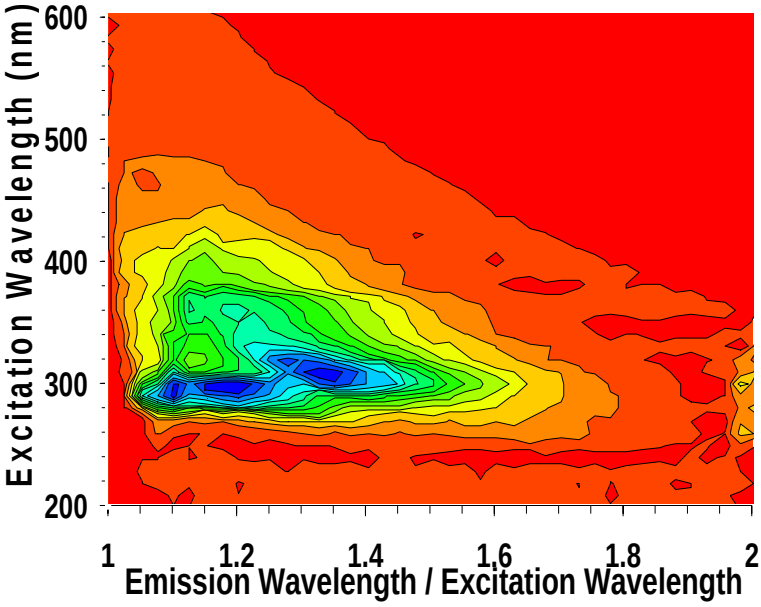

Figure 4.51: Fluorescence contour plot of BG 1 endospores in suspension. The greatest intensity is blue and the least intensity is red.

In most of the other *Bacillus* spores, the CaDPA fluorescence is probably masked by tryptophan. After exposed to broad band UV, we could clearly see the enhanced CaDPA fluorescence peak in all the spore samples in suspension. For convenience, figures will be shown in the following sections.

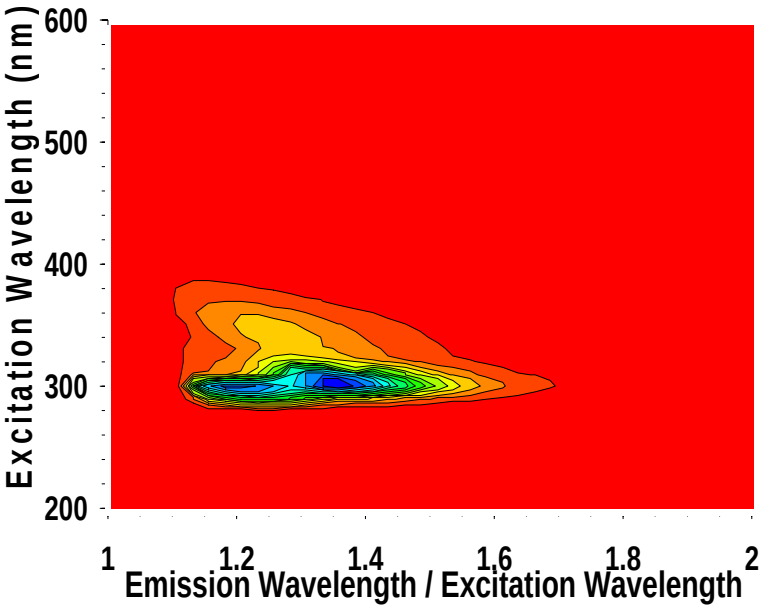

Figure 4.52: Fluorescence spectrum of the mixture of tryptophan and CaDPA in water. The greatest intensity is blue and the least intensity is red.

We identified the major likely components of BG1 fluorescence. In Figure 4.52 we show the fluorescence profile of the mixture of tryptophan and CaDPA in water solution. From these obtained results, we show that these components exist in a nearly wet state or as a wet paste in the spore and CaDPA is the another major fluorophore component along with tryptophan in this study. We could not see any major changes in the dry state and wet paste of the spectrum of the mixture other than the intensity changes. Changes in the fluorescence and absorbance of BG1 spores after exposure to UV irradiation is consistent with changes in the CaDPA fluorescence and absorbance after irradiated to UV (see Figures 4.15, 4.10**,** 4.53 and 4.54).

4.3.3 Fluorescence studies of *Bacillus globigii* spores

In order to further understand and characterize the peaks in the fluorescence spectra of BG were related to CaDPA and tryptophan, the effect of UV irradiation on the fluorescence spectra of BG spores was studied. The fluorescence fingerprint of the BG1 spores in aqueous suspension is presented in Figure 4.51. After exposing the suspension to our broad-band UV irradiation of 80 J, the fluorescence profile changes dramatically as seen in Figure 4.53. The peak intensity (CaDPA region) has been enhanced by a factor of six by the broad band of UV exposure for 15 minutes. The tryptophan peak photo bleached. We also show the changes in the absorption spectra of these samples in Figure 4.54. The changes are very similar to the changes of absorption of CaDPA solution before and after broad band UV irradiation (see Figure 4.3 in section 4.1)

We have observed similar results in the case of BS spores in the previous section. We have also seen the similar results in all of our measurements on other *Bacillus* spores in suspension.

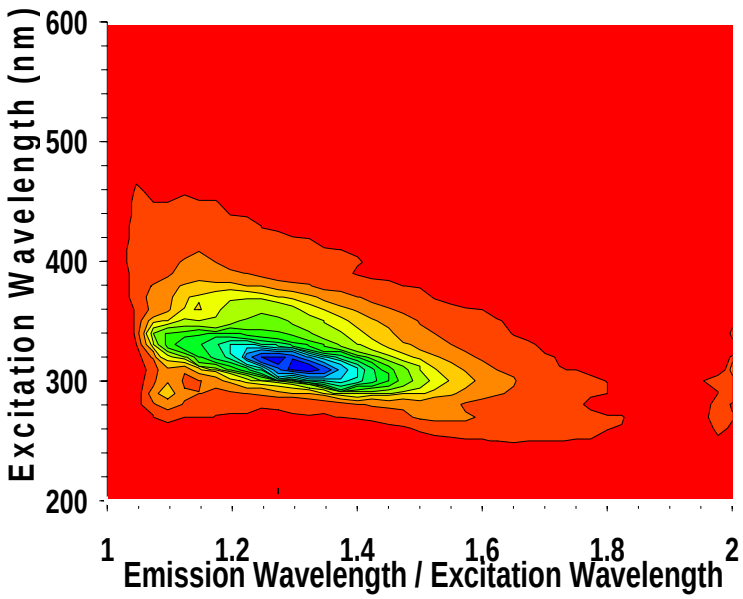

Figure 4.53: Fluorescence spectrum of standard UV irradiated (15minutes) BG1 spores in suspension (of the same sample suspension as shown in Figure 4.51). The greatest intensity is blue and the least intensity is red.

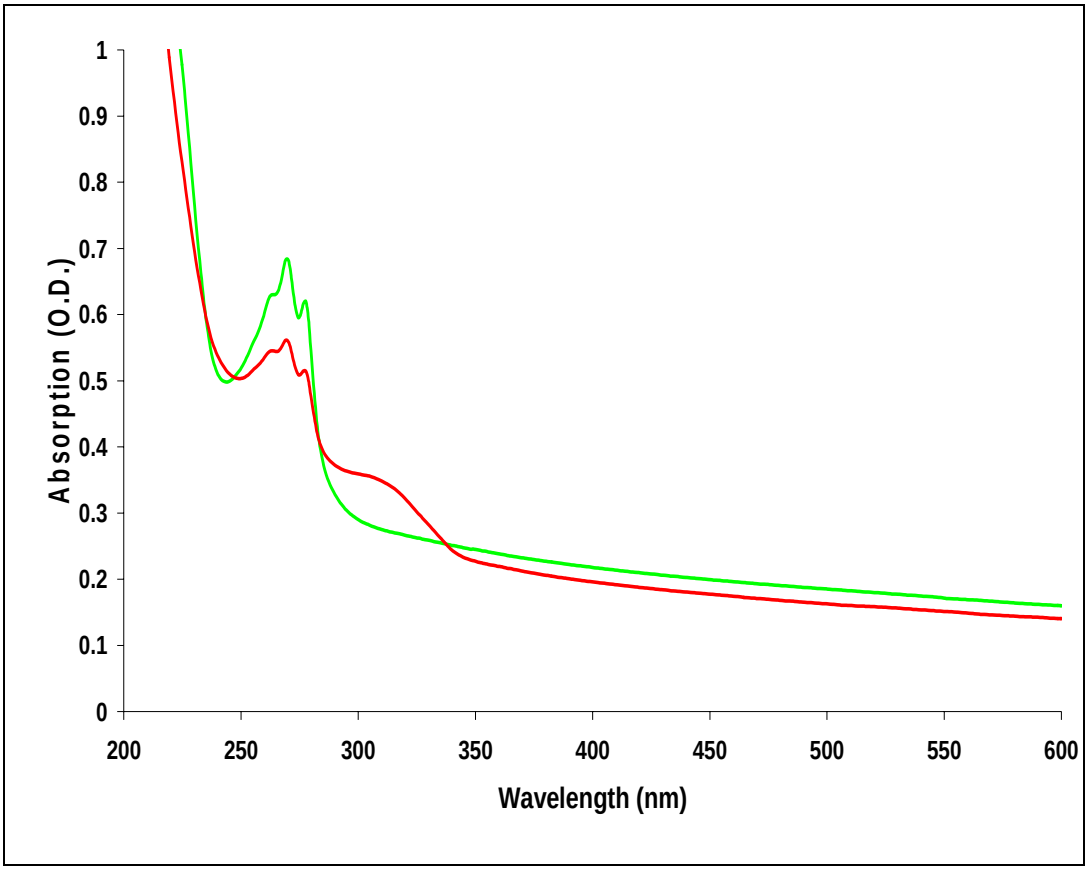

Figure 4.54: The absorption spectra of BG1 in water suspension before exposure to UV light (green) and after exposed to about 80 J of UV light (red)

Figures 4.55 shows the results of a similar experiments performed with BG2 and BG3 spores. After exposing the spore suspension to the broad-band UV irradiation, the fluorescence spectrum changes dramatically in all *Bacillus* spore samples in this study. The tryptophan peak disappeared and a bright peak of CaDPA (at around 300 nm peak excitation and 410 nm peak emission) has appeared in all the spore samples.

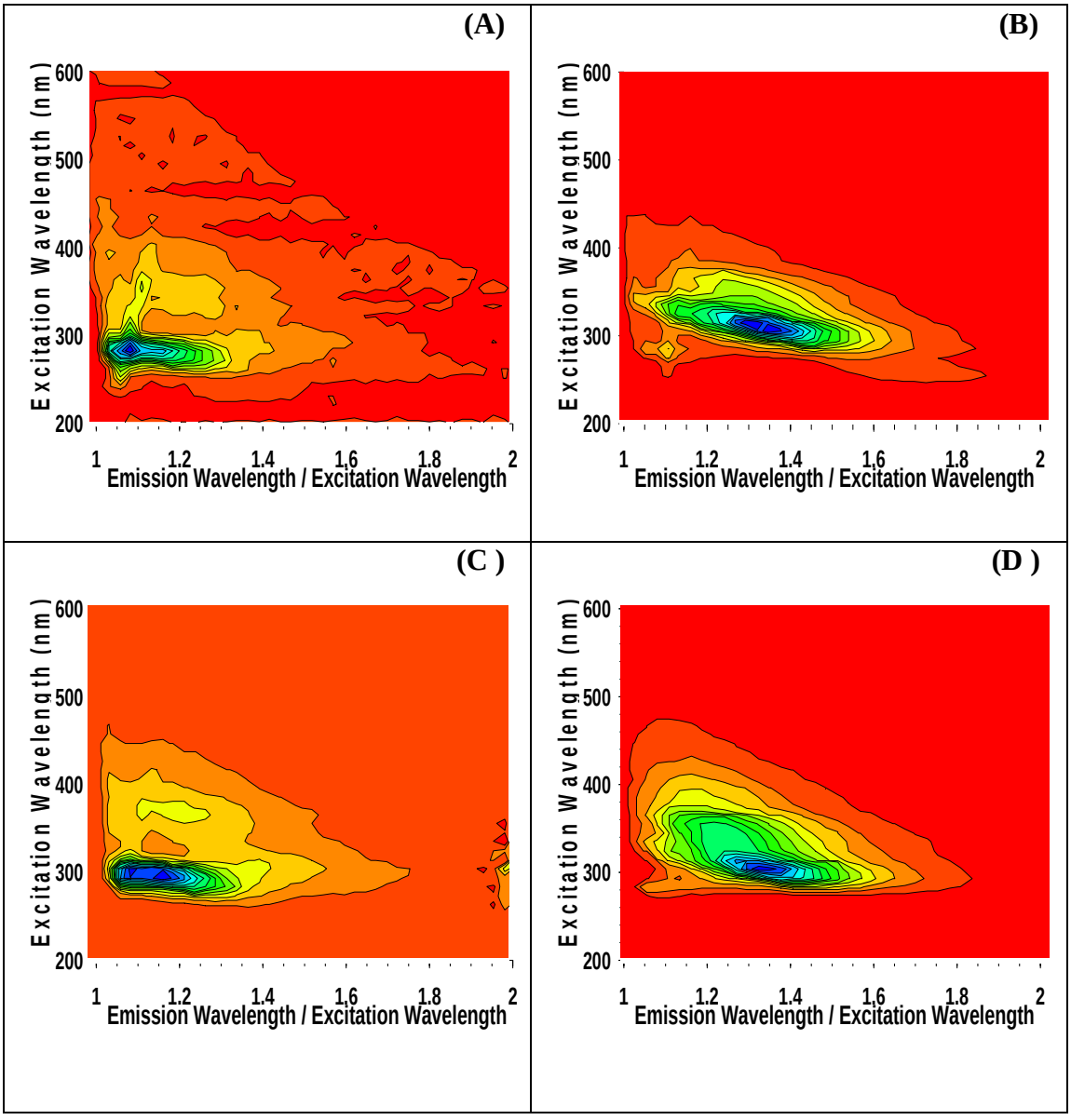

Figure 4.55: Fluorescence signatures from BG3 in suspension (A) before UV, (B) after UV and BG2 in suspension (C) before UV and (D) after UV. The greatest intensity is blue and the least intensity is red.

4.3.4 Fluorescence studies of *Bacillus cereus* spores

Figures 4.56 and 4.57 show the results of a similar experiments performed with BC spores.

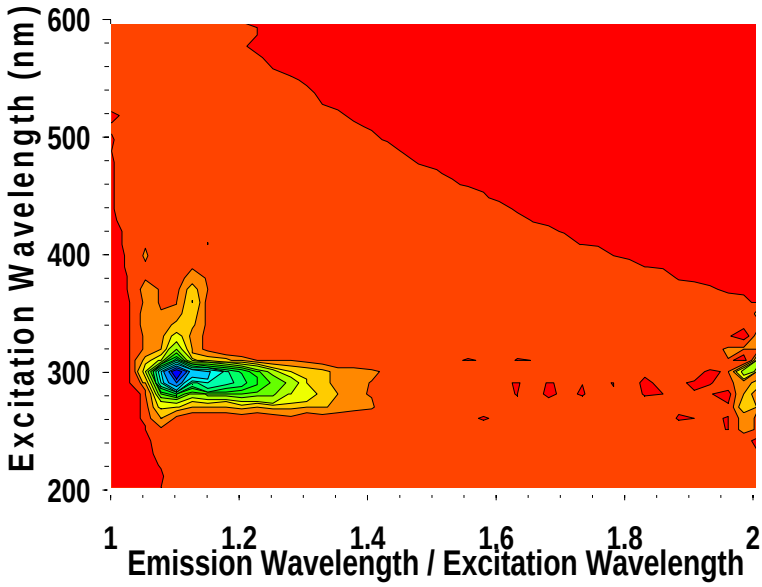

Figure 4.56: The Fluorescence contour plot of BC spores in suspension. The greatest intensity is blue and the least intensity is red.

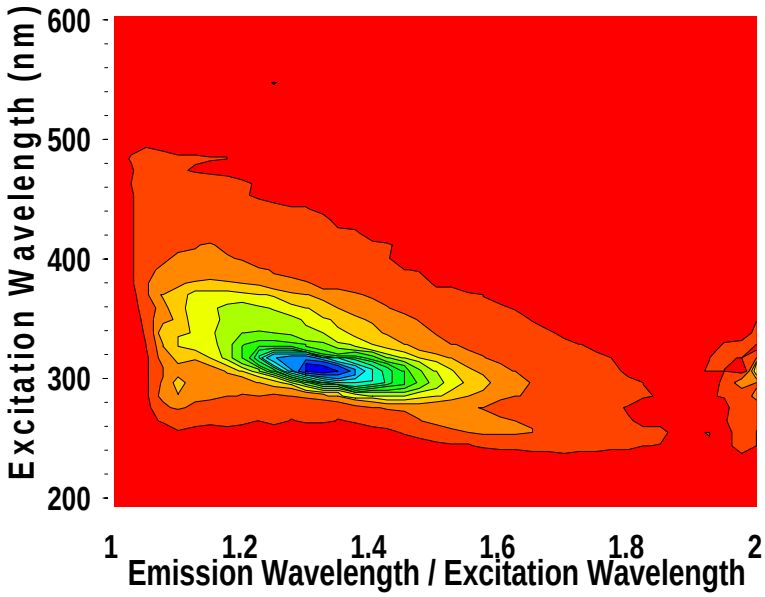

Figure 4.57: Fluorescence spectrum of broad band UV irradiated (15minutes) BC spores in water. The greatest intensity is blue and the least intensity is red.

4.3.5 Fluorescence studies of *Bacillus thuringiensis* spores

Figures 4.58 and 4.59 show the results of a similar experiments performed with BT spores.

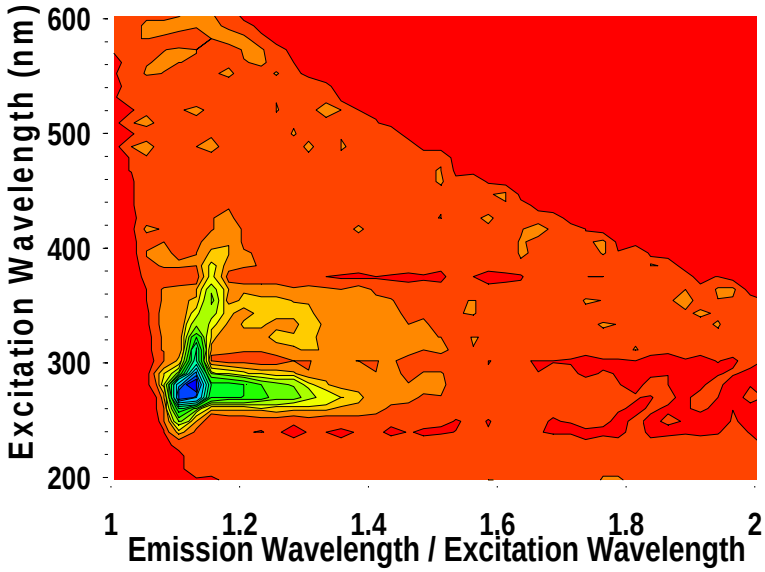

Figure 4.58: The Fluorescence contour plot of BT spores in suspension. The greatest intensity is blue and the least intensity is red.

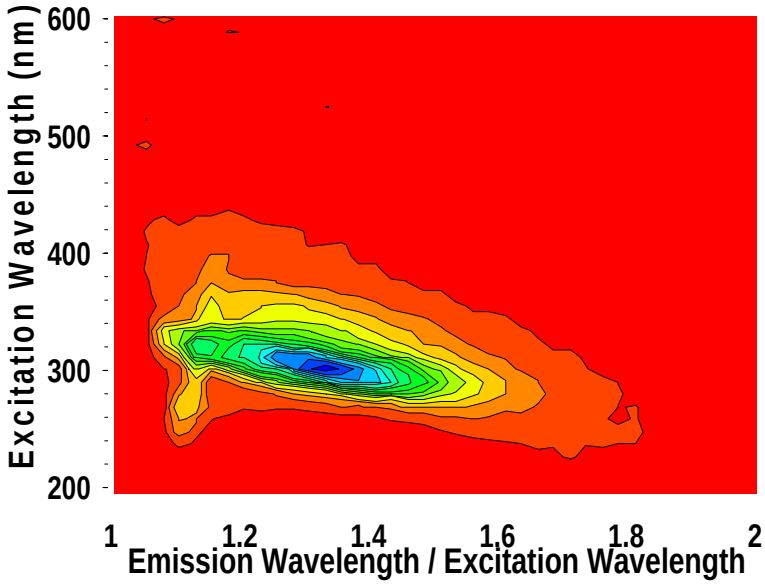

Figure 4.59: Fluorescence spectrum of broad band UV irradiated (15minutes) BT spores in water. The greatest intensity is blue and the least intensity is red.

Figure 4.60 shows the conventional individual fluorescence spectra, of BG1, BS (+DPA) and BC spores in suspension and the enhancement of fluorescence after UV irradiation at excitation wavelength 300nm. We note that the general shape of the emission spectra of these spore species appear rather similar after exposed to broad band UV irradiation but there are noticeable differences before exposure to broad band UV. We also note that there is a measurable amount of fluorescence in the range of 400- 440 nm in the case of BG and BS (+DPA) spore samples but not in the case of BC spores before exposing the samples to broad band UV.

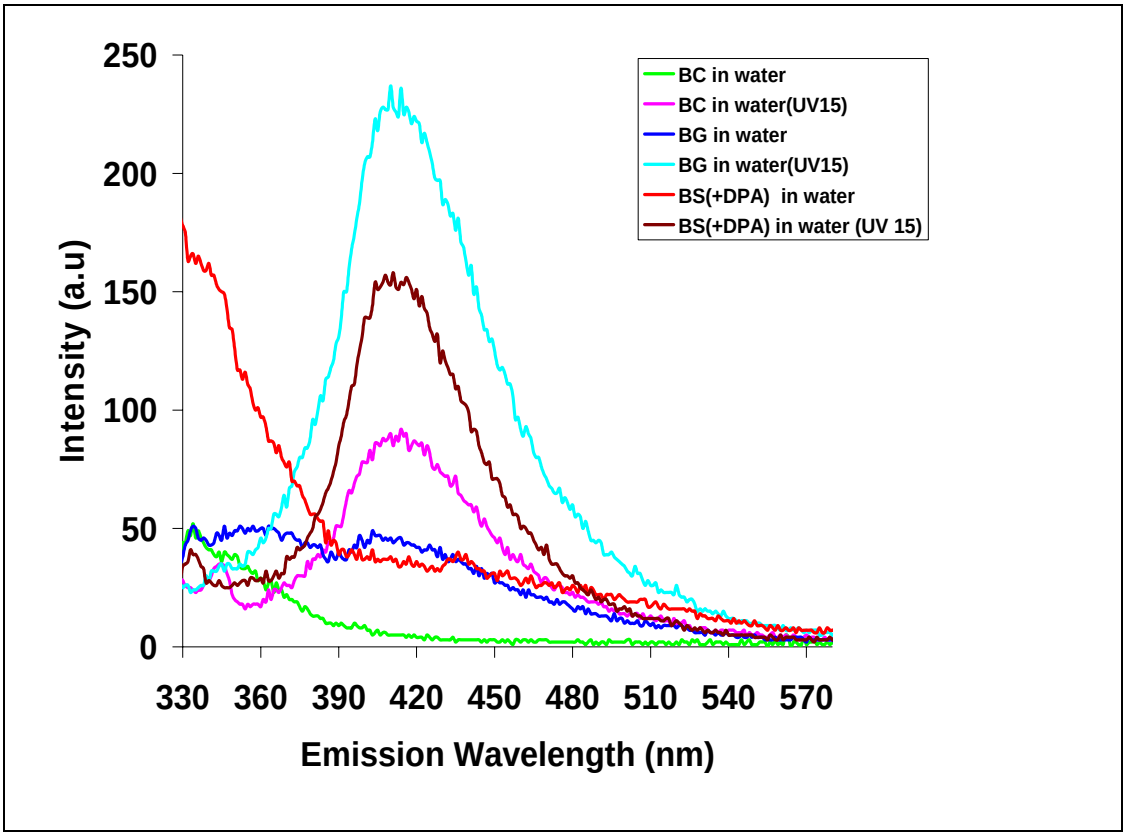

Figure 4.60: The conventional fluorescence emission spectra, excited at 300nm, of BG, BS(+DPA) and BC spores in water suspension before and after exposure to broad band UV light (80 J).

4.3.6 Distinguishing *Bacillus* spores from other biological samples using fluorescence

4.3.6.1 *pigweed*

In order to further gain some insights into the nature of the fluorophores responsible for the spectral changes in *Bacillus* spores and to characterize the unique fluorescence signal from *Bacillus* spores, we also studied some common biological samples in the environment under similar experimental conditions. A fluorescence spectrum of pollen green, pig weed in suspension before and after the broad band UV irradiation for 15 minutes are shown in Figure 4.61. We could not notice any enhancement of fluorescence after UV irradiation other than the suppression of tryptophan peak.

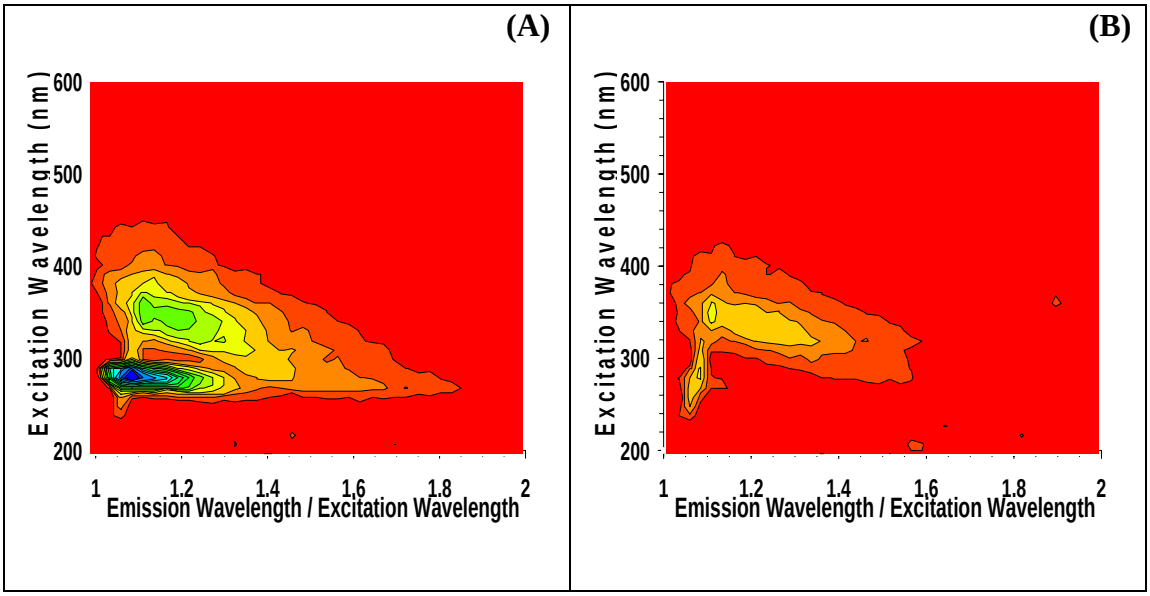

Figure 4.61: Fluorescence signatures from pig weed (A) in suspension before UV, (B) in suspension after UV. The greatest intensity is blue and the least intensity is red.

4.3.6.2 *E.coli bacteria*

An EEM of *E.Coli* vegetative bacteria in log phase in suspension (before and after the broad band UV irradiation for 15 minutes) are shown in Figure 4.62. Again, we could not notice any enhancement of fluorescence after UV irradiation.

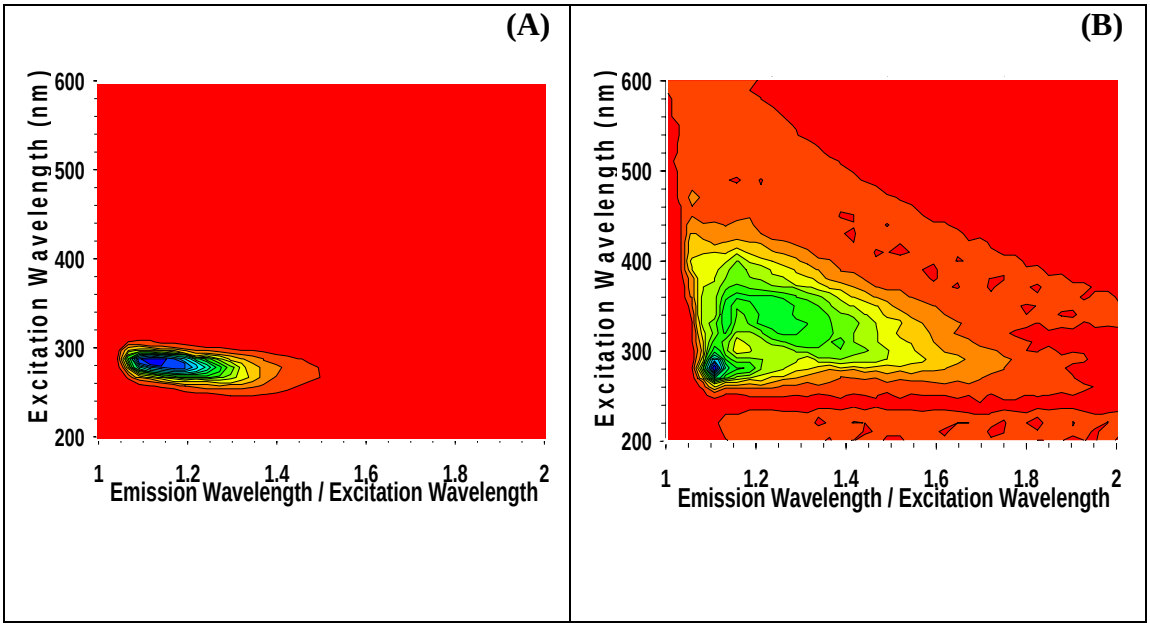

Figure 4.62: Fluorescence signatures from *E.coli* (A) in suspension before UV, (B) in suspension after UV. The greatest intensity is blue and the least intensity is red.

4.3.6.3 *Bacillus subtilis vegetative bacteria*

In Figure 4.63 a 2-D fluorescence spectrum is shown for mid-log phase cells grown in nutrient broth from the (+DPA) *B.sub* vegetative bacteria washed and suspended in saline (0.9% NaCl). The graph for the same cells after UV irradiation with our broad band spectrum of 80 J is shown in Figure 4.64 We also measured the fluorescence of saline water that was used to suspend bacteria. No fluorescence could be seen other than raman scattering as shown in Figure 4.2(A). Notice that although the irradiation suppresses the tryptophan peak and brings a faint fluorescence emission at around 360nm excitation (this may be primarily due to the nutrient broth), the quality of the graph for these vegetative cells is quite different from the corresponding graphs for the (+DPA) spores as shown in Section 4.3.1.

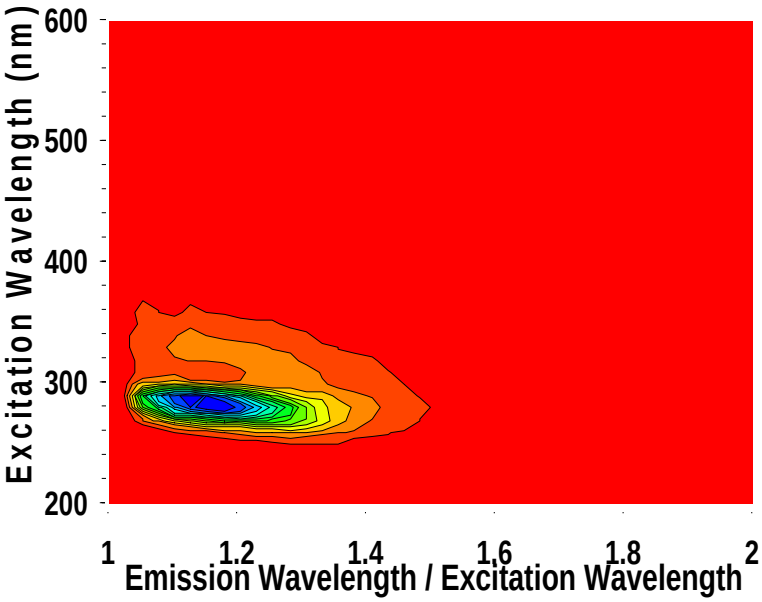

Figure 4.63: Fluorescence fingerprint of vegetative (+DPA) BS cells grown to mid-log phase in 0.9% saline. The greatest intensity is blue and the least intensity is red.

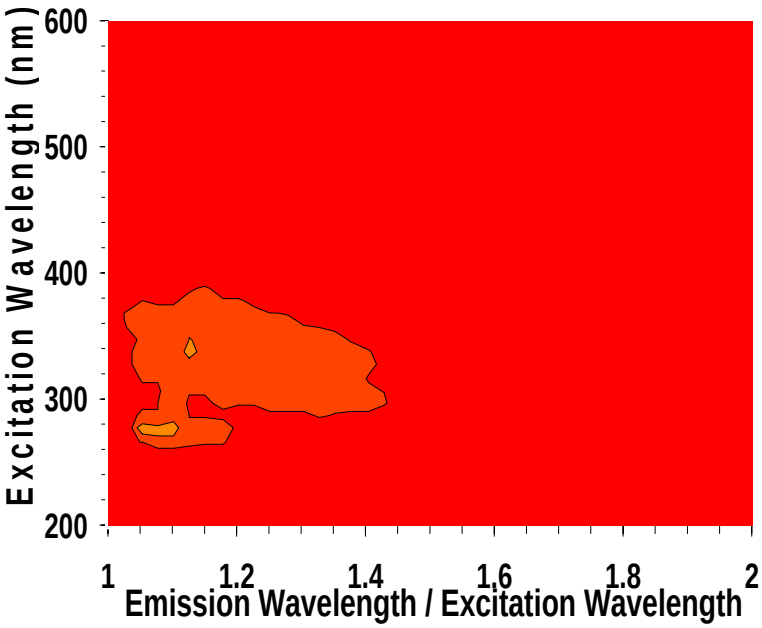

Figure 4.64: Fluorescence fingerprint of vegetative (+DPA) BS cells grown to mid-log phase in 0.9% saline after standard broadband UV irradiation. The greatest intensity is blue and the least intensity is red.

4.3.6.4 *Aspergillus niger* (fungal spore)

Figure 4.65 shows the fluorescence profile of *Aspergilis niger*, a fungal spore, before and after UV irradiation in suspension. Interestingly, we have observed the enhancement of fluorescence in suspension but in different excitation and emission wavelength regions, not in the region of CaDPA or DPA.

The fluorescence enhancement is observed in Figure. 4.65 (B). It has a peak emission wavelength at around 500 nm and occurs with an excitation wavelength around 350 nm. No appreciable changes in the emission spectra around 400 nm were observed after UV irradiation compared to the unexposed solution.

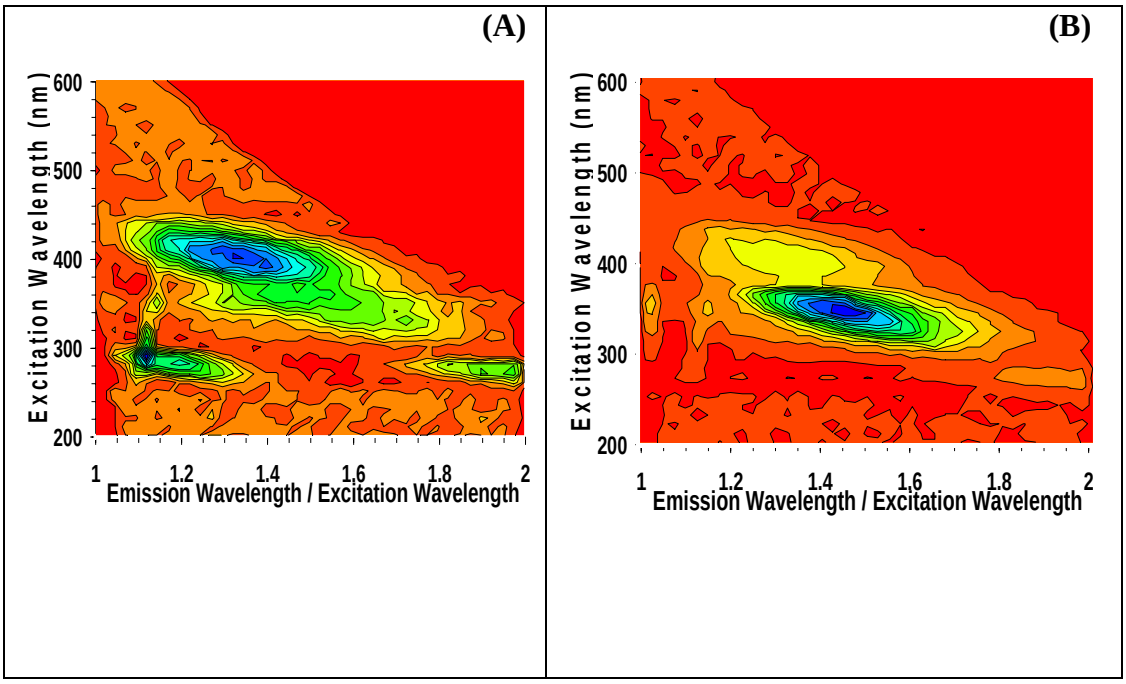

Figure 4.65: Fluorescence signatures from *Aspergillus niger* in suspension (A)before UV, (B) after UV. The greatest intensity is blue and the least intensity is red.

4.3.6.5 PCA analysis of the fluorescence of UV irradiated *Bacillus* spores and other biological samples in water

Several fluorescence spectra were recorded at multi excitation and emission wavelengths, both on controls and irradiated samples (before and after UV irradiation) of different types of biological samples as mentioned in Table 3.1 (Materials and methods). We could not observe any major changes in the fluorescence of these samples after UV irradiation other than the suppressed tryptophan fluorescence. We measured the fluorescence of these samples in water suspension.

Figure 4.66 shows the PCA of the UV irradiated bacterial spores and other biological samples in suspension. We arbitrarily limited the measured spectra to only six excitation wavelengths, as this would be reasonable ranges of wavelengths to show significant fluorescence signals from DPA/CaDPA. We selected 300, 320, 340 360, 380 and 400 nm. To be consistent with previous studies in this thesis, we also did the PCA analysis by using six excitation wavelengths from 280 nm to 430 nm with step 30 nm as shown in Figure 4.66 (B). We could clearly separate the samples of *Bacillus* spores from other biological samples irrespective of small differences in the selection of excitation wavelengths. The separation was more pronounced when we only used the wavelength region resembled with DPA/CaDPA. There are a total of 28 measurements with 14 of the *Bacillus* spores in suspension (five measurements of BG1 spores, replicate measurements of (+DPA) BS, BC spores and one measurement each of BG2, BG3 and BT spores) and 14 of the other biological samples in this research in suspension as mentioned below:

Aspergillus niger- 3 measurements, *Pig weed*- 2 , *E.coli* - 2, *BS vegetative cells*- 2, *Psedomonous aeroginosa*- 2, Ovalbumin – 1, BC vegetative cells-1, *Pinus radiate*-1)

All these samples were irradiated with our broad band UV spectrum of 80 J for 15 minutes. We show these 28 measurements on a plot of the first PC versus the second PC in Figure 4.66**.** This result was reinforced with our 2-D fluorescencent fingerprint of UV irradiated fungal spores as shown in Figure 4.65(B)**.** If we look at the PCA score plot of the second and third component, as shown in Figure 4.67(A), we can see that significant changes along the third PC are seen for these samples. We could even

see some differences within the *Bacillus* spore samples. The larger scatters of other biological samples are due to their much more variable composition

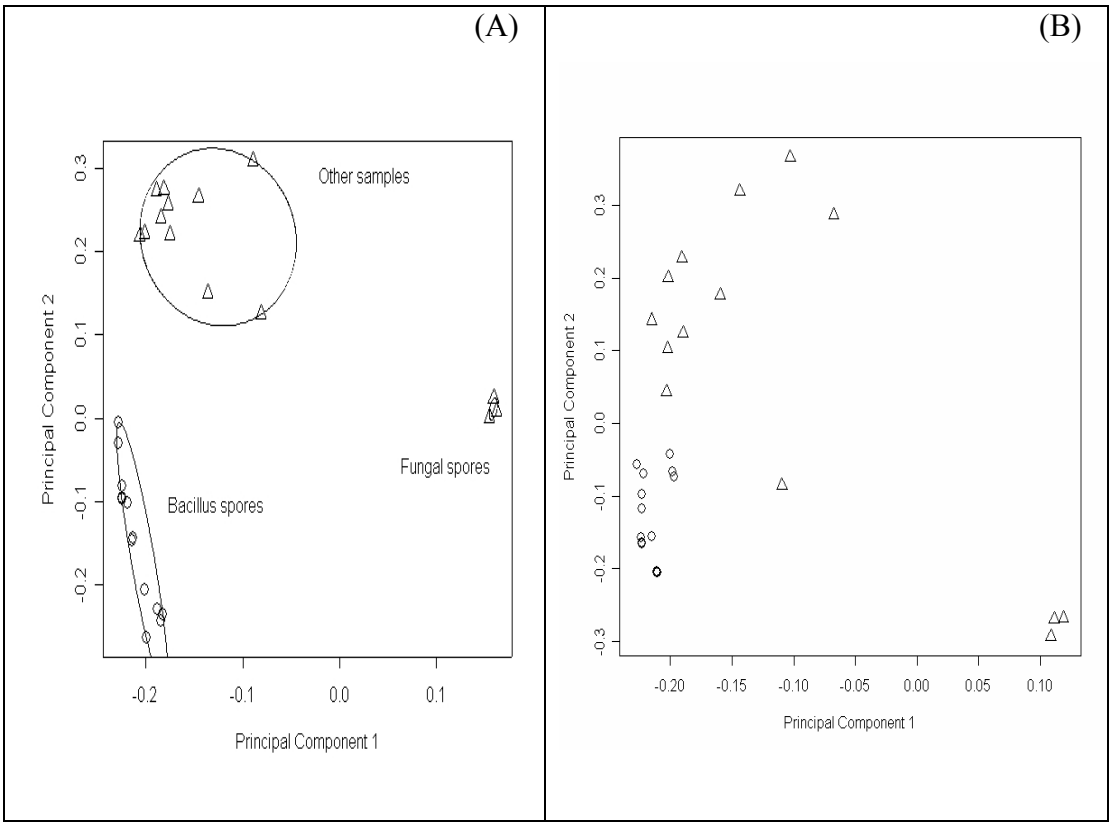

Figure 4.66: The first PC versus the second PC for 28 measurements (A) using excitation wavelengths from 300 to 400 nm with 20 nm step (B) using excitation wavelengths from 280 nm to 430 nm with 30 nm step. The open circles are *Bacillus* spores (BG1, BG2, BG3, BC, BT and BS) the triangles are all other biological samples studied in suspension after a broad band UV irradiation for 15 minutes. The unique three misclassified triangles from other samples are fungal spores, *Aspergillus niger*. The ellipses are minimum area ellipses.

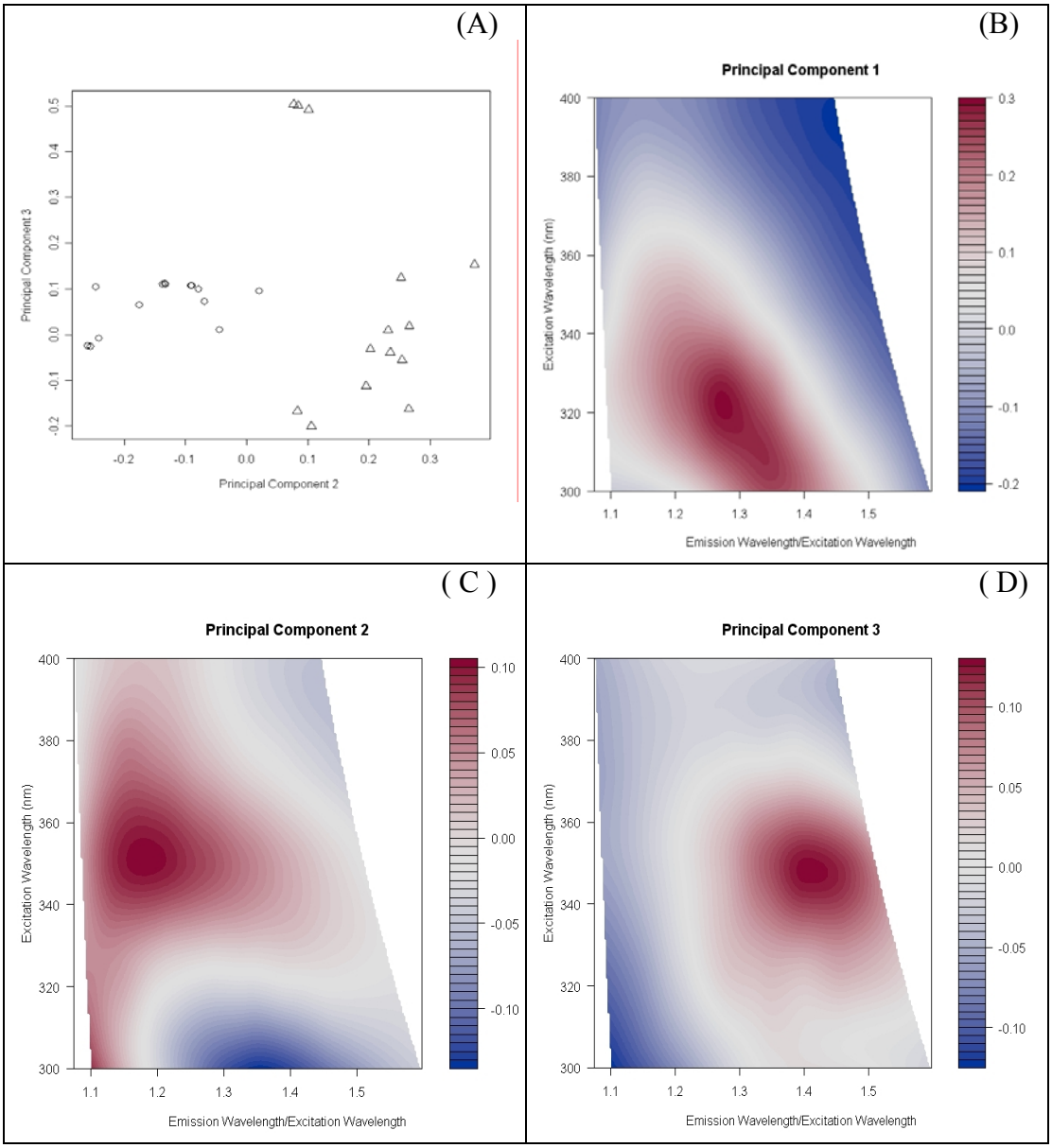

Figure 4.67: (A) PCs two and three for the 28 fluorescence measurements. Contour plot of the Loading spectra of the (B) first and (C) second and (D) third principal components from fluorescence emission spectra of the samples are also shown.

As shown in Figure 4.67, inspection of the fluorescence peaks in the PC loading vectors (PCs) indicates that the first component can be attributed to CaDPA-like peak and the major contribution to the second component is difficult to assign at this stage. The second component is mainly responsible for the separation of *Bacillus* spores from other samples. It is evident that the suggested components of CaDPA matches the fluorescence profile of the pure CaDPA compound fairly well, whereas the third loading vector can be ascribed to the chemical component responsible for the enhancement of fluorescence in *Aspergillus niger*.

4.4 Fluorescence quantum efficiency of major bacterial spore chemical components and spores in water

In this section we present the results of the QE of major spore chemical components and spores in water suspension. Fluorescence QEs are determined by the comparison of the intensities of fluorescence of the test samples with a standard sample of anthracene in ethanol.

4.4.1 Absorbance and fluorescence of anthracene in ethanol

The absorption and fluorescence spectra of seven different concentrations of anthracene in ethanol were measured. The representative absorption and fluorescence spectrum of anthracene in ethanol are shown in Figures 4.68 and 4.69 respectively. The standard anthracene in ethanol produced well-defined absorption spectra in the range of 300-400 nm excitations with a main peak at 356.2 nm. The concentration of the solution was 0.1 mM. The optical density at excitation wavelength 356.2nm was 0.12.

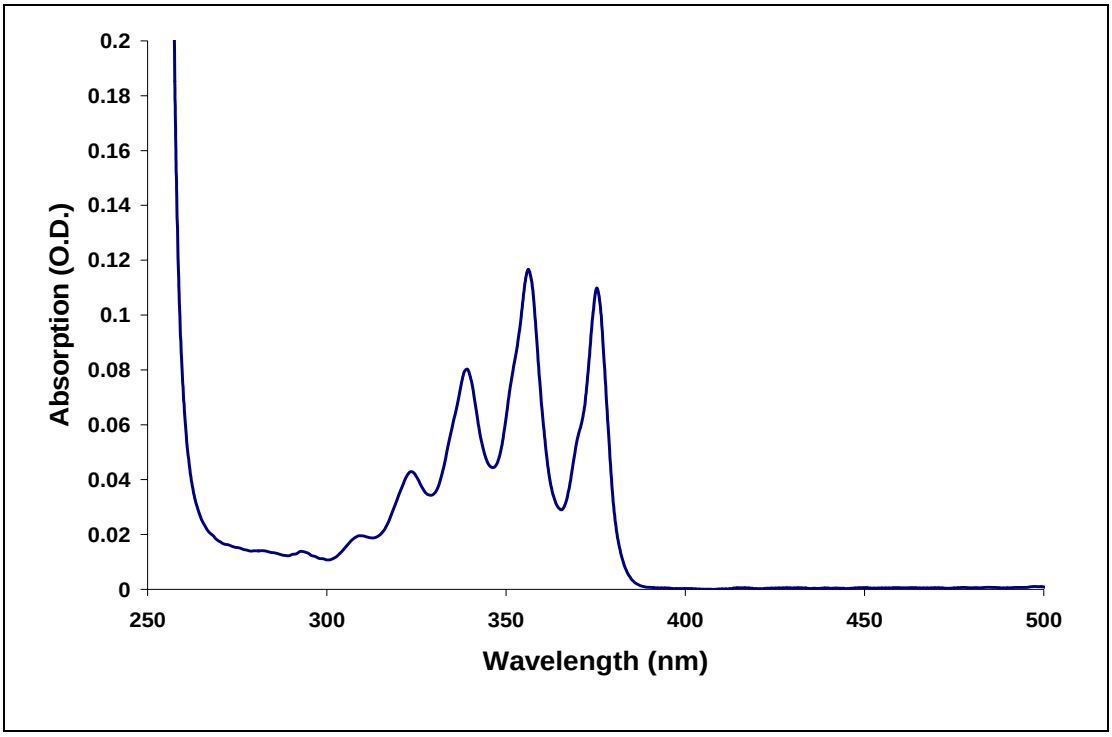

Figure 4.68: Absorption spectra of anthracene in ethanol. The sample measured in a 1-cm quartz cuvette.

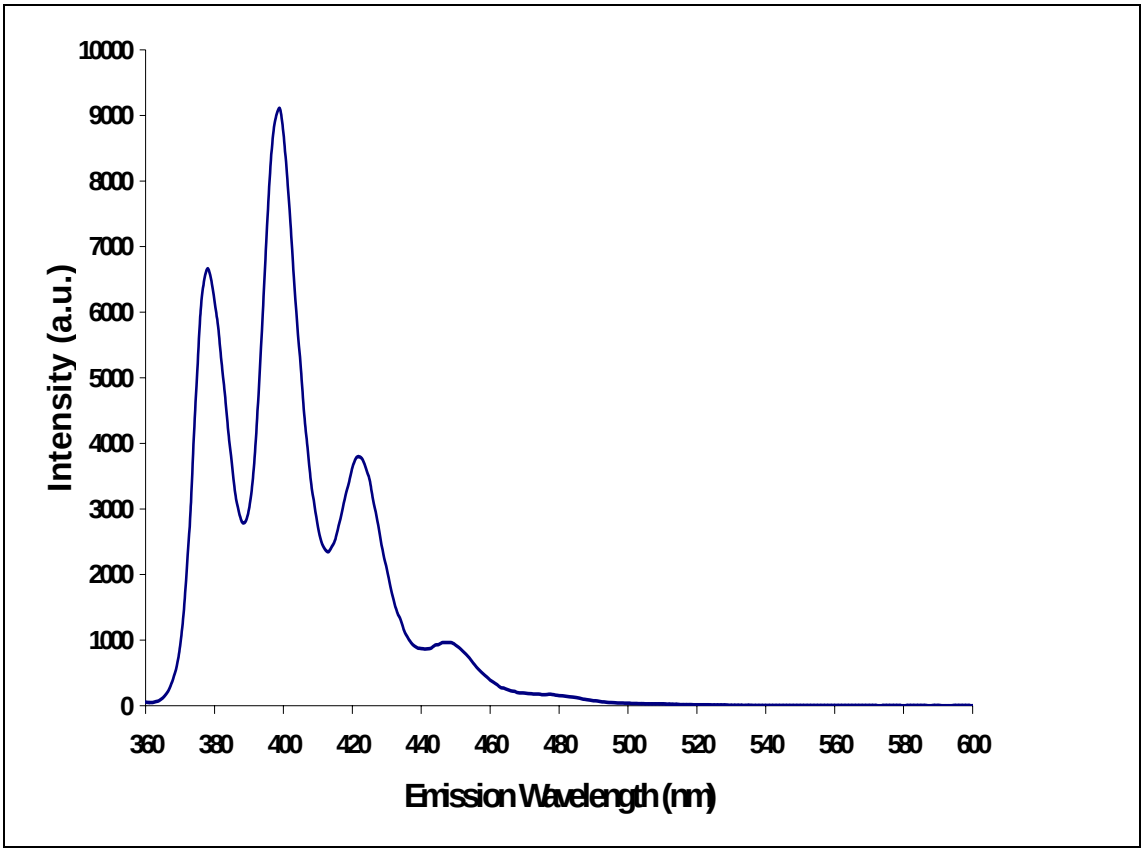

Figure 4.69: Fluorescence spectra of anthracene in ethanol at excitation wavelength 356.2 nm. The sample measured in a 1-cm quartz cuvette.

The classical mirror image representation of absorption and fluorescence is clearly seen. The integrated fluorescence intensity was measured by varying the concentration of the samples. We prepared different concentrations of anthracene in ethanol and measured the absorbance and fluorescence at different excitation wavelengths.

In Figure 4.70 we plotted the integrated fluorescence intensity versus absorbance of anthracene in ethanol at excitation wavelengths 360 nm. The lines are linear least squares fits to the data point and are not restricted to pass through the origin (since we did not subtract the very minimal fluorescence of ethanol alone). We also noticed that the slope value did not change much when the line is forced to pass through the origin (less than 2% changes in the slope values).

Similarly we drew graphs for other excitation wavelengths. These graphs were drawn to find the slope at different excitation measurements to correct the instrument response of the measured fluorescence. Each gradient of the graphs is proportional to the known QE of anthracene in ethanol at the excitation wavelength selected.[143]

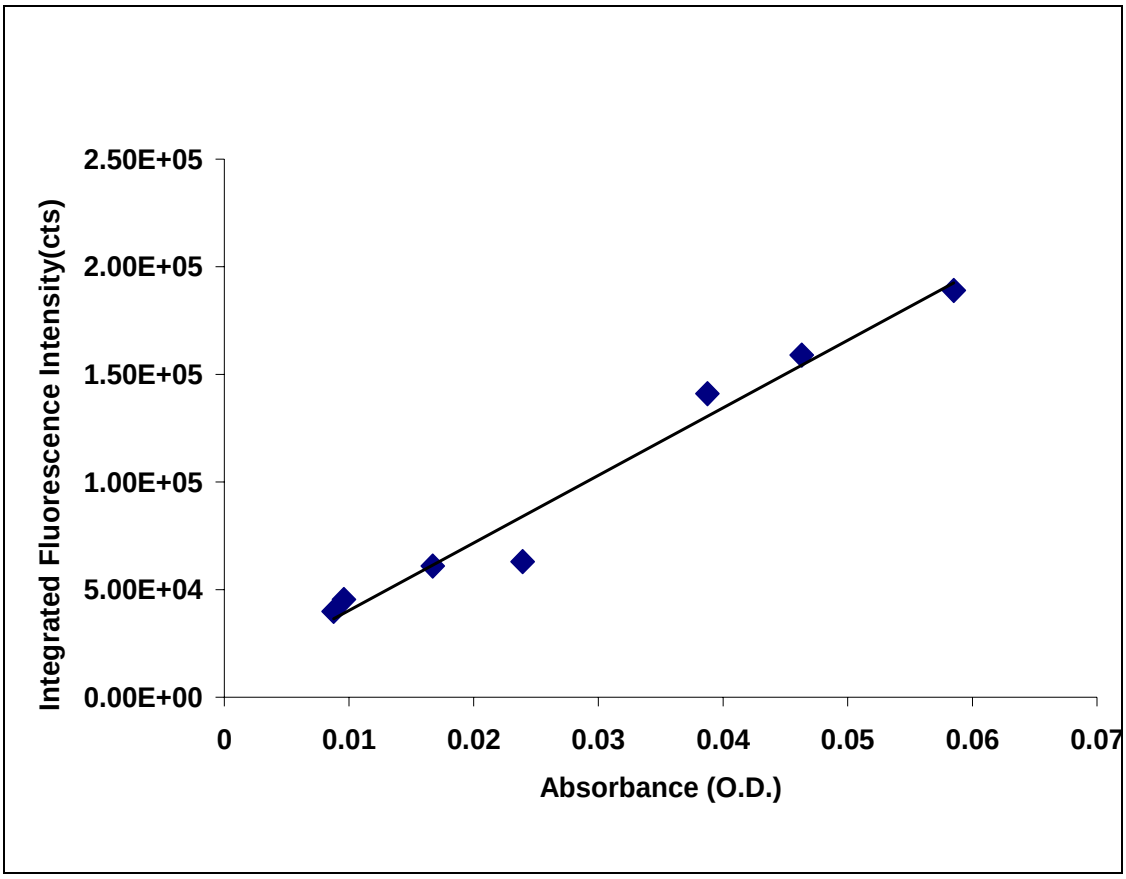

Figure 4.70: The integrated fluorescence intensity (counts) of anthracene in ethanol is shown versus absorption (O.D.) at excitation wavelength 360 nm. The line is drawn as linear least squares fit. The slope of the line is proportional to the QE of anthracene in ethanol at the excitation wavelength selected.

Similarly we drew the graphs of integrated fluorescence intensity versus absorption of anthracene in ethanol at excitation wavelengths of 320, 340, 350 and 356.2 nm (graphs not shown). Table 4.1 shows the measured slope values from the graphs of integrated fluorescence intensity versus absorbance at different excitation wavelengths.

Table 4.1: The gradient (slope) of the graph integrated fluorescence intensity versus absorbance at different excitation wavelengths of anthracene in ethanol.

Excitation Wavelength (nm)	Slope value
360	$314.23 * 10^4$
356.2	$311.67 * 10^4$
350	$254.13 * 10^4$
340	$252.63 * 10^4$
320	$154.75 * 10^4$

We drew a graph excitation wavelength versus the gradient values as shown in Figure 4.71 (i.e., the plot of the slopes versus wavelength for each of the excitations). Since the QE of anthracene is not wavelength dependent, the changes in slope of the lines is the spectral response of the fluorometer. We extrapolate the response to be constant beyond the range measured (dashed lines as shown in the figure). We selected the linear portion of the graph to compare the QE of bacterial spore components and spores in suspension as this region represents the actual fluorometer response to various excitation wavelengths.

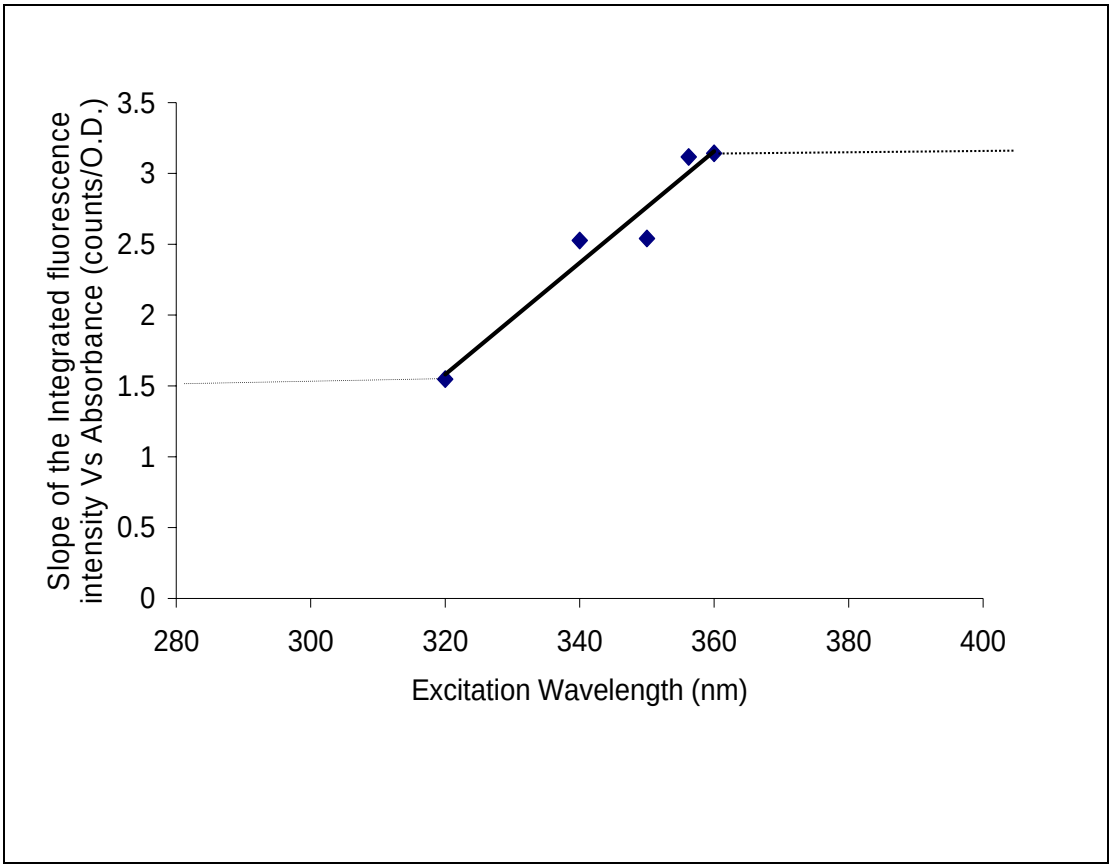

Figure 4.71: Response curve of the fluorometer. The slope of the integrated fluorescence intensity (counts) versus absorption (O.D.) is plotted against the excitation wavelength from 320 to 360 nm as shown in Table 4.3. The straight line is linear least squares fits of the data. The response curve is extrapolated to be constant (dashed lines) at shorter and longer wavelengths.

We used the value of 0.27 as QE of anthracene in ethanol in the linear part of the spectra. Weber and Teale[117] have established that fluorescence QE of several compounds including anthracene in ethanol are constant over a wide range of excitation wavelength. These results are evidence that the measurements are free of any serious variation of systematic error upon change of the excitation wavelength. Therefore we chose the slope value at 320nm excitation of a standard sample of anthracene to calculate the QE of our unknown samples measurements around 300nm excitation and chose the slope value at 360 nm excitation to calculate the QE value of our unknown samples around 360 nm excitation wavelengths.

4.4.2 Quantum efficiency of bacterial spore components

In this section we present the results of QE measurements made with major bacterial spore chemical components. We have already shown in Figures 4.19 and 4.17 the absorption and 2-D fluorescence spectra of tryptophan solution respectively. Figure 4.72(A) shows the integrated fluorescence intensity versus absorbance graph of tryptophan in water suspension at excitation wavelength 280 nm. The tryptophan compound in water suspension produces a well defined fluorescence peak at around 340 nm at excitation wavelengths around 280 nm as shown in Figure 4.17**.**

The solutions were diluted to give absorbances mainly in the range 0.01-0.06 O.D., that is, within the expected linear calibration range of fluorescence emission versus concentration. The QEs were calculated according to equation 2.4 in Chapter 2, Section 2.5 and the results of tryptophan by this method were compared with some literature values, which are given in Table 4.2. The reproducibility of measuring and calculating QE of the same solution in our experiment is within ± 3-5%. Tryptophan fluorescence is decreased with exposure to UV light. We were interested to measure the QE of the tryptophan solution after irradiation using our standard broad band UV irradiation for 15 minutes. In Figure 4.72(B) we show the integrated fluorescence intensity versus absorption of tryptophan in water after the broad band UV exposure of 80 J for 15 minutes. We have primarily measured the QEs of the unknown samples only at excitation wavelengths corresponding to their peak fluorescence emission.

Dipicolinic acid, mainly in the form of CaDPA is thought to be another major chemical component in the fluorescence profile of BG1 spores in suspension in our previous fluorescence results.

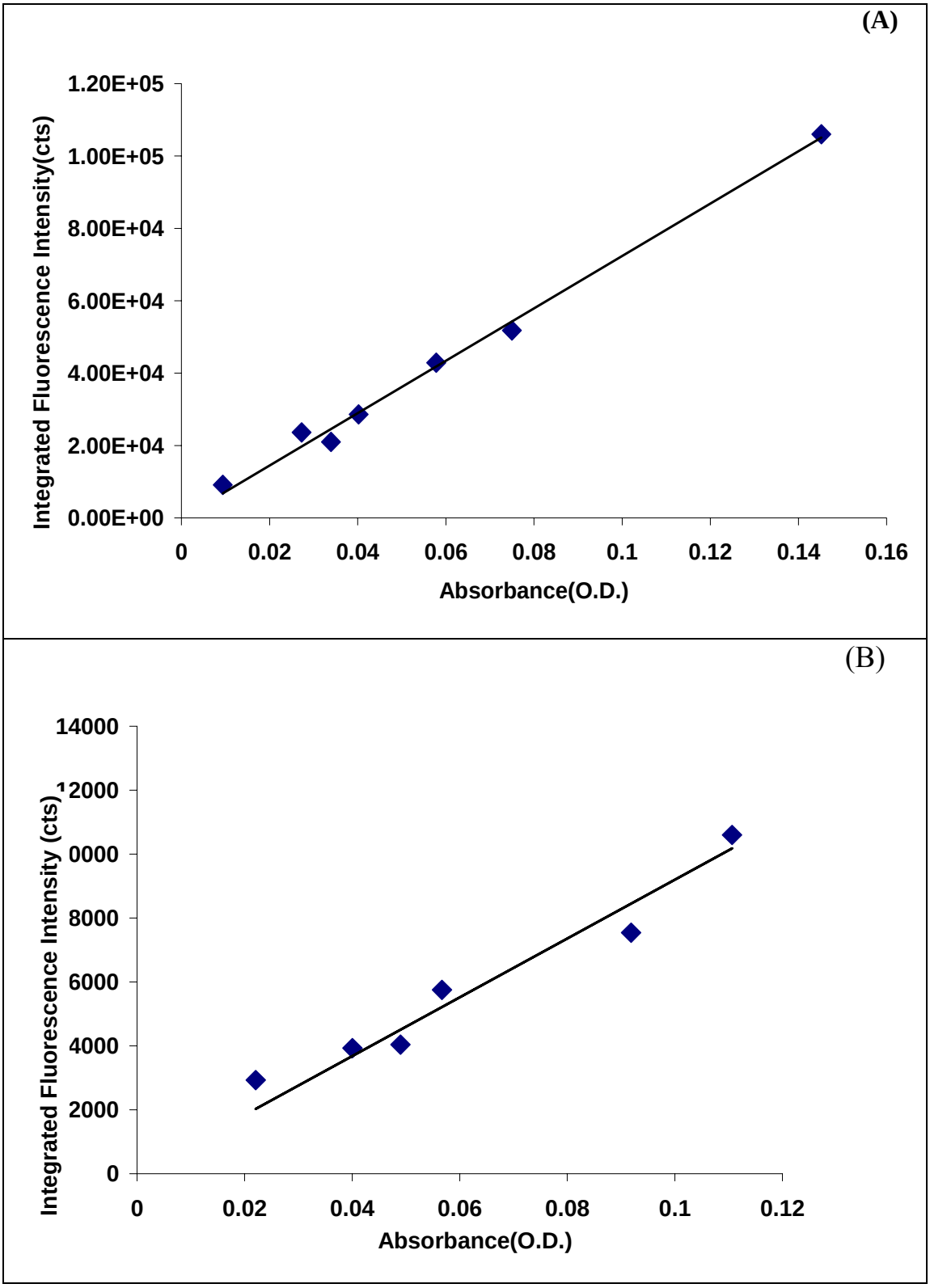

Figure 4.72: Integrated fluorescence intensity versus absorbance graph of tryptophan in water suspension at excitation wavelength 280 nm (A) without broad band UV, (B) with broad-band UV.

CaDPA in water solution (without broad band UV irradiation) produces a well defined fluorescence peak around 290 nm excitation wavelengths (see Figure 4.7). Figures 4.73 and 4.74 show the integrated fluorescence intensity versus absorption graph of CaDPA in solution at excitation wavelengths 290nm and 300nm respectively (without and with the broad band UV irradiation for 15 minutes). It is also interesting to note that the fluorescence peak of UV irradiated CaDPA in water solution appears around 300 nm excitation wavelengths (see Figure 4.8). Therefore we measured the QE of the irradiated CaDPA solution both at 290 nm and 300 nm excitation. It is also interesting to look at the QE of DPA in solution after exposure to UV and the fluorescence QE of dry crystalline sample of CaDPA and DPA.

In Figure 4.75 we show the graph of integrated fluorescence intensity versus absorption of DPA in water solution after irradiation of broad band UV for 15 minutes. Since we could not observe any measurable fluorescence of DPA in solution before UV irradiation, we did not measure the QE of DPA in solution before UV exposure (see Figure 4.1 (A)).

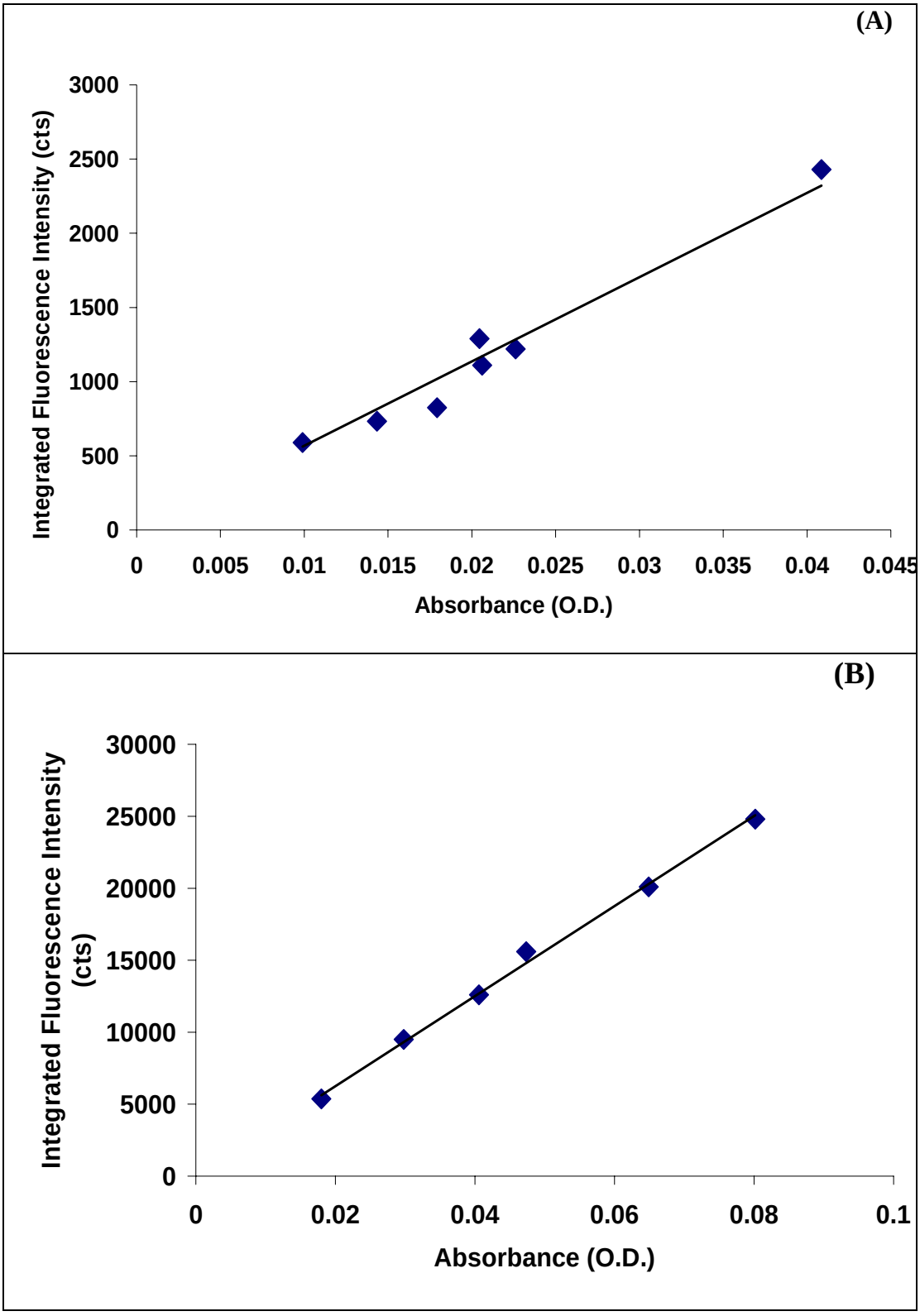

Figure 4.73: Integrated fluorescence intensity versus absorption graph of CaDPA in solution at 290 nm excitation (A) without UV irradiation, (B) with UV irradiation.

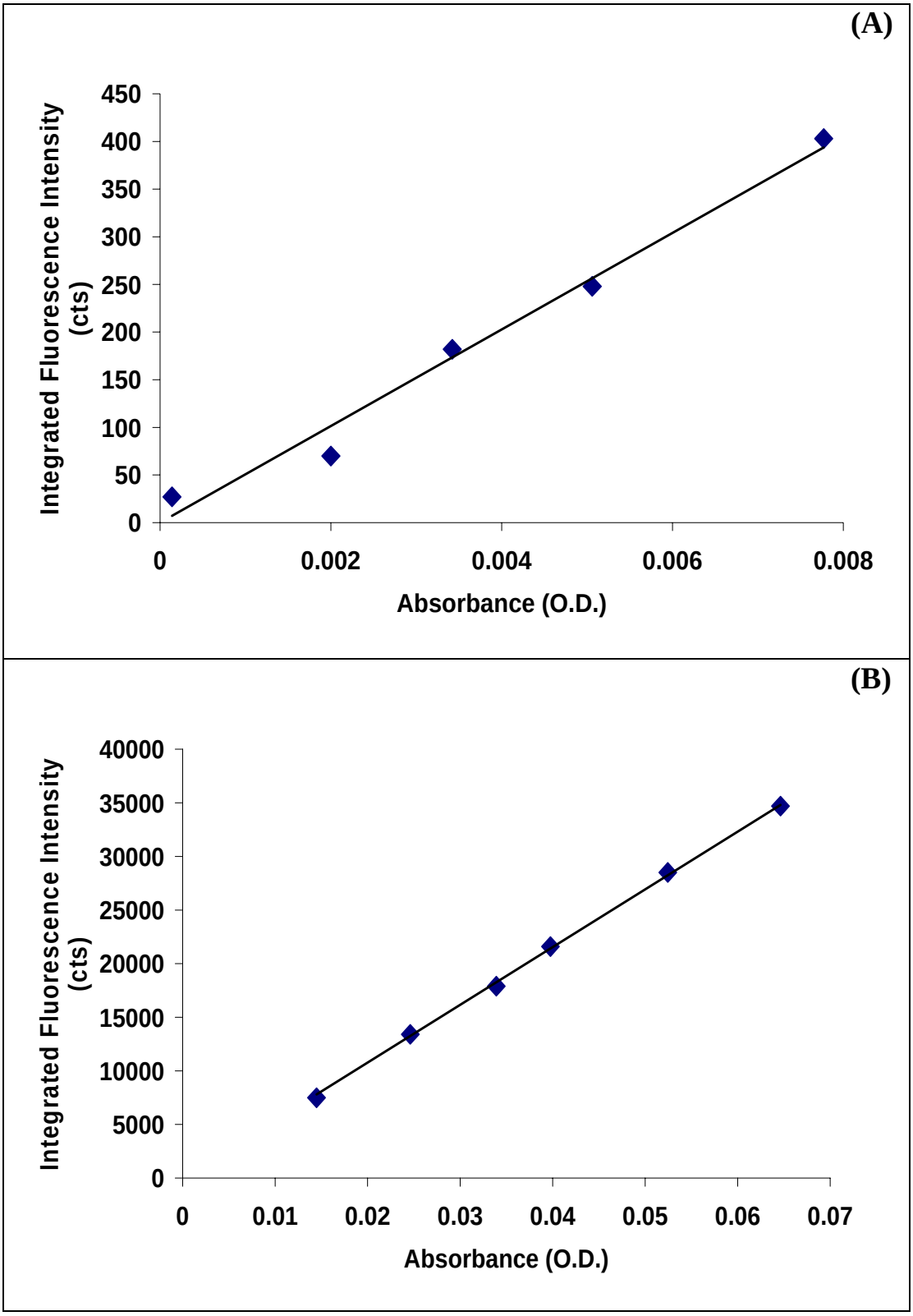

Figure 4.74: Integrated fluorescence intensity versus absorption graph of CaDPA in solution at 300 nm excitation (A)without UV irradiation, (B) with UV irradiation.

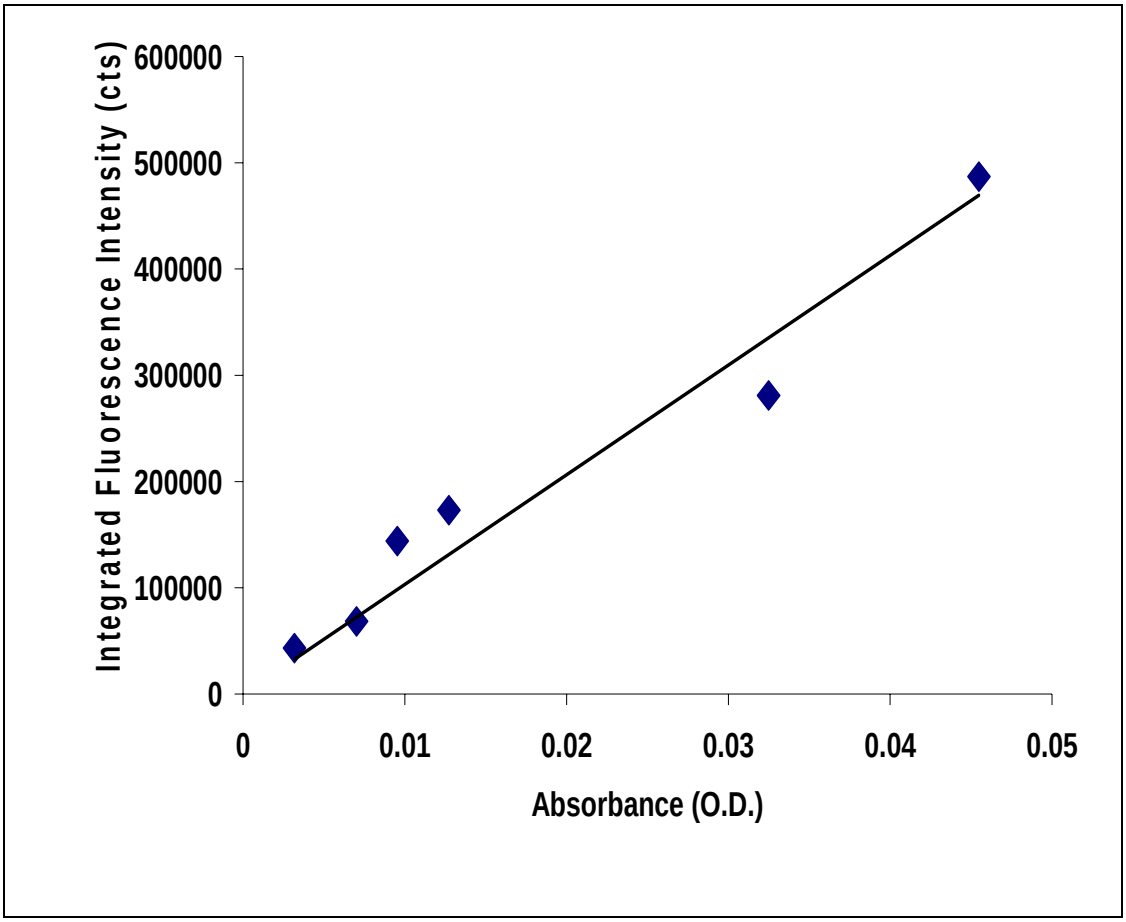

Figure 4.75: Integrated fluorescence intensity versus absorption graph of UV irradiated DPA in solution at 360 nm excitation.

Figure 4.76 (A) shows the absorption spectrum of the dry crystalline of CaDPA. The integrated fluorescence intensity versus absorption graph of dry CaDPA crystalline powder fixed on a quartz slide for measurements is shown in Figure 4.76 (B). The similar plots for dry crystalline DPA powder fixed on a quartz slide are shown in Figure 4.77.

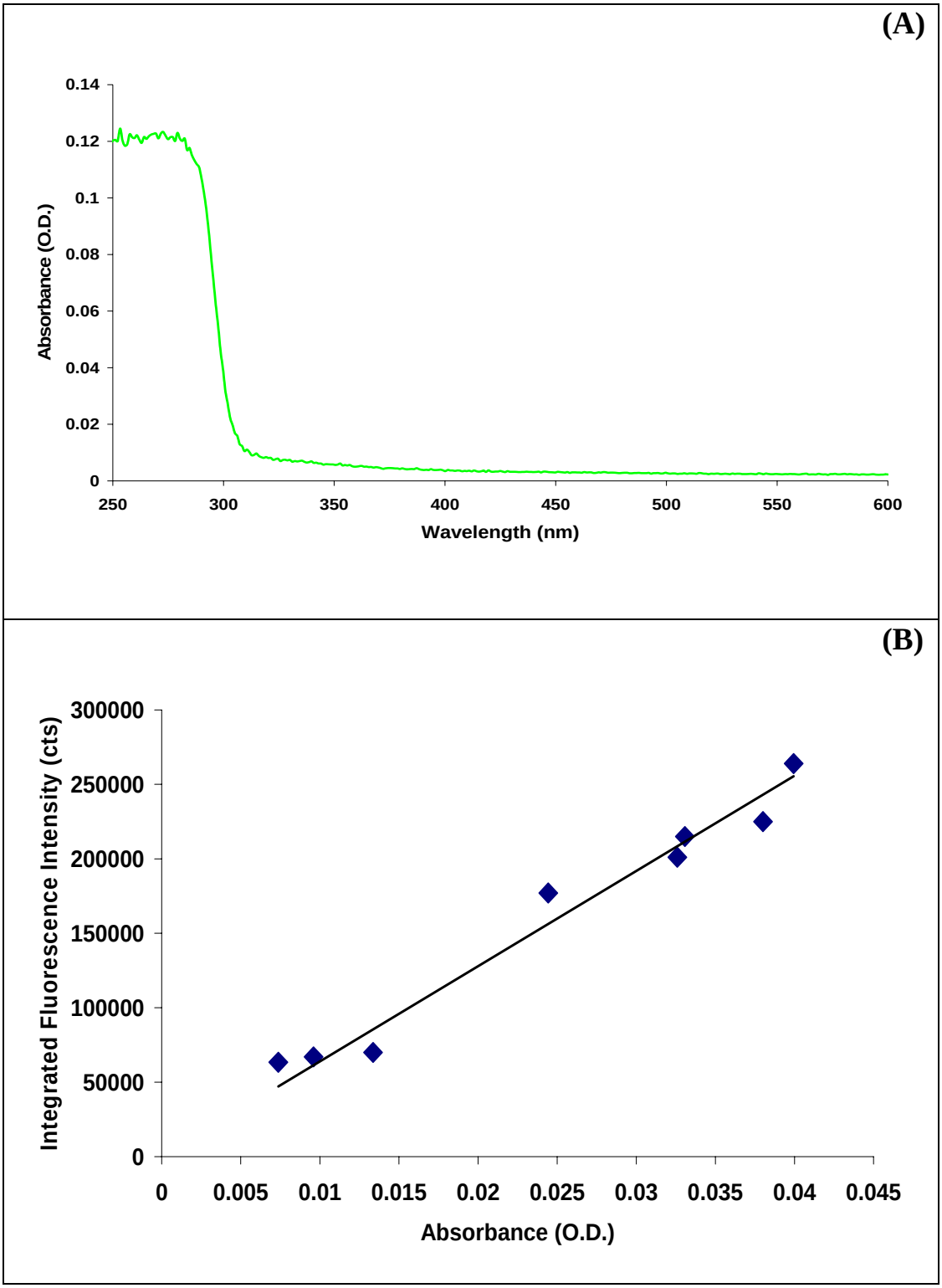

Figure 4.76: (A) The representative absorption spectra of dry CaDPA crystalline and (B) Integrated fluorescence intensity versus absorption graph of dry CaDPA at 300nm excitation

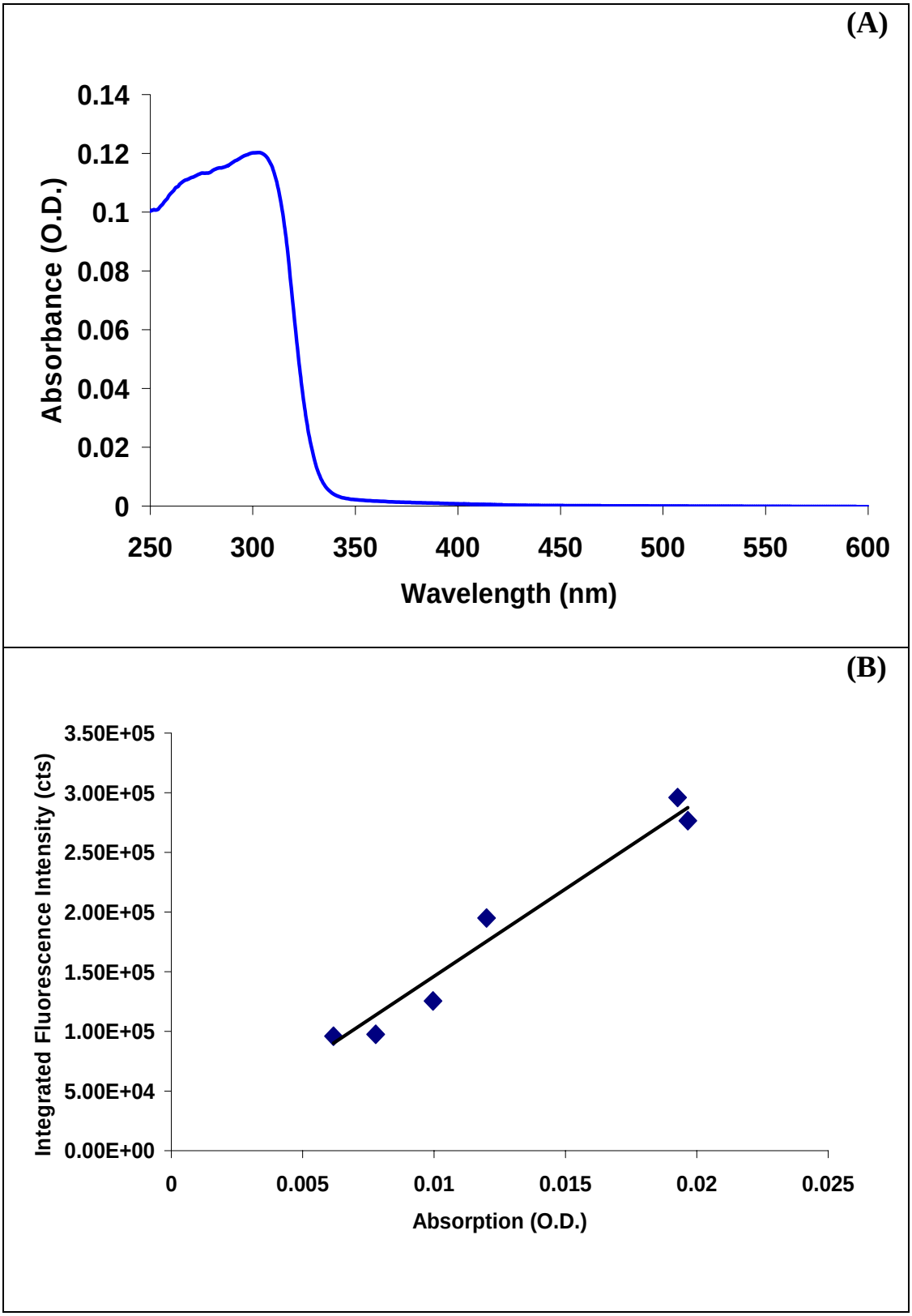

Figure 4.77: (A) The representative absorption spectra of dry DPA crystalline (B) Integrated fluorescence intensity versus absorption graph of dry DPA at 360 nm excitation.

4.4.3 Quantum efficiency of bacterial spores in suspension

In this section we present the results of QE measurements of some *Bacillus* spores in suspension. The QE of BG 1 was calculated before and after washing the spores. In Figure 4.78 we show the fluorescence profile of the supernatant and the pellet of the washed BG 1 spores. There are noticeable differences in the shape of the fluorescence spectrum and the fluorescence peaks of the washed and unwashed BG1 spores in suspension. The CaDPA peak disappears in the washed sample.

Figure 4.54 shows the representative absorption spectrum of BG1 spores in suspension. In Figure 4.79 we show the absorption spectra of the pellet of the washed BG1 spores and BC spores in suspension. We also noticed that the CaDPA peaks disappear in the case of washed BG1 samples.

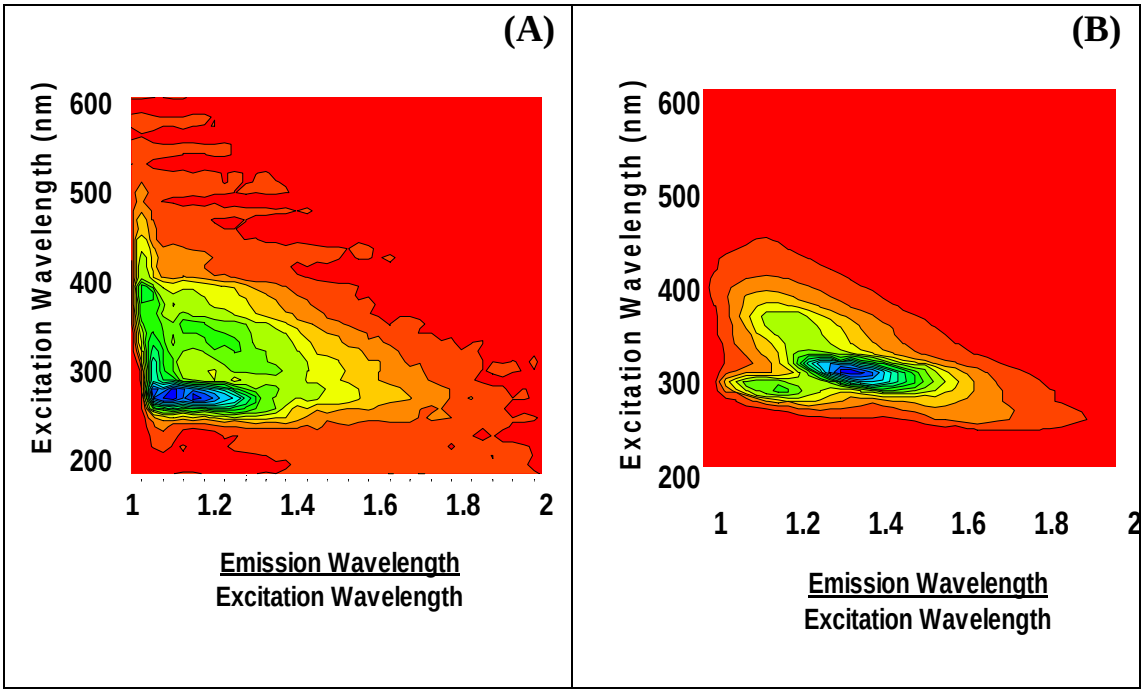

Figure 4.78: Fluorescence contour plot of (A) the pellet and (B) supernatant of the washed BG 1 spores in suspension.

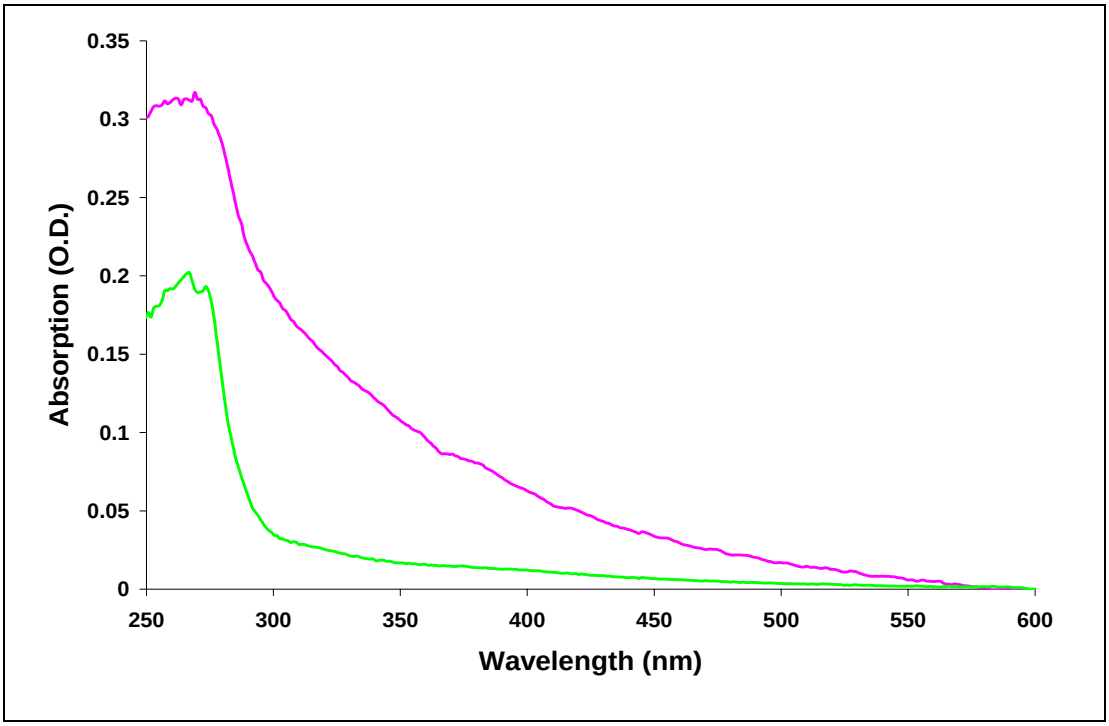

Figure 4.79: The representative absorption spectrum of the pellet of the washed BG(1) spores in suspension (pink) and BC spores in suspension (green).

Figure 4.80 and 4.81 shows the integrated fluorescence intensity versus absorption graph of BG1 spores in suspension at 290 nm and 300 nm excitation wavelengths respectively (before and after washing). The line is linear least squares fit. The slopes are proportional to the QE of BG1 spores in suspension at the selected excitation wavelengths. A similar graph was drawn for BC spores as shown in Figure 4.82. In Table 4.2 we show the summary of the measurements of the samples investigated. Results of both washed and unwashed samples measurements are also shown. We also show the available literature value of the QE of tryptophan solution in the table.

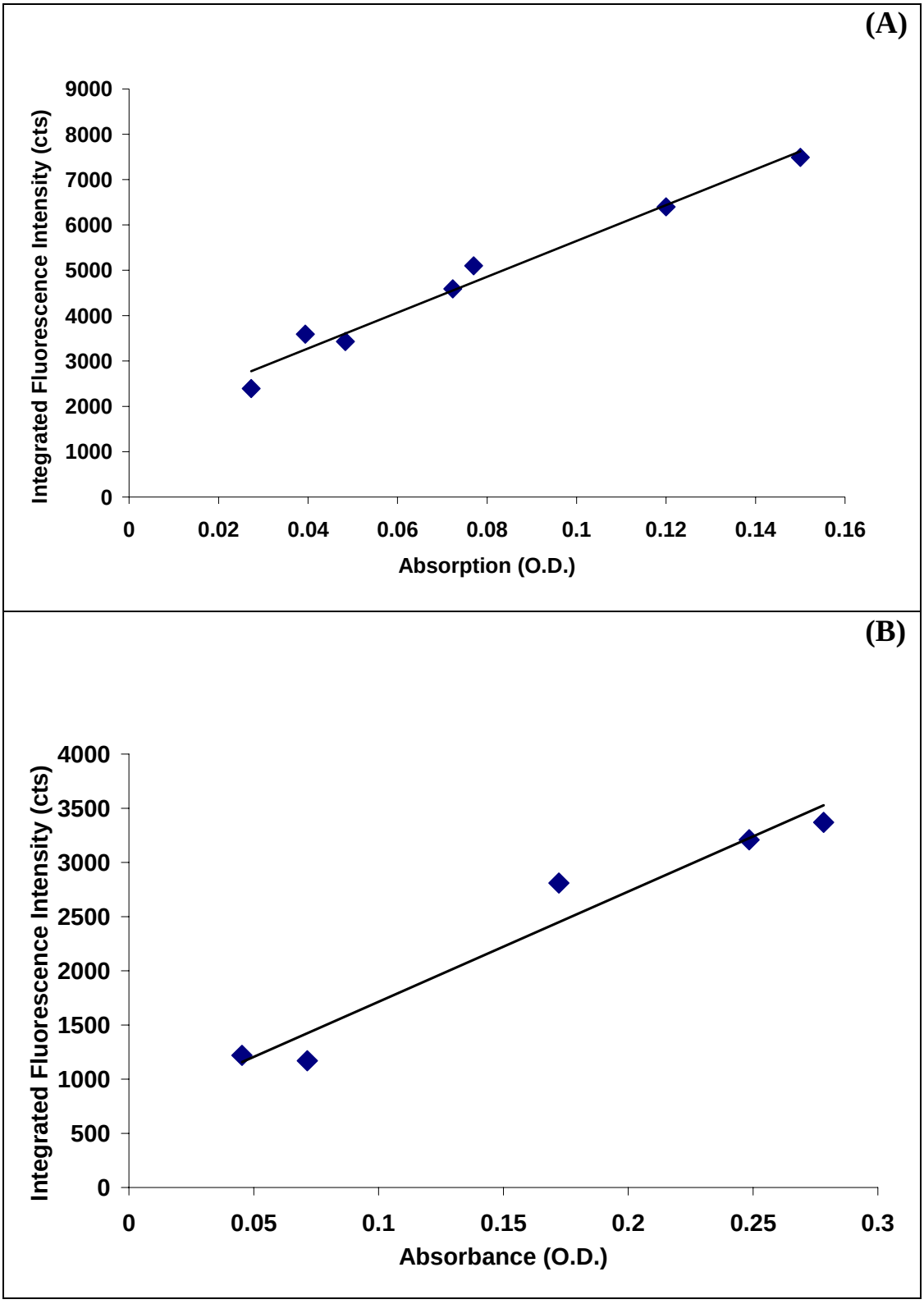

Figure 4.80: The graph of integrated fluorescence intensity versus absorption BG (1) spores in suspension at 290 nm excitation **(A)** before and **(B)** after washing.

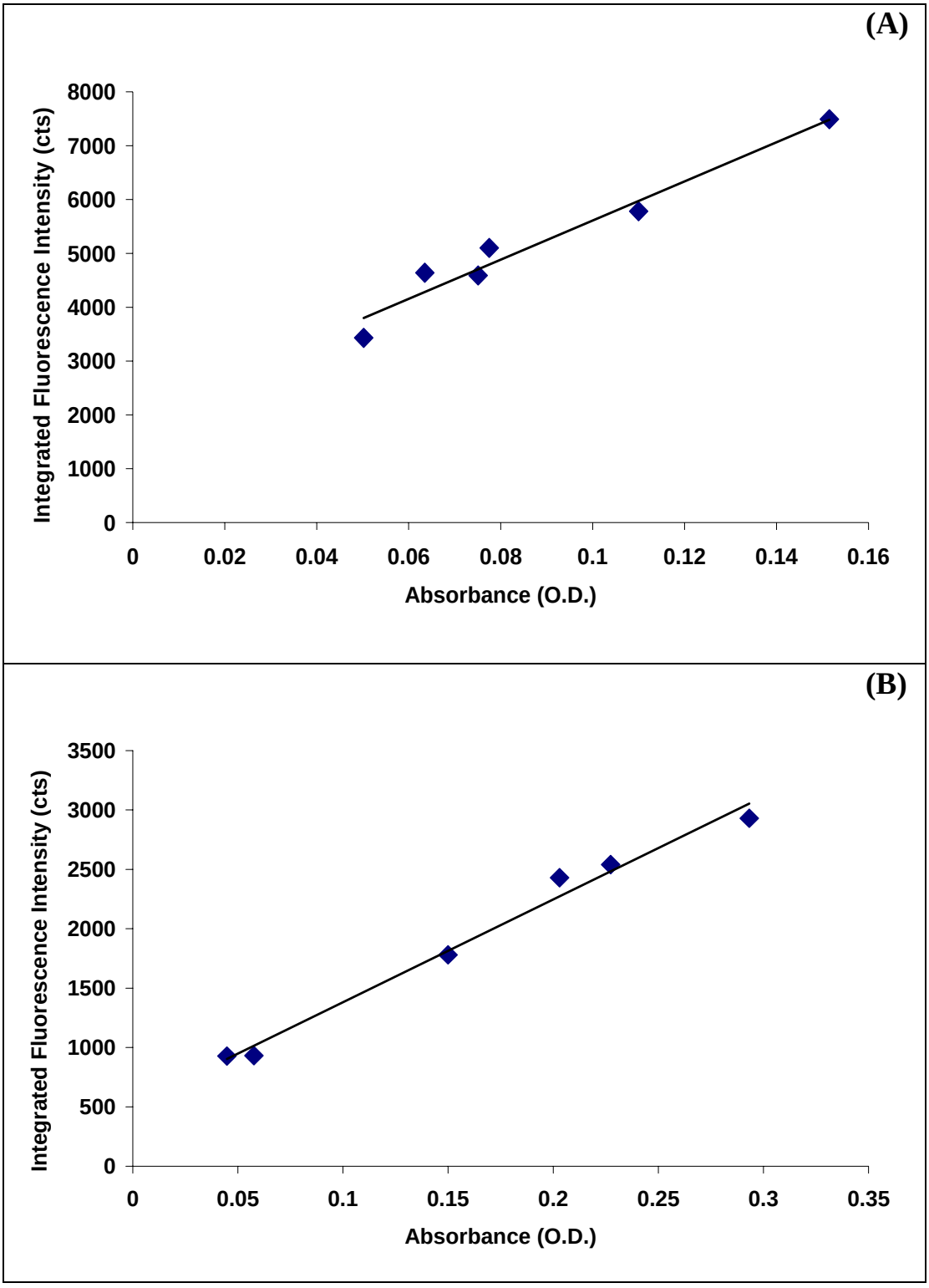

Figure 4.81: The graph of integrated fluorescence intensity versus absorption of BG 1 spores in suspension at 300 nm excitation **(A)** before and **(B)** after washing.

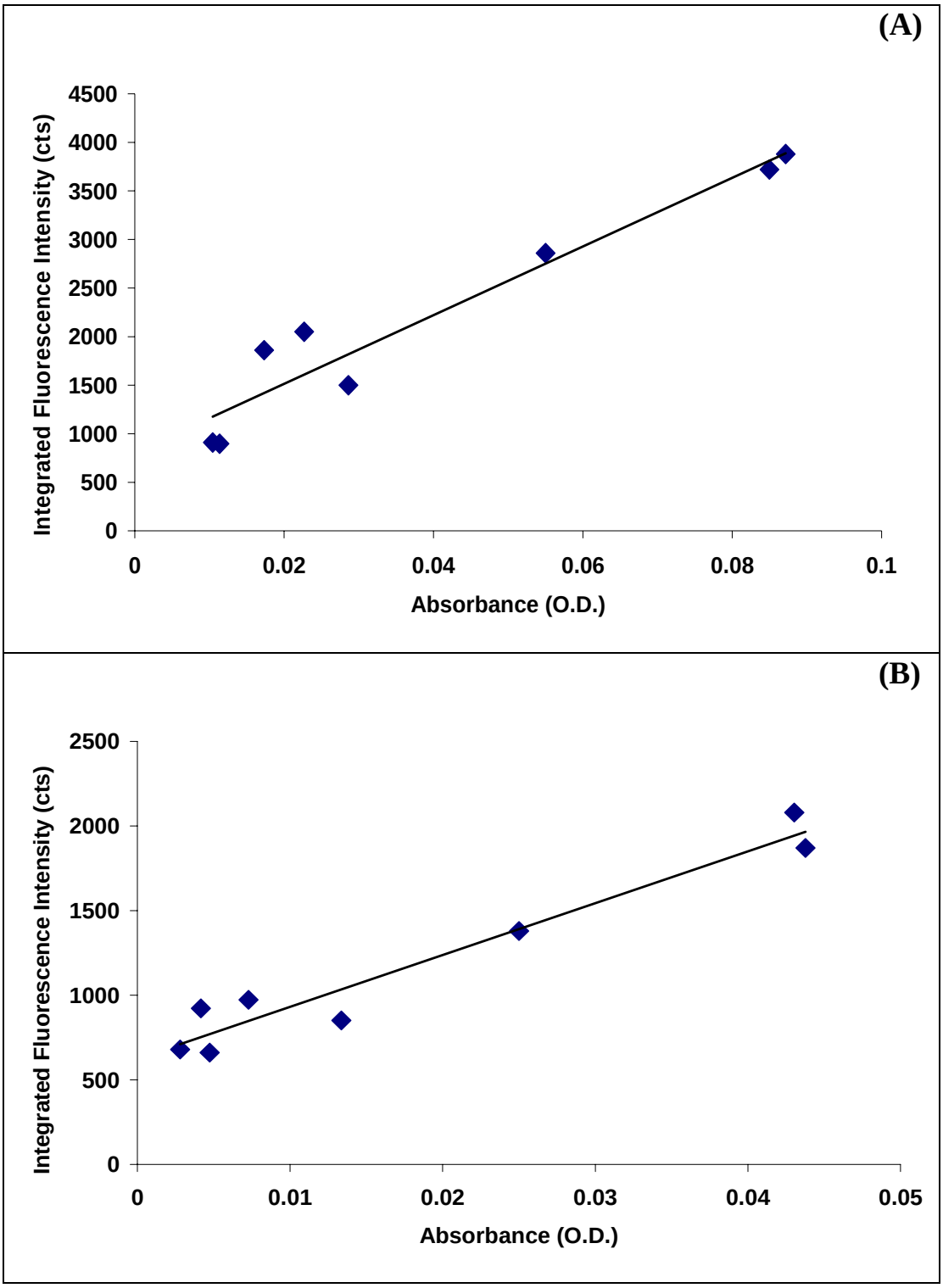

Figure 4.82: The graph of integrated fluorescence intensity versus absorption BC spores in suspension **(A)** at 290 and **(B)** at 300 nm excitation.

Table 4.2: Summary of QE values of samples being investigated.

Compound/Samples	**Solvent**	**Excitation wavelength (nm)**	**Quantum Efficiencies**	**Quantum Efficiencies (Literature values)**
Tryptophan (UV⁻)	water	280	0.12 ± 0.03	0.13[124],0.18[117] and 0.17[105]
Tryptophan (UV+)	water	280	0.02 ± 0.009	Not available
CaDPA(UV⁻)	water	290	0.01 ± 0.003	Not available
		300	0.008 ± 0.003	Not available
CaDPA(UV+)	water	290	0.05 ± 0.01	Not available
		300	0.09 ± 0.02	Not available
DPA(UV+)	water	360	0.74 ± 0.17	Not available
BG1(before wash)	water	290	0.007 ± 0.002	Not available
		300	0.006 ± 0.002	Not available
BG1(after wash)	water	290	0.002 ± 0.001	Not available
		300	0.0014 ± 0.0004	Not available
BC(before wash)	water	290	0.0056 ± 0.002	Not available
		300	0.005 ± 0.002	Not available
CaDPA	Dry powder	300	0.45 ± 0.11	Not available
DPA	Dry powder	360	0.71 ± 0.18	Not available

CHAPTER 5

5 DISCUSSION

5.1 Overview

The techniques of steady-state multi-wavelength UV-Vis fluorescence (EEM) and PCA have been applied to develop a familiarity and predictive ability for the behaviour of *Bacillus* spores in different environments. We have seen that the biological samples can give rise to characteristic spectroscopic fingerprints. Specifically, the samples' physical state and their natural variability in terms of size, shape and chemical composition have been shown to give considerable differences in the spectral characteristic of the spores. We now have a better understanding of the features observed on the fluorescence changes due to hydration and UV irradiation in *Bacillus* spores. The research work presented in this thesis has shown a promising step in the exploration of the autofluorescence characteristics of *Bacillus* spores.

5.2 Two dimensional multi-wavelength fluorescence studies of major *Bacillus* spore chemical components

Knowledge and understanding of the autofluorescent characteristics of some of the components of bacterial spores would help to determine the optimal excitation and emission wavelengths for subsequent study and should also improve the understanding of the chemical/physical system of bacterial spores. The effect of UV irradiation on the fluorescence profile of these components was important in terms of characterisation of the fluorescence from bacterial spores. Knowledge of the EEM of the individual fluorophores can improve the interpretation of *Bacillus* spores' autofluorescence measurements. These results are discussed and compared with the fluorescence properties of bacterial spores in sections 5.3 and 5.4.

5.2.1 Dipicolinic acid (DPA)

In this research we studied different forms of DPA (dry crystalline, wet paste and aqueous solution) and the effect of UV irradiation on these fluorescence profiles with two dimensional multiwavelength fluorescence techniques. We did not observe any measurable fluorescence of a DPA solution[103], but did observe the weak Raman-scattering peak around the vicinity of 290 nm from water as shown in Figure 4.1(A). Raman scattering has a cross section that is roughly proportional to the excitation frequency to the fourth power. This peak decreases and disappears as the wavelength increases.

The selection of suitable substrates to investigate the above mentioned goals was a challenge in the initial days of the research. Any substrate can contribute fluorescence intensity to the sample fluorescence and this may hide or overlap samples features. For the collection and measurement of chemical components and spores in different environments, one should determine the optimal substrate. We tried with different kinds of filter papers and found a suitable one that helped to answer the questions or hypothesis posed at the beginning of this research. The selection of the appropriate filter paper was an important step in this project.

Our measurements confirmed an earlier finding that, even though the DPA absorbs in the UV region, the DPA solution does not appear to fluoresce for excitation between 250 to 300 nm[103] in water solution. We note that the absorption spectrum of DPA shifts slightly (blue shifted) to shorter wavelengths upon exposure to UV light (see Figure 4.3). We also noticed a very small increase in the absorption in the 300 to 400 nm wavelength region. This very small increase does not help to explain the strong fluorescence maximum observed at excitation 360 nm. This behaviour can be partially explained by using our QE measurements and this is discussed in section 5.5. The DPA dissolved in ethanol fluoresced in the blue as shown in Figure 4.2(B) and the shape of the spectrum looks similar to UV exposed DPA in solution. The changes in the absorption spectra, and the well-defined fluorescence emission as a result of UV exposure and the retention of the fluorescence intensity after a week in the dark, indicate the probable irreversible formation of a photochemical compound. In their study of Raman spectra of DPA in solution, Kolomenskii and Schuessler[25] argued

that, at higher excitation laser pulses (above 50 mJ), dipicolinate ions are formed. This results in the formation and dissociation of DPA dimers and polymers. This may be the reason for the observed changes in the fluorescence profile and the absorbance changes of the UV irradiated sample.

Since the DPA inside the *Bacillus* spores is more similar to the dry crystalline state or a wet paste of DPA than the DPA in solution[25], we measured the fluorescence from the exposed DPA dried on filter paper to make a wet paste or a dry sample (see Figures 4.4 (A) and 4.4 (B)). Both of these spectra looked similar to the fluorescence of the UV exposed solution but contained a slightly wider spectral range. The fluorescence profile of crystals of DPA not exposed to UV irradiation is shown in Figure 4.5(A). Probably because of a slightly greater amount of dry DPA exposed on the filter paper compared with the diffuse concentration of the molecules in solution, a fluorescence spectrum can be measured, even without UV exposure. As we mentioned elsewhere in this thesis, the small trail of peaks that occur for short wavelength excitation is an anomalous signal at 420 nm that is observed whenever a large amount of light is reflected into the detection monochromator of the fluorometer.

One might question whether the fluorescence of the dry crystals of DPA is enhanced compared with the small-to-zero fluorescence observed from a DPA solution so, we carefully wet the filter paper with deionized water while it was in the cuvette and remeasured the fluorescence (see Figure 4.6). The fluorescence decreased by nearly a factor of three after the DPA was wet. Since some of the decrease could have been due to DPA going into solution, and being washed away from the portion of the filter paper probed by the fluorometer, we dried the same piece of filter paper with the DPA in the dark and the signal increased by a factor of two. From this, we conclude that there is a measurable increase of fluorescence for DPA when it dries. Dry DPA exhibits about twice the fluorescence of wet DPA. The UV exposed DPA crystals (Figure 4.5 (B)) show a broad fluorescence spectrum and very long wavelength fluorescence that was not observed for unirradiated DPA (in the visible range of excitation wavelengths 500 -600 nm). Thus, the fluorescence spectrum of the DPA molecule exhibits a richness of spectral features before and after UV irradiation useful for its identification.

5.2.2 Calcium dipicolinate (CaDPA)

In this study we again used several forms of CaDPA (dry crystals, wet paste and in aqueous solution). The distinct double peak in the absorption spectrum of CaDPA at 269 and 277 nm with a shoulder at 264 nm does not appear in the absorption spectrum of DPA (see Figure 4.3). Multiple fluorescence scans of the same CaDPA solution showed a slightly increased fluorescence, indicating that the UV light from the fluorometer was affecting the solution and enhancing the fluorescence. This observed fluorescence enhancement and the corresponding fluorescence spectral band was almost identical to our observation with BG1 spores in suspension (after multiple fluorescence scans), as discussed in section 5.3.

In order to prevent the presence of buffer salts from interfering with measurements of dried and partially dry DPA salts we did the CaDPA measurements with unbuffered aqueous solution. Previous spectrophotometric methods[102] for CaDPA estimation used high pHs to ensure the stability of the chelate. These high pHs favour precipitation of calcium carbonates and phosphates, causing turbidity and a loss of DPA by coprecipitation. A more recent method[15], using 100 mM Tris buffer at pH 7.6, provides adequate buffering for the acid extract, and a Ca^{2+} concentration required to achieve essentially complete formation of CaDPA chelate. Other researchers have reported that the reproducibility and consistency of the fluorescence intensity were found to be pH dependent.[103]

The absorption spectrum of UV irradiated CaDPA showed moderate changes compared with the absorption spectrum of an unexposed CaDPA solution (e.g., the absorbance increased at around 300 nm excitation). Nudelman *et al.*[103] reported that low-dose treatment with 254 nm UV irradiation caused only slight changes in the absorption spectrum of CaDPA. However, irradiation of 10μM solutions of CaDPA in a N-2-hydroxyethylpiperazine-N'-2-ethanesulfonic acid (HEPES) buffer at higher intensity and for longer durations resulted in absorption spectra that changed substantially. The CaDPA absorption spectrum also varies with temperature.[102] The changes that we observed in the CaDPA fluorescence and absorbance as a result of UV irradiation remained constant for at least seven days in the dark. The fluorescence

measurements were reproducible qualitatively and quantitatively even without using the buffer.

The increases in the fluorescence of the dry crystals of CaDPA compared with wet crystals again indicate that dry samples fluoresce more intensely than wet samples. We observed a peak similar to the peak measured from exposed DPA in both the dry and wet form of CaDPA spectrum (see Figures 4.10 and 4.11). Some of the DPA in the mixture might not have formed a complex with calcium because of an insufficient excess of calcium ions.

The dry CaDPA also showed enhanced fluorescence after UV exposure. Similar to the dry DPA samples, enhancement was much less for the dry sample compared to the solution. Unlike the dry DPA, no major changes (apart from the intensity change) in the fluorescence spectrum were observed for the dry CaDPA sample. This sample was only exposed to 10 minutes of the UV light instead of 15 minutes. The longer exposure times would have increased the fluorescence too much and the signal would have saturated the detector. We therefore used a shorter exposure time to see whether any changes in the emission spectra would appear. We observed only the increase in intensity. Strahs and Dickerson found that dipicolinate ions in crystal structures of hydrated forms of CaDPA is essentially planar, with the calcium ion as a tridentate ligand.[142] "Two CaDPA units were joined together, forming a dimer where the two DPA units were almost coplanar. This coplanarity of the two DPA units in the CaDPA dimer may be the reason for the much higher fluorescence we detected for CaDPA in comparison with DPA, caused by extended delocalization of π electrons".[103] However the detailed photophysics of the DPA forms remain beyond the scope of the present investigation.

We used a broad band UV irradiation for 15 minutes in all of our measurements in this thesis. We also found that the exposed CaDPA solution for 5 minutes produced the high fluorescence in the measurements. The exposure time for optimal fluorescence enhancement depends upon the intensity of the UV irradiation source and the concentration of the sample. If we use very high power UV irradiation, one might expect to see the peak enhancement within seconds. It would be interesting to investigate whether an intense pulse of UV irradiation could be used to achieve these

results. Changes in absorbance appear to partly explain the changes in fluorescence at different exposure times at 300 nm excitation. After 30 minutes exposure, the two absorbance peak positions (271 and 277 nm) of the CaDPA molecule disappeared (see Figure 4.15). As expected, the UV wavelengths that were more effective at increasing the fluorescence of CaDPA solution were generally in the range of 200 to 300 nm with a maximum fluorescence enhancement observed at around 276 nm exposures. This is an ideal region of the spectrum for assessing fluorescence enhancement. This observation depends on the function of the number of photons absorbed and the activation spectrum resembled with the absorption spectrum of the solution (see Figures 4.15 and 4.16). The changes in fluorescence intensity as a function of time immediately after UV exposure was important to better understand the optical fluorescence characteristics of the CaDPA sample.

The UV irradiation probably induces isomerisation in the DPA/CaDPA molecule as suggested in the literature.[103] It is known that although there may be a small energy difference between reactants and products, many chemical reactions are unlikely to proceed thermally due to the large energy barrier of the transition state.[145] The transition barrier between the isomers is too large for isomerisation to take place thermally. However, there may be a conical intersection between the excited state surface and the ground state that gives an isomerisation pathway. In fact, Chachisvilis *et.al* have shown that a conical intersection exists between the S_2 (π π^*) and S_0 surfaces that allows for the formation of a prefulvenic form of pyridine.[146] Since the absorption profile between pyridine and DPA/CaDPA is so similar, it is suggestive that a similar conical intersection exists in DPA/CaDPA so that the molecules isomerize when irradiated by UV light.

5.2.3 Tryptophan

Fluorescence of tryptophan has been extensively used to study biological samples. Tryptophan in water has produced one well defined peak at 280 nm excitation and emission maxima occurring with peaks at about 340-350 nm (see Figure 4.17). When tryptophan is inside a cell or spore, we note that the emission maxima are shifted to shorter wavelengths and the excitation peak is near 290 nm. The 2-D fluorescence profile for tryptophan in dry powdered form on filter paper and aqueous suspension of tryptophan showed very distinct profiles, as shown in Figures 4.17 and 4.20. The dry tryptophan powder on filter paper has an emission peak at 320nm with excitation of 290 nm. The emission peak of aqueous solution of tryptophan is 350 nm with the excitation at 290 nm. The shift of the peak due to the presence of water is of interest as it may relate to changes of bacterial spore fluorescence on hydration or drying.

Tryptophan fluorescence intensity decreases with exposure to UV irradiation. The decrease in fluorescence intensity for the excitation wavelength 290 nm could be related to the alteration of the aromatic structures of these proteins. “In fact, studies carried out on UV-induced inactivation of enzymes reveal that the protein fluorescence decrease is due to the aromatic amino acids’ destruction and in particular to the chemical conversion of tryptophans to their oxindole derivatives”.[147] The absorbance of the UV exposed tryptophan also changes substantially, as shown in Figure 4.19. The exposed solution absorbs in longer wavelength regions. These changes in fluorescence were observed in all of the biological samples and are discussed in the following sections.

5.3 Multi wavelength fluorescence studies of *Bacillus* spores

We studied the intrinsic steady-state fluorescence spectra of *Bacillus* spores in dry, wet, redried and aqueous forms to increase our knowledge and understanding of *Bacillus* spores in different environments. We observed major differences in fluorescence between the dry and wet samples of the different species of *Bacillus* spores. In contrast to the previous results of dry spores and spores in suspension, the present studies were able show the differences of dry and wet spores in a similar experimental geometry. We believe that the data generated are useful for the development of direct-reading instruments for detecting bacterial spores using the fluorescence technique. As observed earlier, the dried BG1 spores show longer wavelength fluorescence emission than do spores in suspension (see Figures 4.21 and 4.36).[148] We did experiments to determine whether the fluorescence changes that were observed when a spore is hydrated are reversible; to determine whether the spore species of *Bacillus* spores in water can be distinguished and from those in the dry state; and further to attempt to understand whether the underlying spectral patterns related to species and the derived principal components were correlated with the chemical composition of the samples. We also wanted to determine what changes, if any, occur to the autofluorescence of a spore upon autoclaving and washing of the spores.

We measured the fluorescence of spores for three conditions, dry and hydrated on filter paper and spores in water suspension. We note that fully hydrated spores on filter paper were not in a suspension where the solvent could partially index-match the spores. A reduction of contrast reduces scattering and enhances the penetration of light deep into the sample in suspension. The hydrated spores were on wet filter paper that acts as a wick for a small reservoir of water in the bottom of the cuvette. The fluorescence measured from our wet and particularly dry BG spores on filter paper was shifted from the results of tryptophan/CaDPA-like fluorescence observed when the similar spores are in suspension (see Figures 4.21, 4.23 and 4.36). The fluorescence of spores in a dry aerosol-like state is substantially different from that when the spores are suspended in water. The different behaviours of the spores' fluorescence in these conditions were also reflected in the PCA results as discussed below (see Figure 4.38).

The shape differences between wet and dry spore fluorescence on filter paper are not completely obvious when looking only at one or two excitation wavelengths (see Figures.4.25 and 4.26). The number and the distribution of spores on the filter paper may change when the filter paper is wet. Observed changes may be partially due to loss of some spores as the filter paper is wetted and again while it is dried. The multi wavelength 2-D EEM graphs more clearly indicate shape differences between wet and dry spores spectra as shown in Figures 4.21 and 4.23 in the sample of BG spores, in Figures 4.29 and 4.30 in the sample of BC spores. The more subtle changes between spectra of dry and wet are brought out by PCA results (see Figures 4.33, 4.34 and 4.35). There were species-dependent fluorescence changes that suggested hydration might also be utilized for distinguishing *Bacillus* spore species.

Other researchers reported major changes in *Bacillus* spores when the spore is hydrated. Watt[76] showed that the water content of the spores decreased with increasing temperature over the entire humidity range. In the water-wet state, the spore is swollen and a water-filled porous structure exists in accordance with the findings of Black and Gerhardt.[70] Neihof et al.[68] observed that the surface area dramatically decreased for spores that were humidified and subsequently dried and that the degree of surface area reduction depended on the spores' drying procedure. It is also noted from the present experiments that the physical state of the sample (hydrated, partially hydrated or dehydrated) has an influence on the fluorescence spectrum. Marshall and Murrell[69] used deuterated and tritiated water with spores and were able to conclude that at least 97% of the water in spores has the ability to exchange with the environment. Furthermore, they found that water exchange in a population of spores was almost complete in two to three minutes at 0˚C. In our experiment, the population of spores was allowed to stand in water for 15-20 minutes at room temperature before the fluorescence measurements were made.

We suggest that some simple classification of *Bacillus* endospores may be possible from their fluorescence spectral signatures. Whereas the classification of bacteria and bacterial spores has been disappointing when using the fluorescence from a single excitation wavelength, the data are much richer when the fluorescence is measured from multiple excitation wavelengths. The possibility of discriminating between different bacterial spore species in dry, wet and re-dried conditions or in suspension

on the basis of their multiwavelength fluorescence spectra was investigated by using PCA (see Figures 4.28, 4.32, 4.33, 4.34, 4.35 and 4.38). It is also interesting to note the differences between the wet spores in suspension and the wet spores on pieces of filter paper as shown in the PCA (see Figure 4.38). This may be due to an excess number of spores in the filter paper that are unable to become fully hydrated. We also speculate that the fluorescence spectra were influenced by growth media or vegetative cell residue remaining on the outside of the spore. It is possible that some of the material on the exterior of the spore might be washed away upon hydration in suspension and this might lead to the small differences in the spectra from the wet spores on filter paper. These differences were more pronounced when we included long excitation wavelengths in the PCA.

In PCA, only selected excitation/emission wavelength pairs were used for discrimination purposes as explained in the materials and methods section. Such analysis, although simplified and limited to only six excitation/emission wavelength pairs, produced a satisfactory discrimination between different spore samples or between the dry, wet or redried state of samples. These results show that it is not even necessary to record the entire forty-one excitation/emission (EEM) spectra in order to discriminate between spores. Instead, the fluorescence intensity could be measured at selected excitation/emission wavelengths and then subjected to PCA.

The results in the PCA plots are stable if minor changes are made in the analysis. For instance, if different set of excitation wavelengths are used (within the range of fluorescence emission from several chemical components of the spores), the results are not significantly changed (see Figure 4.28). However, if major changes are made, such as using only excitation wavelengths longer than 400nm (except in the sample of BG spores, which produces fluorescence even at 500 nm excitation, as shown in Figures 4.21 and 4.28), or using only three wavelengths (not covered the entire fluorescence excitation-emission range) the results are significantly affected (see Figure 4.38). At these longer wavelengths there is very little fluorescence signal from the spores and signal noise creates spurious results with the PCA. Likewise, if the emission wavelengths include values closer to the excitation wavelengths, then the amount of elastic scattering over the smaller fluorescence signal from the sample dominates the signal and the PCA. While the PCA is reasonably robust to

measurement parameters, the results can be invalidated by a careless selection of measurement parameters.

PCA is well documented for optimizing the evaluation of sample data with minimum loss of information. We have not attempted to subtract any background signal created by the filter paper in the PCA. The first two to three PCs describe more than 90% of the measured signals. This simplification of complex two-dimensional contour plots readily aids in identifying similar and different spectra. To build the similarity map in simple cases, PC1, PC2 and PC3 were used as shown in Figures 4.28, 4.33, 4.34 and 4.35. Likewise, the major components of the spectra were captured in the first two to three PCs, and the small background signals, such as the light scattering off filter paper, therefore, do not necessarily need to be subtracted from the spectra before the analysis. We also used other substrate quartz slides to measure the fluorescence of spores. PCA results combined with the measurements from these two substrates did not show any major difference. The spores measured from filter paper and quartz slide substrates show similar variations in the PCA score plot (see Figure 4.40)**.**

The PCs in Figures 4.28, 4.33, 4.34 and 4.35 show that wet spore fluorescence is clearly different and distinct from dry spore fluorescence. The PCs also show that the re-dried spores look similar, but not identical to the dry spores as shown in Figure 4.28 in the case of BG samples. In the case of BC spores, the dry and re-dried spores were more identical as shown in Figure 4.32. In this case the spores were re-dried in air for seven days. This distinction between dry and re-dried spores is not obvious when looking at the fluorescence contour plots. There are slight variations from sample to sample, and the overall trend is difficult to discern by eye. Also, when considering the data variabilities explained by PCs, it appeared that the hydration effect on spore fluorescence properties was more dramatic than looking at the 2-D fluorescence fingerprint. PCA aids in finding the subtle differences between the spectra of dried and re-dried spores.

The clustering of the spores into overlapping groups is arbitrary. The spores could have been grouped in three distinct and separate groups with one sample mis-identified in Figure 4.28. While we cannot exclude that possibility, it does make more physical sense to have two overlapping groups. The re-dried BG spores have

probably not achieved the same level of dehydration as the original spores. The original spores were lyophilized under vacuum. The re-dried spores were allowed to dry at room temperature for only 24 hours in the sample of BG spores, but in the sample of BC spores, the re-dried spores were allowed to dry at room temperature for seven days. The re-dried BC spores appeared to achieve the same level of dehydration as the original spores (see Figure 4.32).

Fluorescence fingerprints of all the samples studied in this research was reproducible even with a different concentration of samples in each experiment. We also showed that BG spores can be distinguished from other *Bacillus* spores in different environments, even when different laboratories produced the spores. Spore species-specific spectral differences and changes are observed in wet, dry and aqueous environments. The *Bacillus* spores studied using this multiwavelength fluorescence technique showed two main peaks (or spectral bands) for each species. The fluorescence spectra of the samples of *Bacillus* spores at excitation around 290 nm are dominated by tryptophan-like emission peaks and agree with other studies.[35] The exact size and shape of this peak changes with the environment (dry, wet or in aqueous suspension) of the protein (tryptophan). The emission spectra of the dry spores showed a maximum at around 320-330 nm, the wet spores shows a fluorescence shift (red shift) to 340-350 nm. Also the location varied slightly from one spore to another. The other peak (or band) appears at excitation above 360 nm and emission around 470 nm. This peak excitation position varies with spore species from 360 to 420 nm. The spectral width also changes with the environment in addition to emission peak position. These characteristic changes in different environments are the key to the species discrimination with fluorescence technique in dry, wet, re-dried or aqueous samples.

It has been shown very recently that dormant spores are not entirely static but rapidly swell and shrink in response to increases or decreases in relative humidity.[80] The measurement of size increase fits into two diffusion rates. The causes of these two rates are interpreted as water penetrating into the spore coat and cortex, and water penetrating into the spore core. Plomp *et al* studied and reported that the dimensions of individual BG spores decrease reversibly by 12% in response to a change in the environment from fully hydrated to air-dried state indicating the fact that the dormant

spore exhibits a dynamic physical structure.[149] They also determined the intra-and interspecies distributions of spore length and width for four species of *Bacillus* spores in fully hydrated and air-dried states. They found that the individual spore sizes differ significantly depending upon species, environmental conditions and growth regimes.[149] Chada *et.al*,[150] also found that the structures of ridges that encircled the spore differ sufficiently between species of *Bacillus* spores to permit species-specific identification. These studies all support the model of reversible water migration between inner spore compartments and the environment. The changes in the fluorescence spectrum between dried, wet and re-dried spores and the dissimilarity of dried and re-dried spores compared with wet spores suggest that designs of spore detectors and classifiers must incorporate this knowledge.

It is well known that the primary fluorescence signal from spores in a water suspension is tryptophan. As the spores dry the tryptophan-like fluorescence disappears in the case of the BG1 sample as shown in Figures 4.21 (this was an exceptional case). But this was not the case in other spore species in this research. The tryptophan fluorescence was well pronounced in water suspension and the species of wet spores on filter paper in contrast to dry spores. This would lead one to suspect that something near the outside of the spore is preventing the light from penetrating into the spore and contributing its own luminescence signal at longer wavelengths.

These fluorescence studies also suggest that spore species respond consistently to the effect of hydration/drying while maintaining the spore dormancy. Spores require water to germinate into a vegetative bacterium. We found that the changes in fluorescence due to hydration/drying were reversible. This implies that spores still maintain the state of dormancy. Though the nature of water in the spore is not fully understood, our fluorescence measurements and PCA confirm that the water in the spore has important interactions with the proteins and other chemicals in the spore.

It is important to note that we did see major changes in the spore fluorescence profile upon washing and autoclaving the spores (see Figures 4.39 and 4.40). As reported in the literature[52], bacterial spores exhibit significant physical changes following the treatment of autoclaving (distortion or break down) and these changes are reflected in their fluorescence fingerprint. Significant spectral changes in the fluorescence spectral

region of DPA (excitation 300-400 nm) were observed upon washing and autoclaving. Recent literature demonstrated that some DPA from endospores is immediately available in solution without any treatment.[17, 20, 21] We therefore reasonably speculate that some of the DPA (probably from the spore outer coat) could be washed away with the supernatant. During the autoclaving process, DPA undergoes an undetermined transformation.[52] Autoclaving bacterial spores is advantageous, because it is a familiar technique that inherently reduces the risk associated with their handling. "The extreme resistance property of bacterial spores has been taken to test the performance of autoclaves in the laboratories".[54] This study showed that the fluorescence technique is also applicable to situations where unknown bacterial spores previously washed and autoclaved prior to collection need to be distinguished. Spores also can be produced with a varying amount of washing. Together, these studies indicate that the fluorescence spectra of untreated, washed and autoclaved spores are different.

As we mentioned elsewhere in this thesis, fluorescence fingerprints of biological samples contain information derived simultaneously from all chemicals (metabolites and cell components) that are present in the samples. "Major differences were observed in the chemical composition of different species of *Bacillus* spores with respect to levels of DPA, Ca and Ca/DPA ratio".[63] The structure and the fluorescence fingerprint of these samples changes with the environment. We discussed the features of some individual chemical components of *Bacillus* spores in Section 5.2. This is only a preliminary investigation and more research needs to be done, with more samples and other possible components of *Bacillus* spores.

The PCA loadings vectors are more physically interpretable and they correspond to the underlying spectra of the fluorescence components (fluorophores) present in the bacterial spores. PCA score plots enabled to distinguish between the three species of *Bacillus* spores in water suspension as shown in Figure 4.41. The PCA loading vectors (PCs) shown in Figure 4.42 have an advantage in providing good approximations of the excitation and emission profiles of the fluorescence components (fluorophores) present in *Bacillus* spores. The small shifts in the wavelength regions and the alterations in structure can be explained by all the scattering, quenching, reflecting and absorbing phenomena present in the bacterial

spore samples, which make the resulting fluorescence profile a chemical fingerprint rather than a perfect mixture of fluorophores.

The PCA model decomposed the fluorescence matrix into distinct fluorophores that were assigned to tryptophan-like and CaDPA-like emission. The assignment was mainly verified by comparing the derived PCA components with the fluorescence of the pure fluorophores, which increases the reliability of the assignment considerably and thus underlines the advantage of the multivariate PCA approach. The first two loading spectra of the PCs are sufficient enough to explain the original spectral changes. Since PCs are mutually orthogonal they each represent statistically independent modes of variation in the samples. The first PC identifies the major axis in the data set, which is the direction of greatest variance then removes it from the data. The major axis in the remaining data is then identifies the second PC, which is orthogonal, uncorrelated with the first PC. The second PC can be interpreted as the most important relationship among the data after correcting for differences due to first relationship. Tryptophan has mainly contributed to PC1 and CaDPA to PC2. PC3 can be interpreted as a contrast between another chemical component (might be due to DPA and/or broth medium) and tryptophan (see Figure 4.42(C)).

In the fluorescence measurements of samples or fluorophores in water, Raman spectra have very weak bands with narrow bandwidths in comparison to the strong fluorescence spectra. It was shown in this study that the robust nature of PCA makes it possible to resolve a very minute signal of Raman spectra in the measured fluorescence of bacterial spore samples in water suspension (see Figure 4.42(D)). Hasegawa *et.al* has recently shown that Raman scattering arisen from indene was mixed with fluorescence and PCA worked well for the separation of Raman spectrum.[151] It is reasonable to assume that the first one to two PCs represent pure fluorescence signatures from the samples. PCA has shown promise to overcome the Raman problem in the fluorescence measurements of *Bacillus* spores in aqueous suspension or solution form. This result again support to our argument that background signals do not need to be subtracted from the spectra before the analysis.

The main drawback with PCA is that some of the components are not always clearly interpretable, with input variables often contributing significantly to more than one

component due to the effect of orthogonality constraint (If we multiply the elements in one loading with the elements in any other and sum those, the real number is zero). This is a mathematical restriction of PCA and it is not correct for real spectra. The real spectra of the constituent chemical components are not orthogonal and therefore PCA loadings can not be always considered as spectra of real chemical components. The spectra-like PCA loadings are therefore called abstract spectra.[152] But some of the loadings in this spectral analysis (PC1 and PC2) looked like something that is close to real spectra from known chemical components. This is also the reason why some of the PC loadings (PC3) were not perfectly related to specific chemical components and tryptophan being represented in more than one component (see Figure 4.42 (C)). In this case, PC3 can be considered as an average spectrum of different components in the *Bacillus* spore samples. So, one cannot definitely claim that the loading components are real estimates of pure chemical components, but in this particular case some PCs represent these chemical components fairly well. It was recently shown that PCA is a powerful technique to separate various signals when their intensities vary greatly.[152]

5.4 Multi wavelength fluorescence studies on *Bacillus* spores in water under enhanced UV irradiation

5.4.1 Fluorescence studies of *B.subtilis* spores with, and with a lack of, dipicolinic acid

In this study we were interested in determining the role of major chemical components of *Bacillus* spores to the fluorescence of the spores. It is well known that most biological contain tryptophan. DPA which is a major constituent of *Bacillus* spores mainly in the form of CaDPA was rarely found elsewhere in nature. We compared the fluorescence of native BS (+DPA) spores with that of mutant BS (–DPA) spores lacking this chemical. The DPA in the fluorescence of (+DPA) spores were found in the form of CaDPA complex (see Figures 4.42 (B),4.43, 4.51 and 4.60). Spores may contain numerous other chemicals (fluorophores) which could affect the fluorescence of spores, but their contribution to the fluorescence appears to be very small if present.

The most intense fluorescence band observed in each spore studied in diluted suspension, with excitation at ca.250-300 nm and emission at ca. 300-400, has in the past been ascribed to the aromatic amino acids, primarily tryptophan (excitation/emission peak ~280/350 nm) by various research groups (e.g.,Bronk and Reinisch[27]). It is likely that there are small contributions from the other two aromatic amino acids, namely tyrosine (peak at ~275/300 nm) and phenylalanine (peak at ~260/280 nm) but this has not been established. We note that almost all biological specimens examined appear to have a tryptophan type of EEM peak.

In the unirradiated suspensions of (+DPA) spores, very little detectable emission was seen in the region where CaDPA emits according to our results (see Figures 4.43 and 4.60). We did not notice any influence of the presence of CaDPA in their fluorescence fingerprint of unirradiated BS (–DPA) spores in water suspension (see Figure 4.46). However, after our broad band UV irradiation of BS (+DPA) spores in water suspension, there was a substantial emission in the location where the chemical CaDPA fluoresces (see Figures 4.44 and 4.45). This UV effect was very small, if present for the BS (–DPA) spores (see Figures 4.47 and 4.48). It is possible that the

strong fluorescence of the spore's tryptophan hides the fluorescence emission from other molecules which fluoresce in the same region of the EEM graph. For both (+DPA) and (–DPA) spores, we found that the intensity of the tryptophan-like band is greatly suppressed after UV irradiation.

In our visual inspection of the EEM graphs, (+DPA) and (–DPA) spores, appeared to have small distinguishable differences (see Figures 4.43 and 4.46). This observation was confirmed with PCA. The PCA score plot (see Figure 4.49) derived from these spectra, where the similarities between the biological replicate spectra of each individual strain confirms that a very high degree of reproducibility can be achieved with fluorescence across the spectral range. The small differences in the fluorescence fingerprint of these spore strains were observable before exposure to broad band UV irradiation. But after the UV irradiation, there are major changes in the fluorescence fingerprint of spore strains, as again confirmed with PCA.

Our results suggest an interpretation of our studies with structure of spore species. It is well known that BC and BT spores are enclosed by an exosporium. But, BS spores do not have an exosporium. It is not known whether BG spores have an exosporium or not. We could not see any measurable fluorescence from the spore component, CaDPA in the spores of BC and BT before UV irradiation. We observed some CaDPA - like fluorescence in the case of BG and BS spores even before exposed to UV irradiation (see Figure 4.60). These measurements suggest that the exosporium, enclosed in the BC and BT spores may reduce the light from penetrating deep inside the spore to excite the molecule CaDPA. These results support other studies[56] indicating that BS spores do not have an exosporium and further suggest that BG spores do not have an exosporium.

5.4.2 Identifying probable major fluorescence components of *Bacillus* spores

To amplify our understanding that the main chemical contributors to the observed spore fluorescence are trytophan and CaDPA, we attempted to simulate our spore observations with these chemicals alone. In Figure 4.50, we show the 2-D fluorescence profile of the mixture of tryptophan and CaDPA in a wet-paste form on a filter paper. The two main bright peaks appearing in this plot look similar to the 2-D fluorescence spectra of BG1 spores in suspension as shown in Figure 4.51. After exposure to a broad band of UV irradiation, both of these 2-D plots showed only one main peak, which was very similar to the enhanced CaDPA peak, and the suppressed tryptophan peak of the spores (see Figures 4.53 and 4.11). There is another slightly less intense peak observed around the region of 360 nm excitation wavelength (see Figure 4.51). Possibly further studies could confirm assignment of the other fluorescent bands and establish a quantitative relationship between the chemical composition of a *Bacillus* spore and its fluorescence characteristics.

We also note that the DPA in bacterial spores has been primarily identified as CaDPA with IR absorption[114], UV absorption[102] and Raman spectra[113]. However, single wavelength excitation-emission fluorescence from spores in suspension[153] corresponds very closely with our measurements of DPA (wet or dry) and not the CaDPA (wet or dry). Our results revealed mainly the CaDPA-like fluorescence (major peak) in *Bacillus* spores in suspension before and after UV irradiation even though we also observed another DPA-like fluorescence (less intense peak or band) in suspension. We also observed that CaDPA-like fluorescence of *Bacillus* spores in water becomes DPA-like fluorescence when the spores are dried (see Figures 4.21, 4.23, 4.36). The study of Slieman and Nicholson[108] also support this observation. Their study showed that the environment within the spore differs substantially when spores are in the air-dried state versus when they are in water suspension. These studies clearly showed that multiwavelength fluorescence spectroscopy was a very useful technique for informative qualitative analysis.

5.4.3 Distinguishing bacterial spores from other biological samples using fluorescence spectra

The enhanced fluorescence observed in all the *Bacillus* spore species in this research after exposure to UV was appeared to be the existence of DPA mainly in the form of CaDPA. To determine whether the fluorescence behaviour after UV treatment could be used as a reliable indicator to indicate that bacterial spores were present, a number of other biological particles must be examined with the same experimental procedure. We examined a number of other biological samples and other materials to further understand the unique fluorescence characteristic property of bacterial spores. One such experiment is shown in Figure 4.62. This experiment was performed with a similar experimental protocol on *E.coli* vegetative cells after overnight growth in nutrient broth medium. In the case of *E coli,* as shown in Figure 4.62, the broad fluorescence peak at 350nm is mainly from tryptophan. The *E.coli* showed no enhancement of fluorescence after UV irradiation in our studies. We see that the effect of UV on *E.coli* cells differs substantially and recognizably from its effect on *Bacillus* spores.

A very different biological spore which we examined with this approach was the *Aspergillus niger* fungal spore. A characteristic response of these spores in suspension was observed in the excitation band in the range of 340-380 nm (see Figure 4.65). The UV irradiated samples show a peak centered around 500 nm emission whose intensity was enhanced. Such a behavior should indicate the involvement of another chromophore in addition to the contribution of the aromatic amino acids reported above. This fluorescence enhancement did not overlap much with the fluorescence enhancement in *Bacillus* spores after exposure to UV irradiation.

In many environments the dominant background particles are nonbiological. In addition to discriminating between bacterial spores and other biological aerosols, we wanted to distinguish bacterial spores from the dust. Clearly, the bacterial spores can be differentiated from some common biological particles that do not contain any bacterial spores. We have found that only *Bacillus* spores yield a positive response to this UV enhancement, even though the fungal spore also shows the enhancement of fluorescence but in a different spectral excitation-emission band. We had no problem

in discriminating the *Bacillus* spores from the fungal spores both from the fluorescence fingerprint and PCA (See Figures 4.65, 4.66, and 4.67). In Figure 4.66, PCA was applied to two different set of excitation wavelengths, which produced excellent discrimination between the *Bacillus* spores and other biological samples. The range of excitation wavelength in the region of 300- 400 nm produced a good differentiation between *Bacillus* spores and other samples including fungal spores. These wavelength ranges were selected because they show reasonable fluorescence signals corresponding to the fluorophores of CaDPA and DPA, the main interest target molecules for discrimination in this study. The fungal spores have been separated from other biological samples.

Interpretation of the score plots shows that *Bacillus* spores are separated from fungal spores in the first PC and from other biological samples in the second PC (see Figure 4.66). Sources of separation between the samples can be found by interpreting the PC loadings, revealing the spectral regions contributing to the separation. The loadings of the first three PCs for the data set show features in common with individual constituent chemical spectra. For instance, the first loading can be seen to have a strong resemblance to the CaDPA signal (see Figure 4.67(B))**.** It was not easy to find a physical interpretation for the second component. Indeed, the second component is probably a contrast between another undetermined chemical component and CaDPA. The third loading component can be mainly ascribed to the undetermined chemical component responsible for the enhancement of fluorescence in *Aspergillus niger*. Generally, the approach and the results look very promising and can be used for the detection and classification of bacterial spores.

5.5 Fluorescence quantum efficiency

In this section, we studied QE's for the various important peaks in the EEM graphs. This quantitative measurements would be an important parameter in the design of biological detectors using fluorescence and useful in predicting performance of such detectors. Fluorescence yields are determined by the comparison of the intensities of fluorescence of the test samples with a standard sample of anthracene in ethanol. Fluorescence yields from this work are listed in Table 4.2 together with comparable literature values (Only unexposed tryptophan values are available). We found a value of QE of unexposed tryptophan is 0.12, which is reasonably close to the reported values of 0.13[124] 0.18[117] and 0.17[105] in the available literature. The extrapolation of the system response beyond the range measured is perhaps the most questionable aspect of this research study. As we show in Figure 4.71, the extrapolation was a constant for flat spectral response beyond the range measured. We also note that the fluorometer used in this research was designed for a relatively flat system response. Our measured QE value of tryptophan, which is close to the reported values, was evidence for our assumption that the extrapolation was quite reasonable. Clearly, we are justified in not following the straight line system response, which would have yielded a QE of 0.45 for tryptophan.

We found that the apparent QE of tryptophan decreased while that of CaDPA increased with UV exposure with the level of exposure used (15 minutes exposure to broadband UV of 80J). The increase or decrease in fluorescence intensity is partially connected with absorbance changes observed for CaDPA and tryptophan molecules respectively, as shown in Figures 4.3, 4.15 and 4.19. But, due mainly to higher quantum yields of UV exposed CaDPA compared to that of neutral form, which is very weakly fluorescent; the differences cannot be fully explained by these absorbance changes. Calculations showed that the fluorescence QE of CaDPA increased by a factor of 8 from 0.01 to 0.08 at 300 nm excitation after exposure to UV light for 15 minutes. We found a value of QE of tryptophan as 0.01 after exposure to a broad band of UV irradiation for 15 minutes.

The QE closely depends on the environment of the fluorescing molecule, and on processes like internal non-radiative conversion (S_1-S_0) and intersystem crossing (S_1-

T_1). [53] The QE of a sample is highly dependent on temperature, pH and absorbance. We did not take into account the maintaining of the temperature and pH constant during our experiment. "The measurements are complicated in the biological and in the dry samples due to their absorbing and scattering properties".[154] In addition to the UV effect, the samples were exposed to heat for 90 minutes during the multiwavelength fluorescence measurements. "A decrease in the fluorescence quantum yield with temperature has been reported for the indole chromophore as a consequence of temperature dependence of non radiative processes".[155]

The *Bacillus* spores, unlike the anthracene or other chemicals, contain many fluorophores. Therefore,one would not expect the QE to be wavelength independent. Excitation near 290 nm probably excites primarily the tryptophan in the spores. Excitation near 300 nm was mixed up with the major contribution from CaDPA and tryptophan in spores in suspension. Therefore, we measured the QE at 290 nm and 300 nm excitation because the fluorescence is significant in these wavelengths. In a structural study of the proteins of the *Bacillus stearothermophilus* based on intrinsic tryptophan fluorescence, Saavedra *et al.,*[156] reported that the fluorescence QEs were independent of the excitation wavelength in the range 280-310 nm. Overall, the measured fluorescence QE did not vary much at 280 and 300 nm excitation wavelengths. Our values of the QE of spores (unwashed) in suspension agree with the reported values of QE of *B.magatarium* in suspension.[27]

Unwashed samples showed a higher fluorescence QE than washed samples. This is probably due to the cell debris or broth on the exterior of the spore. The other reason is that the DPA and probably some tryptophan in the outer coat of the spore washed away with the supernatant. Although we expected the differences in the QE of the spores to change upon being washed, we did not expect the QE to decrease so dramatically. The decrease might also be due to the spores clumping together (like a paste) after being washed. Before washing, most of the spores were isolated from one another and floating in the suspension. Also after washing, the spores were precipitated very rapidly to the bottom of the cuvette. The other probable reason is that the spores released some amount of the DPA/CaDPA in the outer coat washed away with the supernatant, as shown in Figure 4.78. We also suspect that some of the

tryptophan residue present in the outer coat region of the spores may get washed off with the supernatant.

Our results also agree with the findings of Sivaprakasham *et al.*[38] They found that the fluorescence cross section of dried washed BG Dugway is smaller than the unwashed dried BG Dugway. We speculate that a substantial contribution to the QE value at 280-300 nm is due to a large absorption cross section at this excitation range, mainly due to tryptophan and CaDPA, which are primarily responsible for the fluorescence of *Bacillus* spores in suspension. Many factors, especially inner filter effects (re-absorption of fluorescence emission), can also affect fluorescence signal output.[34] "The QE of a fluorophore may change when it combines with other compounds. For example, the QE of tryptophan in protein can be either higher, lower, or about the same as that of the free amino acid. Its QE can vary from 0.05 for γ-globulin to nearly 0.48 for bovine serum albumin".[157]

Since most of our samples were excited in the absorption maximum range and there was no substantial overlap between absorption and the emission, the correction for re-absorption and re-emission are rendered unnecessary by using an optically dilute technique to calculate the QE values.[121] Several other sources of error cannot be easily avoided. A QE value of the unknown is only as good as the certainty of the yield of the standard. Proper selection of the standard is paramount if the results are to be more accurate. Considerable time is required to scan the emission of both standard and unknown, allowing slow instrumental drift to affect the accuracy. The reproducibility of measuring and calculating QE of the same solution is within ±2-5%. Results in the literature indicate that the reproducibility within a laboratory for the relative yields of two compounds is excellent, within 1-2%.[121] We also note that the relative QEs for the same compounds measured in various laboratories differ substantially, due to the problems inherent in calibrating spectrometers, in purifying materials, and preparing samples.[121] Nighswander-Rempel reported that commonly made assumptions in relative QE calculations (ratio of integrated emission to absorption) may produce errors of up to 25%.[158]

We also calculated the QE of DPA and CaDPA as dry crystalline samples. Secondary emission and scattering also cause trouble in the measurements, especially in the case of dry samples. “The photons that were assumed not to produce a signal can reach the detector and spuriously enhance the apparent yield. It is a highly tedious, exacting procedure which requires a detailed knowledge of all optical paths through the samples, of the absolute reflectance of the exciting light by the scatterer, and of the corrections required for scattered light”.[121] For this reason reliable measurements of QEs for the crystalline dry state are completely lacking, although such measurements are of fundamental importance.

“Because the evidence to date suggests a systematic error for excitation below 300nm, it was highly recommended that the Weber and Teale[117] technique be used only for excitation above 300 nm”.[121] No absolute QEs were measured in most of the above mentioned samples. This makes it very hard to compare the reported results in this research. But our results for tryptophan reasonably agreed with others’ findings. Therefore we remain reasonably satisfied that our results are useful as a reference point for further investigations.

CHAPTER 6

6 SUMMARY AND CONCLUSIONS

This thesis presents a novel and systematic approach to empirically characterizing the autofluorescence spectroscopic properties of the *Bacillus* spores by using the multi wavelength fluorescence technique combined with PCA. A new technique for characterising the unique fluorescence signature from bacterial spores has been introduced based on the chemical fluorescence signature of DPA/CaDPA.

Using autofluorescence spectra, we extended our observations of the spectral properties of DPA, CaDPA and tryptophan in aqueous solution to similar observations with dry crystals and wet paste at room temperature. Upon UV exposure, the fluorescence of DPA and CaDPA increases dramatically for dry as well as wet forms, while the fluorescence of tryptophan decreases in both cases. After exposure to a broad source UV light of the DPA, wet or dry, we observed a large increase in fluorescence with a maximum intensity emission peak at around 440 nm for excitation light with a wavelength of around 360 nm. There was a slight blue shift in the absorption spectra of UV-exposed DPA from the unexposed DPA solution. We could not see any substantial qualitative changes in the DPA exposed as dry or wet crystals, although drying the DPA increased the observed fluorescence and the crystals demonstrated a slightly broader emission peak. CaDPA in solution shows a slight fluorescence with increased fluorescence in the dry form, and a substantial increase of fluorescence was observed after UV exposure with an emission peak of around 410 nm for excitation around 305 nm. There was also a dramatic change in the absorption spectra of UV-exposed CaDPA from the unexposed CaDPA solution. The optimum wavelengths for UV exposure are found to be in the range of 250 to 300 nm with maximum enhancement with UV exposure at around 276 nm. The dry tryptophan powder has an emission peak at 330nm with excitation at around 280 nm. The emission peak of aqueous solution of tryptophan was at 340 nm with the excitation at 280 nm.

We observed that multiwavelength excitation fluorescence provides an additional means for distinguishing DPA and CaDPA. The results of the spectral properties of these chemicals, the enhancement of fluorescence of DPA/CaDPA and the suppression of tryptophan fluorescence due to high doses of UV irradiation were useful for the interpretation of the 2-D fluorescence studies of bacterial spores. From these studies we concluded that DPA and CaDPA show very little or no fluorescence for these chemicals in water solution but the fluorescence is quite visible for the dry chemicals even without UV irradiation. UV exposure increases the fluorescence of these chemicals in all forms and produces very high enhancement in suspension.

The fluorescence emission spectra of the *Bacillus* spores being studied (whether as dry and wet spores on filter paper or in aqueous suspension) at excitation wavelength region 280-290 nm were dominated by tryptophan emission. The emission spectra of dry spores showed a maximum emission of around 320nm. When the spores were either used as wet spores on filter paper or in water suspension, the emission was red shifted to around 340 nm. These changes in fluorescence of *Bacillus* spores in dry and wet environments agree with the changes in fluorescence of tryptophan in similar environments at these wavelength regions. In addition to this band, we also noticed some other pronounced spectral bands at different excitation wavelengths in the region of DPA/CaDPA. These bands also changed with the hydration state of the sample. Characteristic changes in the environment are the key to the species differentiation using PCA combined with fluorescence spectroscopy. Our multiwavelength experiments showed that the spectrum for dried spores of each of the spore species of *Bacillus* spores was different to that of their corresponding wet spores. We identified the wavelengths for the PCA in the UV region and near visible region that is sensitive to the major fluorophores, tryptophan, DPA and CaDPA. We tentatively identified that 280, 310, 340, 370 400, 430 nm are more feasible for discrimination of different species of *Bacillus* spores in dry and wet environment. It was concluded that it is not necessary to record the entire forty one spectra in order to discriminate the samples. Instead, the fluorescence intensity could be measured at selected excitation/emission wavelengths and then subjected to PCA.

The study of *Bacillus* spores in states that perhaps give the extremes of collection shows clear reversible differences between wet and dried *Bacillus* spores. Our results

revealed a stark effect of hydration on the fluorescence spectra of the *Bacillus* spores, implying water migration between inner spore compartments and the environment. Good reproducibility was observed with the results, even for different concentrations of the spores. PCA proved to be a valuable technique for classifying the spores as wet or dry and showed differences between dry and re-dried spores. Our results show that this technique is also applicable to situations where unknown endospores, previously hydrated, washed and autoclaved prior to collection need to be distinguished. It was concluded that the techniques (e.g, bacterial spore detection and identification) relying on fluorescence must take into account the hydration state of the spores and recognize the ability of the spores to rapidly change their state of hydration. Though we were able to discriminate between dry and wet spores, we cannot statistically draw the conclusion that our approach outperforms others studies because of the large number of sample sizes (library of samples) to be distinguished. Further, we should emphasize that the use of PCA in this work is merely illustrative of the potential for UV-Vis fluorescence-based discrimination and that more robust algorithms or other multivariate techniques with a larger sample size would probably be required.

The shape of the loading components made the results of PCA more understandable. PCA indicated that the derived components were correlated with the chemical composition of the spore samples. The PCA decomposed the fluorescence matrix into distinct fluorophores that were assigned to tryptophan and CaDPA. Our simulation studies also support the studies of relating the contribution of tryptophan and CaDPA to the spore fluorescence. It was suggested that minimal experimental inaccuracies, including the back ground Raman scattering, have no serious effect on PCA results and can be resolved when intensity changes of them are independent from each other. Using both techniques, it is possible both to quickly classify samples and identify the components responsible for the differences. Although unambiguous attribution of certain fluorescence bands to spore components requires further studies with other possible fluorophores, the present results show that distinct spectral ranges, such as those corresponding to amino acids, tryptophan and to compounds of the CaDPA may be identified in the spectra and used as markers for differentiation of bacterial spores from other samples.

Due to the presence of strong tryptophan emission, the unirradiated spores in water suspension do not generally show much influence of the presence of DPA/CaDPA in their EEM. However, after the standard UV irradiation, the tryptophan peak is largely reduced in the EEM for (+DPA) spores in water suspension, and the fluorescence increases dramatically in the regions where the chemicals CaDPA/DPA have peaks. For the (−DPA) spores in water, UV irradiation reduced the tryptophan peak, but the DPA and CaDPA influence is quite small, if present. The present use of a mutant strain to resolve a biophysical property of a particular chemical's contribution to the fluorescence spectra is a promising step.

The multiwavelength fluorescence spectroscopy combined with PCA has proved to be a very sensitive and useful technique for characterising the *Bacillus* spores' properties as well as for detecting the UV-induced spectral changes. The results seem to indicate the occurrence of a peculiar response in some specific regions of the fluorescence emission spectra of *Bacillus* spores as induced by UV irradiation. We discovered that the impressive fluorescence enhancement of *Bacillus* spores in water can be caused by UV irradiation with an emission peak of around 410 nm for excitation around 310 nm. We observed very similar enhancement of fluorescence in the case of CaDPA molecule. The identification of the components responsible for the observed spectral changes and their biological significance are also examined on the basis of further results obtained by spectroscopic analysis of other biological samples after exposure to UV irradiation. The specificity and reproducibility of the spectral response, coupled with the emerging importance of the UV radiation stress, seem to suggest that the present fluorescence approach to monitor changes of *Bacillus* spores under UV exposure would be of great interest. The new technique of fluorescence enhancement in *Bacillus* spores demonstrates the utility of a monitor for microbial contamination which is capable of distinguishing bacterial spores from other biological and non biological samples.

The fluorescence QE of DPA and CaDPA increased with UV irradiation while that of tryptophan decreased with UV irradiation with the level of exposure used in this research. We also showed that the QE of *Bacillus* spores decreased upon washing the spores. This is the first research effort known to us of the measured fluorescence QE values of DPA and CaDPA before and after UV irradiation. These measurements are

important to better understand the fluorescence characteristics of bacterial spores and their target molecules. We hope that these measurements will serve as a reference point for further spectroscopic studies of these exciting biomolecular systems.

An effective and sensitive technique was introduced to detect bacterial spores without any reagents, sample contact or applying any chemical or physical treatment, such as heating or autoclaving in contrast to previous technologies. There is no need to lyse the spore, grow the bacteria, hold the temperature constant or maintain pH. The method based on this technique is also seems to be rapid and the experimental conditions for the proposed new detector have not yet been fully optimised; what we present in this thesis is the introduction of this new technique and the preliminary basic investigations. Because biological organisms (for example, pollens, moulds, fungal spores, vegetative bacteria) other than bacterial endospores do not normally contain DPA, this method was relatively immune to their presence.

Whatever the nature of the observed fluorophore or other interferences, our results show that the intrinsic fluorescence of *Bacillus* spores has a huge potential to develop methods allowing the determination of the hydration and UV effect applied to spores. However, this work suggests that further analysis with more samples could differentiate between spores and many other common biological particles. There is also a suggestion that further analysis could reveal the subtle distinctions exposed by these experimental methods. It has been demonstrated that the proposed identification models yield adequate predictions of the spectral fingerprints of the biological samples selected in this research as case studies. We concluded that the 2-D multiwavelength fluorescence technique coupled with effective multivariate analysis is applicable to a wide range of biological samples found in diverse environments. A greater understanding of the fluorescence properties of *Bacillus* spores and their major components in different environments has far reaching consequences. All these efforts are desired in order to combat the adverse effects of the complex dynamic structure of bacterial dormancy – the spore

CHAPTER 7

7 REFERENCES

1. S. J. Gould, "The evolution of life on earth," Scientific American, October, 1994, pp. 85-91.

2. D. Clark, G. Cypret, C. Gonsalves, N. Hoesly, A. Moore, P. Saulnier, P. Scales-Brown, M. Slack, and R. White, "Biological detection system technologies," (North American Technology and Industrial Base Organization (NATIBO), 2001).

3. W. Volk and J. Brown, *Basic Microbiology* (Benjamin Cummings,, New York, 1997).

4. Committee on R&D Needs for Improving Civilian Medical Response to Chemical and Biological Terrorism Incidents, *Chemical and Biological Terrorism*, Research and Development to Improve Civilian Medical Response (National Academy Press, Washington, D.C., 1999).

5. L. M. F. Herman, M. J. M. Vaerewijck, R. J. B. Moermans, and G. M. A. V. J. Waes, "Identification and detection of *Bacillus* sporothermodurans spores in 1, 10, and 100 ml of raw milk by PCR," Appl. Environ. Microbiol **63**, 3139–3143 (1997).

6. P. Belgrader, W. Benett, D. Hadley, G. Long, R. Mariella, F. Milanovich, S. Nasarabadi, W. Nelson, J. Richards, and P. Stratton, "Rapid pathogen detection using a microchip PCR array instrument," Clin. Chem **44**, 2191–2194 (1998).

7. H. Yu, J. W. Raymonda, T. M. McMahon, and A. A. Campagnari, "Detection of biological threat agents by immunomagnetic microsphere-based solid phase fluorogenic- and electro-chemiluminescence," Biosens. Bioelectron **14**, 829–940 (2000).

8. K. A. Uithoven, J. C. Schmidt, and M. E. Ballman, "Rapid identification of biological warfare agents using an instrument employing a light addressable potentiometric sensor and a flow-through immunofiltration-enzyme assay system," Biosens. Bioelectron **14**, 761–770 (2000).

9. N. Velappan, J. L. Snodgrass, J. R. Hakovirta, B. L. Marrone, and S. Burde, "Rapid identification of pathogenic bacteria by single-enzyme amplified fragment length polymorphyism analysis," Microbiol. Infect. Dis **39**, 77–83 (2001).

10. A. Castro and R. T. Okinaka, "Ultrasensitive, direct detection of a specific DNA sequence of *Bacillus* anthracis in solution," Analyst **125**, 9–11 (2000).

11. H. Paulus, "Determination of dipicolinic acid by high-pressure liquid chromatography," Anal. Biochem **114**, 407–410 (1981).

12. D. Helm and D. Naumann, "Identification of some bacterial cell components by FT-IR spectroscopy," FEMS microbiol. Letters **126**(1), 75-80 (1995).

13. N. Grecz and T. Tang, "Relation of dipicolinic acid to heat resistance of bacterial spores," J. Gen. Microbiol **63**, 303–310 (1970).

14. M. W. Tabor, J. MacGee, and J. W. Holland, "Rapid determination of dipicolinic acid in the spores of clostridium species by gas–liquid chromatography," Appl. Environ. Microbiol **31**, 25–28 (1976).

15. A. D. Warth, "Determination of Dipicolinic Acid in Bacterial Spores by Derivative Spectroscopy," Anal.Biochem **130**, 502 -505 (1983).

16. L. E. Sacks, "Chemical germination of native and cation-exchanged bacterial spores with trifluoperazine," Appl.Environ.Microbiol. **56**, 1185-1187 (1990).

17. D. L. Rosen, C. Sharpless, and L. B. McGown, "Bacterial Spore Detection and Determination by Use of Terbium Dipicolinate Photoluminescence," Anal. Chem **69**, 1082-1085 (1997).

18. E. Ghiamati, R. Manoharan, W. H. Nelson, and J. F. Sperry, " UV Resonance Raman Spectra of *Bacillus* Spores," Applied Spectroscopy **46**, 357-364 (1992).

19. A. A. Hindle and E. A. H. Hall, "Dipicolinic acid(DPA) assay revisited and appraised for spore detection.," Analyst **124**, 1599-1604 (1999).

20. P. M. Pellegrino, N. F. Fell Jr, D. L. Rosen, and J. B. Gillespie, "Bacterial Endospore Detection Using Terbium Dipicolinate Photoluminescence in the Presence of Chemical and Biological Materials," Anal. Chem **70**, 1755-1760 (1998).

21. N. F. Fell Jr, P. M. Pellegrino, and J. B. Gillespie, "Mitigating phosphate interference in bacterial endospore detection by Tb dipicolinate photoluminesvence,," Anal.chim.Acta **426**, 43-50 (2001).

22. E. D. Lester and A. Ponce, "An anthrax smoke detector:Online monitoring of aerosilized bacterial spores," IEEE Eng.Med.Biol.Mag, Sept./Oct., 2002, pp. 38-42.

23. E. D. Lester, G. Bearman, and A. Ponce, "A Second-Generation Anthrax "Smoke Detector"-An Inexpensive Front-End Monitor That Detects Airborne Bacterial Spores," IEEE Eng.Med.Biol.Mag,, Jan./Feb., 2004, pp. 130-135.

24. X. Zhang, M. A. Young, O. Lyandres, and R. P. Van Duyne, "Rapid Detection of an Anthrax Biomarker by Surface-Enhanced Raman Spectroscopy," J.Amer.Chem.Soc **127**(12), 4484-4489 (2005).

25. A. A. Kolomenskii and H. A. Schuessler, "Raman spectra of dipicolinic acid in crystalline and liquid environments," Spectrochimica.Acta Part A **61**, 647-651 (2005).

26. J. T. Coburn, F. E. Lytle, and D. M. Huber, "Identification of bacterial pathogens by laser excited fluorescence," Analytical Chemistry **57**, 1669–1673 (1985).

27. B. V. Bronk and L. Reinisch, "Variability of steady state bacterial fluorescence with respect to growth conditions," Applied Spectroscopy **47**, 436–440 (1993).

28. T. M. Rossi and I. M. Warner, eds., *Rapid detection and identification of microorganisms* (Verlag Chemie, 1985), pp. 1-50.

29. L. Reinisch, J. Tribble, J. A. Werkhaven, and R. H. Ossoff, "Non-invasive optical diagnosis of bacteria causing otitis media," Laryngoscope **104**, 264–268 (1994).

30. M. J. Sorrel, J. Tribble, L. Reinisch, J. A. Werkhaven, and R. H. Ossoff, "Bacteria identification of otitis media with fluorescence spectroscopy," Lasers Surgery and Medicine **14**, 155–163 (1994).

31. B. C. Spector, L. Reinisch, D. Smith, and J. A. Werkhaven, "Noninvasive fluorescence identification of bacteria causing acute otitis media in a chinchilla model," Laryngoscope **110**, 1119–1123 (2000).

32. H. E. Giana, L. Silveira, R. A. Zangaro, and M. T. Pacheco, "Rapid Identification of Bacterial Species by Fluorescence Spectroscopy and Classification Through Principal Component Analysis," Journal of Fluorescence **13**, 489-493 (2003).

33. S. A. Glazier and H. H. Weetall, "Autofluorescence detection of Escherichia coli on silver membrane filters,," J.Microbiol.Methods **20**, 23-27 (1994).

34. J. K. Li and A. E. Humphrey, "Use of fluorometry for monitoring and control of a bioreactor," Biotechnology and Bioengineering **37**(11), 1043-1049 (1991).

35. J. Li, E. C. Asali, A. E. Humphrey, and J. J. Horvath, "Monitoring cell concentration and activity by multiple excitation fluorometry," Biotechnol.Prog **7**, 21-27 (1991).

36. P. P. Hairston, J. Ho, and R. Quant, "Design of and instrument for real-time detection of bioaerosols using simultaneous measurements of particle

aerodynamic size and intrinsic fluorescence," J.Aerosol.Science **28**, 471-482 (1997).

37. S. C. Hill, R. G. Pinninck, S. Niles, Y.-L. Pan, S. Holler, R. K. Chang, J. Bottiger, B. T. Chen, and C.-S. Orr, "Real-time measurements of fluorescence spectra from single airborne biological particles," Field Anal Chem Tech **3**, 221-239 (1999).

38. V. Sivaprakasham, A. Huston, C. Scotto, and J. D. Eversole, "Multiple UV wavelength excitation and fluorescence of bioaerosols," Optics Express **12**, 4457-4466 (2004).

39. Y. S. Cheng, E. B. Barr, B. J. Fan, J. Hargis, P.J.,, D. J. Rader, T. J. O'Hern, J. R. Torczynski, B. L. Tisone, B. L. Preppernau, S. A. Young, and R. J. Radloff, "Detection of bioaerosols using multiwavelength UV fluorescence spectroscopy.," Aerosol Science and Technology **30**, 186-201 (1999).

40. L. Leblanc and E. Dufour, "Monitoring the identity of bacteria using their intrinsic fluorescence," FEMS microbiol. Letters **211**, 147-153 (2002).

41. C. E. Alupoaei and L. Garcia-Rubio, H.,, "Growth Behavior of Microorganisms Using UV-Vis Spectroscopy: *Escherichia coli*," Biotechnol.And.Bioeng **86**(2), 163-167 (2004).

42. I. M. Warner, G. D. Christian, E. R. Davidson, and J. B. Callis, "Analysis of Multicomponent Fluorescence Data," Anal. Chem **49**(4), 564-573 (1977).

43. J. A. Werkhaven, L. Reinisch, M. J. Sorrel, J. Tribble, and R. H. Ossoff, "Non Invasive Optical Diagnosis of Bacteria Causing Otitis Media," Laryngoscope **104**, 264-268 (1994).

44. U. Himmelreich, R. L. Somorjai, B. Dolenko, O. C. Lee, H. M. Daniel, R. Murray, E. Mountford, and T. C. Sorrell, "Rapid Identification of *Candida* Species by Using Nuclear Magnetic Resonance Spectroscopy and a Statistical Classification Strategy," Applied and Environmental Microbiology **69**(8), 4566-4574 (2003).

45. J. Saltiel, D. F. Sears Jr, J. O. Choi, Y. P. Sun, and D. W. Eaker, "Fluorescence, Fluorescence-Excitation, and Ultraviolet Absorption Spectra of trans-1-(2-Naphthyl)-2-phenylethene Conformers.," J.Phys.Chem **98**, 35-46 (1994).

46. H. Bhatta, Goldys E,M.,and Learmonth,R.P.,, "Use of fluorescence spectroscopy to differentiate yeast and bacterial cells," Appl Microbiol Biotechnol **71**, 121-126 (2006).

47. J. D. Hybl, G. A. Lithgow, and S. G. Buckley, "Laser-Induced Breakdown Spectroscopy Detection and Classification of Biological Aerosols," Appl Spect **57**(10), 1207-1215 (2003).

48. A. L. Samuels, K. L. DeLucia, K. L. McNesby, and A. Miziolek, "Laser-induced breakdown spectroscopy of bacterial spores,molds,pollens, and protein: initial studies of discrimination potential," Applied Optics **42**(30), 6205-6209 (2003).

49. Y. P. Sun, D. F. Sears, and J. Saltiel, "Three-Component Self-Modelling Technique Applied to Luminescence Spectra," Anal. Chem **59**, 2515-2519 (1987).

50. B. Vandeginste, R. Essers, R. Bosman, T. Reijnen, and G. Kateman, "Three-Component Curve resolution in Liquid Chromatography with Multiwavelength Diode Array Detection," Anal. Chem **57**, 971-985 (1985).

51. D. Helm, H. Labischinski, G. Schallehn, and D. Naumann, "Classification and identification of bacteria by Fourier-transform infrared spectroscopy," J. Gen. Microbiol **137**, 69-79 (1991).

52. D. L. Perkins, C. R. Lovell, B. V. Bronk, B. Setlow, P. Setlow, and M. L. Myrick, "Effects of Autoclaving on Bacterial Endospores studied by Fourier Transform Infrared Microspectroscopy," Appl.Spect **58**(6), 749-753 (2004).

53. J. R. Lakowicz, *Principles of fluorescence spectroscopy* (Plenum Press, New York, 1983).

54. W. L. Nicholson, N. Munakata, G. Horneck, H. J. Melosh, and P. Setlow, "Resistance of *Bacillus* Endospores to Extreme Terrestrial and Extraterrestial Environments.," Microbiology and Molecular Biology Reviews **64**(3), 548-572 (2000).

55. D. J. Ellar and D. J. Lundgren, "Fine Structure of Sporulation in *Bacillus* cereus Grown in a Chemically Defined Medium," Journal of Bacteriology, **92**, 1748-1764 (1966).

56. A. S. Sussman and H. O. Halvorson, *Spores: Their dormancy and germination.* (Harper & Row,, New York, 1966).

57. L. L. Matz, T. Beaman, C.,, and P. Gerhardt, "Chemical Composition of Exosporium from Spores of *Bacillus* cereus," Journal of Bacteriology **101**, 196-201 (1970).

58. S. Charlton, A. J. G. Moir, L. Baillie, and A. Moir, "Characterization of the Exosporium of *Bacillus* cereus," Journal of Bacteriology **87**, 241-245 (1999).

59. A. Driks and P. setlow, ""Morphogenesis and Properties of the Bacterial Spore,"" in *in Prokaryotic Development*, B. Y. V. a. L. J. Shimkets., ed. (American Society of Microbiology,, Washington, D.C, 2000).

60. A. D. Warth, D. F. Ohye, and W. G. Murrell, "The Composition and Structure of Bacterial Spores," The Journal of Cell Biology, **16**, 579-592 (1963).

61. D. L. Popham and P. Setlow, "The Cortical Peptidoglycan from Spores of *Bacillus megaterium* and *Bacillus subtilis* Is Not Highly Cross-Linked," Journal of Bacteriology **175**, 2767-2769 (1993).

62. D. L. Popham, J. Meador-Parton, C. E. Costello, and P. Setlow, "Spore Peptidoglycan Structure in a cwlD dacB Double Mutant of *Bacillus* subtilis," Journal of Bacteriology **181**, 6205-6209 (1999).

63. W. G. Murrell, "Chemical composition of spores and spore structures," in *The Bacterial Spore*, G. W. Gould and A. Hurst, eds. (Academic Press,, London, 1969), pp. 215-273.

64. P. Setlow and E. A. Johnson, ""Spores and Their Significance,"" in *in Food Microbiology: Fundamentals and Fronteirs.*, M. P. Doyle, L. R. Beuchat, and T. J. Montville, eds. (ASM Press,, Washington, D.C, 2001).

65. P. Setlow, "Mechanisms which contributes to the long-term survival of spores of *Bacillus* species.," J.Appl.Bacteriol. **176**, 49S-60S (1994).

66. P. Gerhardt and R. E. Marquis, eds., *Spore thermoresistance mechanisms.*, In Regulation of Procaryotic development (Am.Soc.Microbiol., Washington DC, 1989).

67. V. Sapru and T. P. Labuza "Glassy state in bacterial spores predicted by polymer glass-transition theory," J. Food Sci **58**, 445-448 (1993).

68. R. Neihof, J. K. Thomson, and V. R. Deitz, "Sorption of water vapour and nitrogen gas by bacterial spores," Nature **216**, 1304-1306 (1967).

69. B. J. Marshall and W. G. Murrell, "Symposium on bacterial spores IX. Biophysical analysis of the endospore," Applied Bacteriology **33**, 103-129 (1970).

70. S. H. Black and P. Gerhardt, "Permeability of bacterial spores," Journal of Bacteriology **83**, 960-967 (1962).

71. J. C. Lewis, N. S. Snell, and H. K. Burr, "Water permeability of bacterial spores and the concept of a contracted cortex," Science **132**, 554 (1960).

72. W. G. Murrell and W. J. Scott, "The permeability of bacterial spores to water," Abstr.VII Internal.Congr.Microbiol., 1958, p. 26.

73. B. J. Marshall, W. G. Murrel, and W. J. Scott, "The effect of water activity, solutes and temperature on the viability and heat resistance of freeze-dried bacterial spores.," J.Gen.Microbiol **31**, 451-460 (1963).

74. W. G. Murrell and W. J. Scott, "Heat resistance of bacterial spores at various water activities.," J.Gen.Microbiol **43**(3), 411-425 (1966).

75. W. G. Murrell, "The biochemistry of the bacterial endospore," Adv.Microbiol.Physiol **1**, 133-251 (1967).

76. I. C. Watt, "Water vapour adsorption by *Bacillus* stearothermophilus endospores," presented at the American Society for Microbiology, 1981.

77. R. G. K. Leuschner and P. J. Lillford, "Effects of hydration on molecular mobility in phase-bright *Bacillus* subtilis spores," Microbiology **146**, 49-55 (2000).

78. T. C. Beaman, J. Greenamyre, T. Corner, H. S. Pankratz, and P. Gerhardt, "Bacterial spore heat resistance correlated with water content, wet density, and protoplast/sporoplast volume ratio," Journal of Bacteriology **150**, 870–877 (1982).

79. T. C. Beaman, T. Koshikawa, H. S. Pankratz, and P. Gerhardt, "Dehydration partitioned within core protoplast accounts for heat resistance of bacterial spores," FEMS Microbiology Letters **24**, 47-51 (1984).

80. A. J. Westphal, P. B. Price, T. J. Leighton, and K. E. Wheeler, "Kinetics of size changes of individual *Bacillus* thuringiensis spores in response to changes in relative humidity," Proceedings of the National Academy of Sciences, 2003, pp. 3461-3466.

81. A. Driks, "The dynamic spore," Proc.Natl.Acad.Sci **100**(6), 3007-3009 (2003).

82. I. D. Campbell and R. A. Dwek, *Biological Spectroscopy* (The Benjamin/Cummings Publishing Company,Inc, California, 1984).

83. N. Ramanujam, "Fluorescence Spectroscopy In Vivo," Encyclopedia of Analytical Chemistry, 2000, pp. 20-56.

84. R. S. DaCosta, H. Andersson, and B. C. Wilson, "Molecular Fluorescence Excitation-Emission Matrices Relevent to Tissue Spectroscopy," Photochem. Photobiol. **78**(4), 384-392 (2003).

85. D. W. Johnson, J. B. Callis, and G. D. Christian, "Rapid Scanning Fluorescence Spectroscopy," Anal. Chem **49**(8), 747A-751A (1977).

86. A. P. Demchenko, *Ultraviolet Spectroscopy of Proteins* (Springer-Verlag, New York, 1981).

87. T. D. Brock, M. T. Madigan, J. M. Martinko, and J. Parker, "*Biology of Microorganisms*," 7th ed. (Prentice Hall, Englewood Cliffs, NJ, 1994), p. Chap.19.

88. J. Ho, "Future of biological aerosol detection," Analytica Chimica Acta **457**, 125-148 (2002).

89. V. Agranovski, Z. Ristovski, M. Hargreaves, P. J. Blackall, and Morawska., "Real-time measurement of bacterial aerosols with the UVAPS; Performance evaluation," J.Aerosol.Science **34**, 301-317 (2003).

90. J. F. Powell, " Isolation of dipicolinic acid (pyridine-2:6-dicarboxylic acid) from spores of *Bacillus* megatherium," Biochem.J **54**, 210-211 (1953).

91. P. Setlow, "Germination and Outgrowth," in *The Bacterial Spore*, A. Hurst and G. W. Gould, eds. (Academic Press,, London, U.K, 1984).

92. B. D. Church and H. Halvorson, "Dependence of the heat resistance of the bacterial endospores on their dipicolinic acid content," Nature (London) **183**, 124-125 (1959).

93. G. W. Gould, "Germination," in *The Bacterial Spore*, G.W.Gould and A.Hurst, ed. (Academic Press, New York, 1969), pp. 397-444.

94. R. S. Hanson, M. V. Curry, J. V. Garner, and H. O. Halvorson, "Mutants of *Bacillus* cereus strain T that produce thermoresistant spores lacking dipicolinate and have low levels of calcium," Can.J.Microbiol **18**, 1139-1143 (1972).

95. M. Frobisher, R. D. Hinsdill, K. T. Crabtree, and C. R. Goodheart, *Fundamentals of Microbiology,* 9th ed ed. (W.B. Saunders,, Philadephia, 1974).

96. G. W. Gould and G. J. Dring, "Mechanisms of spore heat resistance," Adv.Microbiol.Physiol **11**, 137-164 (1975).

97. G. Balassa, P. Milhaud, M. Raulet, M. T. Silva, and J. C. Sousa, "A *Bacillus* subtilis mutant requiring dipicolinic acid for the development of heat-resistant spores," J.Gen.Microbiol **110**(2), 365-379 (1979).

98. P. E. Berg and N. Grecz, "Relationship of dipicolinic acid content in spores of *Bacillus* cereus T to ultraviolet and gamma radiation resistance," J.Bacteriol **103**, 517-519 (1970).

99. G. R. Germaine and W. G. Murrell, "Effect of dipicolinic acid on the ultraviolet radiation resistance of *Bacillus* cereus spores," Photochem.Photobiol **17**, 145-154 (1973).

100. S. Kozuka, Y. Y, and Tochikubo K., "Ultrastructural localization of dipicolinic acid in dormant spores of *Bacillus* subtilis by immunoelectron microscopy with colloidal gold particles," J Bact **162**, 1250-1254 (1985).

101. G. Leanz and C. Gilvarg, "Dipicolinic acid location in intact spores of *Bacillus* megaterium," J. Bact **114** p, 455-456 (1973).

102. J. C. Lewis, "Determination of Dipicolinic Acid in Bacterial Spores by Ultraviolet Spectrometry of the Calcium Chelate," Anal.Biochem **19**, 327-337 (1967).

103. R. Nudelman, B. V. Bronk, and Efrima., "Fluorescence Emission Derived from Dipicolinic Acid, its Sodium, and its Calcium Salts," Appl Spect **54**(3), 445-449 (2000).

104. R. Nudelman, N. Feay, M. Hirsch, S. Efrima, and B. V. Bronk, "Fluorescence of Dipicolinic Acid as a possible Component of the Observed UV Emission Spectra of Bacterial Spores," Proc. SPIE **3533**, 190-195 (1998).

105. G. W. Faris, R. A. Copeland, K. Mortelmans, and B. V. Bronk, "Spectrally resolved absolute fluorescence cross sections for *Bacillus* spores," Appl.Opt **36**(4), 958-967 (1997).

105a B. V. Bronk, R. Shoaibi, R. Nudelman, and A. Akinyemi, "Physical Perturbation for Fluorescent Characterization of Microorganism Particles," Proc.SPIE **4036**, 169-180 (2000).

106. J. Wise, A. Swanson, and H. O. Halvorson, "Dipicolinic acid-less mutants of Bacillus cereus," J. Bact. **94**, 2075-2076 (1967).

107. T. H. Zytkovicz and H. O. Halvorson, "Some characteristics of dipicolinic acid-less mutant spores of Bacillus cereus, Bacillus megaterium, and Bacillus subtilis," presented at the Am. Soc. Microbiol.,, Wash. DC., 1972.

108. T. A. Slieman and W. L. Nicholson, "Role of Dipicolinic Acid in Survival of *Bacillus* spores exposed to artificial and solar UV radiation," Appl. & Environ. Microbiol **67**, 1274-1279 (2001).

109. M. Paidhungat, B. Setlow, A. Driks, and P. Setlow, "Characterization of spores of B.subtilis which lack DPA," J.Bact **182**, 5505-5512 (2000).

110. T. C. Beaman and P. Gerhardt, "Heat resistance of bacterial spores correlated with protoplast dehydration, mineralization, and thermal adaptation," Appl. Environ. Microbiol **5s**, 1242-1246 (1986).

111. M. Stewart, A. P. Somlyo, A. V. Somlyo, H. Shuman, J. A. Lindsay, and W. G. Murrel, "Distribution of calcium and other elements in cryosectioned *Bacillus* cereus T spores, determined by high-resolution scanning electron probe x-ray microanalysis," J. Bact. **143**, 481-491 (1980).

112. I. R. Scott and D. J. Ellar, "Study of CaDipicolinic acid release during bacterial spore germination by using a new sensitive assay for dipicolinate," J. Bact **135**, 133-137 (1978).

113. H. Shibata, S. yamashita, M. Ohe, and I. Tani, "Laser Raman spectroscopy of lyophilized bacterial spores," Microbiol.Immunol **30**, 307-313 (1986).

114. D. L. Perkins, C. R. Lovell, B. V. Bronk, B. Setlow, P. Setlow, and M. L. Myrick, "Fourier Transform Infrared Reflectance Microspectroscopy Study of *Bacillus* subtilis Engineered without Dipicolinic Acid: The Contribution of Calcium Dipicolinate to the mid-infrared Absorbance of *Bacillus* subtilis Endospores," Applied Spectroscopy **59**(7), 893-896 (2005).

115. C. A. Parker, *Photoluminescence of Solutions* (Elsevier Publishing Company, New York, N.Y., 1968).

116. C. A. Parker and W. T. Rees, "Correction of fluorescence spectra and measurement of fluorescence quantum efficiency," Analyst **85**, 587-600 (1960).

117. G. Weber and W. J. Teale, "Determination of the absolute quantum yield of fluorescent solutions," Trans.Faraday Soc., **53**, 646 (1957).

118. W. H. Melhuish, "Quantum efficiencies of fluorescence of organic substances: effect of solvent and concentration of the fluorescent solute," J.Phys.Chem **65**, 229-235 (1961).

119. G. T. Wright, "Absolute Quantum Efficiency of Photofluorescence of Anthracene Crystals," presented at the Proc.Phys.Soc.B, 1954.

120. W. R. Dawson and M. W. Windsor, "Fluorescence Yields of Aromatic Compounds.," The Journal of Physicsl Chemistry **72**(9), 3251-3260 (1968).

121. J. N. Demas and G. A. Crosby, "The Measurement of Photoluminescence Quantum Yields. A Review," J.Phys.Chem **75**(8), 991-1024 (1971).

122. S. Dhami, A. J. De Mello, G. Rumbles, S. M. Bishop, D. Phillips, and A. Beeby, "Phthalocyanine fluorescence at high concentration: dimmers or reabsorption effect?," Photochem.Photobiol **61**, 341-346 (1995).

123. T. R. Williams, S. A. Winfield, and J. N. Miller, "Relative fluorescence quantum yields using a computer controlled luminescence spectrometer," Analyst **108**, 1067-1071 (1983).

124. R. F. Chen, "Fluorescence Quantum Yields of Tryptophan and Tyrosine," Analytical Letters **1**(1), 35-42 (1967).

125. S. K. Jenson and F. A. Walty, "Principal components analysis and canonical analysis in remote sensing," presented at the Proc. An. Soc. of Photogrammetry, 1979.

126. K. R. Beebe and B. R. Kowalski, "An Introduction to Multivariate Calibration and Analysis," Anal. Chem **59**, 1007A-1017A (1987).

127. N. Bonnet, "Multivariate statistical methods for analysis of microscope image series," Journal of Microscopy **190**, 2-18 (1998).

128. Basilevsky, "Statistical Factor Analysis and Related Methods, Theory and Applications," (John Wiley & Sons, New York, 1971).

129. B. S. Everit and G. Dunn, *Applied Multivariate Data Analysis* (Oxford University Press, New York, 1992).

130. A. M. Kshirsagar, *Multivariate Analysis* (Marcel Dekker, New York, 1972).

131. I. H. Berstein, Garbin,C.P. and Teng,G.K, *Applied Multivariate Analysis* (Springer-Verlag, New York, 1988).

132. T. Persson, Wedborg,M, "Multivariate evaluation of the fluorescence of aquatic organic matter," Analytica Chimica Acta **434**, 179-192 (2001).

133. G. Paul, *Practical guide to chemometrics,* 2nd ed. ed. (Boca Raton,FL: Taylor & francis, 2006), p. 541 p.

134. K. Y. Yeung and W. L. Ruzzo, "Principal component analysis for clustering gene expression data.," Bioinformatics **17**, 763-774 (2001).

135. I. T. Jolliffe, *Principal Component Analysis* (Springer, NewYork, USA, 1986).

136. B. F. J. Manly, *Multivariate Statistical Methods A Primer,* 2nd ed. (Chapman and Hall, London, 1994).

137. H. F. Kaiser, "The application of electronic computers to factor analysis. Educational and Psychological Measurement," Educational and Psychological Measurement **20**, 141-151 (1960).

138. O. Hammer, D. A. T. Harper, and P. D. Ryan, "PAST - PAlaeontological STatistics, ver. 1.35" (http://folk.uio.no/ohammer/past, 2005), retrieved.

139. L. Kaufman and P. J. Rousseeuw, *Finding Groups in Data. An Introduction to Cluster Analysis* (Wiley–Interscience,, New York., 1990).

140. S. Sarasanandarajah, Kunnil J., E. Chacko, B. V. Bronk, and R. L., "Reversible changes in fluorescence of bacterial endospores found in aerosols due to hydration/drying," J. Aerosol Science **36**, 689-699 (2005).

141. A. Kulmyrzaev and E. Dufour, "Determination of lactulose and furosine in milk using front-face fluorescence spectroscopy," Lait **82**, 725–735 (2002).

142. G. Strahs and R. E. Dickerson, "The Crystal Structure of Calcium Dipicolinate Trihydrate (A Bacterial Spore Metabolite)," Acta Cryst **B24**, 571-578 (1968).

143. I. B. Berlman, *Handbook of Fluorescence Spectra of Aromatic molecules,* (Academic Press,, New York and London, 1971).

144. J. Kunnil, S. Sarasanandarajah, E. Chacko, and L. Reinisch, "Fluorescence quantum efficiency of dry *Bacillus* globigii spores," Optics Express **13**(22), 8969-8979 (2005).

145. D. Zhong, E. W.-G. Diau, T. M. Bernhardt, S. D. Feyter, J. D. Roberts, and A. H. Zewail, "Femtosecond dynamics of valence-bond isomers of azines: transition states and conical intersections," Chem.Phys.Lett **298**, 129-140 (1998).

146. M. Chachisvilis and A. H. Zewail, "Femtosecond Dynamics of Pyridine in the Condensed Phase: Valence Isomerization by Conical Intersections," J.Phys.Chem. A **103**, 7408-7418 (1999).

147. L. I. Grossweiner, "Photochemical inactivation of enzymes.," Curr.Top.Radiat.Res.Q. **11**, 141-199 (1976).

148. J. Kunnil, B. Swartz, and L. Reinisch, "Changes in the luminescence between dried and wet *Bacillus* spores," Applied Optics **43**, 5404–5409 (2004).

149. M. Plomp, T. J. Leighton, K. E. Wheeler, and A. J. Malkin, "The high-resolution architecture and structural dynamics of *Bacillus* spores," Biophys.J **88**(1), 603-608 (2005).

150. V. G. R. Chada, E. A. Sanstad, R. Wang, and A. Driks, "Morphogenesis of *Bacillus* spore Surfaces," J Bact **185**(21), 6255-6261 (2003).

151. T. Hasegawa, Nishijo,J.,Umemura,J., "Separation of Raman spectra from fluorescence emission background by principal component analysis," Chem.Phys.Lett **317**, 642-646 (2000).

152. T. Hasegawa, "Detection of Minute Chemical Species by Principal-Component Analysis," Analytical Chemistry **71**(15), 3085-3091 (1999).

153 A. Alimova, A. Katz, H. W. Savage, M. Shah, G. Minko, D. V. Will, R. B. Rosen, S. A. McCormick, and R. R. Alfano, "Native fluorescence and excitation spectroscopic changes in *Bacillus* subtilis and Staphylococcus aureus bacteria subjected to conditions of starvation," Applied Optics **42**, 4080-4087 (2003).

154. W. F. Cheong and A. J. Welch, "A Review of the Optical Properties of Tissues," IEEE.J.Quantum Electron **26**, 2166-2185 (1990).

155. G. Smith, J., and W. H. Melhuish, "Effect of the temperature and viscosity on the excited singlet state of indoles in polar solvents," J.Phys.Chem **95**, 4288-4291 (1991).

156. C. Saavedra, C. Vasquez, and M. V. Encinas, "Structural studies of the Bst V1 restriction-modification proteins by fluorescence spectroscopy," Eur.J.Biochem. **263**, 65-70 (1999).

157. F. W. J. Teale, "Ultraviolet Fluorescence of Proteins in Natural Solution," J.Biochem **76**, 381-388 (1960).

158 S. P. Nighswander-Rempel, "Quantum Yield Calculations for Strongly Absorbing Chromophores" J.Fluoresc. **16** (4), 483-485 (2006).